Host-parasite associations in the globally invasive *Xenopus laevis*

AL Schoeman

orcid.org/0000-0002-9096-5337

Thesis accepted in fulfilment of the requirements for the degree
Doctor of Philosophy in Science with Environmental Sciences
at the North-West University

Promoter: Prof LH du Preez

Graduation August 2021
29388325

In liefdevolle herinnering
aan my Oupa Thys

"Oupa se oudste
waaraan niemand iets kan doen nie"

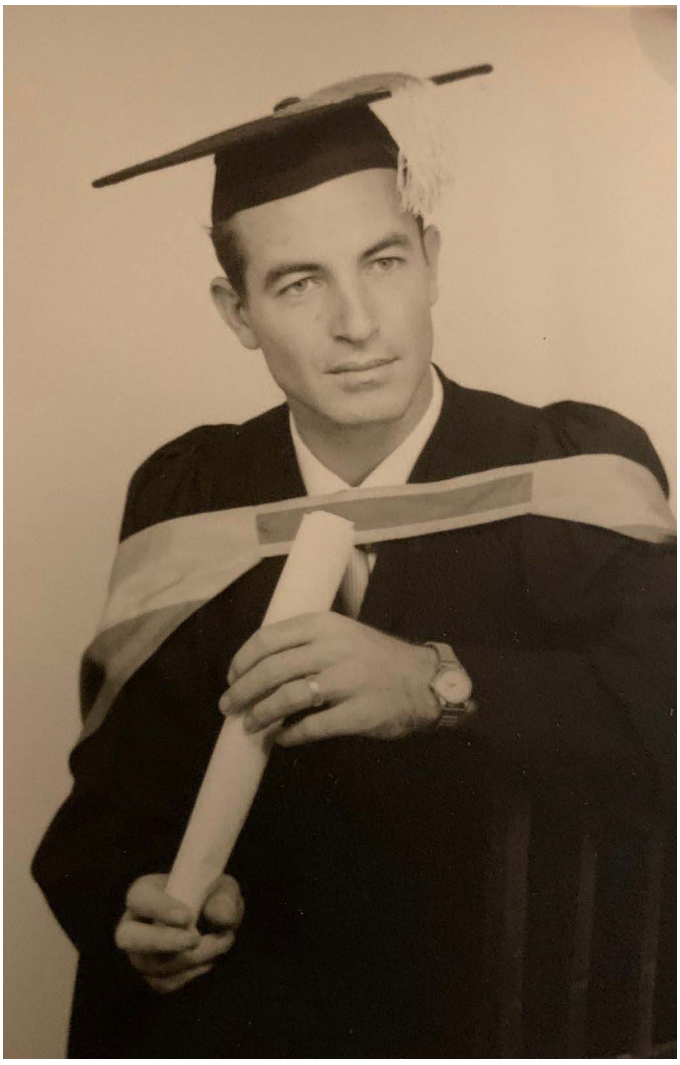

Mathys Stephanus Louis Boshoff

30.iii.1937 tot 18.iii.2020

Declaration

This thesis is compiled in article format and comprises of three published research articles (chapters 2, 3 and 4) and three unpublished manuscripts that are in preparation for submission to academic journals (chapters 5, 6 and 7). I declare that the thesis has been composed by myself and that the work has not be submitted for any other degree or professional qualification. I confirm that the work submitted is my own, except where work which has formed part of jointly-authored publications has been included. For each of these manuscripts, I was primarily responsible for study design, data collection, laboratory work, statistical analyses, writing, manuscript preparation and consolidation of revisions by co-authors. For chapters 3–7, I am the lead author. Sections where co-authors took the lead are noted below. All co-authors have given their permission for the articles and manuscripts to be submitted for degree purposes.

Chapter 2 has been published in *Folia Parasitologica* (Svitin *et al.*, 2018) and was co-authored by Roman Svitin and Louis H du Preez. Dr Svitin was the lead author for this publication. Chapter 3 has been published in *African Zoology* (Schoeman *et al.*, 2020) and was co-authored by Tracy-Lee Joubert, Louis H du Preez and Roman Svitin. Dr Svitin contributed his expertise in nematology to this manuscript. Chapter 4 has been published in *Biological Invasions* (Schoeman *et al.*, 2019) and is co-authored by Natasha Kruger, Jean Secondi and Louis H du Preez. Chapter 5 is in preparation and will be submitted after the examination period. Louis H du Preez, Ané Jacobs, Giovanni Vimercati and Jean Secondi are involved as co-authors. Chapter 6 is in preparation with intended submission to *The Journal of Applied Ecology*. Nikol Kmentová, Louis H du Preez and Maarten PM Vanhove are involved as co-authors. Chapter 7 is in preparation for submission to *Genomics*. Nikol Kmentová, Louis H du Preez and Maarten PM Vanhove are involved as co-authors.

No copyright is involved in the content of any of these manuscripts. The original publications were formatted in accordance with the NWU guidelines for thesis submissions.

This thesis is also available in Afrikaans to honour the financial support of the *Suid-Afrikaanse Akademie vir Wetenskap en Kuns*. Feel free to send an email to Anneke Lincoln Schoeman to obtain this version. More information on the translation process and collaborators and a complete bilingual term list can be found online in English or Afrikaans.

Acknowledgements

If you are reading this, it means that somewhere in the southernmost reaches of a brave continent, a younger version of myself forsook the familiar path of the females of my species and weathered pandemics and publication woes, sacrificed frogs and former amusements, discovered the blessings of community and curiosity and intimately experienced the boundless grace of God in my own life and the beautifully crafted world around me. Moreover, this document is proof of hundreds of helping hands.

Along this journey, the time generously given by others to help this thesis into existence is very precious to me. I am thankful to every family member, friend, colleague and fellow human who made a mark on the past four years of my life. I cherish your tangible input in this project and the emotional, spiritual and intellectual support that you offered me. *Thank you*. *Baie dankie*. *Ke a leboga*. Дякую. *Merci*. *Dank je wel*. *Děkuji*. *Grazie*.

On similarly sincere note, I want to express my gratitude to the funding agencies and institutions that made this project a reality. This project was predominantly funded by a scholarship from the DSI-NRF Centre of Excellence for Invasion Biology. Additional personal funds were provided by the *Suid-Afrikaanse Akademie vir Wetenskap en Kuns*, as well as the North-West University. I am grateful to the NWU Language Directorate who not only ensured that I had a steady income as the interpreter for pregraduate Zoology classes but were also extremely accommodating of a PhD student on the staff. A special word of appreciation for the dear people and fantastic facilities at the Unit for Environmental Sciences and Management at the North-West University, the Centre for Environmental Sciences at UHasselt, the Faculty of Sciences at the Université d'Angers and the Centre for Invasion Biology at the Stellenbosch University.

Finally, I am greatly indebted to Louis du Preez. Dear Prof, I know that it is part of your job to guide PhD students but you went to great lengths to ensure that I flourished as a scientist and a person. In your humble and caring way, you made the research group a family and Potchefstroom a home. May the road ahead be filled with God's blessings and life's wonders.

Abstract

In the Anthropocene, the movement of species takes place at unprecedented rates. As ranges shift in reaction to climate change or through human mediation, we need to understand the complex novel interactions that arise. In the present study, a multidisciplinary approach to invasion biology, exemplifying the application of parasite data, is advanced. To this end, the world's most widespread frog, *Xenopus laevis* (Daudin, 1802) (Anura: Pipidae), and its diverse assemblage of metazoan parasites are proposed as a model host-parasite system during range expansion.

As a baseline for further bio-invasion investigations, "integrative taxonomy" was applied to address knowledge gaps regarding the associations between native *X. laevis* and nematode parasites. Thus followed the redescription of three members of the Camallanidae, providing indispensable molecular data, as well as the first report of seven more nematode species that are associated with *X. laevis*. The parasite dynamics revealed in this survey highlights the need for the inclusion of DNA barcodes, emphasises the role of *X. laevis* as a parasite reservoir and provides insight on the origin of the parasite species of *X. laevis* in the invasive range.

As a next step, the geographic replicates of parasitological surveys of *X. laevis* in its native southern Africa and the invasive populations in France, Portugal, California and Chile, acted as a "natural experiment" to identify over-arching patterns in the host-parasite dynamics of invasive species. This approach demonstrates the Enemy Release Hypothesis for this globally invasive amphibian host yet also reveals complex parasite dynamics of *X. laevis* populations in South Africa and western France upon closer inspection. The parasite communities of expanding populations of *X. laevis* are typified as more variable than the communities from host populations from natural habitats. The divergent responses of parasite taxa to range expansion show that these systems merit further study to predict the future of host-parasite associations amidst global change.

Finally, this study proves the concept that parasite data sets can provide an independent line of evidence to address questions in invasion biology. This approach was applied to trace the intraspecific cryptic invasions of *X. leavis* in its native range with the help of its highly associated polystomatid parasite, *Protopolystoma xenopodis* (Price, 1943)

Bychowsky, 1957 (Monogenea: Polystomatidae). The comparative phylogeography of these ”holistic specimens” revealed widespread lineage-level invasion events of *X. laevis* across southern Africa, provided insight on the origin of the French invasive population of the host and even revealed the role of small-scale human-mediated translocation of this frog via the recreational fishing community in shaping its dispersal patterns in the native range. In order to aid future investigators in the development of mitochondrial markers when using polystomatid parasites as tags for host phylogeography, the complete mitochondrial genome of *P. xenopodis* was sequenced and annotated. Intraspecific comparison of the mitogenome sequences of this polystomatid identified promising gene regions for phylogeographic analyses.

Ultimately, a multidisciplinary approach that incorporates both host and parasite data holds great potential in invasion biology. This study demonstrates this approach via the lens of a well-studied model host-parasite system.

Keywords: Anthropocene; Biological invasion; Co-phylogeography; Cryptic invasion; Integrative taxonomy; Metazoan parasite; Mitogenomics; Multidisciplinary; Natural experiment; Range expansion.

Opsomming

Die Antroposeen word gekenmerk deur spesies wat teen 'n ongeëwenaarde gang beweeg. Soos wat gebiede in reaksie op klimaatsverandering of as gevolg van menslike inmenging skuif, is dit noodsaaklik om die komplekse nuwe interaksies wat te voorskyn kom, te verstaan. Die huidige studie beveel aan dat 'n multidissiplinêre benadering tot indringerbiologie gevolg word, waar die toepassing van parasietdata uitdrukking vind. Ten einde hierdie doel te verwesenlik word die wêreld se mees wydverspreide padda *Xenopus laevis* (Daudin, 1802) (Anura: Pipidae) en sy diverse metasoönparasietgemeenskap as 'n model vir die gasheer-parasiet-sisteem tydens gebiedsuitbreiding voorgestel.

As basis vir verdere navorsing in bio-indringing, is "geïntegreerde taksonomie" toegepas om gapings in ons kennis van die verband tussen inheemse *X. laevis* en nematoodparasiete aan te spreek. Gevolglik is drie lede van die Camallanidae herbeskryf wat onontbeerlike molekulêre data gelewer het. Verder is nog sewe nematoodspesies wat met *X. laevis* verband hou vir die eerste keer bekend gemaak. Die parasietdinamiek wat hierdie opname aan die lig gebring het, beklemtoon die belang van DNA-staafkodes in indringerbiologie en die rol van *X. laevis* as 'n parasietreservoir. Verder word die oorsprong van die parasietspesies van *X. laevis* in die vreemde gebied toegelig.

As 'n volgende stap is die geografiese replikate van die parasitologiese opnames van *X. laevis* in sy inheemse suidelike Afrika en die uitheemse bevolkings in Frankryk, Portugal, Kalifornië en Chili as 'n "natuurlike eksperiment" benut om oorkoepelende patrone in die gasheer-parasiet-dinamiek van indringerspesies uit te lig. Hierdie benadering bevestig die vyandsvrystellingshipotese vir hierdie wêreldwye indringeramfibie, maar by nadere ondersoek illustreer dit ook die komplekse parasietdinamiek van *X. laevis*-bevolkings in Suid-Afrika en westelike Frankryk. Die parasietgemeenskappe van die uitbreidende bevolkings van *X. laevis* word uitgeken aan hulle veranderlikheid in vergelyking met die gemeenskappe van gasheerbevolkings van ongerepte habitatte. Die uiteenlopende reaksies van parasiettaksa tot gebiedsuitbreiding toon aan dat verdere studie nodig is om die toekomstige gasheer-parasiet-vennootskappe te midde van 'n veranderende wêreld te voorspel.

Ten laaste is hierdie studie 'n konsepbewys dat parasietdata onafhanklike bewyse kan

lewer waarmee vraagstukke in indringerbiologie aangespreek kan word. Hierdie benadering is gebruik om die intraspesifieke kriptiese indringings van *X. leavis* met die hulp van ’n hoogs geassosieerde polistomatiedparasiet, *Protopolystoma xenopodis* (Price, 1943) Bychowsky, 1957 (Monogenea: Polystomatidae), in die inheemse gebied na te spoor. Die vergelykende filogeografie van die “holistiese eksemplare” het wydverspreide intraspesifieke indringingsgebeurtenisse van *X. laevis* regoor suidelike Afrika uitgeken, tot insigte gelei oor die oorsprong van die Franse uitheemse bevolking van die gasheer en selfs die rol van kleinskaalse antropogeniese verskuiwings van hierdie padda via die hengelarygemeenskap as rolspelers in verspreidingspatrone in die inheemse gebied geëien. As hulpbron vir toekomstige navorsers in die ontwikkeling van mitochondriese merkers tydens die gebruik van polistomatiede as aanwysers van gasheerfilogeografie, is die volledige mitochondriese genoom van *P. xenopodis* gekarakteriseer. Intraspesifieke vergelykings van die mitogenoom van hierdie polistomatied het belowende geenstreke vir filogeografiese analises geïdentifiseer.

Oplaas is daar aangetoon dat ’n multidissiplinêre benadering, wat beide gasheer- en parasietdata betrek, groot potensiaal in indringerbiologie inhou. Hierdie studie demonstreer die benadering aan die hand van ’n welbestudeerde model van ’n gasheer-parasietsisteem.

Sleutelterme: Antroposeen; Biologiese indringing; Gebiedsuitbreiding; Geïntegreerde taksonomie; Ko-filogeografie; Kriptiese indringing; Meersellige parasiete; Mitogenomika; Multi-dissiplinêr; Natuurlike eksperiment.

Contents

1 Introduction to a parasite taxi **1**

1.1 Biological invasions, a sign of the times 1

1.2 Parasites, the clandestine passengers of range expansion 2

1.3 Model host-parasite systems needed in invasion biology 2

1.4 A globally invasive frog and its parasites as model 3

1.5 Aim: Application of the frog-parasite model to issues in invasion biology . . 4

1.5.1 Objective 1: The use of integrative taxonomy to strengthen knowledge on native parasite associations 4

1.5.2 Objective 2: Parasite infra- and component community analyses to compare parasite dynamics in the native and invasive range 5

1.5.3 Objective 3: Comparative phylogeography as a more holistic approach to tracing invasions 6

1.6 Methodological considerations 7

1.6.1 Parasitological surveys 7

1.6.2 Ethical considerations 8

1.6.3 Sampling design 8

2 Taxonomic update of native nematodes **9**

2.1 Introduction 9

2.2 Methods 11

2.3 Results . . . 13
2.3.1 Morphological descriptions . . . 13
2.3.2 Molecular analysis . . . 21
2.4 Discussion . . . 22

3 New reports of native nematodes **25**
3.1 Introduction . . . 25
3.2 Methods . . . 27
3.3 Results . . . 29
3.3.1 Nematode descriptions . . . 30
3.3.2 Role of *Xenopus laevis* in the transmission of nematode species . . . 41
3.4 Discussion . . . 42

4 Repeated parasite loss in invasive range **46**
4.1 Introduction . . . 46
4.2 Methods . . . 48
4.2.1 Host and parasite collection in France . . . 48
4.2.2 Parasite identification in the French population . . . 50
4.2.3 Host and parasite collection in South Africa . . . 50
4.2.4 Parasite identification in South Africa . . . 50
4.2.5 Parasitological surveys from the literature and clarification of parasitological parameters . . . 51
4.2.6 Statistical analyses . . . 52
4.3 Results . . . 53
4.3.1 Parasitological survey in France and South Africa . . . 53
4.3.2 Effect of sampling effort . . . 55

4.3.3 Parasitism of hosts in native and invasive ranges 55
4.3.4 Characteristics of accompanying parasites 56
4.3.5 Susceptibility of invasive hosts to parasitism 57
4.3.6 Parasite community dissimilarity analyses 57
4.4 Discussion 59

5 Complex parasite dynamics during range expansion 63

5.1 Introduction 63
5.2 Methods 65
5.2.1 Host collection 65
5.2.2 Parasite collection and identification 66
5.2.3 Calculation of scaled mass index of hosts 68
5.2.4 Habitat classification in the native range 69
5.2.5 Calculation of least cost path from introduction site in invasive range 69
5.2.6 Quantification of parasitism 70
5.2.7 Selection of predictors 71
5.2.8 Statistical analyses 71
5.3 Results 74
5.3.1 Parasite assemblages of *X. laevis* in the native and invasive range . 74
5.3.2 Intrinsic and extrinsic factors affecting parasitism in the native range 76
5.3.3 Effect of range expansion on parasitism in the invasive range 77
5.4 Discussion 77
5.4.1 Host body size has some effect on crowding and cestode, but not monogenean, abundance of native *Xenopus laevis* 78
5.4.2 Extrinsic factors primarily shape parasitism of native *Xenopus laevis* 80

5.4.3 Cestode abundance decreases with distance from the introduction point in invasive *Xenopus laevis* . . . 82

5.4.4 Implications for the domestic and global invasion of host-parasite systems . . . 84

6 Parasites reveal cryptic introduction of hosts **85**

6.1 Introduction . . . 85

6.2 Methods . . . 88

6.2.1 Host and parasite sampling . . . 88

6.2.2 Molecular data collection . . . 90

6.2.3 Haplotype networks . . . 91

6.2.4 Phylogenetic analyses . . . 91

6.2.5 Co-phylogenetic analyses . . . 92

6.3 Results . . . 93

6.3.1 Sequence diversity . . . 93

6.3.2 Host and parasite phylogeographic clustering . . . 94

6.3.3 Host and parasite phylogeny and congruence . . . 96

6.4 Discussion . . . 99

6.4.1 Parasite clustering mirrors the intraspecific phylogeography of the host 99

6.4.2 Parasite spill-over is an indication of contact between divergent host lineages . . . 100

6.4.3 Parasite phylogeography as an underutilised tool in invasion biology 102

6.4.4 Conclusions and recommendations . . . 103

7 Monogenean mitogenome for invasion genomics **104**

7.1 Introduction . . . 104

7.2 Methods . . . 107

7.3 Results . . . 112
7.3.1 Sequencing and assembly . . . 113
7.3.2 Annotation . . . 114
7.3.3 Mitogenome architecture, gene content and intraspecific variation . 117
7.3.4 Comparison with other polyopisthocotylean mitogenomes . . . 123
7.3.5 Mitogenome phylogeny . . . 124
7.4 Discussion . . . 126

8 General discussion and future perspectives 133

8.1 The role of integrative taxonomy in invasion biology . . . 134
8.2 Discerning patterns in invasion biology with global replicates of co-introduced host-parasite systems . . . 136
8.3 Parasites as supporting evidence in bio-invasion research . . . 137
8.4 The future of invasion biology from the perspective of a parasitologist . . . 138

A Information on collection localities 185

B Additional morphometrics of a polystomatid 190

B.1 Background and aim . . . 190
B.2 Morphometrics . . . 191
B.3 Statistical analyses . . . 191
B.4 Significant morphological variation among South African *Protopolystoma xenopodis* . . . 192
B.5 Implications . . . 193

List of Figures

2.1 *Batrachocamallanus slomei* Southwell *et* Kirshner, 1937 from *Xenopus laevis* (Daudin), photomicrographs. 14

2.2 *Camallanus kaapstaadi* Southwell *et* Kirshner, 1937 from *Xenopus laevis* (Daudin), photomicrographs. 16

2.3 *Camallanus xenopodis* Jackson *et* Tinsley, 1995 from *Xenopus laevis* (Daudin), photomicrographs. 19

2.4 *Camallanus xenopodis* Jackson *et* Tinsley, 1995 from *Xenopus laevis* (Daudin), male, line-drawings. 20

2.5 Phylogenetic tree of seven species of *Camallanus* Railliet *et* Henry, 1915 based on partial *28S* sequences. 21

2.6 Phylogenetic tree of four species of *Camallanus* Railliet *et* Henry, 1915 based on partial *COX1* sequences. 22

3.1 Distribution of seven previously undescribed species of nematodes recovered at ten localities across South Africa during the parasitological screening of *Xenopus laevis*. 29

3.2 Adult female of *Capillaria* sp. from the digestive tract of *Xenopus laevis*, photomicrographs. 31

3.3 Third stage larval *Contracaecum* sp. encysted in *Xenopus laevis*, photomicrographs. 33

3.4 Adult *Falcaustra* sp. from the digestive tract of *Xenopus laevis*, photomicrographs. 35

3.5 Third stage larval *Paraquimperia* sp. from the digestive tract of *Xenopus laevis*, photomicrographs. 37

3.6 Third stage larval *Tanqua* sp. from the digestive tract of *Xenopus laevis*, photomicrographs. 39

3.7 Unidentified second stage nematode larvae sp. 1 & 2 from the lungs, liver and kidneys of *Xenopus laevis*, photomicrographs. 40

3.8 Hypothesised trophic transmission in a freshwater ecosystem of seven nematode parasites associated with *Xenopus laevis*. 42

4.1 Recovered parasite species richness at 47 sites where full parasitological surveys of *Xenopus laevis* were conducted. 49

4.2 Metazoan parasite species richness of *Xenopus laevis* populations in the invasive range is lower than in the native range. 56

4.3 Per-site prevalence of a monogenean parasite of *Xenopus laevis* is higher in the native range than in the invasive range, but does not differ significantly in the case of a cestodean parasite. 58

4.4 Non-metric multidimensional scaling of compositional dissimilarity reveals that metazoan parasite communities from native (southern Africa) and invasive (California, Chile, France, Portugal) *Xenopus laevis* populations cluster separately due to enemy loss in invasive hosts. 59

5.1 Distribution of localities in western France and South Africa where adult *Xenopus laevis* were collected along with their metazoan parasite assemblages. 67

5.2 Summaries of the estimated posterior distributions for the fixed and random effects from the three Bayesian generalised linear mixed models with measures of parasitism of *Xenopus laevis* in South Africa as response. . . 75

5.2 Summaries of the estimated posterior distributions for the fixed and random effects from the three Bayesian generalised linear mixed models with measures of parasitism of *Xenopus laevis* in South Africa as response (*continued*). 76

5.3 Summaries of the estimated posterior distributions for the fixed and random effects from the three Bayesian generalised linear mixed models with measures of parasitism of *Xenopus laevis* in western France as response. . 78

6.1 Localities in southern Africa where 46 adult *Xenopus laevis* were collected along with the flatworm parasite *Protopolystoma xenopodis*. 89

6.2 Median spanning haplotype networks of the concatenated partial *COX1* and *rrnS* genes of 59 *Xenopus laevis* specimens and their corresponding 59 *Protopolystoma xenopodis* parasites from their native and invasive range. 95

6.3 The interaction network and maximum likelihood phylogenies of the frog *Xenopus laevis* and its polystomatid *Protopolystoma xenopodis*. 97

7.1 Mitochondrial genome of the polystomatid flatworm *Protopolystoma xenopodis*.112

7.2 Predicted secondary structures of transfer RNAs encoded by the two newly annotated mitochondrial sequences of *Protopolystoma xenopodis*. 120

7.2 Predicted secondary structures of tRNAs encoded by the two newly annotated mitochondrial sequences of *Protopolystoma xenopodis* (*continued*). . 121

7.3 Nucleotide diversity (π) between the two newly annotated *Protopolystoma xenopodis* mitochondrial sequences. 123

7.4 Gene order rearrangement scenarios among nine polyopisthocotylean mitogenomes based upon the pairwise comparison of seven complete mitogenomes to the newly annotated sequences of *Propopolystoma xenopodis*.124

7.5 Majority-rule consensus tree from the Bayesian inference (BI) of phylogeny of 14 mitochondrial genes from 12 polyopisthocotylean species. 126

B.1 Principal components analysis of the morphological traits of *Protopolystoma xenopodis* from two phylogeographic lineages of the host *Xenopus laevis*. . 193

List of Tables

2.1 Geographic origin, habitat and level of infection of three nematodes of 97 *Xenopus laevis* (Daudin) from 11 localities in South Africa. 12

3.1 Complete locality data and infection parameters, *sensu* Bush *et al.* (1997), of the seven nematode species reported for the first time from the African Clawed Frog *Xenopus laevis* from ten localities in South Africa. 30

4.1 Distribution and level of infection of the two parasites of *Xenopus laevis* from its invasive range in western France. 54

5.1 Bayesian R^2 values of the six generalised linear mixed models where infracommunity crowding and *Cephalochlamys namaquensis* and *Protopolystoma xenopodis* abundance in both the native and invasive range of *Xenopus laevis* were modelled in response to intrinsic and extrinsic factors. 77

6.1 Primers used for DNA amplification and sequencing of the *COX1* and *rrnS* genes of *Xenopus laevis* and *Protopolystoma xenopodis*. 90

7.1 Polyopisthocotylean species with available mitochondrial genomes. 109

7.2 Best partitioning scheme for the concatenated alignment of 14 mitochondrial genes from 14 monogenean flatworm species. 111

7.3 GC content and compositional asymmetry in the two newly assembled mitogenome sequences of *Protopolystoma xenopodis* and the re-annotated draft mitogenome of *Diplorchis hangzhouensis*. 113

7.4 Localisation of genes and non-coding regions in the mitochondrial genome of *Protopolystoma xenopodis*. 114

7.5 Proposed changes in gene position, length and start, stop and anticodons to the annotations in some of the polyopisthocotylean mitogenomes available on GenBank. 116

7.6 Codon frequency in the mitochondrial protein-coding genes of *Protopolystoma xenopodis*. 119

7.7 Comparison of the general features of all previously published complete polyopisthocotylean mitochondrial genomes with the newly annotated mitogenome sequences of *Protopolystoma xenopodis*. 125

A.1 Detailed information on collection localities from four continents where *Xenopus laevis* specimens were sampled for parasitological surveys. 186

Table of abbreviations

aa	Amino acid
ATP6	Gene for ATP synthase F0 subunit 6
bp	Nucleotide base pair(s)
COX1–3	Genes for subunits I–III of cytochrome *c* oxidase
cytb	Gene for cytochrome *b*
F	Empirical base frequencies
G	Discrete Gamma model (Yang, 1994)
GTR	General time-reversible DNA model of evolution (Tavaré, 1986)
HKY	Hasegawa-Kishino-Yano DNA model of evolution (Hasegawa *et al.*, 1985)
I	Allowing for a proportion of invariant sites (Gu *et al.*, 1995)
ITS	Internal transcribed spacer gene region
mitogenome	Mitochondrial genome
***NAD1–6*; NAD4L**	Genes for subunits 1–6 and 4L of NADH dehydrogenase
NGS	Next-generation sequencing
PCR	Polymerase chain reaction
R	FreeRate model (Soubrier *et al.*, 2012)
rRNA	Ribosomal RNA
rrnL*; *rrnS	Genes for the large (16S) and small (12S) subunits of ribosomal RNA
SD	Standard deviation
TIM	Transitional DNA model of evolution (Posada, 2003)
tRNA	Transfer RNA
trnX	Genes encoding for transfer RNA molecules with corresponding amino acids denoted by the one-letter code
TPM	3-parameter DNA model of evolution (Kimura, 1981)

Chapter 1

Introduction to *Xenopus laevis*, a parasite taxi amidst global change

1.1 Biological invasions, a sign of the times

The year 2020 has been a lesson in the damage that can be wrought by the rampant spread of organisms (Morens *et al.*, 2020). In deeply personal yet universal ways, we were all confronted by the fact that we will increasingly live in a world characterised by the movement of species and their associated parasites and pathogens (Chinchio *et al.*, 2020). Indeed, this reality of sweeping, human-mediated biological invasions that are profoundly changing the world is one of the hallmarks of the Anthropocene (Bar-On *et al.*, 2018; Blackburn *et al.*, 2019; Capinha *et al.*, 2015; Ellis *et al.*, 2012; Ricciardi, 2007).

Biological invasion is the displacement of organisms to areas beyond their natural ranges where new populations establish and fan out (Blackburn *et al.*, 2011). Although the impacts of invasion events are not necessarily always negative, it is generally agreed upon that invaders have the potential to transform their non-native habitats in subtle, yet far-reaching ways (Simberloff, 2011). It is especially the spread of highly competitive and generalist invasive species that drive declines in biodiversity in their new environments (Bellard *et al.*, 2016; Ricciardi, 2007). Case in point, the lasting scar of invaders is felt in their role in bringing about a third of species extinctions since the sixteenth century (Blackburn *et al.*, 2019).

1.2 Parasites, the clandestine passengers of range expansion

Where free-living species go, their parasites follow. For every one successful biological invader, there are an estimated three co-introduced parasites (Torchin *et al.*, 2003). Like their hosts, alien parasites have the potential to alter their novel habitats, even if they might not be one of the major drivers of their host's invasion success (Blackburn & Ewen, 2017). Indirectly, the subtle shift in species interactions brought about by biological invaders and exacerbated by their associated parasites can lead to dramatic ecosystem-wide changes (Amundsen *et al.*, 2013; Dunn *et al.*, 2012; Roy & Lawson Handley, 2012). More pointedly, the movement of symbionts along with their hosts to new geographic ranges puts human and animal wellbeing at peril through the emergence of novel interactions (Chinchio *et al.*, 2020; Daszak, 2000).

Yet, the pervasive repercussions of parasites in invasions are not validated by an equal share of research on the alteration of parasite dynamics during host range expansion (Blackburn & Ewen, 2017). Because of this, our understanding of the nature of potential novel host-parasite interactions and the overall transformation of the intricate dynamics that arise because of biological invasions remains limited.

1.3 Model host-parasite systems needed in invasion biology

Biological invasions, although often devastating in their effects, provide the unique opportunity to test hypotheses in ecology and evolution as a result of their large scale, geographically repeated ecosystem manipulation (Blackburn, 2008; Morand *et al.*, 2015; Richardson *et al.*, 2011a). The scientific world has much to gain from studying the disruptions of ancient interactions and the formation of novel associations that characterise the range expansions of species, especially in the preparation of our response to looming global change. Yet, as with any other natural process, there are many unknowns regarding the patterns underpinning invasions (Crystal-Ornelas & Lockwood, 2020), even more so when we take the added complication of co-introduced parasites into account (Blackburn & Ewen, 2017). This paucity of knowledge may hamper our ability to study the factors that shape the newfangled dynamics of invasive host-parasite systems.

The use of well-studied model systems can be invaluable to explore hypotheses and discern patterns in invasion biology, precisely because there are fewer unknowns to grapple with (Gundale *et al.*, 2014). According to Gundale *et al.* (2014), such a model system will be most valuable if it possesses three features. Firstly, the introduction of this species to a wide range of different localities should be well-documented. Secondly, the growth form of the species should be easily noticeable and evaluable. Thirdly, knowledge on the propagule pressure, genetic composition and biotic and abiotic factors at play in

the introduced ranges will be a plus. In the context of the neglected study of host-parasite relationships during invasions, a fourth criterion can be added. A broad knowledge of the associated parasites of the species in both its native and invasive ranges will greatly help invasion biologists along their way in incorporating symbionts in their studies.

1.4 A globally invasive frog and its parasites as model

In light of this, the globally invasive amphibian *Xenopus laevis* (Daudin, 1802) (Anura: Pipidae) and its associated parasite assemblage is an inviting candidate to explore the behaviour of host-parasite systems during invasions.

This host species is no stranger to being a model research animal (Gurdon & Hopwood, 2000). In fact, this is the very reason for its prolific spread from its native southern Africa to its current near-worldwide distribution (Measey *et al.*, 2012). Its range expansion was initiated in the 1930s due to its use as a pregnancy assay (Shapiro & Zwarenstein, 1934). Because of its hardy nature and ease of maintenance, it was readily adopted as a vertebrate model animal in research, especially in developmental biology (Gurdon & Hopwood, 2000). Nowadays, the pet trade seems to be the biggest culprit in the spread of *X. laevis* (e.g. Wang *et al.*, 2019).

As things stand, *X. laevis* boasts with invasive populations on four continents outside Africa that represent multiple independent invasion pathways and reasonably well-studied introductions (reviewed in Measey *et al.*, 2012). Some invasive populations, such as those in the United Kingdom, have since collapsed (Tinsley *et al.*, 2015). Others have been successfully eradicated (Measey *et al.*, 2012). Yet others represent established feral populations with limited dispersal capacity (Hill *et al.*, 2017; Measey *et al.*, 2012). However, the vast majority of these invasive populations are dispersing at rapid rates into unrealised niche space that will only be made more accessible due to climate change (Ihlow *et al.*, 2016; Measey *et al.*, 2012; Rödder *et al.*, 2017; Vimercati *et al.*, 2020).

Within its native range in southern Africa, the genetic divergence of *X. laevis* has drawn the attention of a number of investigators (du Preez *et al.*, 2009; Furman *et al.*, 2015; Grohovaz *et al.*, 1996; Measey & Channing, 2003; Measey, 2004). Building upon this knowledge of the genetic composition of the native populations of *X. laevis*, investigators have been able to establish the approximate geographical origin of several *X. laevis* populations in the invasive range (de Busschere *et al.*, 2016; Lillo *et al.*, 2013; Lobos *et al.*, 2014). As a consequence, the genetic composition of a number of these invasive populations has also been brought to light.

There exist detailed records of the official export routes of *X. laevis* (van Sittert & Measey, 2016; Weldon *et al.*, 2007). In addition to hundreds of consignments from the Cape Town

area and surrounds to the global market, the domestic market constituted the bulk of the historical trade in *X. laevis* (van Sittert & Measey, 2016; Weldon *et al.*, 2007). These widespread human-mediated translocations of *X. laevis* in its native range joins natural overland and aquatic dispersal networks to earn *X. laevis* a reputation as domestic exotic (de Villiers & Measey, 2017; Measey, 2004, 2016; Measey *et al.*, 2012).

All in all, *X. laevis* is arguably the world's most widely distributed and well-studied amphibian (Measey *et al.*, 2012; van Sittert & Measey, 2016). As illustrated above, many aspects of its invasive history are broadly known. Moreover, what makes this invader even more valuable for the study of parasite dynamics during invasion is its extraordinarily rich and extensively investigated parasite fauna, with more than 25 associated parasitic genera in the native range (see parasite surveys in Cosgrove & Jared, 1974; Macnae *et al.*, 1973; Pritchard, 1964; Southwell & Kirshner, 1937; Thurston, 1970; Tinsley, 1996; Vercammen-Grandjean, 1960). There is even a number of parasite records and surveys from invasive populations of *X. laevis* (Castillo *et al.*, 2017; Jackson & Tinsley, 2001a; Kuperman *et al.*, 2004; Lafferty & Page, 1997; Rodrigues, 2014; Tinsley & Jackson, 1998b). These surveys have demonstrated that *X. laevis* and its symbionts are inseparable when it comes to range expansion. Therefore, it becomes clear that in *X. laevis* and its parasites, we have at our disposal an intimately associated and widely distributed host-parasite system that holds great promise to inform general trends in invasion biology.

1.5 Aim: Application of the frog-parasite model to issues in invasion biology

Consequently, this study exemplifies a multidisciplinary approach to test the value of a globally distributed host-parasite system in addressing long-standing questions in "invasion parasitology" – that under-explored subfield of invasion ecology which concerns itself with the most widespread lifestyle among non-native species (Blackburn & Ewen, 2017).

1.5.1 Objective 1: The use of integrative taxonomy to strengthen knowledge on native parasite associations

In their review of *X. laevis*' ongoing worldwide invasion, Measey *et al.* (2012) cautioned that "comparatively few reports exist of *X. laevis* in its natural habitat, and we continue to be ignorant of the native ecology and natural dispersal of this globally invasive species". Naturally, this gap in our knowledge is to the detriment of the management of *X. laevis* in its invasive range. As an addition to that statement, a parasitologist would argue that this ignorance includes several aspects of its native parasite ecology, the most notable being robust species identifications that is based upon both morphological and molecular data.

The development of novel techniques in advanced microscopy and DNA barcoding has paved the way for an integrative approach to taxonomy (Schlick-Steiner *et al.*, 2010). From the perspective of invasion biology, the correct classification of species lays the groundwork for future bio-invasion research and should therefore not be neglected (Mazzamuto *et al.*, 2016).

In the current study, the first two chapters (2 and 3) are devoted to a pluralistic approach to the taxonomy of both previously documented and hitherto undocumented parasite species of *X. laevis* in its native range. Here, the focus of the investigation is the Nematoda, the second most speciose taxon among the parasites of *X. laevis* (reviewed in Tinsley, 1996). As part of this endeavour, the available information of three species of Camallanidae from *X. laevis* across South Africa is augmented in terms of infection levels, locality information, amended morphological descriptions and molecular data (Chapter 2, hereafter referred to as Svitin *et al.*, 2018).

Parasitological surveys of *X. laevis* in the invasive range have pointed out that novel parasite associations within the invasive range are most likely to occur with nematode larvae from the native parasite assemblage of the novel environments (Castillo *et al.*, 2017; Kuperman *et al.*, 2004). In the native range, there are reports of interactions between *X. laevis* and unidentified nematodes (Brayton, 1992; Cosgrove & Jared, 1974; Thurston, 1970), which suggests the possibility of *X. laevis* playing a role in parasite cycling as a paratenic or intermediate host. To this end, seven nematode species parasitising this host in South Africa that have not been documented before are reported, an astounding number of neglected parasite associations for such a well-studied host-parasite system (Chapter 3, hereafter referred to as Schoeman *et al.*, 2020). In the spirit of the multisource approach of integrative taxonomy, short morphological descriptions are provided based upon advanced microscopy, as well as molecular data and distribution information. Furthermore, possible avenues of parasite transmission are explored, based upon a survey of the literature, to elucidate the role of native *X. laevis* in parasite cycling in its native range.

1.5.2 Objective 2: Parasite infra- and component community analyses to compare parasite dynamics in the native and invasive range

The great strength of comparative biogeography in the light of biological invasions is the existence of independent geographical replicates of the same system (Blackburn, 2008). Nonetheless, the ramifications of single invasive species are rarely documented across multiple ecosystems (Crystal-Ornelas & Lockwood, 2020) and this is even more true for bio-invasion investigations that involve parasites (Blackburn & Ewen, 2017). For example, comparatively few studies have investigated the Enemy Release Hypothesis (ERH) across the many geographical replicates of globally distributed animals, with exceptions the studies on the European house sparrow and the European green crab (Marzal *et al.*, 2011;

Torchin *et al.*, 2001).

In the present study, a geographically representative data set of *X. laevis* parasitological surveys was available that could be used to identify unifying mechanisms within this host-parasite system. These included previously conducted surveys in Chile, Portugal and the United States (Castillo *et al.*, 2017; Kuperman *et al.*, 2004; Rodrigues, 2014), in conjunction with the surveys conducted for this project in western France and southern Africa. This places the *X. laevis* host-parasite system in a unique position to inform a global perspective on the fate of associated parasites during the process of invasion. Furthermore, an understanding of the spatial component of parasite dynamics during range expansion will afford predictions of the reactions of host-parasite systems to global change (Poulin, 2007).

In the first instance, the applicability of this model is demonstrated on a test of the ERH, the first conducted for a globally invasive amphibian with several geographic replicates (Chapter 4, hereafter referred to as Schoeman *et al.*, 2019). Utilising this novel model system, a comparison is made between the native and invasive parasite assemblages of *X. laevis* in terms of species richness, infection levels and community composition.

Secondly, the drivers of parasitism in the parasite infracommunities of *X. laevis* in the native and invasive range are investigated, with a specific focus on the effects of range expansion (Chapter 5). Thus, this investigation attempted to uncover general responses to range expansion in the parasites associated with a globally invasive amphibian by investigating the factors that determine the make-up of its parasite assemblages in both its native and invasive range.

1.5.3 Objective 3: Comparative phylogeography as a more holistic approach to tracing invasions

When incorporating parasite data sets in bio-invasion research, we are not only interested in the role of parasites in the process of invasion or the novel interactions that may arise. On a more fundamental level, data from parasites provide an independent line of evidence that can corroborate or expound upon evidence provided by the host data set.

This is the basis of the idea of the ”holistic specimen”, where hosts are sampled along with their symbionts for multidisciplinary approaches to questions in biology (Cook *et al.*, 2017). A more holistic approach to solving the origin and range shifts of hard-to-trace invasive species may involve molecular data from co-introduced parasites (Clavero *et al.*, 2016). Monogenean parasites have been suggested and occasionally used as tags for introductions and other forms of host movement (Baldwin *et al.*, 2012; Hahn *et al.*, 2015; Huyse *et al.*, 2017; Kmentová *et al.*, 2018, 2020). Using the *X. laevis* host-parasite model

once again, the performance of this integrative approach in the detection of intraspecific cryptic invasions in the native range was assessed (Chapter 6). Specifically, orthologous mitochondrial markers were employed for the host and the parasite phylogeographic analyses to demonstrate how equal sampling effort for both data sets can provide different insights.

The choice of markers for co-phylogeographic studies such as these is very important, as sufficient resolution must be provided to discern among parasite lineages at the intraspecific level. The mitochondrial markers *COX1* and *rrnS* are the only two available markers for which primers have been developed for polyopisthocotylean Monogenea (Héritier *et al.*, 2015; Littlewood *et al.*, 1997). Yet, the interspecific comparison of the mitochondrial genomes of diplozoid, gyrodactylid and dactylogyrid monogeneans have indicated that other genes might be more suitable for species identification or even population-level studies within these families (Huyse *et al.*, 2008; Vanhove *et al.*, 2018; Zhang *et al.*, 2018b). The rise of mitochondrial genomics has provided invasion biologists with the tools to incorporate more sophisticated molecular data into their investigations. As a closing addition to this study, the mitogenome of *Protopolystoma xenopodis* (Price, 1943) Bychowsky, 1957 (Monogenea: Polystomatidae), one of the most highly associated parasites of *X. laevis*, both in the native range and beyond, is assembled (Chapter 7). This mitogenome serves as a reference for future investigators of the globally co-invasive parasite family Polystomatidae who might want to incorporate molecular markers with higher discriminating power in their studies.

1.6 Methodological considerations

The project features the largest data set of its kind from more than 350 frogs and 45 localities (refer to Appendix A for full locality data) – a statistically, geographically and taxonomically representative survey that was lacking in previous investigations of this host-parasite system.

1.6.1 Parasitological surveys

In the context of the shortcomings of the previous parasitological surveys of *X. laevis*, this study was conceptualised with some qualifications in mind. Firstly, only the parasites of southern African *X. laevis sensu stricto*, according to the classification of Furman *et al.* (2015), were investigated. Secondly, data from sampling localities were only pooled in cases where the frogs were captured within the same aquatic system. For example, frogs collected on the same property from farm dams and connecting irrigation channels or natural rivers were seen as members of the same population. The intention was to keep

data as locality-specific as possible in order to compare the parasite community indices of independent populations of *X. laevis*, unlike previous studies where all the sampled hosts were regarded as a unit (e.g. Cosgrove & Jared, 1974; Macnae *et al.*, 1973; Pritchard, 1964; Southwell & Kirshner, 1937; Thurston, 1970; Tinsley, 1996; Vercammen-Grandjean, 1960). Finally, parasites were mainly fixed in molecular grade ethanol to facilitate later molecular analyses, because very few previous studies on the parasites of *Xenopus* provide genetic information. Thus, at least the first recovered representative of each parasite species from every locality was placed in ethanol.

1.6.2 Ethical considerations

Animal welfare should be a chief concern during the planning and execution of any project in zoology. The postgraduate students of the African Amphibian Conservation Research Group have permission to investigate the parasites of southern African amphibians at large from the AnimCare research ethics committee at the North-West University (NWU-00006-14-A3). The committee further approved the execution of this specific study on *X. laevis* and its parasites, allowing the capture and euthanasia of ten specimens per collection locality in southern Africa (NWU-0380-16-A5-01). Permits for the collection of these frogs were obtained from the various provincial governments (0056-AAA007-00224: CapeNature; FAUNA 1343-2017: Northern Cape) and all sampling activities took place with the written consent of the landowners. Upon collection, the frogs were kept in water from the source, replaced by borehole water on a weekly basis in accordance with the standard operating procedure for the restraint of frogs (AACRG-SOP-03). Subsequent anaesthesia with tricaine-3-methanosulphonate, commonly known as MS222 (Sigma-Aldrich Co., Steinheim, Germany), followed by cutting the spine and destroying the brain prior to dissection, was done in accordance with the standard operating procedure for the euthanasia of amphibians (NWU-00492-16-A5). Finally, frog carcasses were disposed of by the University's medical waste removal contractors.

1.6.3 Sampling design

In view of the divergence of *X. laevis* in its native range (Furman *et al.*, 2015), care was taken to include representative populations of all the previously defined phylogeographic lineages of *X. laevis* in southern Africa in the sampling effort of this study.

Another consideration during the sampling design was the number of individuals necessary to obtain statistically meaningful parasite community indices. Logistical and ethical constraints lead us to limit the number of individuals sampled per locality to ten. In some cases, sample size was even lower due to low capture success.

Chapter 2

New information on morphology and molecular data of camallanid nematodes parasitising *Xenopus laevis* (Anura: Pipidae) in South Africa

2.1 Introduction

Over 25 parasite genera from seven invertebrate groups have been reported to be associated with the African Clawed Frog *Xenopus laevis* (Daudin, 1802) (Anura: Pipidae) in its native southern African range (Tinsley, 1996). Some of these parasites have followed their invasive hosts out of Africa to North America, as well as to Europe (Kuperman *et al.*, 2004; Lafferty & Page, 1997). One group of parasites that, to date, has not been reported from feral populations of *X. laevis* is the nematodes of the family Camallanidae that primarily parasitise marine and freshwater fish and less often amphibians, turtles and snakes (Stromberg & Crites, 1974).

In clawed frogs across the southern African subcontinent, representatives of camallanids are widespread – in Kenya, Nigeria, Rwanda, Uganda and Zimbabwe (Avery, 1971; Thurston, 1970; Tinsley *et al.*, 1979). Specifically, three species of camallanids are associated with *X. laevis* in South Africa: *Camallanus kaapstaadi* Southwell *et* Kirshner, 1937, *Camallanus xenopodis* Jackson *et* Tinsley, 1995 and *Batrachocamallanus slomei* (Southwell *et* Kirshner, 1937).

Camallanus kaapstaadi was described from *X. laevis* from Cape Town (South Africa) (Southwell & Kirshner, 1937). Subsequently, it was identified from clawed frogs (*X. laevis* and other *Xenopus* spp.) from Cameroon, Ghana, Kenya, Nigeria, Rwanda, northern and southeastern parts of South Africa (previously known as Transvaal and Transkei), Sudan, Tanzania, Togo, Uganda and Zimbabwe (Avery, 1971; Jackson & Tinsley, 1995a). Furthermore, the junior synonym of *C. kaapstaadi*, *Camallanus johni* Yeh, 1960, was described from Tanzania (Yeh, 1960b) and later also reported from Zimbabwe, Uganda and Nigeria under this name (Thurston, 1970). In the meantime, Tinsley *et al.* (1979) recorded the presence of a species of *Camallanus* Railliet *et* Henry, 1915 in *X. wittei* Tinsley, Kobel *et* Fischberg from central Africa, which was later identified as *C. kaapstaadi* (Jackson & Tinsley, 1995a). Therefore, *C. kaapstaadi* can be regarded as a widespread parasite of clawed frogs across Africa.

The second camallanid from *X. laevis*, *C. xenopodis*, was described based only on six female specimens from the Cape (South Africa) and one female specimen which was recovered in Kenya from *X. borealis* Parker (Jackson & Tinsley, 1995a). Neither of these species has been recorded since.

The third species, *B. slomei*, was also described as *Procamallanus slomei* Southwell *et* Kirshner, 1937 from *X. laevis* from the Cape (South Africa) (Southwell & Kirshner, 1937) and was formally recorded for the first time since its original description as *B. slomei* from clawed frog hosts in South Africa and Zaire (Jackson & Tinsley, 1995b). Jackson & Tinsley (1995b) also synonymised *Procamallanus brevis* Kung, 1948 from *X. laevis* in South Africa (Kung, 1948) with *B. slomei* and reidentified a *Spirocamallanus xenopodis* Southwell *et* Kirshner, 1937 in a clawed frog from Kenya (Thurston, 1970) as belonging to the same species.

The redescription of *B. slomei* as a member of the genus *Batrachocamallanus* Jackson *et* Tinsley, 1995 is not without controversy (Jackson & Tinsley, 1995b). The genus *Batrachocamallanus* was erected specifically for the four species of *Procamallanus* Baylis, 1923 parasitising African amphibians, based upon the large number of mucrons (more than five) on the female tail, relatively smaller body size and the almost identical cephalic morphology, male caudal structures and female reproductive system that differentiate the amphibian parasites from all other species of *Procamallanus* (see Jackson & Tinsley, 1995b).

Moravec *et al.* (2006) considered differences in female mucron number and affinity to an amphibian host as not sufficient generic characters and advocated for the reduction of *Batrachocamallanus* to a junior synonym of *Procamallanus*. This decision was based on the description of *Procamallanus pacificus* Moravec, Justine, Würtz, Taraschewski *et* Sasal, 2006 from Pacific eels (*Anguilla* sp.) (Actinopterygii: Anguillidae) bearing four to nine mucrons on the female tail (Moravec *et al.*, 2006) and the discovery of *B. siluranae* Jackson

et Tinsley, 1995, previously described from *Xenopus tropicalis* Gray (Anura: Pipidae), from the polypteroid fish *Erpetoichthys calabaricus* Smith (Actynopterigii: Polypteridae) (Řehulková *et al.*, 2005). However, only one immature female specimen of *B. siluranae* was recovered from the polypteroid fish, which was a specimen imported for the pet trade, leading the authors to believe this to be an accidental infection (Řehulková *et al.*, 2005). Moreover, the small processes on the tail of female *P. pacificus* are 6 μm to 9 μm long whereas the mucrons of *Batrachocamallanus* spp. vary from 10 μm to 15 μm (Jackson & Tinsley, 1995b; Moravec *et al.*, 2006). Therefore, the mucrons of *P. pacificus* might not represent the same structures as in *Batrachocamallanus* and probably cannot be used for suppression of the genus. Taken as a whole, these factors cast doubt on the validity of the suppression of *Batrachocamallanus*, leading us to assign our specimens to *B. slomei*.

It is clear that information on the camallanids from *X. laevis* are in need of augmentation, especially on the molecular front. The present studies of three species of camallanids collected from *X. laevis* in different regions of South Africa add information on the infection level, localities, morphology and molecular data of the *28S rRNA* and *COX1* genes.

2.2 Methods

In total, 97 *X. laevis* were collected in chicken liver baited funnel traps from eight localities across the northern regions of South Africa during November of 2016 and March to May of 2017 and from three localities in the southwestern regions during June and July of 2017 (Table 2.1).

The hosts were anaesthetised in 6% ethyl-3-aminobenzoate methanesulfonate (MS222) (Sigma-Aldrich Co., Steinheim, Germany) and subsequently euthanised through severing the spine and destroying the brain, according to internationally accepted standard operating procedures. During the total dissection, the alimentary canal was removed and opened in 0.6% amphibian saline. After removal from the oesophagus, stomach and intestine, nematodes were washed in saline, fixed in 70% hot ethanol and subsequently stored in 70% ethanol.

Prior to microscopic examination, the nematodes were cleared in lactophenol. The morphology of the nematodes was studied and photomicrographs were taken using the Nikon E800 and Nikon ECLIPSE Ni compound microscopes. Apical and transverse sections were prepared manually. In total, 601 specimens of *B. slomei*, 39 of *C. kaapstaadi* and 53 of *C. xenopodis* were studied of which 50 (20 males and 30 females), 18 (nine males and nine females) and 28 (four males and 24 females), respectively, were measured. All measurements in the text are given in micrometres, unless otherwise indicated and presented as ranges followed by mean values in parentheses. The representative sample (30 specimens) is expressed as mean with standard deviation.

Table 2.1: Geographic origin, habitat and level of infection of three nematodes of 97 *Xenopus laevis* (Daudin) from 11 localities in South Africa. Mean intensity of infection is given with median intensity in square brackets and minimum and maximum values in parentheses. Fields with 'n/a' refer to absent infection level values due to absence of nematodes in the digestive tract.

Nematode	Localities	Coordinates	Habitat	Number of hosts	Intensity	Prevalence	Mean abundance
Batrachocamallanus slomei Southwell *et* Kirshner, 1937	Imvubu Lodge, KwaZulu Natal	28°47'34"S; 26°03'02"E	Vegetated pond	15	1	7%	0.1
	Potchefstroom, North-West	26°45'20"S; 27°03'38"E	Shallow vlei (marshland)	9	14 [10] (1–37)	100%	13.7
	Modimolle, Limpopo	24°26'18"S; 28°26'13"E	Ornamental garden pond	6	18 [14] (2–45)	83%	15.2
	Jacana Estate, White River, Mpumalanga	25°20'21"S; 31°01'21"E	Dam in vlei (marshland)	8	9 [8] (4–16)	63%	5.6
	Tasselberry, White River, Mpumalanga	25°19'55"S; 31°02'36"E	Ornamental garden pond	6	24 [26] (9–37)	100%	24.3
	Dullstroom, Mpumalanga	25°23'53"S; 30°02'17"E	Dam in mountain stream	10	13 [12] (1–30)	100%	13.0
	Letsitele, Limpopo	23°47'56"S; 30°11'42"E	Vegetated pond	10	6 [5] (2–12)	100%	5.5
	Hermanus, Western Cape	34°22'13"S; 19°15'25"E	Vegetated pond	7	3 [2] (1–6)	57%	1.6
Camallanus kaapstaadi Southwell *et* Kirshner, 1937	Dullstroom, Mpumalanga	25°23'53"S; 30°02'17"E	Dam in mountain stream	10	4 [4] (1–8)	80%	3.4
	Site A, Cape Town, Western Cape	33°50'21"S; 18°36'01"E	Urban recreational pond	5	2 [2] (1–2)	60%	1.0
Camallanus xenopodis Jackson *et* Tinsley, 1995	Dullstroom, Mpumalanga	25°23'53"S; 30°02'17"E	Dam in mountain stream	10	6 [6] (1–13)	90%	5.3
No camallanids present	Site B, Cape Town, Western Cape	33°50'08"S; 18°33'10"E	Urban recreational pond	14	n/a	n/a	n/a
	Rondepan, Limpopo	23°46'10"S; 29°24'17"E	Dam in inundated grass	7	n/a	n/a	n/a

For the molecular studies, the middle fragments of males were used while taxonomically important anterior and posterior parts were reserved for the morphological identification of species. DNA was extracted using the KAPA Express Extraction Kit DKAPKK7103 (Sigma-Aldrich Co., Steinheim, Germany). *COX1* amplicons were obtained using the primer pair 'LCO1490' (5'-GGTCAACAAATCATAAAGATATTGG-3') and 'HCO2198' (5'-TAAACTTC-AGGGTGACCAAAAAATCA-3'). The thermocycling profile was: 3 min denaturation at 94°C, 10 cycles of 94°C for 30 s, 45°C for 30 s, 72°C for 1 min and 40 cycles of 94°C for 30 s, 51°C for 1 min, 72°C for 1 min for amplification and 72°C for 10 min for extension.

The *28S* amplicons were amplified using forward primer 'LSU5' (5'-TAGGTCGACCCGC-TGAAYTTAAGCA-3') and reverse primer 'n900r' (5'-GGTTCGATTAGTCTTTCGCC-3'). The thermocycling profile was as follows: 5 min denaturation at 95°C; 40 cycles of 30 s at 95°C, 30 s at 55°C, 2 min at 72°C for amplification; and a final 7 min extension at 72°C. Sequences were obtained using BigDye® Terminator v3.1 Cycle Sequencing on an ABI3500XL sequencer. DNA products were sequenced in both directions using the pairs of PCR primers; for the nuclear gene the following additional primers were used: internal primers, '300F' (5'-CAAGTACCGTGAGGGAAAGTTG-3') and 'ECD2' (5'-

CTTGGTCCGTGTTTCAAGACGGG-3'). Contiguous sequences were assembled, edited using Geneious 9.0 software (Biomatters Ltd., Auckand, New Zealand) and submitted to GenBank.

For the phylogenetic analysis, Bayesian inference in the MrBayes programme *version* 3.2.2 was used. Prior to analysis, sequences were aligned using the ClustalW tool in Mega *version* 7 software and trimmed to the shortest sequence (497 nucleotides of *28S* and 312 nucleotides of *COX1* genes). The Bayesian analyses were run with the following nucleotide substitution model settings: `nst = 6`, `rates = invgamma`, `ncat = 4`, `shape = estimate`, `inferrates = yes` and `basefreq = empirical`, that correspond to a general time reversible model GTR+G+I (Gu *et al.*, 1995; Tavaré, 1986; Yang, 1994). The nucleotide substitution model was determined using JModelTest *version* 2.1.7 software. Further analysis was provided using the following parameters: `mcmc ngen = 200000` for *28S* alignments and `ngen = 100000` for *COX1* alignments, `samplefreq = 100`, `printfreq = 100` and `diagnfreq = 1000`. Trees were visualised using the FigTree *version* 1.4.3 software (Rambaut, 2018).

2.3 Results

2.3.1 Morphological descriptions

***Batrachocamallanus slomei* (Southwell *et* Kirshner, 1937)**

Host: *Xenopus laevis* (Daudin) (Amphibia: Anura: Pipidae).

Localities: KwaZulu Natal, Mpumalanga, Limpopo, North-West, Western Cape (see Table 2.1).

Site of infection: Stomach, oesophagus.

Representative DNA sequences: MG948463 (*COX1*), MG947390 (*28S*).

Figure 2.1

General description. Body small, usually coiled ventrally, comparatively thick, with maximum width at level of anterior third. Cuticle with prominent transverse striations. Apical (Figure 2.1b): oral opening rounded, surrounded by six flat elevations (two larger lateral and four submedian); six labial papillae; four cephalic papillae; two amphids. Buccal capsule with well sclerotised walls, somewhat longer than wide with conspicuous basal ring and without internal ridges (Figure 2.1a,c). Muscular oesophagus opening surrounded with three tooth-like projections of basal ring (Figure 2.1c). Muscular oesophagus club-shaped with elongated posterior bulb. Glandular oesophagus somewhat longer than muscular

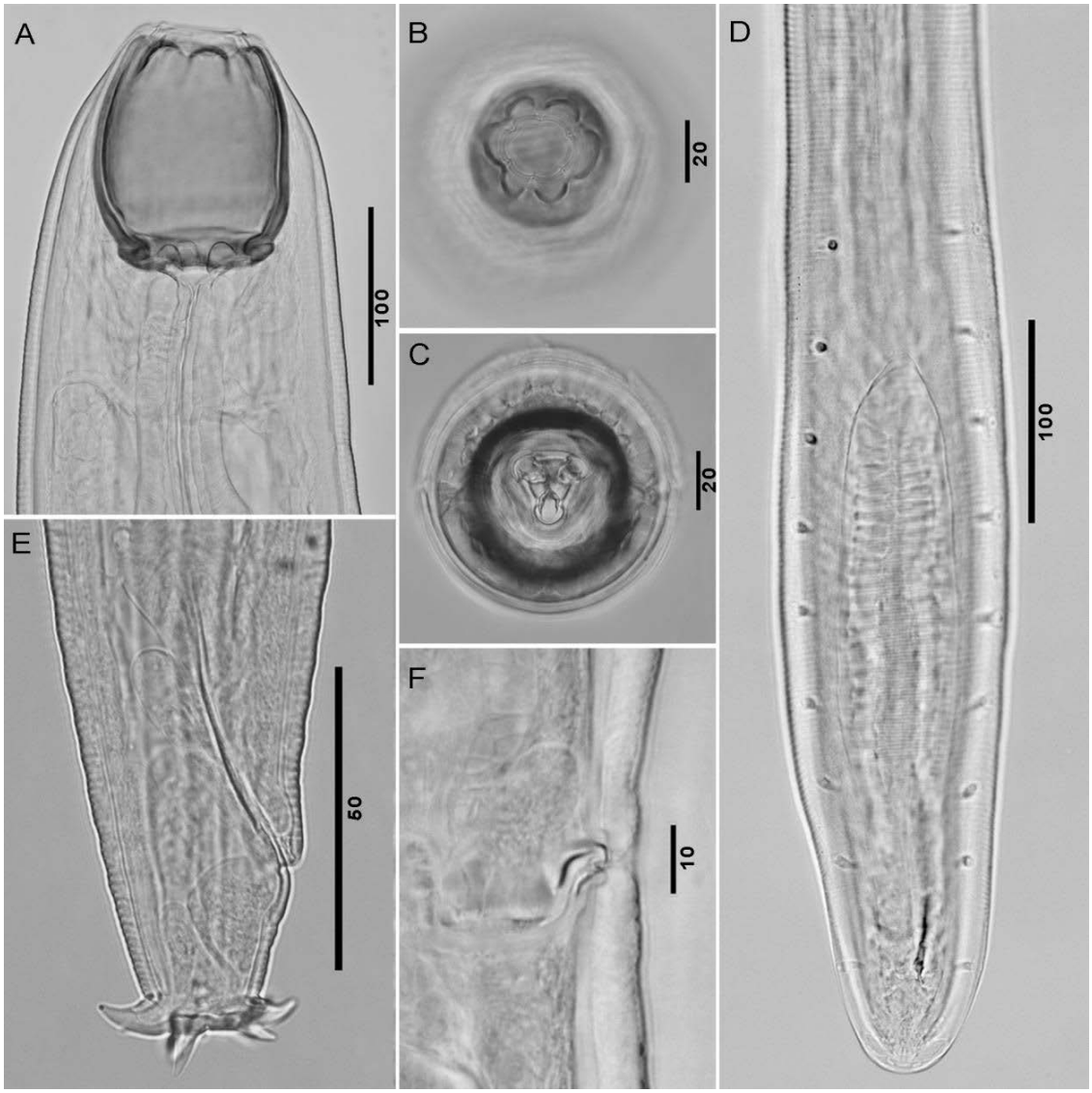

Figure 2.1: *Batrachocamallanus slomei* Southwell *et* Kirshner, 1937 from *Xenopus laevis* (Daudin), photomicrographs. **a** – anterior end, female, lateral view; **b** – anterior end, male, apical view; **c** – anterior end, male, optical section at base of buccal capsule level; **d** – caudal end, male, ventral view; **e** – posterior end, female, lateral view; **f** – part of female genital system at vulva level, lateral view.

oesophagus, almost cylindrical but slightly widened posteriorly. Nerve ring encircling muscular oesophagus at level of its proximal third. Excretory pore opening at level of muscular oesophageal mid-length. Minute papilliform deirids situated at level of excretory pore. Intestine straight, narrow. Rectum straight, with thin walls (Figure 2.1e). Tail tapering with numerous mucrons in females (Figure 2.1e) and rounded tip in males (Figure 2.1d).

Male (morphometry based on 20 specimens). Body 1.94–2.80 mm (2.32 mm) long, 96–157 (120) maximum width. Buccal capsule 93–112 (102) long, including basal ring 7–14 (11) long, 53–75 (61) wide with maximum width 67–94 (76) at mid-length and minimum width 26–53 (35) at anterior extremity. Minimum and maximum thickness of buccal capsule walls close to oral opening 2–4 (2.5) and to basal ring 4–10 (6). Muscular oesophagus

188–282 (235) long, 9–12% (10%) of body length; 33–56 (43), 33–43 (38) and 60–97 (75) wide at anterior, mid-length and bulb level, respectively. Glandular oesophagus 208–366 (301) long, 10–15% (13%) of body length; 46–81 (58), 32–68 (52) and 32–88 (65) wide at anterior, mid-length and posterior level, respectively. Nerve ring at 153–200 (177) from anterior extremity. Excretory pore and deirids situated at 127–280 (217), 6–11% (9%) of body length and 213–260 (238), 9–12% (10%) of body length from anterior extremity, respectively. Posterior end coiled ventrally, provided with well-developed vesicular caudal alae supported by pedunculate papillae near mid-length. Posterior part of alae slightly elevated and joined on ventral surface forming pseudosucker. Tail conical with rounded tip, 37–50 (42) long. Caudal region possessing pedunculate papillae (Figure 2.1d): eight pairs of pre-cloacal; one pair of ad-cloacal and three pairs of post-cloacal. Three pairs of sessile papillae surrounding cloaca (one slightly anterior to and two somewhat posterior to). Spicules unequal, simple-shaped with sharply pointed distal ends. Right spicule clearly visible, 90–115 (101) long; left one less sclerotised, 15–37 (25) long. Gubernaculum absent.

Female (morphometry based on 30 specimens). Body 1.67–3.51 mm (2.87 mm $\pm$ 0.54) long, 163–284 (225 $\pm$ 39) maximum width. Buccal capsule 105–138 (122 $\pm$ 9) long, including basal ring 10–17 (14 $\pm$ 2) long, 63–90 (76 $\pm$ 7) wide; maximum width 86–113 (103 $\pm$ 6) at mid-length and minimum width 34–71 (48 $\pm$ 9) at anterior extremity. Minimum and maximum thickness of buccal capsule walls close to oral opening 2–6 (3 $\pm$ 1) and to basal ring 4–11 (8 $\pm$ 2). Muscular oesophagus 242–337 (288 $\pm$ 22) long, 8–17% (10% $\pm$ 2) of body length; 38–72 (51 $\pm$ 8), 40–60 (49 $\pm$ 5) and 68–116 (95 $\pm$ 12) wide at anterior, mid-length and bulb level, respectively. Glandular oesophagus 248–526 (369 $\pm$ 62) long, 9–18% (13% $\pm$ 2) of body length; 48–78 (65 $\pm$ 8), 38–76 (60 $\pm$ 9) and 57–108 (78 $\pm$ 15) wide at anterior, mid-length and posterior level, respectively. Nerve ring at 161–221 (206 $\pm$ 14) from anterior extremity. Excretory pore and deirids situated at 184–326 (246 $\pm$ 27), 7–13%, (9% $\pm$ 2) of body length, and 196–298 (242 $\pm$ 27), 6–11% (9% $\pm$ 1) of body length, from anterior extremity, respectively. Vulva (Figure 2.1f) situated near body mid-length at 1.13–1.94 mm (1.61 mm $\pm$ 0.27) from anterior extremity; 42–60% (54% $\pm$ 3) of body length. Tail 34–59 (48 $\pm$ 6) long with five to seven mucrons at its tip (Figure 2.1e).

***Camallanus kaapstaadi* Southwell *et* Kirshner, 1937**

Host: *Xenopus laevis* (Daudin) (Amphibia: Anura: Pipidae).

Localities: Mpumalanga, Western Cape (see Table 2.1).

Site of infection: Oesophagus, stomach.

Representative DNA sequences: MG948461 (*COX1*), MG947391 (*28S*).

Figure 2.2

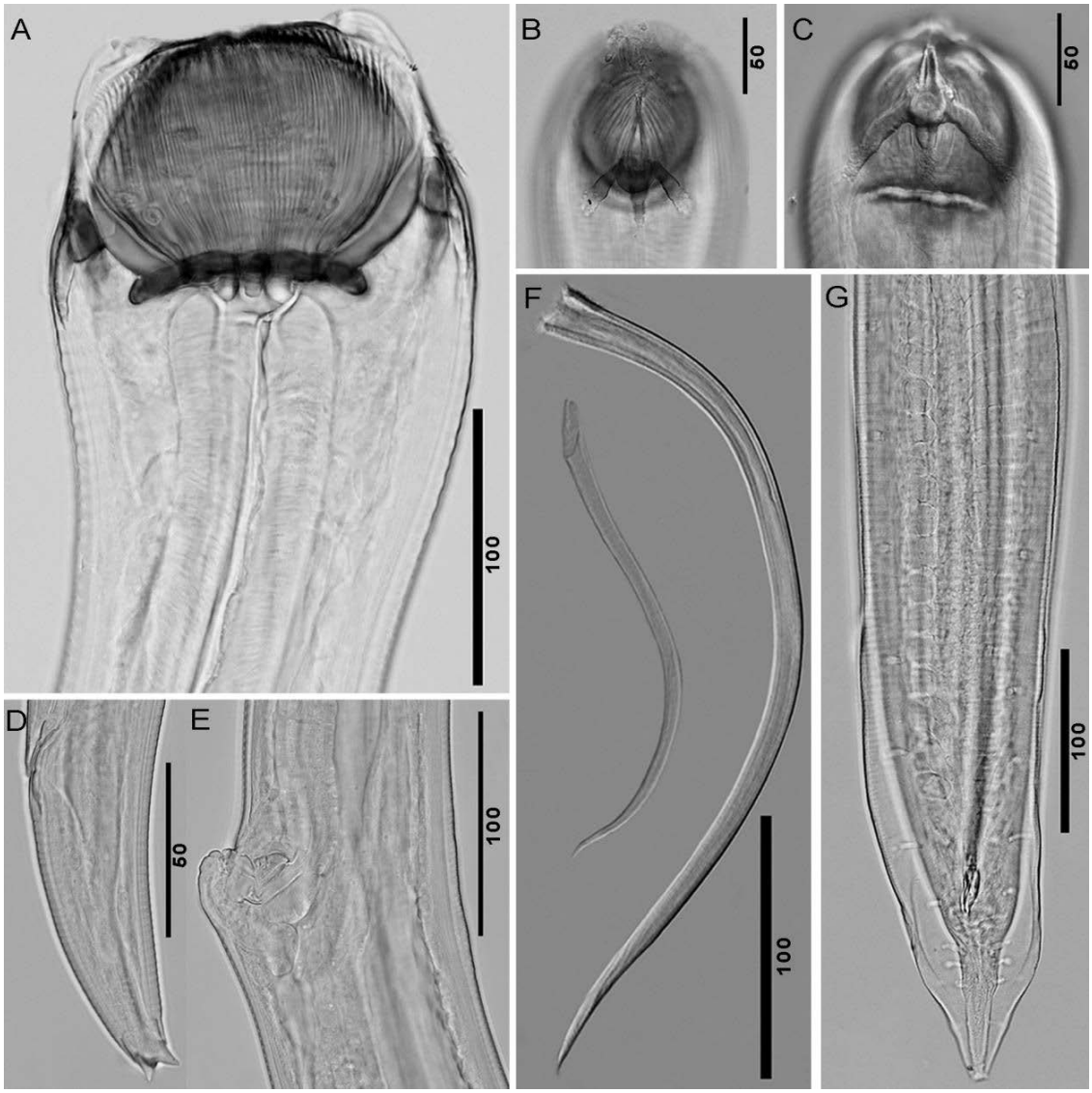

Figure 2.2: *Camallanus kaapstaadi* Southwell *et* Kirshner, 1937 from *Xenopus laevis* Daudin, photomicrographs. **a** – anterior end, male, lateral view; **b** – dorsal trident, male, lateral view; **c** – ventral trident, male, lateral view; **d** – posterior end, female, lateral view; **e** – part of female genital system at vulva level, lateral view; **f** – left and right spicules, lateral view; **g** – caudal end, male, ventral view.

General description. Medium-sized worms, coiled dorsally, body comparatively thick with maximum width at anterior third level. Cuticle with prominent transverse striations along whole body, except at buccal capsule. Apical: oral opening transversely slit; four conspicuous submedian cephalic papillae. Buccal capsule consisting of two valves each supported with numerous primarily completed ridges (Figure 2.2a,b). Four sclerotised plates situated on external surface of valves near their anterior margin. Thick sclerotised basal ring present at buccal capsule base. Buccal capsule valves supported by two prominent tridents on dorsal and ventral side (Figure 2.2b,c). Each trident consisted of three posteriorly directed prongs. Central prongs somewhat longer than sublateral ones. Tridents usually unequal, beginning at level of buccal capsule mid-length and ending

slightly posterior to level of basal ring. Muscular oesophagus club-shaped with elongated posterior bulb. Glandular oesophagus almost equal in length to muscular oesophagus, cylindrical to $^{3}/_{4}$ length with slightly widened posterior quarter. Nerve ring encircling muscular oesophagus at level of its anterior quarter. Excretory pore opening on ventral side somewhat posterior to nerve ring level. Deirids minute, papilliform, situated at level of posterior third of muscular oesophagus. Intestine and rectum straight, narrow. Tail tapering.

Male (morphometry based on nine specimens). Body 2.66–3.28 mm (3.04 mm) long, 102–171 (149) wide. Buccal capsule valves 62–100 (83) long, 65–118 (106) wide, supported by 16–31 (26) ridges, of which 7–10 (8) incomplete. Basal ring 7–14 (10) long, 52–89 (77) wide. Dorsal trident 51–72 (66) long and 15–23 (19) wide in lateral projection, ventral one 48–67 (58) long and 17–23 (20) wide. Muscular oesophagus 261–381 (338.4) long, 9.8–12.3% (11.1%) of body length; 53–63 (58.8), 46–61 (53.9) and 58–95 (86.1) wide at anterior, mid-length and bulb level, respectively. Glandular oesophagus 275–461 (368.5) long, 9.1–14.9% (12.1%) of body length; 35–96 (61.5), 44–82 (59.5) and 42–76 (59.9) wide at anterior, mid-length and posterior level, respectively. Nerve ring, excretory pore and deirids (distance to deirids measured in three specimens) at 150–246 (182.9), 191–277 (216.1) and 226–257 (241.7) from anterior extremity, respectively. Caudal alae narrow, ventrolateral, supported by papillae: six pairs of pre-cloacal pedunculated papillae (Figure 2.2g); one pair of pedunculated papillae at cloaca level; five pairs of post-cloacal pedunculated papillae (three prominent pairs somewhat posterior to cloaca and two pairs of small papillae close to tail end). Additionally, two pairs of sessile ad-cloacal papillae situated slightly anterior and posterior to cloaca. Spicules unequal, simple-shaped with sharpened tips (Figure 2.2f). Right spicule prominent, 287–468 (422.5) long; left one less sclerotised (measured in three specimens), 198–220 (211.7) long. Tail conical with two minute spines on tip (Figure 2.2g), 74–104 (91.5) long, 2.5–3.2% (3.0%) of body length.

Female (morphometry based on nine specimens). Generally larger than males. Body 2.80–5.13 mm (3.62 mm) long, 201–293 (242) wide. Buccal capsule valves 95–149 (116) long, 81–174 (147) wide, supported by 31–38 (34) ridges, of which 7–10 (9) incomplete. Basal ring 9–20 (13) long, 71–125 (106) wide. Dorsal trident 72–102 (86) long and 21–29 (25) wide in lateral projection, ventral one 63–88 (76) long and 14–35 (24) wide. Muscular oesophagus 373–451 (414) long, 7–14% (12%) of body length; 58–87 (76), 46–79 (69) and 97–140 (123) wide at anterior, mid-length and bulb level, respectively. Glandular oesophagus 313–531 (390) long, 6–15% (11%) of body length; 50–91 (72), 49–91 (66) and 52–105 (79) wide at anterior, mid-length and posterior level, respectively. Nerve ring, excretory pore and deirids (distance to deirids measured in five specimens) at 183–242 (220), 229–307 (266) and 261–375 (306) from anterior extremity, respectively. Vulva post-equatorial, opening posterior to distinct projection of body wall at 1.67–2.64 mm (2.16 mm) from anterior extremity (Figure 2.2e), 51–63% (60%) of body length. Tail tapering, 124–179 (143) long, 3–5% (4%) of body length, bearing three mucrons 5–11 (8) long at its

tip (Figure 2.2d).

Camallanus xenopodis Jackson *et* Tinsley, 1995

Host: *Xenopus laevis* (Daudin) (Amphibia: Anura: Pipidae).

Locality: Western Cape (see Table 2.1).

Site of infection: Intestine.

Representative DNA sequences: MG948462 (*COX1*), MG947389 (*28S*).

Figures 2.3 & 2.4

General description. Medium-sized worms, coiled dorsally, body comparatively thick with maximum width at anterior third level. Cuticle with transverse striations clearly visible from level of basal ring to posterior extremity. Apical: oral opening transversely slit; four conspicuous submedian cephalic papillae. Buccal capsule comparatively small, consisting of two valves, supported by longitudinal ridges, with four thin plates on anterior margin, sclerotised basal ring at base and two tridents (Figure 2.3b–d, 2.4a–c). Tridents prominent, equal in shape, almost equal in size, with central prongs somewhat longer than sublateral ones (Figure 2.3c,d, 2.4b,c). Tridents beginning at level of buccal capsule mid-length, ending somewhat posterior to basal ring. Muscular oesophagus club-shaped with elongated posterior bulb. Glandular oesophagus almost same length as muscular oesophagus, cylindrical along almost entire length with slightly widened or narrowed posterior quarter. Position of nerve ring varying within level of muscular oesophagus anterior third. Excretory pore opening on ventral side somewhat posterior to nerve ring level. Deirids minute, papilliform, situated at level of muscular oesophageal mid-length. Intestine and rectum straight, narrow. Tail tapering.

Male (morphometrics based on four specimens). Body 2.88–3.30 mm (3.04 mm) long, 113–127 (118) wide (Figure 2.3a). Buccal capsule valves 62–70 (66) long, 72–82 (77) wide, supported by 18–22 (20) ridges, of which 4–6 (5) incomplete. Basal ring 5–11 (9) long, 50–55 (53) wide. Dorsal trident (Figure 2.3c, 2.4b) 57–69 (62) long and 10–18 (15) wide at lateral projection, ventral one (Figure 2.3d, 2.4c) 51–63 (59) long and 9–16 (13) wide. Muscular oesophagus 257–305 (284) long, 9–11% (9%) of body length; 43–51 (45.5), 38–45 (41) and 59–74 (65) wide at anterior, mid-length and bulb level, respectively. Glandular oesophagus 209–313 (271) long, 7–11% (9%) of body length; 39–61 (47), 38–58 (49) and 34–73 (53) wide at anterior, mid-length and posterior level, respectively. Nerve ring, excretory pore and deirids (distance to deirids measured in one specimen) at 140–159 (149), 184–211 (198) and 213 from anterior extremity, respectively. Caudal alae comparatively narrow, ventrolateral, supported by papillae (Figure 2.3f, 2.4f): six pairs of pre-cloacal pedunculated papillae; one pair of pedunculated papillae at cloaca

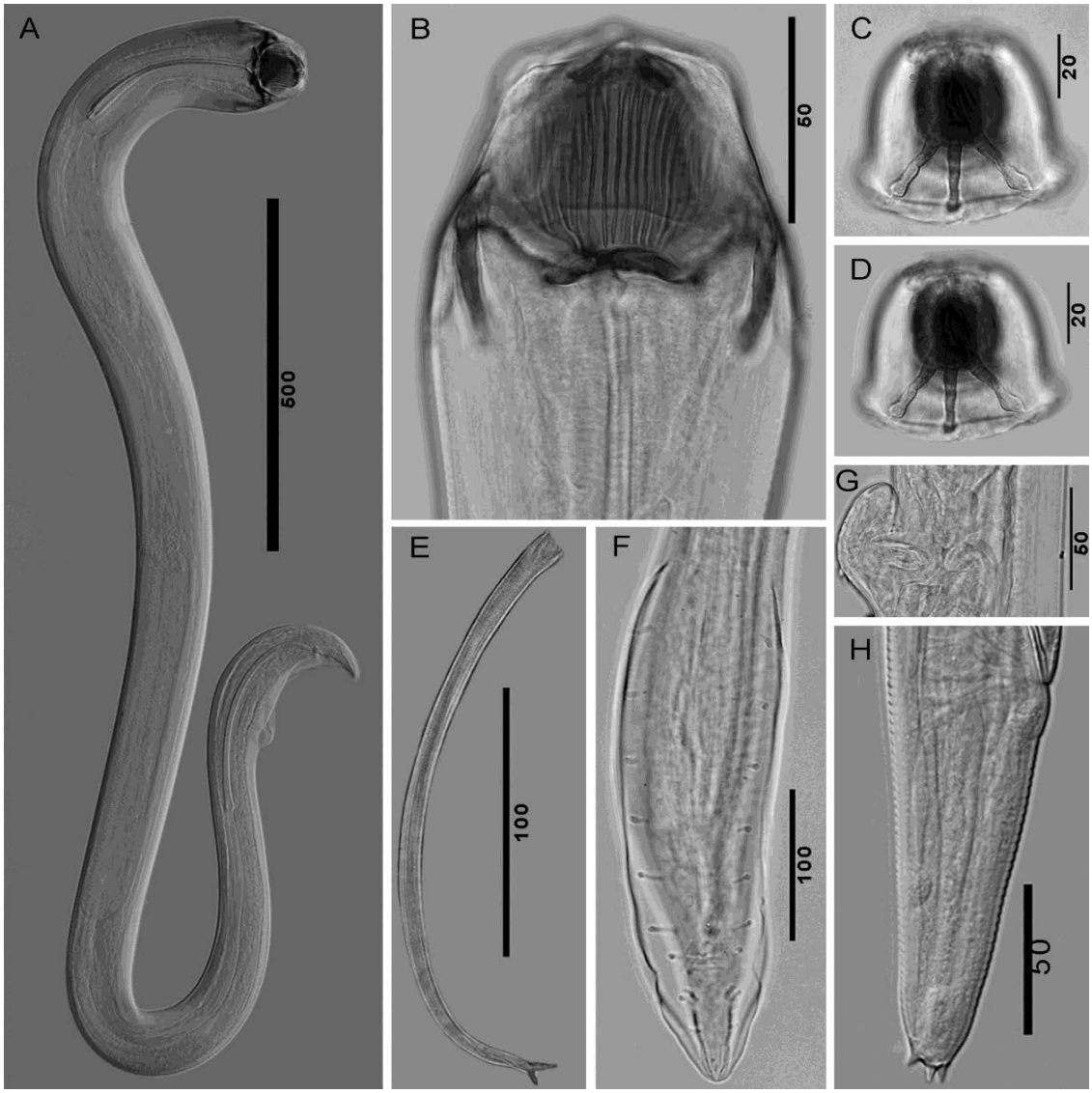

Figure 2.3: *Camallanus xenopodis* Jackson *et* Tinsley, 1995 from *Xenopus laevis* (Daudin), photomicrographs. **a** – male, general view; **b** – anterior end, female, lateral view; **c** – dorsal trident, male, lateral view; **d** – ventral trident, male, lateral view; **e** – right spicule, lateral view; **f** – caudal end, male, ventral view; **g** – part of female genital system at vulva level, lateral view; **h** – posterior end, female, lateral view.

level; four pairs of post-cloacal pedunculated papillae (two prominent pairs somewhat posterior to cloaca, one pair at tail mid-length and one pair of small papillae close to tail end). Two pairs of sessile ad-cloacal papillae situated slightly anterior and posterior to cloaca. Spicules unequal. Right spicule (Figure 2.3e, 2.4e) 323–356 (335) long with short conical process directed dorsally at its tip. Left spicule shorter, 96–98 long (measured in two specimens), poorly sclerotised, with simple-shaped sharpened tip (Figure 2.4d). Tail tapering with smoothly rounded tip (Figure 2.3f, 2.4f).

Female (morphometrics based on 24 specimens). Generally larger than males. Body 3.33–5.13 mm (4.20 mm) long, 136–241 (177) wide. Buccal capsule valves 73–85 (81) long, 73–104 (93) wide, supported by 14–22 (18) ridges, of which 3–7 (5) incomplete.

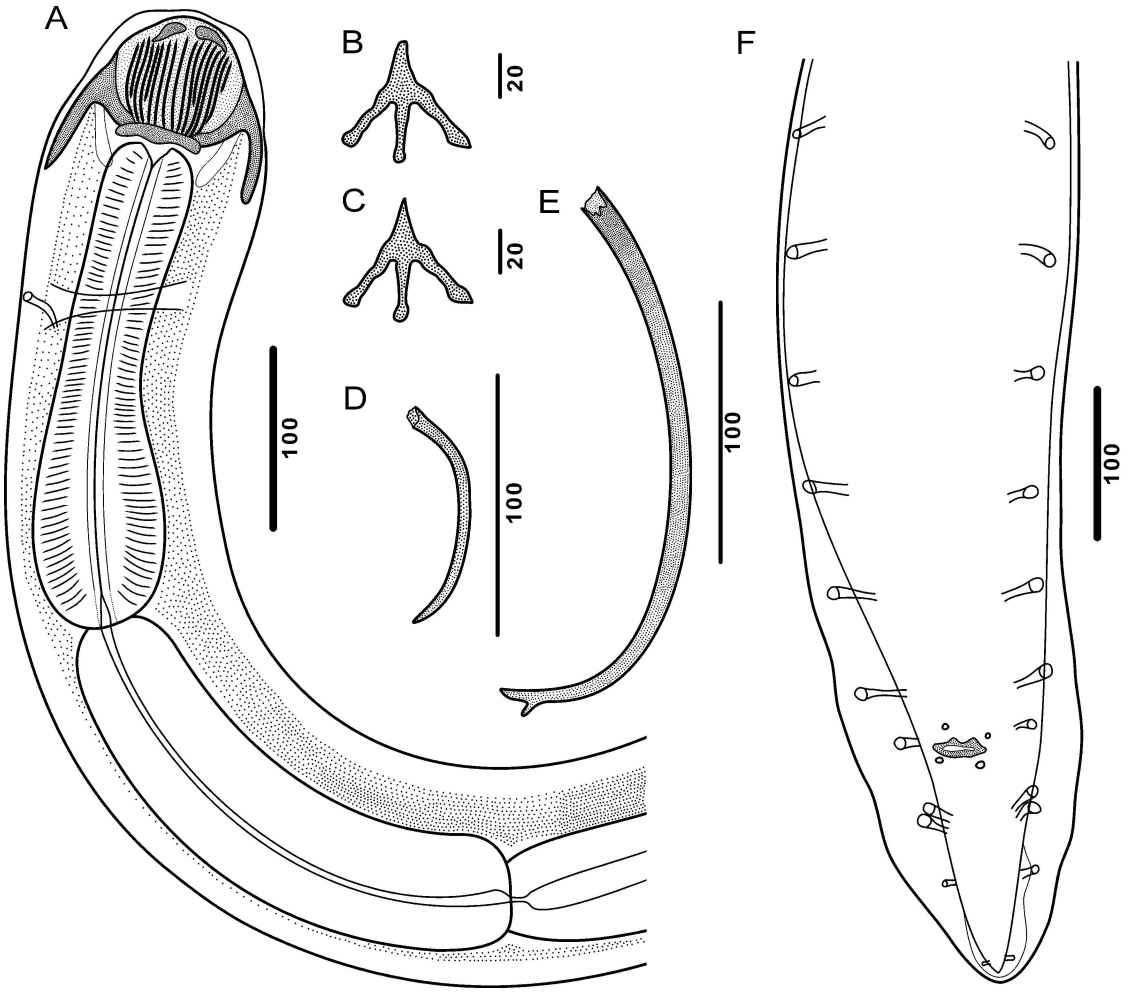

Figure 2.4: *Camallanus xenopodis* Jackson *et* Tinsley, 1995 from *Xenopus laevis* (Daudin), male, line-drawings. **a** – anterior end, lateral view; **b** – dorsal trident, lateral view; **c** – ventral trident, lateral view; **d** – left spicule, lateral view; **e** – right spicule, lateral view; **f** – caudal end, ventral view.

Basal ring 8–14 (11) long, 62–74 (67) wide. Dorsal trident 53–93 (76) long and 11–25 (16) wide at lateral projection, ventral one 61–85 (75) long and 12–20 (16) wide. Muscular oesophagus 326–433 (353) long, 7–12% (9%) of body length; 48–68 (58), 39–59 (51) and 76–104 (89) wide at anterior, mid-length and bulb level, respectively. Glandular oesophagus 310–455 (374) long, 7–11% (9%) of body length; 42–84 (61), 51–111 (71) and 48–85 (66) wide at anterior, mid-length and posterior level, respectively. Nerve ring, excretory pore and deirids (distance to deirids measured in eight specimens) at 171–212 (186), 210–256 (228) and 180–291 (247) from anterior extremity, respectively. Vulva opening posterior to distinct projection of body wall almost at level of mid-body at 1.72–2.59 mm (2.14 mm) from anterior extremity (Figure 2.3g), 47–54% (51%) of body length. Tail tapering, 94–165 (129) long, 3–4% (3%) of body length, bearing three mucrons, 5–7 (6) long, at its tip (Figure 2.3h).

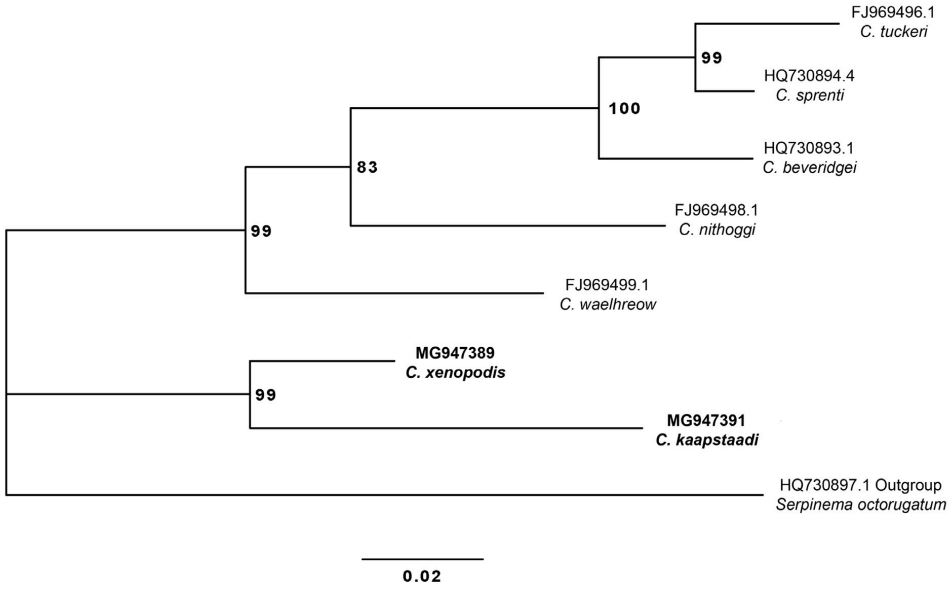

Figure 2.5: Phylogenetic tree of seven species of *Camallanus* Railliet *et* Henry, 1915 based on partial *28S* sequences.

2.3.2 Molecular analysis

For all three species, partial *28S* gene and *COX1* fragments were sequenced. Only for five species of *Camallanus* from Australian freshwater turtles partial sequences of the *28S* subunit are available in GenBank. These species were used for the phylogenetic analysis and *Serpinema octorugatum* (Baylis, 1933) was used as outgroup since it represents the most related genus to *Camallanus* (see Kuzmin *et al.*, 2011). The resulting tree (Figure 2.5) confirmed the interrelationships among *C. tuckeri* Kuzmin, Tkach, Snyder *et* Maier, 2009, *C. sprent*i Kuzmin, Tkach, Snyder *et* Bell, 2011, *C. waelhreow* Rigby, Sharma, Hechinger, Platt *et* Weaver, 2008, *C. nithoggi* Rigby, Sharma, Hechinger, Platt *et* Weaver 2008 and *C. beveridgei* Kuzmin, Tkach, Snyder *et* Bell, 2011 showed by Kuzmin *et al.* (2011) and showed their distant relations to *C. kaapstaadi* and *C. xenopodis*.

The *COX1* sequences were available for only two species of *Camallanus*, namely *C. cotti* Fujita, 1927 and *C. hypophthalmichthys* Dogel *et* Akhmerov, 1959, originally described from fishes in the Eastern Palaearctic (Moravec & Justine, 2006; Moravec *et al.*, 2004). For this analysis, *Spirocamallanus istiblenni* Noble, 1966 was used as outgroup. Phylogenetic tree topology showed distant relationships between *Camallanus* from African frogs and from Asian fishes which grouped in two strongly supported clades (Fig. 2.6).

Since neither *28S* nor *COX1* sequences of *Batrachocamallanus* and *Procamallanus* were available in GenBank, we were not able to provide phylogenetic analysis for *B. slomei*. Therefore, representative sequences of that species were simply submitted to GenBank.

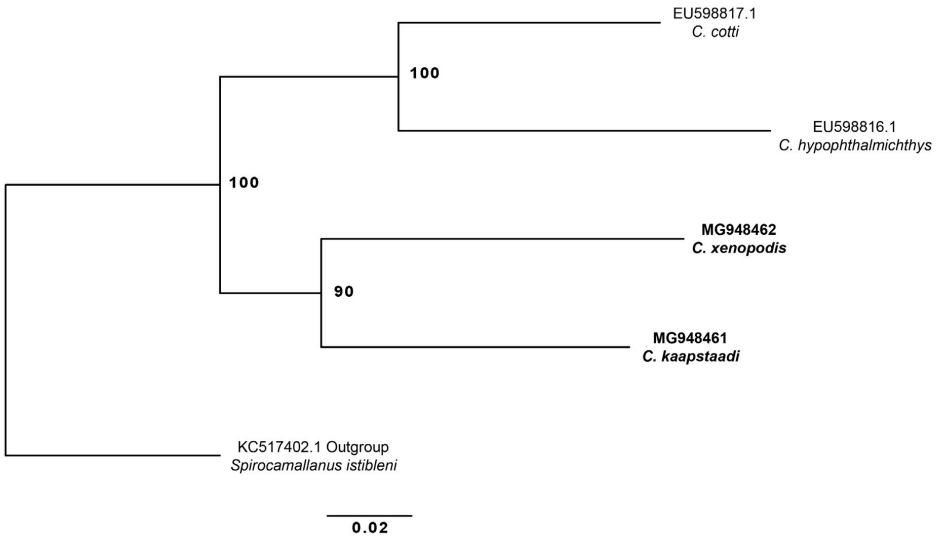

Figure 2.6: Phylogenetic tree of four species of *Camallanus* Railliet *et* Henry, 1915 based on partial *COX1* sequences.

2.4 Discussion

During the course of the present study, all three species of camallanid nematodes that have previously been reported from *X. laevis* were found. The most common nematode encountered in the present study was *B. slomei*, reported from all but three localities with prevalence ranging from 7% to 100% (Table 2.1). Conversely, the other two species were found only in two localities. Both *C. kaapstaadi* and *C. xenopodis* were only found at one locality, namely a series of dams in a mountain stream near Dullstroom (Mpumalanga Province, northern region of South Africa) and only *C. kaapstaadi* was found at one locality in Cape Town (Western Cape Province). The higher level of nematode diversity at this specific locality where both *Camallanus* species occur, corresponds with the higher numbers of other parasites (cestodes, monogeneans, digeneans and parasitic arthropods) also found here in comparison to other localities (unpublished data). In our opinion, this can be explained by the pristine condition of the habitat and lack of human disturbance allowing a better environment for parasite circulation.

Our results confirm the presence of *C. kaapstaadi* in South Africa, in the light of the fact that many previous records are from more northern regions in Africa such as Cameroon, Ghana, Kenya, Nigeria, Rwanda, Sudan, Tanzania, Togo, Uganda and Zimbabwe (Avery, 1971; Jackson & Tinsley, 1995a; Thurston, 1970; Tinsley *et al.*, 1979; Yeh, 1960b). We found *C. xenopodis* in the north of South Africa, indicating a less disjunct distribution than the two previous records from the Cape and Kenya suggest (Jackson & Tinsley, 1995a). We hypothesise that species of *Camallanus* in clawed frogs are more widespread than previous studies imply, which will be outlined in further studies.

Batrachocamallanus slomei is found primarily in the stomach, but also in some cases in the oesophagus. Our findings suggest no correlation between the number of nematodes in the stomach and their presence in the oesophagus of the same frog. For example, the frog with the highest infection of *B. slomei* harboured 36 nematodes in the stomach and one nematode in the oesophagus, whereas another frog harboured 15 in the stomach and 17 in the oesophagus. Only one specimen of *C. kaapstaadi* was found in the stomach while all other specimens inhabited the oesophagus in four frogs sharing this site with *B. slomei*. *Camallanus xenopodis* is found only in the intestine of *X. laevis* and no other nematode species are known from this part of the digestive tract.

The reported morphometric characters of *B. slomei* vary widely and correspond to the previously known data (Jackson & Tinsley, 1995b; Southwell & Kirshner, 1937). Our data slightly expand the existing ranges of body length and width, length of male spicules and distance to vulva from anterior part of body in females. Overall, no differences in morphometric characters of *B. slomei* were observed between localities.

Metrical characters of *C. kaapstaadi* and *C. xenopodis* also vary greatly in the studied samples, though most of them fall within the ranges of previously known data (Jackson & Tinsley, 1995a; Southwell & Kirshner, 1937; Thurston, 1970). In the first description of *C. kaapstaadi*, the authors mentioned that the male left spicule is about 200 μm long and less sclerotised than the right one (Southwell & Kirshner, 1937). In the later redescription, the authors concurred that the left spicule is poorly visible, but did provide a mean measurement of 155 μm (Jackson & Tinsley, 1995a). In our specimens, all males of *C. kaapstaadi* possessed a conspicuous left spicule with a mean length of about 212 μm. This measurement is longer than that reported for *C. kaapstaadi* from *X. laevis* by Jackson & Tinsley (1995a), probably due to the fact that the specimens in our study were generally bigger (2.25 mm in Jackson & Tinsley (1995a) *vs* 3.04 mm in the present study). This discrepancy is also found in the mean measurement of the right spicule (273 μm *vs* 423 μm). At the same time, the left spicule of *C. xenopodis* is truly inconspicuous under light microscopy, even when viewed under high magnification with differential interference contrast. Nevertheless, the existence of the left spicule is confirmed based on dissection of the caudal part of male.

In our specimens, more females than males of all the species were found, although only in *C. xenopodis* the females are four times more frequent. Therefore, it is clear why the species was previously described only by females (Jackson & Tinsley, 1995a). Males in our samples of *C. xenopodis* possess several characters, such as structure of buccal capsule, number of ridges on its valves, size and shape of tridents and male right spicule, that are similar to *C. mazabukae* Kung, 1948. Despite that, two characters, namely number of mucrons (five or at least four in *C. mazabukae vs* only three in *C. xenopodis*) and the shape of the body (*C. mazabukae* coiled in the ventral direction whilst all found specimens of *C. xenopodis* coiled dorsally) led us to assign the collected specimens to *C. xenopodis*.

However, the image of the female tail of *C. mazabukae* in the original description (Kung, 1948) shows that the specimen might really be coiled dorsally. Moreover, the species was described based on only two specimens from the poorly identified host, marked as "bullfrog". Since no *Camallanus* have been found in the Giant Bullfrog (*Pyxicephalus adsperus* Tschudi) or African Bullfrog (*Pyxicephalus edulis* Peters) (Halajian *et al.*, 2013, unpublished data) before this record or ever since, we suppose that it might represent an opportunistic infection or host misidentification. Given these points, we prefer to identify our specimens as *C. xenopodis* while the taxonomic status of *C. mazabukae* should be illuminated by further studies of *Camallanus* from different amphibians in Africa.

The lack of available DNA alignments in GenBank did not allow us to provide robust phylogenetic analysis of the found species. Both phylogenetic trees (based on partial *28S* and *COX1* alignments) show that species of *Camallanus* from South African amphibians form a well-supported clade separate from clades of species from Asian fish or Australian freshwater turtles. Unfortunately, we are not able to consider that group as monophyletic, since no data are available of *Camallanus* from fish (*C. polypteri* Kabre *et* Petter, 1997) or turtles (*C. chelonius* Baker, 1983) in Africa.

Our study revealed only one species of *Batrachocamallanus*, which limits us in our ability to draw conclusions about the status of the genus. Both the opinions of Jackson & Tinsley (1995b) and Moravec *et al.* (2006) are based on the morphological characters of nematodes. Recent molecular studies of different groups of nematodes established that morphological characters (especially apomorphies) may appear independently in different lineages and are often not suitable for phylogenetic studies (Carreno & Nadler, 2003; Tkach *et al.*, 2014). Therefore, in our opinion, the real phylogeny and evolutionary relationships between Camallanidae and their hosts will be illuminated in further molecular studies of more species from different hosts around the globe.

Chapter 3

Xenopus laevis as UberXL for nematodes

3.1 Introduction

Biological invasion, or the translocation of animals, plants and pathogens to novel habitats, often with human help, is one of the distinguishing characteristics of the Anthropocene (Capinha *et al.*, 2015; Ellis *et al.*, 2012). In numerous cases, declines in biodiversity are directly linked to the spread of highly competitive, generalist invasive species (Bellard *et al.*, 2016; Ricciardi, 2007) and many invasive species impact their new ecosystems negatively (Simberloff, 2011).

In particular, the role of invasive species in the alteration of parasite dynamics in their novel habitats is frequently overlooked (Blackburn & Ewen, 2017). Conversely, introduced hosts could cause the amplification of native parasite dynamics, by acting as reservoirs for native parasites that can eventually spill back to native hosts, or conversely, they can dilute these interactions by acting as dead-end hosts for native parasites (Telfer & Bown, 2012). These ripples can be felt several links down the food chain, especially in the case of parasites transmitted via trophic interactions (Amundsen *et al.*, 2013).

The globally invasive African Clawed Frog, *Xenopus laevis* (Daudin, 1802) (Anura: Pipidae) is one of the world's most widely distributed amphibian invaders. Its human-mediated range expansion was initiated in the 1930s through its use as a biological pregnancy assay and a model research animal and later with the help of the pet trade (Gurdon & Hopwood, 2000; van Sittert & Measey, 2016; Weldon *et al.*, 2007). Currently, its invasive range spans four continents, with established populations mainly in areas with a Mediterranean climate (Lobos & Measey, 2002; Measey *et al.*, 2012). However, climate and niche modelling have made it clear that *X. laevis* still has many potential environments to fill across the globe

(Ihlow *et al.*, 2016; Measey *et al.*, 2012; Rödder *et al.*, 2017; van Sittert & Measey, 2016). In addition to its status as global invader, *X. laevis* exhibits recurring range expansion within its native range (Measey & Davies, 2011; Measey *et al.*, 2017). These domestic invasions were brought about by its frequent translocation for research and training purposes in the past (van Sittert & Measey, 2016) and continues to the here and now through natural dispersal via overland movement and artificial waterbodies (de Villiers & Measey, 2017; Measey, 2004, 2016; Measey *et al.*, 2012).

The parasite fauna of *X. laevis* has received extensive attention since the early 1900s, with more than 25 parasitic genera, representing all invertebrate parasite groups except acanthocephalans, described in association with this host in its native range (Tinsley, 1996). Although the parasite communities of invasive *X. laevis* are significantly impoverished (Schoeman *et al.*, 2019), at least three of its co-evolved parasites have been co-introduced across the invasive range (Jackson & Tinsley, 2001a; Kuperman *et al.*, 2004; Rodrigues, 2014; Schoeman *et al.*, 2019; Tinsley & Jackson, 1998b). These are the monogeneans *Protopolystoma xenopodis* Price, 1943 and *Gyrdicotylus gallieni* Vercammen-Grandjean, 1960 and the cestode *Cephalochlamys namaquensis* Cohn, 1906 (see Schoeman *et al.*, 2019).

Notably, host-specific parasites with complex life cycles are absent from the accompanying parasite assembly (Schoeman *et al.*, 2019). Notwithstanding, it is specifically the digeneans and nematodes native to the invasive range of *X. laevis* that have been able to form novel host-parasite associations with the new invader (Castillo *et al.*, 2017; Kuperman *et al.*, 2004; Rodrigues, 2014; Schoeman *et al.*, 2019).

In the case of nematodes, Kuperman *et al.* (2004) reported juvenile stages of *Contracaecum* Rialet *et* Henry, 1912 (Ascaridoidea: Anasakidae) from the body cavity and *Eustrongylides* Jägerskiöld, 1909 (Dioctophymatoidea: Dioctophymidae) from the subcutaneous tissue in the Californian invasive population of *X. laevis*. In addition, *Contracaecum* larvae were also recorded at very low infection levels encapsulated in the intestinal serosa of *X. laevis* invasive in Chile (Castillo *et al.*, 2017). Both sets of authors proposed the native parasite fauna of California and Chile to be the source of the infections, because none of these parasites have been reported in association with *X. laevis* from southern Africa (Castillo *et al.*, 2017; Kuperman *et al.*, 2004).

In turn, in the native range, the Nematoda is the second most speciose taxon among the parasites of *X. laevis* after the Digenea (Tinsley, 1996). Of these, three species belong to the family Camallanidae (Camallanoidea), namely *Batrachocamallanus slomei* (Southwell *et* Kirshner, 1937), *Camallanus kaapstaadi* Southwell *et* Kirshner, 1937 and *Camallanus xenopodis* Jackson *et* Tinsley, 1995. These species are found across Africa in *Xenopus* spp. (Avery, 1971; Jackson & Tinsley, 1995a,b; Kung, 1948; Southwell & Kirshner, 1937; Svitin *et al.*, 2018; Thurston, 1970; Tinsley *et al.*, 1979; Yeh, 1960a) and *C. kaapstaadi*

has been found to infect crocodilians through post-cyclic parasitism (Junker *et al.*, 2019). Another described nematode is *Pseudocapillaroides xenopi* Moravec *et* Cosgrove, 1982 (Enoplida: Capillariidae), of which all the life stages infest the skin of *X. laevis* (see Brayton, 1992; Cohen *et al.*, 1984; Cosgrove & Jared, 1974, 1977; Feldman & Ramirez, 2014; Moravec & Cosgrove, 1982; Stephens *et al.*, 1987; Wade, 1982).

A few reports of unidentified nematodes described in association with *X. laevis* across its native range have arisen over the years, ranging from a single specimen of probably *Rhabdias* Stiles *et* Hasal, 1905 (Rhabditoidea: Rhabdiasidae) in the lung (Cosgrove & Jared, 1974) and two species of quimperiid nematodes (Ascaridoidea: Quimperiidae) in the intestine (Thurston, 1970), to unidentified nematodes encysted in body tissues (Cosgrove & Jared, 1974). Larval nematodes in the glomerular space were also reported (Brayton, 1992; Cosgrove & Jared, 1974). These reports, though rare, suggest that *X. laevis* could act as a paratenic or intermediate host for some nematodes in its native range, as it has already proven itself to be capable of in the invasive range.

In light of the pervasive effects of trophically transmitted parasites in biological invasions (Amundsen *et al.*, 2013; Dunn *et al.*, 2012; Roy & Lawson Handley, 2012), it is paramount to have a better understanding of the role of *X. laevis* in the parasite dynamics of its native ecosystems. To this end, as part of a larger parasitological survey of *X. laevis* across the whole of its native range, the current study is the first report of seven nematode species parasitising this host in South Africa. Short morphological descriptions, supported by photomicrographs and molecular data (*18S* and *28S rRNA* and the *COX1* gene sequences), as well as distribution information, are provided for future reference in the native range and beyond. Furthermore, possible avenues of parasite transmission are explored, based upon a survey of the literature.

3.2 Methods

In total, 181 adult individuals were collected in chicken liver baited funnel traps from 28 localities across South Africa from March 2017 to April 2019 (see Appendix A for detailed information on all collection sites). The frogs were anaesthetised in 6% ethyl-3-aminobenzoate methanesulfonate (MS222) (Sigma-Aldrich Co., Steinheim, Germany) and subsequently euthanised through pithing, according to internationally accepted standard operating procedures. For the external parasite examination, the epidermis, lateral line, eyes, buccal cavity, eustachian tubules and nostrils were examined. Thereafter, the body was slit open longitudinally and the alimentary tract, kidney, excretory bladder, gallbladder with bile ducts, liver, lungs, heart and reproductive organs were removed and examined separately using a stereomicroscope in 0.6% amphibian saline, prepared according to Ringer's method (du Preez & van Wyk, 2007), for internal parasites. The

acquired nematodes were washed in saline, fixed in 70% hot ethanol and subsequently stored in 70% ethanol.

Prior to microscopic examination, the nematodes were placed in distilled water for about 20 min and then cleared in lactophenol for a period of time ranging from 30 min to 24 h, depending on the size of the respective nematode. The morphology of the nematodes was studied and photomicrographs were taken using ZEISS Axio Z1, Nikon AZ100, Nikon E800 and Nikon ECLIPSE Ni compound microscopes. Measurements were taken with the aid of the software ZEN (blue edition) (Carl Zeiss Microscopy GmbH, Jena, Germany) and NIS-Elements Documentation *version* 3.22.09 (Nikon Instruments Inc., Tokyo, Japan). In total, two of nine *Capillaria* sp. Zeder, 1800, females, nine of 183 *Contracaecum* sp. larvae, seven *Falcaustra* sp. Lane, 1915 (three females and four males), two of four *Paraquimperia* sp. Baylis, 1934, larvae, four of nine *Tanqua* sp. Blanchard, 1904, larvae, 14 of approximately 1 035 unidentified nematode larvae sp. 1, and eight of approximately 150 unidentified nematode larvae sp. 2 were measured. All measurements in the text are given in micrometres, unless stated otherwise, and presented as ranges, followed by mean values in parentheses. For molecular studies, the middle fragments of specimens were used, whereas the taxonomically important anterior and posterior parts were reserved for the morphological identification of species.

DNA was extracted using the PCRBIO Rapid Extract PCR Kit (PCR Biosystems Ltd., London, United Kingdom). Cytochrome oxidase *c* subunit I (*COX1*) amplicons were obtained using the primer pair 'LC01490' (5'-GGTCAACAAATCATAAAGATATTGG-3') and 'HCO2198' (5'-TAAACTTCAGGGTGACCAAAAAATCA-3') (Folmer *et al.*, 1994). The thermocycling profile was as follows: 3 min denaturation at 94 °C, 20 cycles of 94 °C for 30 s, 45 °C for 30 s, 72 °C for 1 min and 40 cycles of 94 °C for 30 s, 51 °C for 1 min, 72 °C for 1 min for amplification and finally 72 °C for 10 min for extension. The *18S rRNA* was amplified by the primer pair 'F18ScF1' (5'-ACCGCCCTAGTTCTGACCGTAAA-3') and 'F18ScR1' (5'-GGTTCAAGCCACTGCGATTAAAGC-3'), with the following thermocycling profile: 5 min denaturation at 95 °C, 40 cycles of 95 °C for 30 s, 58 °C for 30 s, 72 °C for 1 min 30 s for amplification, followed by an extension of 7 min at 72 °C (Lefoulon *et al.*, 2015). The *28S rRNA* was amplified using the primer pair 'LSU5' (5'-TAGGTCGAC-CCGCTGAAYTTAAGCA-3') and 'LSU3' (5'-TAGAAGCTTCCTGAGGGAAACTTCGG-3') (Littlewood *et al.*, 1997), with the thermocycling profile as follows: one initial step of 5 min at 95 °C for long denaturation; 35 cycles of 1 min at 95 °C for denaturation, 2 min at 48 °C for annealing and 2 min at 72 °C for elongation and one final step of 10 min at 72 °C for terminal elongation (Verneau *et al.*, 2009). For purification and sequencing, PCR products were sent to a commercial company (Inqaba Biotec, Pretoria, South Africa) that used the ExoSAP protocol (New England Biolabs Ltd., Massachusetts, United States) for purification. Sequencing was performed via BigDye® Terminator *version* 3.1 Cycle Sequencing, utilising the corresponding primer pairs used for the final PCR, on an ABI3500XL analyser (Applied Biosystems™). Contiguous sequences were assembled and edited using Geneious

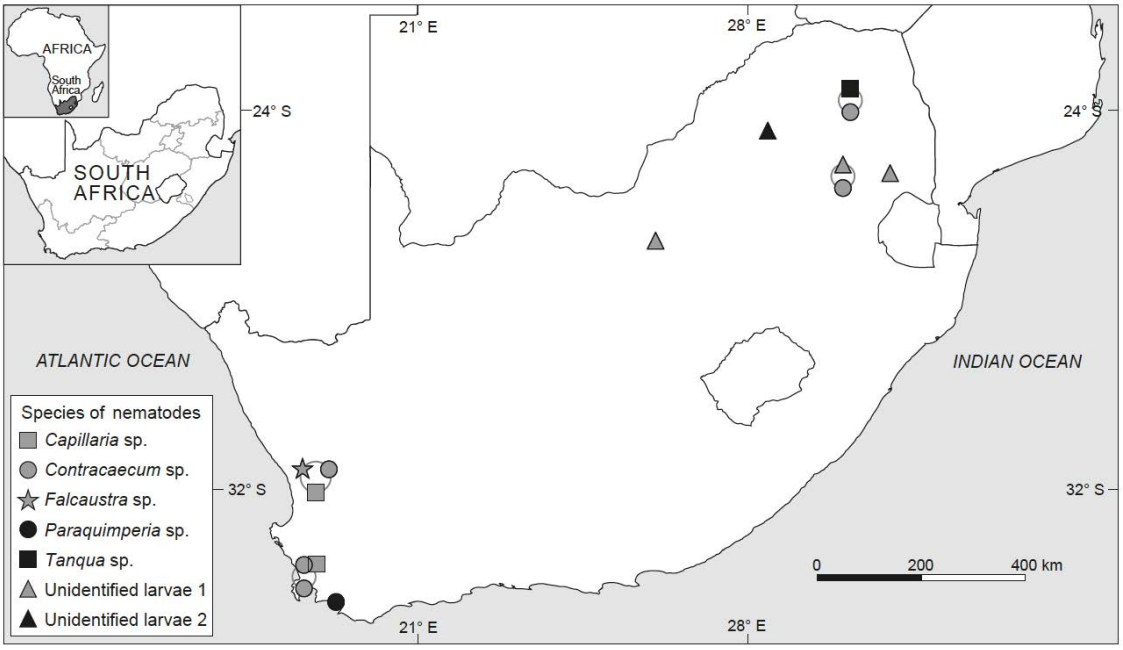

Figure 3.1: Distribution of seven previously undescribed species of nematodes recovered at ten localities across South Africa during the parasitological screening of *Xenopus laevis*. The presence of more than one nematode species in hosts from a single locality (Dullstroom, Vanrhynsdorp and Tzaneen), or from two localities in close proximity (in Cape Town), is denoted by the arrangement of the symbols in a ring around the central point. All maps utilise the Mercator projection and were created in QGIS *version* 3.4.3 Madeira.

version 9.0 (Biomatters Ltd., Auckand, Nieu-Seeland) and submitted to GenBank.

For each nematode species, prevalence, mean infection intensity and mean abundance were calculated for the localities where the species was present, *sensu* Bush *et al.* (1997). All applicable institutional, national and international guidelines for the care and use of animals were followed under the North-West University ethics approval number NWU-00380-16-A5-01.

3.3 Results

During the course of the current study, seven species of nematodes were discovered in association with *X. laevis* at ten localities across South Africa (Figure 3.1). Some species, such as the *Contracaecum* sp. encysted third stage larvae, were quite common across the region, whereas other infections were more localised. The unidentified second stage larvae from the lungs had the highest abundance and infection intensity of all at the three localities where it occurred (Table 3.1).

Table 3.1: Complete locality data and infection parameters, *sensu* Bush *et al.* (1997), of the seven nematode species reported for the first time from the African Clawed Frog *Xenopus laevis* from ten localities in South Africa. Locality names are given as farm name, nearest town and province. Values are reported as the mean for a given locality and species, with the median in square brackets and the range in round brackets.

Nematode	Localities	Coordinates	Number of hosts	Intensity	Abundance	Prevalence
Capillaria sp.	7-Fontein Farm, Vanrhynsdorp, Western Cape	31°44'09.8"S; 18°49'31.7"E	7	2 [2] (1–2)	0.4	29%
	Loekiesfontein Farm, Wellington, Western Cape	33°34'16.9"S; 18°50'24.4"E	6	2 [1] (1–4)	0.8	38%
Contracaecum sp.	7-Fontein Farm, Vanrhynsdorp, Western Cape	31°44'09.8"S; 18°49'31.7"E	7	2 [2] (1–2)	0.4	29%
	Bloemendal Wine Estate, Cape Town, Western Cape	33°50'21.2"S; 18°36'01.0"E	5	3	0.6	20%
	Burgundy Estate, Cape Town, Western Cape	33°50'07.8"S; 18°33'10.1"E	14	5 [5] (4–6)	0.7	14%
	Crimson Creek Cherry Farm, Dullstroom, Mpumalanga	25°23'53.2"S; 30°02'16.9"E	10	3 [2] (1–8)	1.7	50%
	Letsitele, Tzaneen, Limpopo	23°47'55.7"S; 30°11'42.5"E	10	1	0.1	10%
Falcaustra sp.	7-Fontein Farm, Vanrhynsdorp, Western Cape	31°44'09.8"S; 18°49'31.7"E	7	2 [2] (1–3)	1.1	57%
Paraquimperia sp.	Hermanus, Western Cape	34°22'12.6"S; 19°15'25.4"E	10	4	0.4	10%
Tanqua sp.	Letsitele, Tzaneen, Limpopo	23°47'55.7"S; 30°11'42.5"E	10	5 [5] (1–8)	0.9	20%
Unidentified nematode larvae sp. 1	Crimson Creek Cherry Farm, Dullstroom, Mpumalanga	25°23'53.2"S; 30°02'16.9"E	10	76 [76] (1–150)	15.1	20%
	Jacana Estate, White River, Mpumalanga	25°20'20.7"S; 31°01'21.2"E	8	11 [11] (5–16)	2.6	25%
	Potchefstroom, North-West Province	26°45'19.7"S; 26°03'02.2"E	9	145 [30] (5–720)	112.7	78%
Unidentified nematode larvae sp. 2	Placidus Farm, Modimolle, Limpopo	24°26'18.1"S; 28°26'12.8"E	6	150	25.0	17%

3.3.1 Nematode descriptions

Capillaria sp.

Site of infection: Stomach, intestine and rectum.

Representative DNA sequence: MN526255 (*28S*).

Figure 3.2

Female (morphometrics based on two gravid specimens). Body elongated, thin at anterior part widening posteriorly, 9.4–15.6 mm long, 58–66 wide. Anterior and posterior ends rounded. Muscular oesophagus elongated, evenly widening towards posterior end, 272–324 long. Stichosome almost cylindrical along whole length, 2.3–2.7 mm long. Stichocytes wider than long, with often indistinct merges. Total oesophagus 2.7–3.0 mm long. Nerve ring encircling oesophagus at level of its anterior half, 107–121 from anterior end of body. Vulva pre-equatorial, with thick walls, situated at 2.9–4.6 mm from anterior end of body, comprising 29–31% of body length. Vulva with 76–238 eggs, arranged in one row near

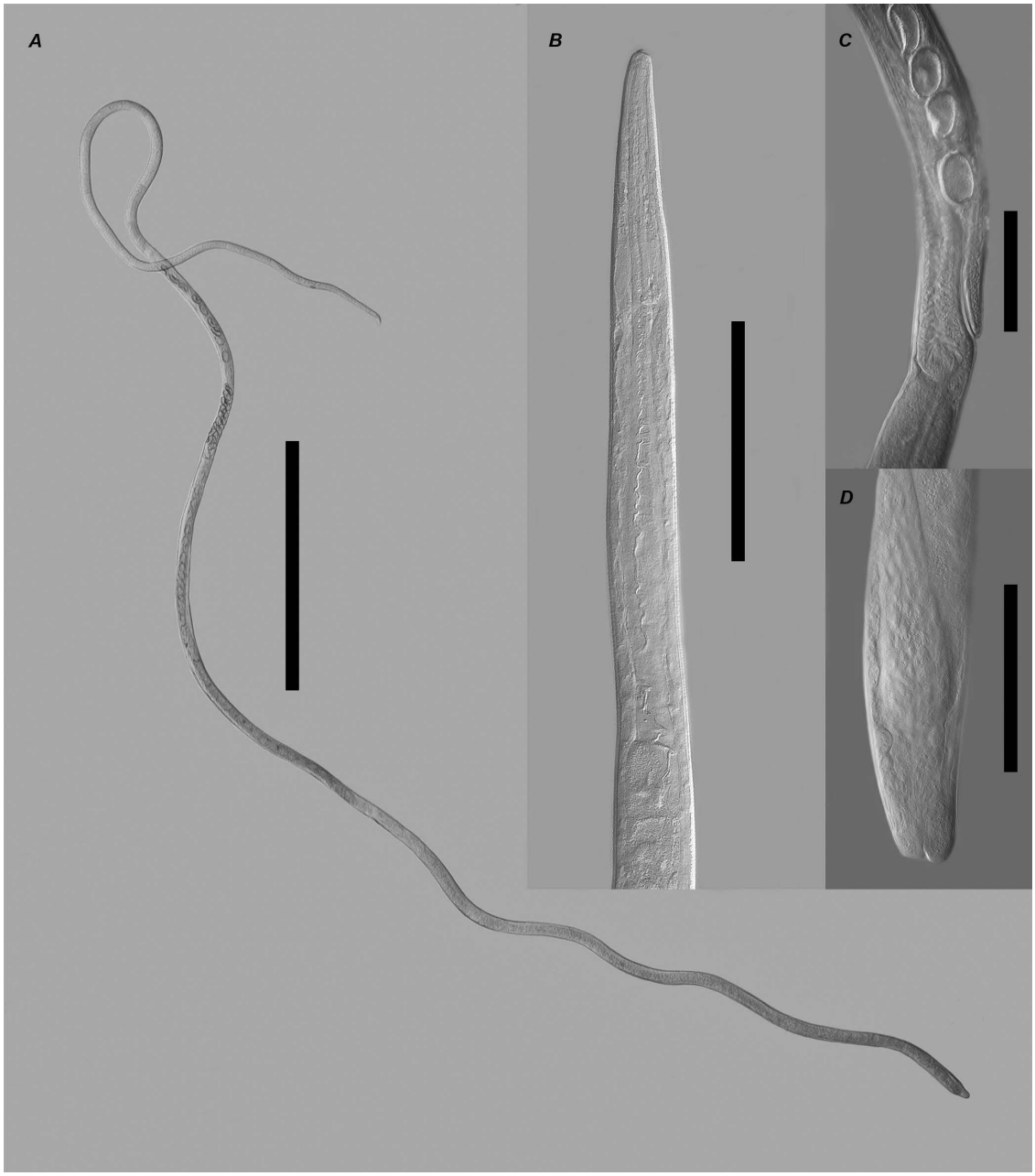

Figure 3.2: Adult female of *Capillaria* sp. from the digestive tract of *Xenopus laevis*, photomicrographs. **a** – general view; **b** – anterior end of body, lateral view; **c** – part of body at vulva region, lateral view; **d** – posterior end of body, lateral view. Scale bars: **a:** 1 mm; **b–d:** 100 μm

vulva and in three rows posteriorly. Eggs 50 (41–54) long, 23 (20–26) wide (n = 10). Intestine straight, narrow, rectum short, with thick walls. Tail short, rounded, subterminal.

Remarks

Of the capillariid nematodes, only *Pseudocapillaroides xenopi* has been described in association with *X. laevis* imported to Europe from South Africa (Moravec & Cosgrove, 1982; Wade, 1982). This species was described by Moravec & Cosgrove (1982) as *Pseudocapillaroides xenopi*. In the same year, Wade (1982) described it as *Capillaria*

xenopodis. These two names were used interchangeably. However, *P. xenopi* is regarded as the generally accepted one (Feldman & Ramirez, 2014), because the species clearly belongs to a genus separate from *Capillaria*, based upon both phylogenetic and morphological evidence. Representatives of *Pseudocapillaroides* Moravec *et* Cosgrove, 1982 are characterised by the eggs containing developed larvae, small body size and the subcutaneous site of infection (Moravec & Cosgrove, 1982; Wade, 1982).

Other reports of capillariids from Africa have been registered throughout southern Africa from different species of clariid and cyprinid fish. However, in most cases, these nematodes were recorded without descriptions and identified only to genus level (Boomker, 1994a; Moyo *et al.*, 2009). In our material, only female specimens (of which two harboured well-developed eggs) were found in the host intestines. Based on the general body measurements, the morula stage of the eggs and the site of infection, as well as the molecular data, we assign our specimens to the genus *Capillaria*. Unfortunately, because of an absence of males and a lack of clear molecular data, we could not identify them to the species level.

***Contracaecum* sp.**

> Site of infection: Encysted in the body cavity and on the outer surfaces of stomach and liver.
>
> Representative DNA sequences: MN526248 (*COX1*), MN526250 (*18S*), MN526256 (*28S*).

Figure 3.3

Third stage larva (morphometrics based on nine specimens). Body comparatively thick, robust, 28–49 mm (42 mm) long, 550–925 (810) wide. Along entire body cuticle, with conspicuous transverse striations. Anterior end rounded, bearing small ventral cuticular tooth. Excretory pore situated near tooth. Oesophagus elongated, almost cylindrical in anterior half, widening posteriorly. Oesophagus 2.8–3.5 mm (3.1) long, 6.6–11.0% (8.0%) of body length; 77–116 (92), 106–192 (143) and 99–230 (180) wide at anterior, mid-length and posterior part, respectively. Nerve ring encircling oesophagus at level of its anterior end, at 363–547 (492) from anterior end of body; 12–18% (16%) of oesophagus length. Intestine straight, narrow. Rectum short, with thick walls. Tail tapering, 135–247 (186) long.

Remarks

Third stage larvae of *Contracaecum* have been found encapsulated in the body cavity of numerous fish species throughout southern Africa: spot-tail robber *Brycinus imberi*, African sharp-tooth catfish *Clarias gariepinus* and African blunt-tooth catfish *C. ngamensis*, canary

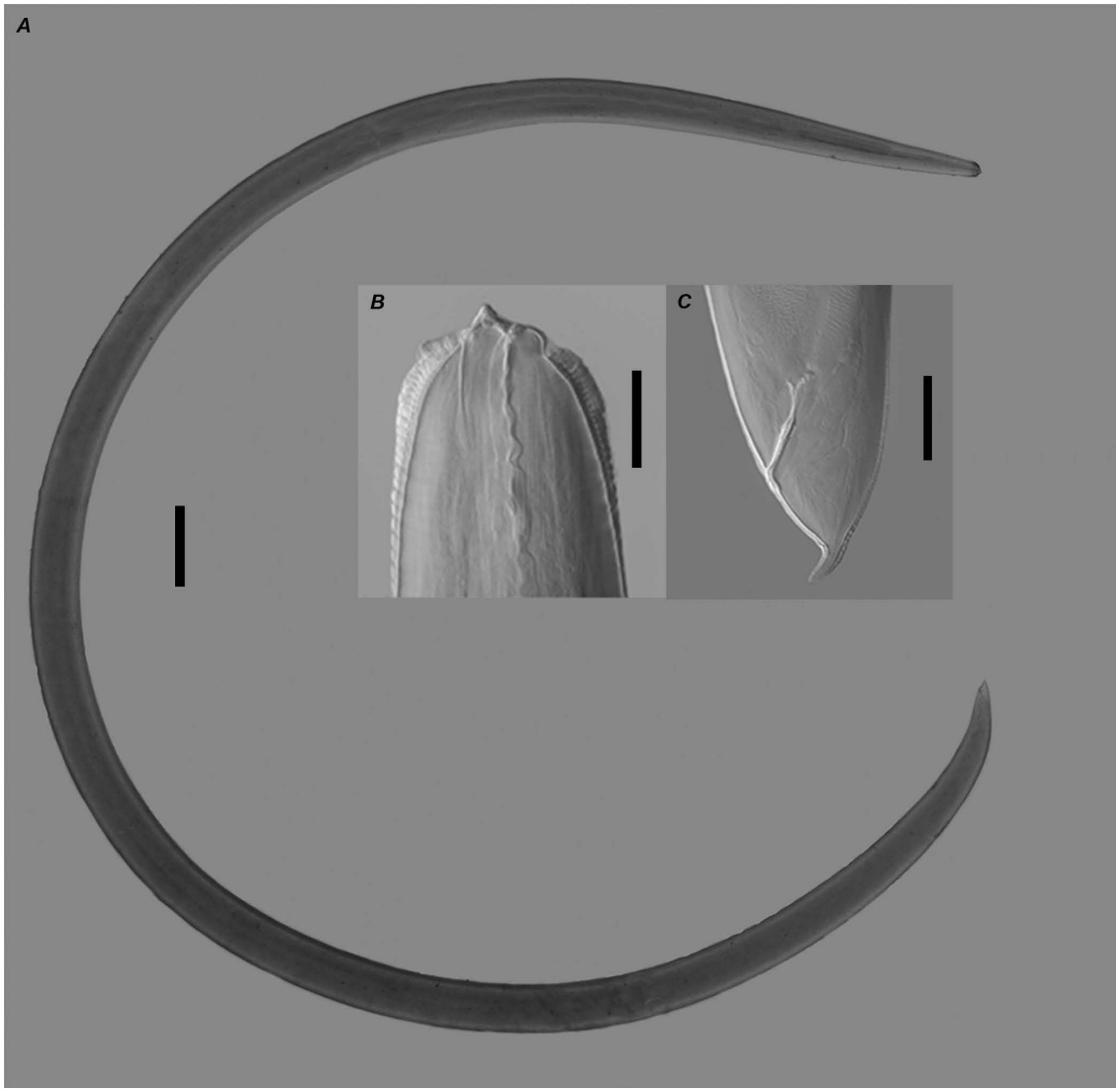

Figure 3.3: Third stage larval *Contracaecum* sp. encysted in *Xenopus laevis*, photomicrographs. **a** – general view; **b** – anterior end of body, lateral view; **c** – posterior end of body, lateral view. Scale bars: **a:** 1 mm; **b,c:** 100 μm

kurper *Chetia flaviventris*, redbreast tilapia *Coptodon rendalli*, common carp *Cyprinus carpio*, papermouth *Enteromius mattozi*, threespot barb *E. trimaculatus*, African pike *Hepsetus odoe*, tigerfish *Hydrocynus vittatus*, largescale yellowfish *Labeobarbus marequensis*, bulldog *Marcusenius macrolepidotus*, largemouth bass *Micropterus salmoides*, Mozambique tilapia *Oreochromis mossambicus*, threespot tilapia *O. andersonii*, greenhead tilapia *O. macrochir*, Cape kurper *Sandelia capensis*, dusky bream *Sargochromis codringtonii*, butter catfish *Schilbe intermedius*, Zambezi bream *Serranochromis robustus*, purpleface largemouth *S. macrocephalus*, blackspotted squeaker *Synodontis nigromaculatus* and banded tilapia *Tilapia sparrmanii* (see Barson, 2004; Barson & Avenant-Oldewage, 2006; Barson *et al.*, 2008; Boane *et al.*, 2008; Boomker, 1982, 1994a,b; Madanire-Moyo *et al.*, 2010; Mashego, 1989; Mashego & Saayman, 1981; Mbokane *et al.*, 2015; McHugh *et al.*, 2016; Moravec *et al.*, 2016; Moravec & van As, 2015; Moyo *et al.*, 2009; Sara *et al.*,

2014; Smit & Luus-Powell, 2012; Tavakol *et al.*, 2015; Whitfield & Heeg, 1977; van As & Basson, 1984). Nevertheless, only Moravec *et al.* (2016) provided detailed descriptions (including line drawings and SEM images) of *Contracaecum* sp. from the Cape kurper *S. capensis* from South Africa. Of the *Contracaecum* species known from South Africa, only the gene fragments of *C. ogmorhini* Johnston *et* Mawson, 1941 from the Cape fur seal *Arctocephalus pusillus* are available in GenBank (Jabbar *et al.*, 2013; Nadler *et al.*, 2000; Shamsi *et al.*, 2009; Zhu *et al.*, 2001). Because the morphology of the third stage larvae of different *Contracaecum* species is almost indistinguishable and our specimens clearly differed from *C. ogmorhini* (KU558726) in the *COX1* alignments (only 582 of 689 bp are identical for both species), we could only identify the recovered specimens to genus level.

Falcaustra sp.

Site of infection: Intestine and stomach.

Sequences for this species could not be obtained.

Figure 3.4

General description. Comparatively short nematodes, with maximum width at body mid-length. Apical: three large anterior labia, with two circles of papillae (six inner and six outer), oral opening rounded-triangular shape. Oesophagus long, consisting of short anterior pharyngeal region, long cylindrical corpus, short, slightly expanded isthmus and well-developed posterior bulb. Nerve ring encircling oesophagus at level of its anterior quarter. Excretory pore at level of oesophageal bulb. Tail tapering, with sharpened end in both sexes.

Male (morphometrics based on four specimens). Body 5.4–9.3 mm (7.3 mm) long, 143–281 (197) wide. Oesophagus 1.1–1.5 (1.3) long, 16–21% (19%) of body length; 31–47 (37), 44–77 (62) and 110–159 (136) wide at anterior, mid-length and posterior level, respectively. Nerve ring at 294–345 (321) from anterior end, 22–29% (24%) of oesophagus length. Excretory pore at 741–1193 (1038) from anterior end. Posterior end of body coiled ventrally. Spicules equal, sharpened at tips, 318–453 (380) long. Gubernaculum short, narrowing towards posterior end, 65–102 (84) long. Caudal end with papillae: three pairs pre-cloacal, one unpaired papilla just anterior to cloaca, six pairs post-cloacal (three pairs of subventral papillae and one pair of lateral papillae anterior to cloaca plus two subventral pairs close to tail tip). Phasmids at level of tail mid-length. Tail tapering, 240–321 (285) long.

Female (morphometrics based on three specimens). Body 6.7–9.7 mm (8.3 mm) long, 163–222 (191) wide. Oesophagus 1.5–1.9 mm (1.6 mm) long, 19–22% (20%) of body length; 41–57 (48), 65–72 (68) and 142–165 (152) wide at anterior, mid-length and

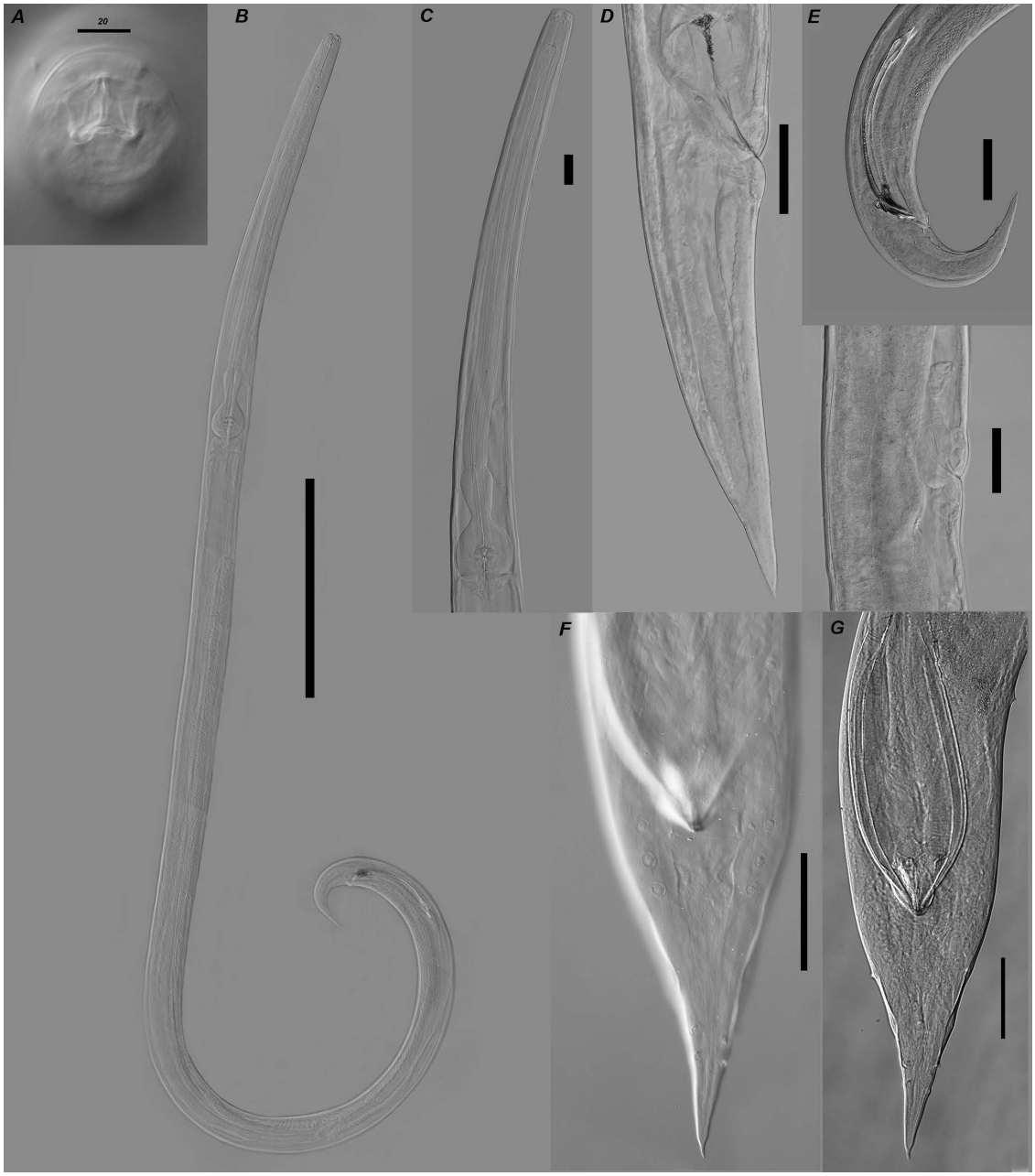

Figure 3.4: Adult *Falcaustra* sp. from the digestive tract of *Xenopus laevis*, photomicrographs. **a** – anterior end of body, male, apical view; **b** – male, general view; **c** – anterior end of body, male, lateral view; **d** – posterior end of body, male, lateral view; **e** – posterior end of body, female, lateral view; **f** – part of body at vulva region, lateral view; **g,h** – posterior end of body, male, ventral view. Scale bars: **a:** 50 μm; **b:** 1 mm; **c–h:** 100 μm

posterior level, respectively. Nerve ring at 370–390 (380) from anterior end, 21–25% (23%) of oesophagus length. Excretory pore at 1110–1396 (1277) from anterior end. Vulva post-equatorial, 4.3–6.6 mm (5.5 mm) from anterior end, 64–68% (66%) of body length. Tail tapering, 355–489 (403) long.

Remarks

The examined specimens were assigned to the genus *Falcaustra* because of the presence of three well-developed labia and a differentiated oesophageal bulb with well-developed valves (Anderson, 2000). Our specimens differed from most of the other African species of *Falcaustra* described from fish and terrapins by the absence of a pseudosucker on the male tail (Baker, 1983; Moravec & Scholtz, 2017). The same parameter is described for the three fish-parasitising species, namely *F. piscicola* (von Linstow, 1907), *F. verbekei* Campana-Rouget, 1961 and *F. therezieni* Petter, 1979 and for the two species from amphibians, namely *F. hinkeli* Jackson, 2000 and *F. puylaerti* Jackson, 2000 from *Xenopus* spp. (including *X. laevis*) (Jackson, 2000). The specimens from our material differ from the latter two species in metrical characters, such as size of the gubernaculum (65–102 μm in *Falcaustra* sp. *vs* 44–65 μm and 42 μm in *F. hinkeli* and *F. puylaerti*, respectively), length of the spicules (318–453 μm in *Falcaustra* sp. *vs* 151 μm in *F. puylaerti*) and length of the female tail (350–489 μm in *Falcaustra* sp. *vs* 560–1060 μm in *F. hinkeli*) in comparably sized worms. *Falcaustra* sp. also clearly differs from the fish-parasitising species by the number of post-cloacal papillae: it has six pairs, whereas *F. piscicola* possesses eight pairs and *F. verbekei* and *F. therezieni* possess seven pairs (Bursey *et al.*, 2018; Yorke & Maplestone, 1926). Despite the clear morphological differences, we prefer not to describe a new species but rather to assign the recovered specimens to *Falcaustra* sp. as a result of the limited sample size and lack of gravid females.

***Paraquimperia* sp.**

Site of infection: Intestine.

Representative DNA sequences: MN526249 (*COX1*), MN526251 (*18S*), MN526257 (*28S*).

Figure 3.5

Third stage larva (morphometrics based on two specimens). Body thin, elongated, 4.0–5.7 mm long, 77–114 wide. Oesophagus club-shaped, 416–712 long, 7–18% of body length; 12–13, 21–25, 20–27 and 52–69 wide at anterior, anterior dilation, mid-length and posterior bulb level, respectively. Nerve ring encircling oesophagus at anterior half, at 170–211 from anterior end of body; 30–41% of oesophagus length. Excretory pore (found in one specimen) at 436 from anterior end of body. Genital primordium small, situated at mid-body region. Tail short, tapering, 218–290 long.

Remarks

The recovered specimens corresponded to *Paraquimperia africana* (JF803925) in 99% of their *18S rRNA* fragments (683 of 684 bp are identical for both species) (Moravec, 2007). The genus *Paraquimperia* currently includes only three species, found in the intestines of eels and additionally reported from several cyprinid and percid fish (Baylis, 1934; Cone

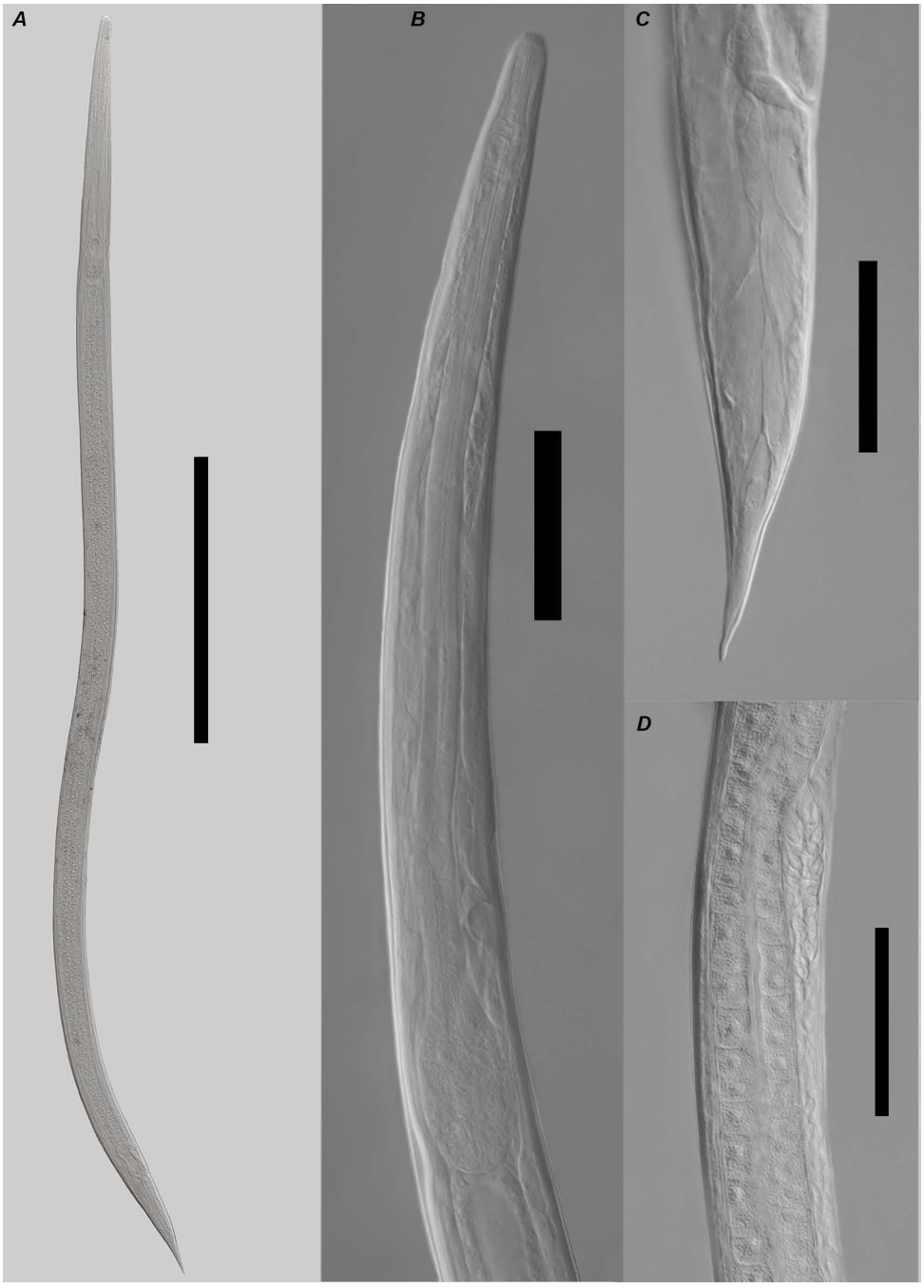

Figure 3.5: Third stage larval *Paraquimperia* sp. from the digestive tract of *Xenopus laevis*, photomicrographs. **a** – general view; **b** – anterior end of body, lateral view; **c** – posterior end of body, lateral view; **d** – fragment of body at genital primordium region, lateral view. Scale bars: **a:** 1 mm; **b–d:** 100 μm

et al., 1993; Gupta & Bakshi, 1984; Hanek & Molnar, 1974; Hanek & Threlfall, 1970; Ivashkin & Khromova, 1976; Jackson, 1978; Karve, 1941; Køie, 1988; Lin *et al.*, 2015; Marcogliese & Cone, 1996; Moravec, 1966a,b, 1994, 2007; Moravec *et al.*, 2000; Mueller, 1934; Naidu, 1983; Nie & Kennedy, 1991; Saraiva & Chubb, 1989; Sasal *et al.*, 2008; Šrámek, 1901; Thielin *et al.*, 2007; Yamaguti, 1961). The only species described from Africa is *P. africana* Moravec, Boomker *et* Taraschewski, 2000 (Jackson, 1978; Moravec

et al., 2000). Because *18S rRNA* is very conservative, a difference of one nucleotide in a comparatively short fragment could be considered as interspecific. Therefore, until numerous sequences of different genes from different species have been obtained, we prefer to assign the recovered specimens to *Paraquimperia* sp.

***Tanqua* sp.**

Site of infection: Encysted in the intestine.

Representative DNA sequences: MN526252 (*18S*), MN526258 (*28S*).

Figure 3.6

Third stage larva (morphometrics based on four specimens). Body thin, elongated, with maximum width at mid-length level. Body 8.8–10.8 mm (10.0 mm) long, 281–315 (292) wide. Anterior end with two minute pseudolabia, not reaching each other. Oesophagus elongated, evenly widening towards posterior end, 2.6–3.0 mm (2.8 mm) long, 27–30% (28%) of body length; 37–47 (41), 79–137 (117) and 153–203 (174) wide at anterior, mid-length and posterior level, respectively. Nerve ring encircling oesophagus at its anterior end, 294–338 (316) from anterior end, 11–11% (11%) of oesophagus length. Excretory pore situated at 372–443 (411) from anterior end, 4–4% (4%) of body length. Tail short, tapering, with rounded tip, 162–197 (180) long.

Remarks

Representatives of the genus *Tanqua* are specific parasites of various species of *Varanus* lizards. Only *Tanqua tiara* (von Linstow, 1879) has previously been reported from South Africa from *V. albigularis* and *V. ornatus* (Baylis, 1939; Hering-Hagenbeck & Boomker, 2000; Leiper, 1908; von Linstow, 1879). A very close relative of *T. tiara*, possibly a congeneric species, based upon Bayesian inference of phylogeny, has previously been recorded as encysted third stage larvae from the swim bladder of the African longfin eel *Anguilla mossambica* from the Eastern Cape in South Africa (Laetsch *et al.*, 2012). The partial *28S rRNA* sequence (JF805627) of this specimen is identical (702 of 702 bp) to the corresponding base pairs of our slightly longer *28S rRNA* sequence (990 bp), but no morphological description or taxonomic identification is provided by the authors (Laetsch *et al.*, 2012). Moreover, our collected specimens differed in less than 1% (one of 681 bp) of their *18S rRNA* fragments from *T. tiara* (JF934728), reported by the same authors from *Varanus indicus* in Australia (Laetsch *et al.*, 2012). Nevertheless, as a result of the comparatively short fragment of *18S rRNA* available and its high level of conservatism, in addition to the fact that we only have larval stages, we prefer to assign our specimens to *Tanqua* sp.

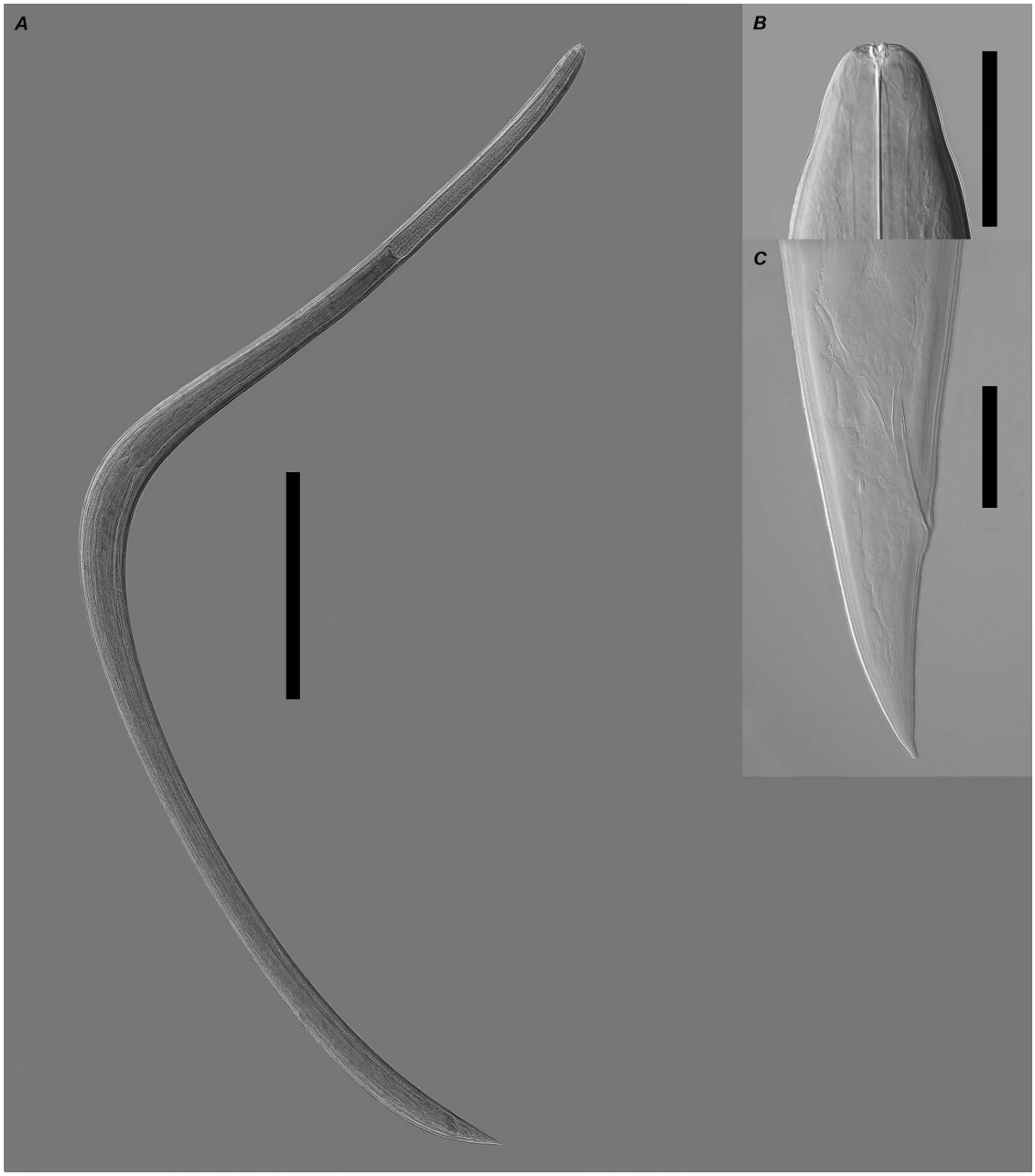

Figure 3.6: Third stage larval *Tanqua* sp. from the digestive tract of *Xenopus laevis*, photomicrographs. **a** – general view; **b** – anterior end of body, lateral view; **c** – posterior end of body, lateral view. Scale bars: **a:** 1 mm; **b,c:** 100 μm

Unidentified nematode larva sp. 1

Site of infection: Lungs and liver.

Representative DNA sequence: MN526253 (*18S*).

Figure 3.7a

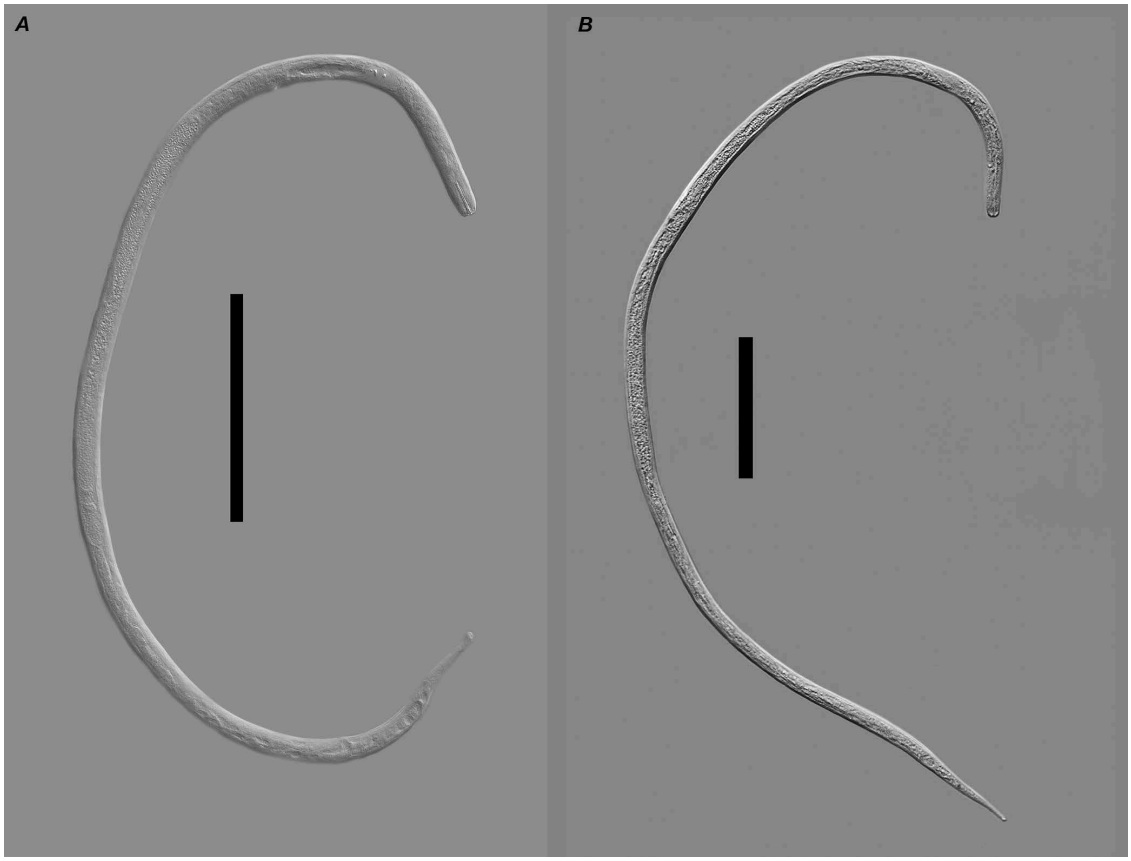

Figure 3.7: a – Unidentified second stage nematode larva sp. 1 from the lungs and liver of *Xenopus laevis*, photomicrographs. **b** – Unidentified second stage nematode larva sp. 2 from the kidneys of *Xenopus laevis*, photomicrographs. Scale bars: **a,b:** 100 μm

Second stage larva (morphometrics based on 14 specimens). Minute nematodes, body thin, elongated, 530–619 (583) long, 12–14 (13) wide at mid-length level. Stoma elongated, cylindrical, 13–18 (15) long. Oesophagus narrow, oesophageal-intestinal junction poorly visible. Genital primordium not found. Tail short, with rounded end, 14–32 (24) long.

Unidentified nematode larva sp. 2

Site of infection: Kidneys.

Representative DNA sequence: MN526254 (*18S*).

Figure 3.7b

Second stage larva (morphometrics based on eight specimens). Minute nematodes, body thin, elongated, 665–921 (800) long, 13–17 (15) wide at mid-length level. Stoma elongated, cylindrical, 7–14 (9) long. Oesophagus narrow, oesophageal-intestinal junction poorly visible. Nerve ring at 45–69 (60) from anterior end. Genital primordium not found. Tail short, tapering, with rounded tip.

Remarks for unidentified sp. 1 and 2
Two different species of larvae were recovered from the lungs and kidneys, respectively. The perceived differences in morphological characters (body length, stoma length) and the site of infection were also confirmed by the molecular data of the *18S rRNA* alignment (94.6% pairwise identity). Nevertheless, BLAST (Altschul *et al.*, 1990) searching places both species closest to nematodes from the family Thelastomatidae and the genera *Blattophila* Cobb, 1920 and *Travassosinema* (Rao, 1958). Representatives of these taxa are commonly found in arthropods (insects and myriapods). Both species were found in high numbers in organs other than the digestive tract, accordingly post-cyclic or occasional infection is rather unlikely. In our opinion, they could well represent some primitive species of nematodes using *X. laevis* as an intermediate or paratenic host.

3.3.2 Role of *Xenopus laevis* in the transmission of nematode species

Of the seven species of nematodes reported here, subadult and ovigerous females were found for *Capillaria* sp.; adult males and females for *Falcaustra* sp.; third stage larvae for *Contracaecum* sp., *Paraquimperia* sp. and *Tanqua* sp.; and second stage larvae of unidentified larvae sp. 1 and unidentified larvae sp. 2. Based on the available information on the life cycles, sites of infection and developmental stages of the retrieved nematodes, we propose the role that *X. laevis* could play in their transmission (Figure 3.8).

Both direct and indirect life cycles have been described for fish-parasitising capillariids (Køie, 1988; Moravec *et al.*, 1987). Because subadult and adult stages were found in the intestines, we consider *X. laevis* as a definitive host for the recovered *Capillaria* sp.

Third stage larvae of *Contracaecum* sp. were found encysted on the surface of the internal organs and in the body cavity, similar to previous findings of these nematodes in fish species (Moravec *et al.*, 2016). Accordingly, we consider *X. laevis* as an intermediate and possible paratenic host for *Contracaecum* sp.

Because all the retrieved *Falcaustra* sp. specimens were adults and members of this genus usually make use of one intermediate host during their life cycle (Skrjabin *et al.*, 1964), *X. laevis* could well be the definitive, or less likely paratenic, host for these nematodes.

Third stage larvae of *Paraquimperia* sp. (known as a fish-parasitising genus) were found in the intestines of the studied frogs. Because of a lack of information on the life cycle of these nematodes, *X. laevis* could equally be considered as either a definitive or paratenic host for the recovered *Paraquimperia* sp.

Third stage larvae of *Tanqua* sp. were observed encysted in intestines of *X. laevis*. Because the life cycle of this genus is poorly studied, *X. laevis* could either play a role as an intermediate or a paratenic host for the retrieved *Tanqua* sp.

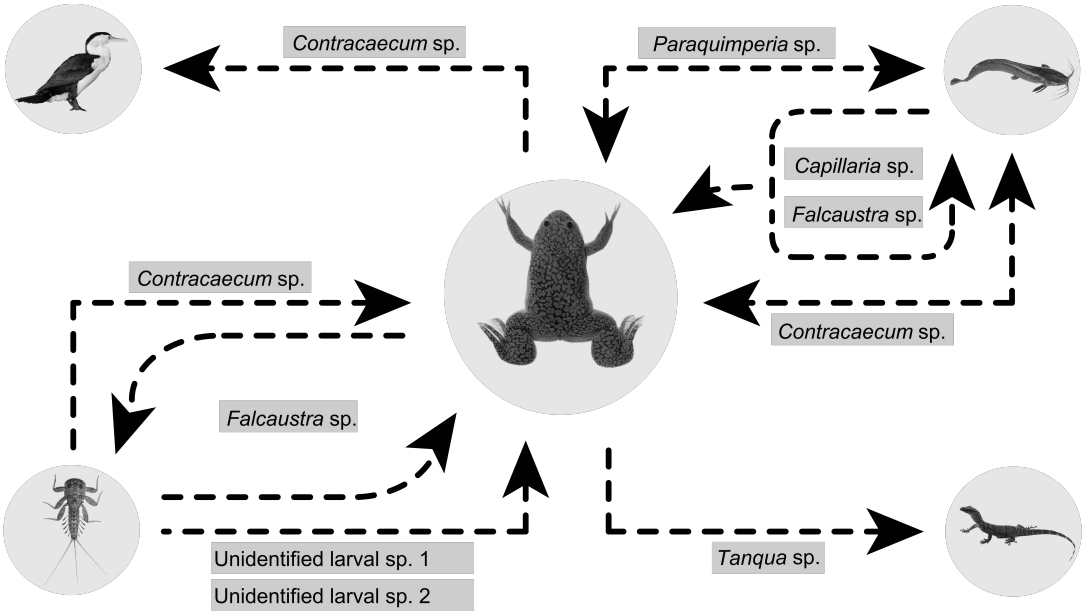

Figure 3.8: Hypothesised trophic transmission in a freshwater ecosystem of the seven nematode parasites recovered in the current study. *Xenopus laevis* (centre) acts as an intermediate or paratenic host for the larval stages of *Contracaecum* sp., *Paraquimperia* sp., *Tanqua* sp. and two other unidentified second stage larvae and is a possible definitive host for the adult stages of *Capillaria* sp. and *Falcaustra* sp. Other hosts include, from the top left corner in a clockwise direction, fish-eating birds, fish, semi-aquatic lizards and aquatic invertebrates. Arrow heads point in the direction of the predator.

Both of the unidentified larval species were found unencapsulated and in high numbers in blood-filled organs (lungs and kidneys). Therefore, these species most likely use *X. laevis* as an intermediate host.

3.4 Discussion

In total, approximately 1400 specimens of seven species of nematodes from ten localities throughout South Africa were found parasitising *X. laevis*. The most widespread were encysted *Contracaecum* sp. third stage larvae, with a total of 183 specimens parasitising between 10 and 50% of the hosts at five of the studied localities. The other two species that were also recovered as third stage larvae, namely four *Paraquimperia* sp. and nine *Tanqua* sp. specimens, were recovered at just one locality each. Of the adult specimens, nine female *Capillaria* sp. were recovered from hosts at two localities in the Western Cape, whereas three females and four males of *Falcaustra* sp. were recovered from only one locality in the same area. The first species of unidentified second stage larvae was present in very high numbers (about a thousand larvae in total) in the lungs of half of the hosts at three localities. Conversely, approximately 150 specimens of the second species of unidentified second stage larvae were observed in the kidneys of only one frog.

Of these nematodes, only representatives of the genus *Contracaecum* have previously been reported from *X. laevis*, not in the native range, but in California and Chile (Castillo *et al.*, 2017; Kuperman *et al.*, 2004). The other six species are recorded from *X. laevis* for the first time herein, although the possibility of associations with nematodes in the native range has been suggested by a few earlier reports (Brayton, 1992; Cosgrove & Jared, 1974; Thurston, 1970). Surprisingly, this high number of novel parasite associations is reported despite more than 100 years of investigations and numerous parasitological surveys of *X. laevis* since the early 1900s (Aisien *et al.*, 2004; Avery, 1971; Beverley-Burton, 1963; Bruňanská *et al.*, 2012; Cohn, 1906; Cosgrove & Jared, 1974; Crous & du Preez, 1997; de Puytorac & Grain, 1965; Dick, 1959; Dollfus, 1968; du Preez *et al.*, 1996; Elkan & Murray, 1952; Feldman & Ramirez, 2014; Ferguson & Appleton, 1988a,b; Fischthal & Thomas, 1968; Harris & Tinsley, 1987; Metcalf, 1923; Jackson & Tinsley, 1988, 1995a,b, 1997, 1998a,b, 2001a,b; King & van As, 1992, 1997, 2000; Kruger *et al.*, 1991; Kruger & du Preez, 2015; Mettrick, 1963; Macnae *et al.*, 1973; Manter & Pritchard, 1964; Moravec & Cosgrove, 1982; Nigrelli & Maraventano, 1944; Porter, 1938; Price, 1943; Pritchard, 1964; Sandon, 1941; Southwell & Kirshner, 1937; Svitin *et al.*, 2018; Theunissen *et al.*, 2014; Thurston, 1967, 1970; Tinsley, 1996; Tinsley & Sweeting, 1974; Tinsley & Whitear, 1980; Tinsley & Wynne Owen, 1975, 1979; Tinsley & Jackson, 1995, 1998a,b; Vercammen-Grandjean, 1960; Wade, 1982; Williams, 1959; Yeh, 1960a,b). We suggest that these new host-parasite associations could be a result of the continuous domestic expansion (de Villiers & Measey, 2017; Measey & Davies, 2011; Measey *et al.*, 2017) and deliberate translocation (van Sittert & Measey, 2016) of *X. laevis* in its native range, with underrepresentation in the literature possibly heightened by the oversight of larval stages of nematodes in this frog in past investigations.

Unfortunately, as a result of a lack of molecular data, absence of clear morphological descriptions of larval stages and poorly studied life cycles of the recovered nematodes, we were not able to identify any of the collected nematodes to the species level and some not even to the family level. Indeed, even those specimens that were recovered in their adult stage could only be identified to the genus level. This was true for *Capillaria* sp. that lacked males and *Falcaustra* sp. that lacked gravid females. In the case of the five species recovered as second or third stage larvae, it is almost impossible to distinguish larval stages of congeneric nematode species without applying molecular tools, because of high levels of morphological similarity at this stage of development (Anderson, 2000). Unfortunately, very few species of nematodes parasitising ectothermic vertebrates from Africa have sequences available in GenBank and none of those available clearly correspond to the obtained sequences of the nematodes from the current study.

What is more, as a result of a lack of information on life cycles of African nematodes at large, we cannot specify the exact role of *X. laevis* in the transmission of the nematode species recovered during the current study. Nevertheless, in light of the data available on nematode life cycles, distribution, sites of infection and preferred host taxa from the region,

we propose that *X. laevis* could be a definitive host for two species (*Capillaria* sp. and *Falcaustra* sp.), a paratenic host for three species (*Contracaecum* sp., *Paraquimperia* sp. and *Tanqua* sp.) and an intermediate host for four species (*Contracaecum* sp., *Tanqua* sp. and both species of unidentified larvae). These findings highlight the key role of *X. laevis* in the parasite dynamics of the freshwater ecosystems it forms part of. In many cases, it seems to act as a host for nematodes previously only associated with fish, as could be expected of an amphibian with a predominantly aquatic ecology (Elephandt *et al.*, 2000). This is illustrated by the past records of *Capillaria* sp. (Boomker, 1994a; Moyo *et al.*, 2009), *Contracaecum* sp. (Barson, 2004; Barson & Avenant-Oldewage, 2006; Barson *et al.*, 2008; Boane *et al.*, 2008; Boomker, 1982, 1994a,b; Madanire-Moyo *et al.*, 2010; Mashego, 1989; Mashego & Saayman, 1981; Mbokane *et al.*, 2015; McHugh *et al.*, 2016; Moravec *et al.*, 2016; Moravec & van As, 2015; Moyo *et al.*, 2009; Sara *et al.*, 2014; Smit & Luus-Powell, 2012; Tavakol *et al.*, 2015; van As & Basson, 1984; Whitfield & Heeg, 1977) and *Paraquimperia* sp. (Jackson, 1978; Moravec *et al.*, 2000), which hail from freshwater fish in Africa. Furthermore, previously undescribed routes of trophic nematode transmission via *X. laevis* to piscivorous birds, in the case of *Contracaecum* sp. (Barson, 2004; Whitfield & Heeg, 1977), and semi-aquatic varanid lizards, in the case of *Tanqua* sp. (Baylis, 1939; Hering-Hagenbeck & Boomker, 2000; Leiper, 1908; von Linstow, 1879), are suggested.

Clearly, as has been shown for other invasive species (Amundsen *et al.*, 2013; Dunn & Smyth, 2005; Roy & Lawson Handley, 2012), the potential effects of *X. laevis* on freshwater ecosystems go beyond direct interactions. The current study demonstrates that *X. laevis* is a versatile parasite reservoir in its native range where it is a known domestic exotic, embarking on frequent pioneer and expansion events (Measey & Davies, 2011; Measey *et al.*, 2017). Potentially, it alters the parasite dynamics of not only nematodes associated with other amphibians, but also those of fish, reptile, bird and even invertebrate fauna, ultimately modifying trophic interactions at a large scale. Studies from the invasive range imply a similar role in the new habitats of *X. laevis*, where it has been shown to form novel associations with both larval nematodes and digeneans (Castillo *et al.*, 2017; Kuperman *et al.*, 2004; Rodrigues, 2014).

Previous authors have warned that we remain ignorant of the native ecology of *X. laevis* to the detriment of its management elsewhere (Measey *et al.*, 2012). The current study provides an example of how that might play out. Notably, third stage larvae of *Contracaecum* have been reported before from *X. laevis* in the invasive range on two occasions (Castillo *et al.*, 2017; Kuperman *et al.*, 2004). Yet, because there had been no records of *Contracaecum* associated with *X. laevis* in the native range before, the records in the invasive range were assumed to originate from the native fauna of the invasive regions. Whether this claim is true could probably only be ascertained by sufficient molecular data and morphological descriptions, both of which are lacking for *Contracaecum* in the native and invasive range.

When investigating the ecology of invasive species, the far-reaching effect of parasites should not be underestimated. It is specifically trophically transmitted parasites, of which all the recovered species are examples, that play the most prominent role in the alteration of networks post introduction (Amundsen *et al.*, 2013). Introduced hosts could cause amplification and dilution effects for native parasite dynamics (Telfer & Bown, 2012). For example, the arrival of another invasive amphibian in Australia, the cane toad, has been associated with lowered lungworm burdens in native toads, because they act as ”dead-ends” for native parasites (Nelson *et al.*, 2015; Selechnik *et al.*, 2017).

Regrettably, these effects are not known for *X. laevis*, an invasive amphibian with a much greater global footprint than the cane toad. As a starting point to remedy this gap in our knowledge, the current study clearly shows the importance of the inclusion of molecular data, morphological descriptions and qualitative illustrations in parasitological surveys in Africa, even when reporting on the presence of larval stages. In addition, future investigations of *X. laevis* in its invasive range should not discount the insidious effects of parasites, both co-invading and newly associated, when determining the impact and subsequent management strategies of this globally invasive amphibian.

Chapter 4

Repeated reduction in parasite diversity in invasive populations of *Xenopus laevis*: a global experiment in enemy release

4.1 Introduction

In the Anthropocene, the world's biota is experiencing modification at unprecedented rates (Bar-On *et al.*, 2018; Ceballos *et al.*, 2015). The increasing magnitude of human-mediated animal, plant and pathogen translocation to novel environments has led to growing interest in the discipline of invasion science (Richardson & Ricciardi, 2013). Since the inception of modern invasion ecology following Charles Elton's seminal book (1958), several hypotheses have been developed to explain the disproportionate success of invasive species (Jeschke, 2014). Opportunely, the natural experiment arising from the global distribution of certain invasive species, such as rats and Australian acacias, has presented conservationists with a unique opportunity to test evolutionary and ecological hypotheses across independent geographical replicates (Morand *et al.*, 2015; Richardson *et al.*, 2011a).

Oft cited among the hypotheses in invasion ecology is the Enemy Release Hypothesis (ERH), which ascribes the increased fitness of invasive species to a release from the effects of natural enemies, such as co-evolved parasites, during the process of co-invasion (Keane & Crawley, 2002; Torchin & Mitchell, 2004). The ERH is empirically supported across a wide range of invasive taxa, particularly in terms of parasite loss, which holds true for the majority of invasive species in their non-native ranges (Heger & Jeschke, 2014;

Lui & Stiling, 2006; Torchin *et al.*, 2003; Torchin & Mitchell, 2004). However, the validity of the ERH as a unifying theory in invasion ecology suffers, among other concerns, from a lack of studies conducted on a global scale (Blackburn & Ewen, 2017; Lester *et al.*, 2015; Prior *et al.*, 2015; Prior & Hellmann, 2015; Schultheis *et al.*, 2015). For example, in invasive amphibians, the only two studies which have investigated parasite loss to date were conducted on two species of tree frog, *Eleutherodactylus coqui* and *Osteopilus septentrionalis*, that are both native in and invasive to Central America (Marr *et al.*, 2008; Ortega *et al.*, 2015). In fact, comparatively few studies have investigated the ERH in globally distributed animals from any class, notable exceptions being the repeated parasite loss demonstrated in both the European house sparrow and the European green crab (Marzal *et al.*, 2011; Torchin *et al.*, 2001).

In the light of this, the globally invasive frog, *Xenopus laevis* (Daudin, 1802) (Anura: Pipidae), with its multiple invasive populations on four continents, is eminently suited to test the ERH on a global scale (Measey *et al.*, 2012). Its spread from southern Africa to other continents was initiated in the early 1930s, when it was widely adopted as a biological pregnancy assay and later as a model animal for research and education (Gurdon & Hopwood, 2000; Shapiro & Zwarenstein, 1934; van Sittert & Measey, 2016). The global range expansion of *X. laevis* has not been halted since, with climate change and an inherent adaptability to novel environments boosting their invasive potential in many regions (Ihlow *et al.*, 2016; Rödder *et al.*, 2017; van Sittert & Measey, 2016). Furthermore, as a domestic exotic in southern Africa, the invasiveness of *X. laevis* is not just confined to populations outside of its native range (Measey & Davies, 2011; Measey *et al.*, 2017). Since the onset of trade in this frog, *X. laevis* has been translocated in the native range in large numbers (van Sittert & Measey, 2016), further expanding its range without direct human mediation by moving overland or via farm dams and artificial waterways (de Villiers & Measey, 2017; Fouquet & Measey, 2006; Measey, 2004, 2016; Measey *et al.*, 2012).

Moreover, the fact that its parasite fauna has been well studied, makes *X. laevis* the ideal model to test the ERH in terms of parasites as natural enemies. Since the description of its first associated parasite (Cohn, 1906), over 20 metazoan parasite species have been associated with it in its native range (Avery, 1971; Beverley-Burton, 1963; Cosgrove & Jared, 1974; Crous & du Preez, 1997; Dick, 1959; du Preez *et al.*, 1996; Elkan & Murray, 1952; Ferguson & Appleton, 1988a,b; Fischthal & Thomas, 1968; Harris & Tinsley, 1987; Héritier *et al.*, 2015; Jackson & Tinsley, 1995a,b, 1997, 1998b, 2001a; King & van As, 1992, 1997, 2000; Kruger & du Preez, 2015; Macnae *et al.*, 1973; Manter & Pritchard, 1964; Moravec & Cosgrove, 1982; Nigrelli & Maraventano, 1944; Pritchard, 1964; Prudhoe & Bray, 1982; Southwell & Kirshner, 1937; Svitin *et al.*, 2018; Theunissen *et al.*, 2014; Thurston, 1967, 1970; Tinsley & Jackson, 1995; Tinsley & Whitear, 1980; van der Lande & Tinsley, 1976; Vercammen-Grandjean, 1960; Wade, 1981, 1982). Likewise, the parasitic fauna of the established invasive populations, although not as well studied as in the native range, nonetheless have been surveyed on three continents. Hitherto, two full

parasitological surveys have been conducted in California and Chile (Castillo *et al.*, 2017; Kuperman *et al.*, 2004). A third investigation into the parasites of *X. laevis* in Portugal remains unpublished (Rodrigues, 2014).

Few host-parasite systems lend themselves to inform a global perspective on the fate of co-evolved parasites during the process of invasion. This study aimed to address this gap by testing the ERH on geographical replicates of metazoan parasite communities of a globally distributed amphibian. To this end, this study included full parasitological surveys of *X. laevis* across the whole of the native range and in the invasive population in Western France to enhance the existing data available from the invasive populations in Chile, California and Portugal (Castillo *et al.*, 2017; Kuperman *et al.*, 2004; Rodrigues, 2014). Specifically, we aimed to address the questions of (1) whether invasive *X. laevis* populations exhibited loss of metazoan parasites, both in terms of species richness and infection levels, (2) what factors caused parasites to accompany *X. laevis* to the invasive range, (3) whether these accompanying parasites attained as high infection levels in the invasive range as in the native range and (4) how the metazoan parasite community compositional dissimilarities correlate with the geographical origin of *X. laevis* populations.

4.2 Methods

4.2.1 Host and parasite collection in France

In June 2017, a total of 43 adult *X. laevis*, 17 males and 26 females, were collected by the eradication programme in baited funnel traps from six sites across the invasive range of *X. laevis* in western France (Figure 4.1b). After five weeks of experimental breeding, where the live animals were kept separately by collection site, the frozen corpses of the frogs were made available for parasitological analysis. Although laboratory conditions can be stressful for hosts, the metazoan parasites of *X. laevis* that have been examined in this regard all have the ability to survive even longer periods of laboratory maintenance (Elkan & Murray, 1952; Jackson & Tinsley, 1988; Thurston, 1970; Tinsley, 1972, 1996; Tinsley & Whitear, 1980; Tinsley & Sweeting, 1974; Tinsley & Wynne Owen, 1979), meriting the inclusion of this survey in this comparative study. All frogs were screened for parasites approximately two weeks *post mortem*. Before dissection, the thawed frogs were measured and the epidermis, lateral line, eyes, buccal cavity, Eustachian tubules and nostrils were examined for external parasites. Thereafter, the body was slit open longitudinally and the alimentary tract, kidney, excretory bladder, gall bladder with bile ducts, liver, lungs, heart and reproductive organs were removed and examined separately for internal parasites using a stereomicroscope. Helminths were collected, counted, fixed in warm ethanol and stored in 70% ethanol.

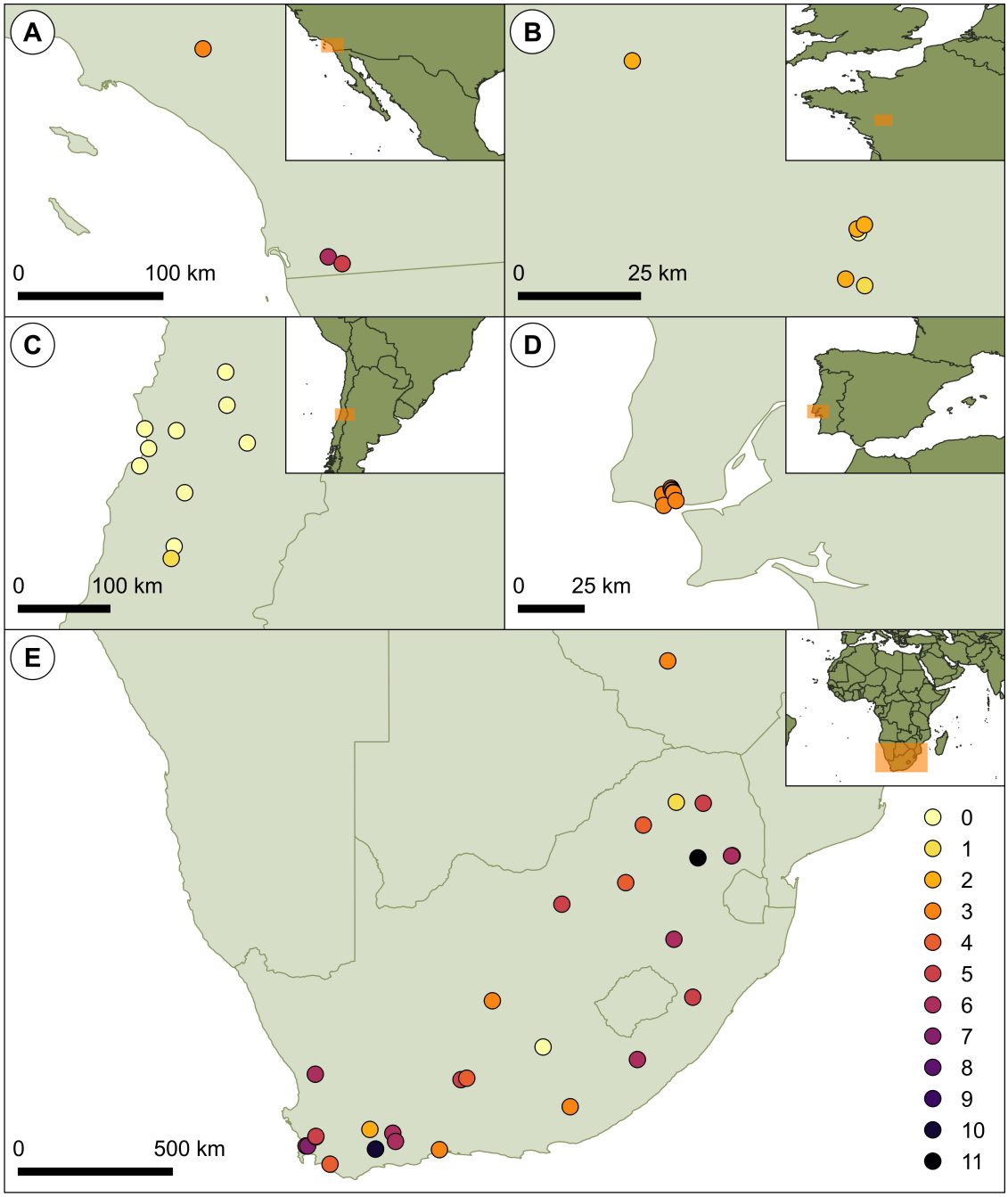

Figure 4.1: Recovered parasite species richness at 47 sites where full parasitological surveys of *Xenopus laevis* were conducted. This includes data from three previously published works from the invasive range, namely **a** – three sites in California, North America (Kuperman *et al.*, 2004), **b** – nine sites in Chile, South America (Castillo *et al.*, 2017) and **d** – eight concatenated sites in Oeiras, Portugal, Europe (Rodrigues, 2014). Newly generated data from **e** – 27 sites from across the native range in Southern Africa and **c** – six sites from western France, Europe are also included. The parasite species richness at a site is indicated by its position on the colour scale, ranging from zero (light yellow) to eleven (black). All maps are displayed according to the Mercator projection.

4.2.2 Parasite identification in the French population

Since freezing can be damaging to the internal structures of soft-bodied parasites, traditional morphological methods could not be used to identify the recovered parasites. Rather, the specimens were tentatively identified to morphospecies based upon site of infection and general body structure. These identities were confirmed through molecular techniques with the DNA barcoding gene, *COX1*, by using two specimens per morphospecies as representative of the whole population. DNA was extracted from two specimens per morphospecies (one from a core site and one from a peripheral site) using the PCRBIO Rapid Extract PCR Kit (PCR Biosystems Ltd., London, United Kingdom). The *COX1* amplicons were obtained using the forward primer 'L-CO1p' (5'-TTTTTTGGGCATCCTGAGGTTTAT-3') and the reverse primer 'H-Cox1p2' (5'-TAAAGAAAGAACATAATGAAAATG-3') (Littlewood *et al.*, 1997). The thermocycling profile proposed by Verneau *et al.* (2009) was implemented. Sequences were obtained on an ABI3500XL sequencer using BigDye® Terminator *version* 3.1 Cycle Sequencing. Specifically, DNA products were sequenced in both directions using the PCR primer pair, yielding a sequence of approximately 450 bp. Sequences were assembled, edited using Geneious *version* 9.0 software (Biomatters Ltd., Auckand, Nieu-Seeland) and compared with existing *COX1* sequences on GenBank to confirm species identity (Héritier *et al.*, 2015; Waeschenbach *et al.*, 2017). Sequences were submitted to the GenBank database under the accession numbers MK342937–40.

4.2.3 Host and parasite collection in South Africa

A total of 172 adult *X. laevis* were collected from March 2017 to February 2018 in baited funnel traps from 27 sites across the native range in southern Africa, specifically including collection localities from the known distribution of all the mitochondrial lineages (de Busschere *et al.*, 2016; Furman *et al.*, 2015) (Figure 4.1e). All frogs were sacrificed within a month of collection according to internationally accepted standard operating procedures. Anaesthesia in 6% ethyl-3-aminobenzoate methanesulfonate (MS222) (Sigma-Aldrich Co., Steinheim, Germany) was followed by euthanasia through cutting the spine and destroying the brain. Subsequent host measurements and parasite screening and collection were performed immediately *post mortem* using the same methods as for the hosts and parasites in France. All parasites were preserved in 70% ethanol.

4.2.4 Parasite identification in South Africa

Morphological species identification was sufficient for the majority of the parasites recovered in South Africa, since the parasites of *X. laevis* are well-described in the native range. In addition, the parasites were removed from the hosts whilst still alive and could

be optimally fixed for morphological studies. For this reason, molecular techniques were only employed for the identification of some of the larval nematodes and digenean metacercariae. Extraction and sequencing followed exactly the same procedure as for the parasites from France. The larval nematodes were distinguished from one another and species on GenBank with the help of the *COX1* gene, for which amplicons were obtained with the forward primer 'LCO1490' (5'-GGTCAACAAATCATAAAGATATTGG-3') and the reverse primer 'HCO2198' (5'-TAAACTTCAGGGTGACCAAAAAATCA-3') (Folmer *et al.*, 1994) and the following thermocycling profile: initial denaturation at 95℃ for 2 min, followed by 35 cycles of denaturation at 95℃ for 30 s, annealing at 50℃ for 30 s and elongation at 72℃ for 2 min, terminated by one cycle of elongation at 72℃ for 7 min. The digenean metacercariae were told apart by the complete internal transcribed spacer (*ITS*) gene region, which was amplified by the forward and reverse primers 'D1' (5'-AGGAATTCCTGGTAAGTGCAAG-3') and 'D2' (5'-CGTTACTGAGGGAATCCTGGT-3') (Galazzo *et al.*, 2002) with the following thermocycling profile: initial denaturation at 95℃ for 3 min, followed by 35 cycles of denaturation at 95℃ for 1 min, annealing at 56℃ for 1 min and elongation at 72℃ for 2 min, terminated by one cycle of elongation at 72℃ for 5 min.

4.2.5 Parasitological surveys from the literature and clarification of parasitological parameters

Three full parasitological surveys of invasive *X. laevis*, conducted in California (Kuperman *et al.*, 2004), Chile (Castillo *et al.*, 2017) and Portugal (Rodrigues, 2014), were included for comparison (Figure 4.1a,c,d). Comparable locality-specific data does not exist for the native range, therefore only the results of our parasitological survey were included, along with our results from France. Results from sites in the same aquatic systems (such as dams on the same property connected by one river) were concatenated. In total, 47 sites were included in the comparison (refer to Appendix A for detailed information on all sites). Only metazoan parasites, including mites, leeches and helminths, were included in the analyses, owing to the fact that freezing of hosts, such as in France, will make it impossible to recover protozoan parasites. For each site, parasite species richness (number of parasites in all hosts from one site) and the per-site prevalence of each parasite species (percentage of hosts from one site infected with a given parasite species) were calculated, *sensu* (Bush *et al.*, 1997). Other parasitological parameters, namely mean intensity and mean abundance (Bush *et al.*, 1997) could not be calculated from the information available in all the source publications and were only calculated for the newly generated data from France. For further analyses, summed parasite prevalence (the sum of the prevalences of each of the parasite species at a site) and mean parasite prevalence (prevalences averaged across all parasite species present at a site) were also calculated, following Torchin *et al.* (2003). Summed prevalence gives an indication of the potential impact of the parasitism on the host population, as it is a measure of the unweighted cumulative extent

of the parasitism hosts experience at a site (Torchin *et al.*, 2003). Finally, for each of the parasite species present in the African hosts, frequency of occurrence across South Africa (percentage of sites where the parasite occurs) and mean species prevalence (per-site prevalence averaged across all sites in South Africa, excluding those with zero prevalence) were calculated.

4.2.6 Statistical analyses

Host sample size often strongly influences the number of parasite species collected at a site (Engemann *et al.*, 2015; Luque & Poulin, 2007). To determine whether the unbalanced sampling effort at the 47 sites, ranging from one individual in Zimbabwe to 132 in Dulzura Creek, California, could potentially confound our results by correlating with the recovered species richness at these sites, the Spearman's rank correlation coefficient was calculated.

To resolve whether hosts from the invasive and native ranges experienced similar levels of parasitism, the 27 native localities were compared with the 20 invasive localities in terms of parasite species richness and the summed and mean parasite prevalence with the Wilcoxon-Mann-Whitney test.

The effect of several factors on the likelihood of parasites to follow *X. laevis* out of Africa was evaluated separately. Only the parasites from the native range which could be identified to the point where sufficient life history information could be obtained, were included for analysis. The effect of parasite taxonomical class (Acari, Cestoda, Digenea, Hirudinea, Monogenea, or Nematoda), type of life cycle (direct, or indirect), life stage when present in *X. laevis* host (all stages, adult, cyst, or larva) and presence in the Western Cape province, where most of the invasive *X. laevis* originated from (de Busschere *et al.*, 2016), were assessed though the Fisher's exact test of independence. The Wilcoxon-Mann-Whitney test was employed to test the effect of host specificity (high to low: that is, recorded from a single host species, a single host genus, or multiple host genera), mean species prevalence across sites, excluding zero prevalence sites, and frequency of occurrence in South Africa on the presence or absence of a parasite in invasive populations.

We specifically selected two parasites that were the most common in both in the native and invasive ranges to examine whether parasites can attain similar infection levels in native and invasive populations. The Student's *t* test was preferred to test the effect of geographic origin on per-site prevalence, since the response variables were normally distributed for each group with equal variance.

To investigate the parasite community composition of the two ranges, two methods were utilised—firstly to test for a significant difference in community composition based upon the geographic origin of the hosts and then to visually interpret the dissimilarities. Prior

to the analyses, per-site species prevalence data were Hellinger transformed (Legendre & Gallagher, 2001), utilising the package *vegan* in R (Oksanen *et al.*, 2019). Since some sites did not share parasite species, a dummy parasite species was added to each site at a per-site prevalence level of 50%. This was done to avoid a situation of undefined dissimilarity indices between sites (see also Locke *et al.* (2012) and Warburton *et al.* (2016)). This technique is especially appropriate in cases where assemblages are impoverished for biological reasons, as is the case with invasive animals and their parasite communities (Clarke *et al.*, 2006). Bray-Curtis distances, which are not only sensitive to the presence or absence of species, but also to differences in prevalence of specific species between sites, were utilised to measure compositional dissimilarity of parasite communities between sites (Ricotta & Podani, 2017). The Bray-Curtis is a semi-metric dissimilarity index and therefore better suited to impoverished communities where species prevalence is not normally distributed. An analysis of similarity (ANOSIM) was conducted in the R package *vegan* (Oksanen *et al.*, 2019) with 999 permutations based upon the Bray-Curtis distances to test whether there was indeed a significant difference in community composition between the native and invasive ranges. Non-metric multidimensional scaling (NMDS) was also employed utilising the *vegan* R package to visualise whether the parasite communities from each of the sites fell into clearly separated geographical groups based upon compositional dissimilarity (Oksanen *et al.*, 2019). The wrapper function `metaMDS()` was exploited with 20 random starts to compute both the Bray-Curtis distances in an initial step and subsequently the solution of the ordination to visualise the parasite community dissimilarity. Ellipses were computed according the standard deviation around the centroid (weighted mean) for each group. The parasite species richness was overlaid onto the two-component ordination space, assuming a non-linear relationship *a priori*, via the fitting of a generalised additive model produced in the function `ordisurf()` (Oksanen *et al.*, 2019). The generalised additive model estimated whether there might be a significant relationship between the observed clustering and variation in species richness between the sites (Marra & Wood, 2011).

All statistical analyses were performed in the built-in package *stats* in the program R *version* 3.4.4 (R Core Team, 2018), unless mentioned otherwise. Summary statistics were computed in the R package *Rmisc* (Hope, 2013), or alternatively in *dplyr* (Wickham *et al.*, 2017). Results were visualised through the package *ggplot2* (Wickham, 2016).

4.3 Results

4.3.1 Parasitological survey in France and South Africa

The *X. laevis* from France ranged in snout-urostyle length from 25.2 to 99.3 mm (mean = 69.3 mm, SD $\pm$ 14.08). From these 43 frogs, two parasite species were morpholog-

ically and genetically identified. The parasite from the bladder was the monogenean *Protopolystoma xenopodis* (Price, 1943) Bychowsky, 1956, from the Polystomatidae and the cestode inhabiting the intestine was similarly confirmed to be *Cephalochlamys namaquensis* (Cohn, 1906), from the Cephalochlamydidae. Both species were widespread across the region, hailing from both northern and southern peripheral sites, as well as core sites close to the introduction site, with a mean species prevalence of 19% and mean intensity of two worms per host for *P. xenopodis* across four sites and a mean species prevalence of 63% and mean intensity of four worms per host for *C. namaquensis* across five sites (Table 4.1).

Table 4.1: Distribution and level of infection of the two parasites of *Xenopus laevis* from its invasive range in western France, namely *Protopolystoma xenopodis* (**p**) and *Cephalochlamys namaquensis* (**c**). The population is represented by 43 frogs from six localities. Sites 1 to 3 are towards the edge of the invasive range (periphery) and sites 4 to 6 are close to the original introduction site (core). Mean intensity of infection is given with median intensity in square brackets and minimum and maximum values in parentheses. Mean values averaged across sites include sites with zero prevalence. Absent infection level values due to absence of a parasite species at a specific collection site is denoted by 'n/a'.

Locality	Number of hosts	Prevalence		Mean abundance		Intensity	
		p	**c**	**p**	**c**	**p**	**c**
Site 1	8	38%	88%	0.9	3.3	2 [3] (1–3)	4 [1] (1–11)
Site 2	10	n/a	70%	n/a	1.0	n/a	1 [1] (1–2)
Site 3	10	20%	40%	0.2	2.0	1	5 [4] (2–10)
Peripheral sites	28	18%	64%	0.3	2.0	2 [1] (1–3)	3 [2] (1–11)
Site 4	5	n/a	n/a	n/a	n/a	n/a	n/a
Site 5	4	25%	100%	0.8	1.5	3	2 [2] (1–2)
Site 6	6	33%	83%	0.3	5.7	1	7 [3] (1–18)
Core sites	15	20%	60%	0.3	2.7	2 [1] (1–3)	4 [2] (1–18)
All sites	**43**	**19%**	**63%**	**0.3**	**2.2**	**2 [1] (1–3)**	**4 [2] (1–18)**

The frogs collected from South Africa were similar in size to those from France, ranging in snout-urostyle length from 38.3 to 110.2 mm (mean = 71.5, SD $\pm$ 15.66). From a total of 172 frogs collected from 27 sites, 21 different metazoan parasites species were recovered. These parasites represented six different taxonomic classes, namely Acari, Hirudinea, Digenea, Monogenea, Cestoda and Nematoda. Parasite species richness varied considerably, ranging from zero parasite species in the frogs from a swimming pool near Colesberg, Northern Cape, to 11 parasite species in the frogs from dams in a pristine mountain stream near Dullstroom, Mpumalanga (Figure 4.1e). The seven sites which hosted less than four parasite species in total all originated from recently disturbed or newly established habitats. These habitats included swimming pools, ornamental garden ponds, urban recreational dams, drainage from abattoirs and crop irrigation systems, temporary mountain streams, dams downstream of informal settlements and artificial ponds in botanical gardens. On the contrary, the nine host populations with parasite species richness of six or more hailed mostly from natural or permanent artificial water bodies in natural environments, such as farm dams and their connecting rivers or dams

and pools in mountain streams. Some populations with six or more parasite species were sampled in ornamental garden ponds, but from sites in the vicinity of large natural water bodies in undisturbed areas. The two most common parasite species by far were *P. xenopodis* and *C. namaquensis*, both present in 25 of the 27 sites (92.6%). The rest of the parasite species were much rarer across South Africa, only present in ten or less of the sites (maximum 37.0%). The mean species prevalence of *P. xenopodis* across all sites, including sites with zero prevalence, was higher than in France at 56%. In the case of *C. namaquensis*, the same value was 65%.

In the Chilean invasive *X. laevis*, only one parasite species, identified as a nematode larva of the genus *Contracaecum*, has been reported at a mean species prevalence of 3.4% from 179 hosts from 10 sites (Figure 4.1c) (Castillo *et al.*, 2017). The Californian *X. laevis* parasite communities, collected from 230 hosts from three sites, were much more diverse and represented parasites native to both South Africa and California (Kuperman *et al.*, 2004). Parasite species richness ranged from three to six at the three sites, with a total of seven parasite species across sites (Figure 4.1b) (Kuperman *et al.*, 2004). All three parasite communities included three South African parasites, namely the two monogeneans, *Gyrdicotylus gallieni* Vercammen-Grandjean, 1960 (mean species prevalence of 12%) and *P. xenopodis* (mean species prevalence of 47%), and the cestode, *C. namaquensis* (mean species prevalence of 47%) (Kuperman *et al.*, 2004). The Portuguese invasive *X. laevis*, represented by 80 hosts from two streams in Oeiras, harboured South African *P. xenopodis* at a mean species prevalence of 55% and two other parasites that were native to the invasive range (Figure 4.1d) (Rodrigues, 2014).

4.3.2 Effect of sampling effort

Despite great variation in sampling effort between the sites, parasite species richness was not significantly correlated with sample size (Spearman's rank correlation, $\rho_S = 0.15$, n = 47, $p = 0.31$). This did not mean that a full account was given of all the species at each site, but this result cancelled out variation in sample size as a possible confounding factor. Therefore, we did not make use of species richness estimators to correct for potential inaccuracies in subsequent analyses (Engemann *et al.*, 2015).

4.3.3 Parasitism of hosts in native and invasive ranges

Of the 21 metazoan parasite species recorded from hosts in the native range, only three parasite species successfully accompanied *X. laevis* during the process of invasion. In addition, a total of seven new parasite species, which were native to the different invasive ranges, colonised invasive *X. laevis* upon arrival. Parasite species richness was significantly higher in hosts from the native range (mean = 4.7 species per population, SD $\pm$

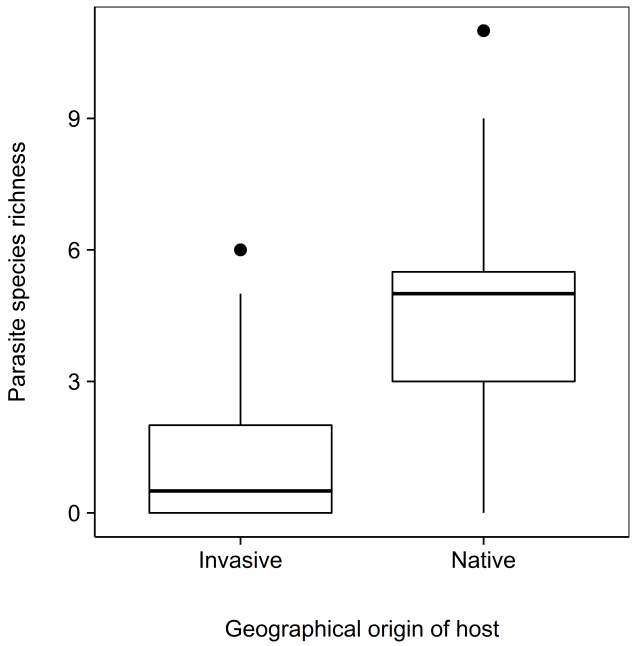

Figure 4.2: Metazoan parasite species richness of *Xenopus laevis* populations in the invasive range is lower than in the native range. Minimum, first quartile, median, third quartile and maximum species richness values are shown for 20 invasive sites from Europe and North and South America and 27 native sites from Africa. Outliers are indicated by black dots.

2.35) in comparison to those from the invasive ranges (mean = 1.4 species per population, SD $\pm$ 1.79) (Wilcoxon-Mann-Whitney test, $p < 0.001$) (Figure 4.2). This was also the case for summed parasite prevalence (Wilcoxon-Mann-Whitney test, $p < 0.001$), where hosts in the native range (mean = 254%, SD $\pm$ 130.5) experienced greater cumulative effects of parasitism than in the invasive range (mean = 49%, SD $\pm$ 60.5). Similarly, mean parasite prevalence was significantly higher in the native (mean = 56%, SD $\pm$ 24.1) than in the invasive range (mean = 20%, SD $\pm$ 25.7) (Wilcoxon-Mann-Whitney test, $p < 0.001$).

In opposition to the general trend of parasite loss from the native to the invasive ranges, great variation in parasite species richness could be observed within the native range (from zero parasites to 11) and among the various invasive ranges (from zero parasites to six) (Figure 4.1a–e). Notably, the parasite species richness at the native sites did not vary with relation to climatic region or biomes, with high richness sites being fully interspersed by lower richness sites across the range (Figure 4.1e).

4.3.4 Characteristics of accompanying parasites

Of the 13 South African parasites species that were sufficiently identified for the distinguishing of traits, only three managed to co-invade with their host, namely *P. xenopodis*, *C. namaquensis* and *G. gallieni*. Taxonomic class was a significant indicator of whether

a species would accompany the host in the process of invasion (Fisher's exact test, p = 0.005), because all the monogenean and cestodean parasites were present in at least one of the invasive populations and none of the mites, leeches, digeneans or nematodes managed co-invasion. Likewise, parasites with direct life cycles were significantly over-represented in the accompanying parasite species pool (Fisher's exact test, p = 0.04). On the other hand, the level of host specificity was not a significant predictor of co-invasion (Wilcoxon-Mann-Whitney test, p = 0.10). However, it is interesting to note that the co-invading parasites with higher host specificity possessed a direct life cycle, whilst the co-invading parasite with low host specificity possessed an indirect life cycle. The life stage of the parasite when infecting adult *X. laevis* had no effect on its presence in the invasive range (Fisher's exact test, p = 0.07). Neither were the non-accompanying parasites significantly absent in the Cape host population (Fisher's exact test, p = 0.16). However, presence in the Cape host population was a prerequisite for co-invasion. The parasite species that did not accompany their hosts tended to be those that were present in fewer of the host populations across the native range (median = 17%) as compared to those that did manage the co-invasion (median = 93%) (Wilcoxon-Mann-Whitney test, p = 0.03). Conversely, mean species prevalence across all hosts was not significantly different between accompanying (median = 60%) and non-accompanying parasites (median = 54%) (Wilcoxon-Mann-Whitney test, p = 0.57).

4.3.5 Susceptibility of invasive hosts to parasitism

The two most prevalent parasite species in both the native and invasive ranges were *P. xenopodis* and *C. namaquensis*. The per-site prevalence of these species in the sites where they were present was compared between the native and invasive ranges to determine whether parasites can attain similar infection levels across the distribution of *X. laevis* (Figure 4.3). In the case of *C. namaquensis*, there was no significant difference in the percentage of hosts infected in the native (mean = 65%, SD $\pm$ 35.1) as compared to in the invasive range (mean = 25%, SD $\pm$ 35.4) (Student's t test, t = -0.583, p = 0.57). However, the opposite was true for *P. xenopodis*, seeing that per-site prevalence was significantly higher in the native (mean = 56%, SD $\pm$ 31.3) versus the invasive range (mean = 16%, SD $\pm$ 21.0) (Student's t test, t = -2.984, p = 0.006).

4.3.6 Parasite community dissimilarity analyses

The global ANOSIM indicated that the overall parasite community composition among sites was significantly different when taking into account the geographical origin (native versus invasive range) of the hosts (ANOSIM, R = 0.41, p = 0.001). Qualitative visualisation of parasite community dissimilarity between the native and invasive ranges through NMDS

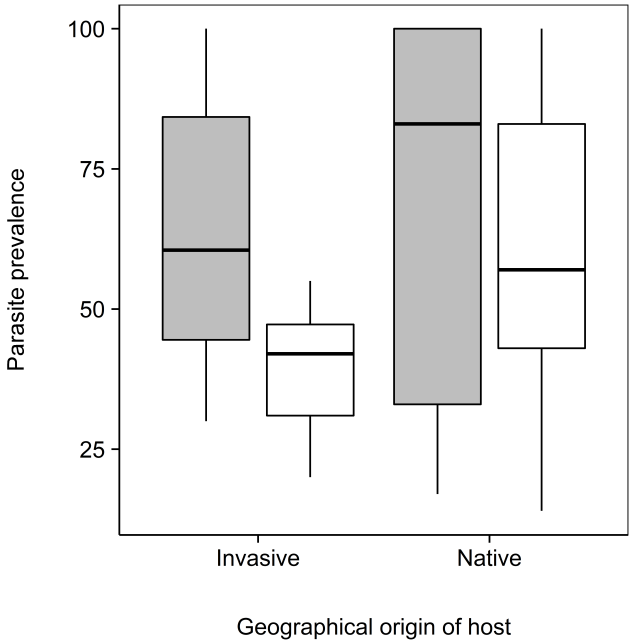

Figure 4.3: Per-site prevalence of a monogenean parasite of *Xenopus laevis* is higher in the native range than in the invasive range, but does not differ significantly in the case of a cestodean parasite. The minimum, first quartile, median, third quartile and maximum prevalence values of the cestode, *Cephalochlamys namaquensis*, across eight sites in the invasive and 25 sites in the native range are indicated in grey. The same values for the monogenean, *Protopolystoma xenopodis*, also across 8 sites in the invasive and 25 sites in the native range, are indicated in white.

yielded a stable solution (stress = 0.13) and agreed with the results of the ANOSIM in that sites did cluster together based upon the geographic origin of the hosts (Figure 4.4). This is clearly illustrated by the non-overlapping ellipses that encircled all sites that occurred within one standard deviation of the centroid of each of the geographic groups. The percentage of variance in species richness that was explained by the statistically significant response surface fitted by the generalised additive model was 94% ($F_{8.03,9}$ = 72.29, $p < 0.001$). This confirmed that the highest species richness scores tended to be associated with the native range and lower species richness with the invasive range. Two notable exceptions in the native range are Colesberg and Polokwane, where the hosts harboured zero and one parasites species respectively. These sites did not cluster with the rest of the native sites. This relationship also indicated that native sites with less parasite species tended to cluster more closely with invasive sites. Specifically, impoverished communities in the native range were almost identical in community composition to the four French sites that harboured both *P. xenopodis* and *C. namaquensis*. In contrast, invasive sites with acquired parasites, such as those from Chile, California and Portugal, tended to be more dissimilar to native sites.

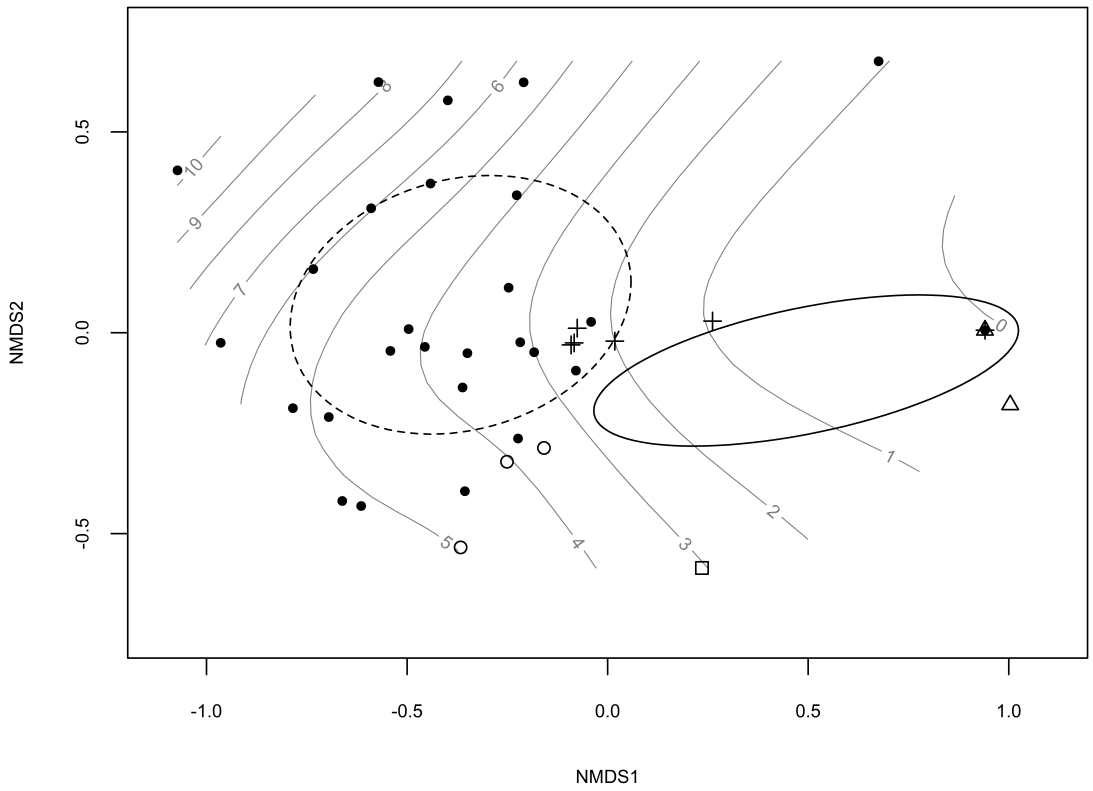

Figure 4.4: Non-metric multidimensional scaling of compositional dissimilarity reveals that metazoan parasite communities from native (southern Africa) and invasive (California, Chile, France, Portugal) *Xenopus laevis* populations cluster separately due to enemy loss in invasive hosts. Included are 27 sites from southern Africa (filled circles), three sites from California (open circles), nine sites from Chile (open triangles), six sites from France (crosses) and one site from Portugal (open square). Two native sites are fully interspersed with the invasive sites, namely Polokwane, top right corner, and Colesberg, which clusters with the Chilean sites. The fitted smooth response surface (grey contour lines) corresponds to species richness at each site. The ellipses encircle all sites that fall within one standard deviation of the centroid of the invasive (solid line) and native ranges (dotted line).

4.4 Discussion

This study is the first to demonstrate that a globally invasive amphibian species underwent repeated loss of metazoan parasites during the process of invasion. Only three parasites accompanied *X. laevis* on its invasion pathway and seven parasites colonised it upon arrival across the various invasive ranges, in contrast to the 21 parasite species that were recovered from *X. laevis* in the native range. In addition, decreased cumulative effects of parasitism and decreased levels of infection by certain parasites in the invasive range suggest that there might also be release from some of the negative effects of parasitism, lending support to the ERH in terms of release from metazoan parasites. Parasite loss from the native to the invasive range is a given in most organisms (Heger & Jeschke, 2014; Lui & Stiling, 2006; Torchin *et al.*, 2003) and colonisation by new parasites from the invasive range typically cannot make up for this loss (Torchin *et al.*, 2003). Specifically, this

is also the case for the only two other amphibians that have been assessed in a similar manner, albeit on a regional scale, namely the Puerto Rican tree frog, *E. coqui* (Marr *et al.*, 2008), and the Cuban tree frog, *O. septentrionalis* (Ortega *et al.*, 2015).

In opposition to the two amphibian species evaluated to date, this pattern of metazoan parasite loss in *X. laevis* is observed across different pathways of range expansion, on different continents and in different climatic regions. In most of the invasive populations, *X. laevis* was introduced into the wild after many generations of laboratory cultivation (Crayon, 2005; Lobos *et al.*, 2013; Measey *et al.*, 2012; van Sittert & Measey, 2016; Weldon *et al.*, 2007). This invasion history is reflected by the fact that the two most common accompanying parasites, *P. xenopodis* and *C. namaquensis*, can both survive for at least a year in captive hosts (Jackson & Tinsley, 1988; Tinsley, 1996). In its native range, *X. laevis* is known to be one of the first aquatic vertebrates to populate new habitats, which they frequently reach via overland migration, or via jump dispersal with the aid of farms dams or artificial waterways (de Villiers & Measey, 2017; Measey, 2016; Measey & Channing, 2003; Measey *et al.*, 2017). The results from the present study indicate that these pioneer populations harbour distinct parasite communities with lowered parasite species richness that are similar to those in invasive populations elsewhere, particularly in France. In addition, parasite loss occurs in all of the climatic regions where invasive *X. laevis* is found, be it temperate, Mediterranean or subtropical.

Rather, despite the shared loss of parasites across continents and modalities of expansion, the mechanisms behind the loss can probably not be ascribed to a single factor. In the majority of cases, it is probably an artefact of long periods of captivity. After subsequent release into the wild, parasite loss may be due to habitat unsuitability for the parasite cycle, specifically in terms of loss of intermediate hosts or unfavourable environmental conditions. For example, *P. xenopodis* relies on specific temperature optima for egg production (Jackson & Tinsley, 1988) and *C. namaquensis* on the availability of a suitable copepod as intermediate host (Ferguson & Appleton, 1988a; Thurston, 1967). On the other hand, it might be a result of greater investment in immunological defence on the part of the host during range expansion, especially in the native range. For instance, dispersing *X. laevis* differ in some respects from *X. laevis* from established habitats. In France, *X. laevis* populations from the range edge exhibit lowered investment in reproduction and increased stamina, which might enhance their dispersal ability (Courant *et al.*, 2017; Louppe *et al.*, 2017). Immunological defence against parasites in *X. laevis* has received little attention to date and might not increase fitness *per se* in the light of the low pathogenicity of its parasites (Tinsley, 1996), but cannot be ruled out as a potential factor.

With this in mind, it is interesting to note that the three accompanying parasites, namely the monogeneans *P. xenopodis* and *G. gallieni* and the cestode *C. namaquensis*, reveal some characteristics that might have facilitated their co-invasion. Not only are all three parasites present in the Cape, where the majority of *X. laevis* was exported from (van

Sittert & Measey, 2016; Weldon *et al.*, 2007), they are also present in significantly more of the screened native populations than the parasites that did not transfer. Their likelihood to co-invade along with *X. laevis* was not significantly influenced by their mean prevalence in the native range, a likely consequence of the magnitude of the repeated, enduring export of *X. laevis* (van Sittert & Measey, 2016). Since invaders generally do not experience such high levels of propagule pressure, it makes sense why accompanying parasites in *X. laevis* do not need high prevalence in the native range to facilitate co-invasion, as opposed to the trend in many other co-invading parasites (Torchin *et al.*, 2003). Equally important, the majority of the accompanying parasites of *X. laevis* have direct life cycles, a trait that has long been linked to a greater likelihood to manage co-invasion (Kuperman *et al.*, 2004; Torchin & Mitchell, 2004). However, our results show that parasites with complex life cycles can also be involved in co-invasion, in agreement with the findings of a recent review (Lymbery *et al.*, 2014). Host specificity of the accompanying parasites reveals a similar dichotomy. Contrary to the findings of the majority of studies reviewed by Heger & Jeschke (2014), our results demonstrate that the tight link between the host and the accompanying host-specific monogenean parasites promotes co-invasion, rather than suppresses it, as in the case of the highly host-specific *P. xenopodis* and *G. gallieni*. On the other side of the spectrum, the only parasite of *X. laevis* that has ever been recorded from hosts that are not from the genus *Xenopus*, namely *C. namaquensis*, also managed co-invasion (Dollfus, 1968; Mettrick, 1963).

Loss of parasite species is not the only factor that contributes to the distinctness of the parasite communities of invasive hosts. At least one parasite, *P. xenopodis*, displays lowered prevalence in invasive populations of the host. Coupled with the fact that the summed prevalence, an indication of the cumulative effect of parasitism, is also lower in the invasive range compared to the native range, this hints at a form of release from the effects of parasitism in invasive populations (Torchin *et al.*, 2003). However, this must be stated with great caution (Prior *et al.*, 2015; Prior & Hellmann, 2015). Not only might these values be somewhat inaccurate due to the unevenness of sampling effort in this study (Jovani & Tella, 2006), but lowered levels of parasitism might not directly lead to increased invasive success, especially in the case of *X. laevis* that possesses a host of other traits that contribute to its invasiveness (Rödder *et al.*, 2017). The acquisition of parasites upon establishment can also completely counter the effects of parasite loss given enough time (Kołodziej-Sobocińska *et al.*, 2018; Schultheis *et al.*, 2015). Eventually, acquired parasites may even contribute to the population regulation of the invasive *X. laevis*, since their association with the host is much more recent, which may translate to higher virulence than in the case of co-evolved parasites (Dunn *et al.*, 2012; Ricklefs, 2010).

All things considered, this study demonstrates that there is an overall pattern of metazoan parasite release, both with regards to species richness and prevalence, in *X. laevis* during invasion that is not yet countered by acquisition of new parasites. This process is repeated across continents and even in the ever-changing landscape of the native range.

In line with two similar studies on the protozoan parasites of birds and the metazoan parasites of crustaceans (Marzal *et al.*, 2011; Torchin *et al.*, 2001), the repeated loss of metazoan parasites across independent geographical replicates observed in the present study supports the ERH, irrespective of continent, climate, mechanism of parasite loss, or invasion history. The assessment of co-invading parasites is rarely considered in control programmes, unless these parasites have high pathogenicity. However, the role of parasites in biological invasions should not be underestimated, because both host and accompanying parasite may fundamentally modify ecosystems and trophic interactions in invaded ranges (Amundsen *et al.*, 2013; Dunn *et al.*, 2012; Roy & Lawson Handley, 2012). In the long run, we must realise that the accompanying parasites of *X. laevis* are also invaders in their own right. Predicting the future occurrences of these parasites is an important step in the control of *X. laevis* as an invasion package.

Chapter 5

The multiplex response of co-introduced parasites to the range expansion of their globally invasive frog host

5.1 Introduction

Biological invasion is the translocation of organisms beyond the limits of their native distributions where new populations may establish and spread (Blackburn *et al.*, 2011). During the Anthropocene, the frequency of biological invasions and the detrimental consequences linked to them are on the rise in a way that is completely redefining the distribution of flora and fauna on earth (Bar-On *et al.*, 2018; Blackburn *et al.*, 2019; Capinha *et al.*, 2015; Ricciardi, 2007). One aspect of this redistribution of biomass that is not only hidden from the eye but also frequently overlooked in invasion research is co-introduced parasites (Blackburn & Ewen, 2017).

Even though the majority of parasites might miss the boat during the process of invasion (Torchin *et al.*, 2003), it is still reasonable to assume that they make up a sizeable fraction of all non-native species on the planet (Blackburn & Ewen, 2017). In fact, for every one host species that invades a new area, a mean of three parasite species accompany it (Torchin *et al.*, 2003). An excellent example of this is the globally invasive amphibian *Xenopus laevis* (Daudin, 1802) (Anura: Pipidae), which has indeed been accompanied by at least three species of its natively associated metazoan parasite fauna to various parts of its invasive range (reviewed in Schoeman *et al.*, 2019). Specifically, the cestode *Cephalochlamys namaquensis* (Cohn, 1906) (Cestoda: Cephalochlamydidae) and the

monogenean *Protopolystoma xenopodis* (Price, 1943) Bychowsky, 1957 (Monogenea: Polystomatidae) emerge as its two most highly associated parasites.

Nonetheless, the simple comparison of parasite species richness between the native and invasive ranges of host species greatly oversimplifies the complexity of the parasite dynamics in both native and non-native host populations (Dunn & Hatcher, 2015; Poulin, 2007). Aquatic parasite communities are not uniform in space (Poulin, 2007) and we are only beginning to understand the forces shaping parasite dynamics during the range expansion of their hosts (Blackburn & Ewen, 2017). The recent comparison of the parasite component communities of *X. laevis* between its native and invasive range pointed towards extensive spatial heterogeneity in parasite dynamics, even more so in the native than the invasive range (Schoeman *et al.*, 2019). One of the most striking findings of this study was that *X. laevis* populations from less pristine localities in the native range harboured parasite communities that were more similar to those from invasive *X. laevis* than to their native counterparts from more pristine localities (Schoeman *et al.*, 2019).

This frog is well-known for its ability to colonise both pristine and less pristine water bodies in its native range of southern Africa, where it often arrives via overland migration and dispersal via artificial waterways as a pioneer species (de Villiers & Measey, 2017; Measey, 2016). Indeed, its widespread translocation in this region is definitely helped along by anthropogenic activities, which often includes deliberate long range translocation (Measey *et al.*, 2017; van Sittert & Measey, 2016; Weldon *et al.*, 2007). Therefore, it comes as no surprise that some populations of native *X. laevis* may harbour parasite communities that resemble those of translocated and expanding *X. laevis* populations in the invasive range. Yet, the drivers behind these shared patterns are much harder to discern and a plethora of factors have been invoked as explanations of heterogeneity in parasitism.

On the one hand, intrinsic factors, such as host traits, are thought to affect the number and diversity of parasites that an individual host may carry. Popularly, the application of ”island biogeography theory” to the richness of parasite communities has underscored the effect of host traits on rates of parasite colonisation and extinction (Poulin & Morand, 2004). In particular, host body size, as a proxy for age and exposure and a representation of a more diverse, resource-rich environment, emerges as a good predictor of parasite species richness in various amphibian hosts (Campião *et al.*, 2015).

On the other hand, extrinsic factors, those from the environment and not the host, can be highly influential in shaping parasitism. However, the effect of environment is complex and potentially conflicting, especially when there is more than one host involved in the life cycle of a parasite (Hartson *et al.*, 2011). Generally, parasite communities of frogs tend to be richer with higher abundance of species in more natural freshwater environments (Hartson *et al.*, 2011), but this varies between parasite species (King *et al.*, 2007).

Finally, range expansion and the accompanying spatial sorting in both host and parasite

traits can also be the agent of change in the parasite communities of invasive frogs (Kelehear *et al.*, 2012; Mayer *et al.*, 2021). As a result, hosts at the range edge of an expanding population experience less parasitism, a phenomenon that has been confirmed for a wide range of invasive host taxa (Barnett *et al.*, 2018; Coates *et al.*, 2017; Coon & Martin, 2014; Phillips *et al.*, 2010; Stuart *et al.*, 2020).

Biological invasions represent widespread natural experiments, in some cases with independent global replicates, that can reveal the workings of nature (Blackburn, 2008). Understanding the spatial component of parasite dynamics during range expansion will allow us to predict the reactions of host-parasite systems to global change (Poulin, 2007). In this sense, *X. laevis* and its parasites, both in the native range of South Africa, where it is widely translocated, and the invasive range in western France, where its expansion is well-documented, pose the ideal model. In the past 40 years since its introduction in western France, the invasive range of *X. laevis* in this region has grown to approximately 4 000 km^2 (Vimercati *et al.*, 2020). Several studies on this invasive population of *X. laevis* have shown that spatial sorting in traits linked to dispersal and reproduction has taken place, even at a relatively small spatial and geographical scale (Courant *et al.*, 2017, 2019a,b; Louppe *et al.*, 2017, 2018).

Our study focused on the parasites of *X. laevis* in these two ranges and investigate the drivers of parasitism, with a specific focus on the effects of range expansion. Firstly, to explore trends in the native parasite ecology of *X. laevis* across South Africa, we investigated whether intrinsic or extrinsic factors contribute to the abundance of the two most common parasite species in particular and to parasite infracommunity crowding in general. Secondly, to identify possible extrinsic factors that may affect native parasite ecology in *X. laevis*, we interpreted the variation in parasite abundance and crowding in terms of the broader habitat types of the studied localities. Thirdly, to explore the effect of *X. laevis* range expansion on parasite dynamics, we analysed the relationship between distance from introduction point and the abundance of common parasite species and parasite infracommunity crowding in the invasive range of western France.

5.2 Methods

5.2.1 Host collection

From March 2017 to November 2019, 186 adult *X. laevis* were captured from 31 water bodies across South Africa (Figure 5.1; Appendix A for detailed information on collection sites). Funnel traps with liver bait were used to capture frogs overnight. Frogs were kept for up to 43 days (median = 5 days) in water from the source, replaced by unchlorinated water as necessary, prior to dissection.

In addition to collection in the native range, 114 adult *X. laevis* were collected during May to July 2019 from 11 water bodies in the invasive range in western France at various distances from the introduction point (Figure 5.1; Appendix A for detailed information on collection sites). Frogs were captured in baited traps by members of the EU LIFE CROAA team as part of the regional eradication programme for invasive amphibians. After capture, frogs were kept with others from the same site in plastic aquaria filled with aged chlorinated tap water. Parasite screening took place from the day of capture to up to two weeks after capture (median = 7 days).

Prior to dissection, all frogs underwent double euthanasia with anaesthesia in 6% ethyl-3-aminobenzoate methanesulfonate (MS222) (Sigma-Aldrich Co., Steinheim, Germany) followed by pithing. Euthanised frogs were sexed, weighed and the length from snout to urostyle (SVL) was recorded.

Relevant institutional, national and international guidelines for the care and use of animals were followed under the North-West University AnimCare ethics number NWU-0380-16-A5-01. The data set for the present study was obtained as part of a larger project with the aim of characterising the parasite fauna of *X. laevis* in South Africa and western France.

5.2.2 Parasite collection and identification

Euthanised frogs were examined both externally and internally for metazoan parasites. External examination included the skin and webbing between toes, eyes, nostrils, Eustachian tubules and buccal cavity. Frogs were cut open on the ventral side and the heart with pericardium intact, lungs, liver lobes, gall bladder and bile ducts, excretory bladder, digestive tract from oesophagus to rectum and kidney were removed, placed separately in 0.6% amphibian Ringer's solution (du Preez & van Wyk, 2007) and examined under a stereomicroscope.

The observed parasites were carefully removed, counted, fixed and preserved in molecular grade 70% ethanol. Adult cestodes and digeneans were heat killed in tap water under coverslip pressure. Encysted cestodes and digeneans were carefully excysted with sharp needles and placed directly in 70% ethanol. Monogeneans were placed in a drop of tap water on a microscope slide which was gently heated from underneath with a buthane flame until the worms relaxed, following Snyder & Clopton (2005). A coverslip was placed over the worm and the tap water was gradually replaced by 70% ethanol. Nematodes were fixed in hot 70% ethanol. Mites and leeches were placed directly in 70% ethanol.

Many of the parasite specimens in our data set have already been identified in previous analyses that formed part of an ongoing survey of the parasite fauna of *X. laevis* (Schoeman *et al.*, 2019, 2020; Svitin *et al.*, 2018). For the purpose of our ecological analy-

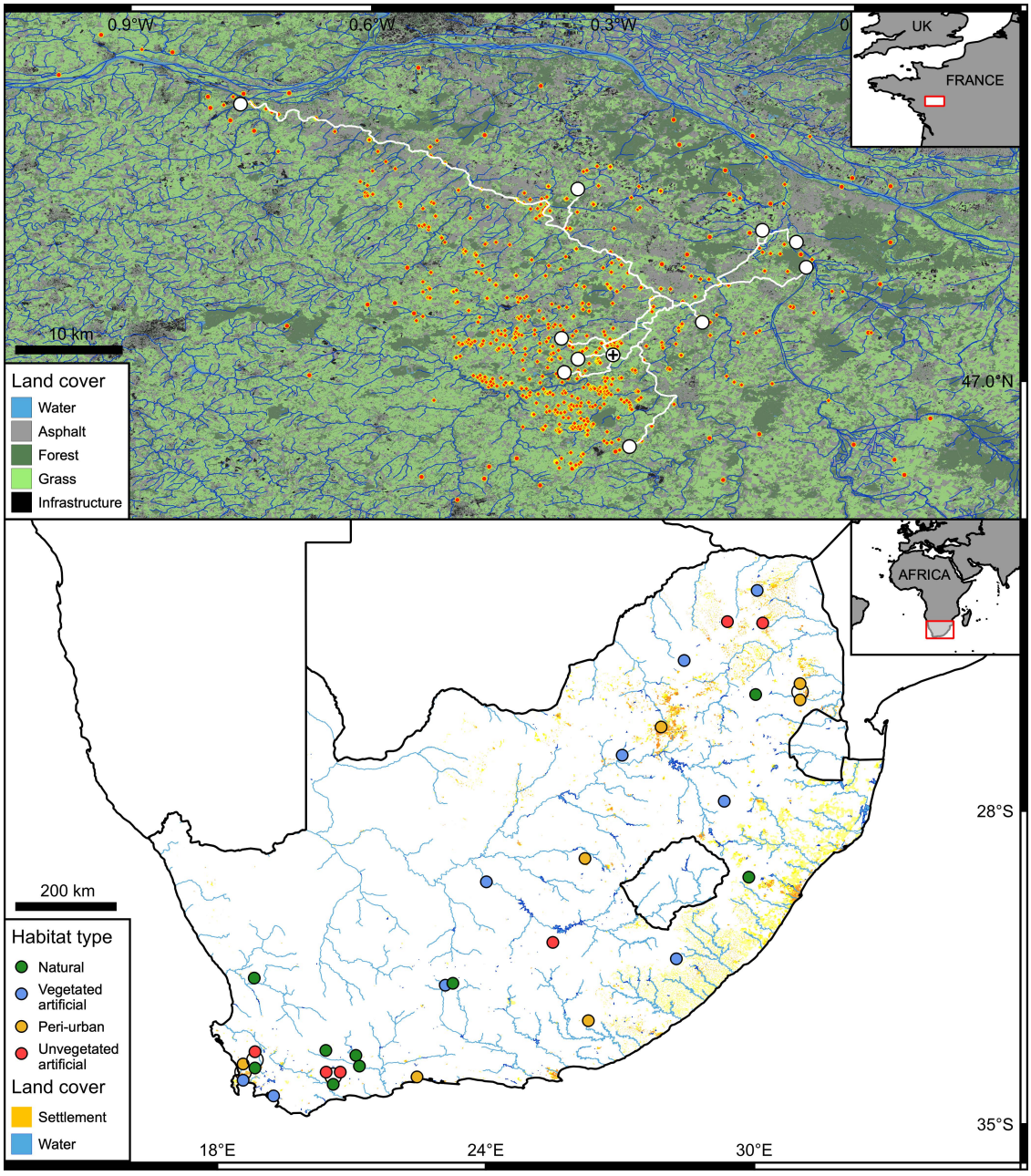

Figure 5.1: Distribution of localities (coloured circles) in western France (top) and South Africa (bottom) where adult *Xenopus laevis* were collected along with their metazoan parasite assemblages. Predominant land use of each 25 m^2 grid cell in France, according to Vimercati *et al.* (2020), is shown along with waterways derived from BD CARTHAGE® *version* 3.0. Historical introduction site (black cross) and occurrence data (orange dots; Vimercati *et al.*, 2020) of invasive *X. laevis* are shown. White lines indicate the calculated least cost paths between the introduction site and each collection locality in France. In South Africa, major water bodies and human population density data were obtained from the 2012 Water Resources of South Africa database. Habitat type of water bodies at South African localities were classified based upon on-site observations and the 2018 South African National Land Cover dataset. The map was constructed in QGIS *version* 3.10.2-A Coruña (QGIS Development Team, 2018) with the Mercator projection.

ses, specimen identifications to species level was only necessary for the monogenean *P. xenopodis* and the cestode *C. namaquensis*. These morphologically distinct species

were identified based upon morphological features as observed under light microscopy, infection site and host identity. As for the rest of the parasites – digenean, monogenean, mite and leech species present as adults could be distinguished from one another and, in most cases, identified based upon morphology under light microscopy and infection site in the body. Nematodes were identified with the use of both the molecular and morphological tools as in previous studies (Schoeman *et al.*, 2020; Svitin *et al.*, 2018). The molecular approach of Schoeman *et al.* (2019) was applied to distinguish among the digenean metacercariae recovered in the present study with the internal transcribed spacer (*ITS*) gene region in cases where morphological examination was insufficient.

5.2.3 Calculation of scaled mass index of hosts

Host condition was approximated with the scaled mass index (SMI), an accurate body condition index for anurans, including *X. laevis* (Brodeur *et al.*, 2020; Courant *et al.*, 2017; MacCracken & Stebbings, 2012). As opposed to being derived from the ordinary least square regression of body mass *vs* SVL, the SMI relies on the standardised major axis (SMA) regression (Peig & Green, 2009). The SMA delivers a superior estimation of body condition in anurans, especially in the case of heteroscedastic and overdispersed data where frogs are from different populations or sites (Jakob *et al.*, 1996; Peig & Green, 2010). The SMI, denoted $\hat{M}_i$, is calculated according to the following formula:

$$\hat{M_i} = M_i \cdot \left(\frac{L_0}{L_i} \right)^{b_{SMA}}$$

where M_i is the mass and L_i the SVL of frog i, L_0 is the mean of all the frogs in the sample and the scaling factor b_{SMA} is the slope of the SMA regression of body mass on SVL with both variables transformed by the decadic logarithm.

In order to make the SMI comparable among sites and sexes, the SMI for all frogs should be standardised to the same length (L_0), which can be any arbitrary value chosen by the researcher (Peig & Green, 2009). In cases where the slope of the SMA does not differ significantly between groups in the sample, one can reliably use a single scaling factor to calculate the SMI of the whole sample (Brodeur *et al.*, 2020; Peig & Green, 2009). The R package *smatr* (Warton *et al.*, 2012) is commonly used in allometry to fit bivariate lines using the SMA. The function `sma()` can further test for common slope amongst several SMA regressions, fitted separately for each level of the grouping factor (Warton & Weber, 2002). Thus, we fit the SMA of the decadic logarithms of mass *vs* SVL to compare the slopes between males and females whilst assuming common elevation. Since there were no outliers present, we did not employ the robust version of the regression (Taskinen & Warton, 2011).

Regression slope was found to not be significantly different between males and females in South Africa ($LR_{df=1}$ = 3.536, $p > 0.05$) or France ($LR_{df=1}$ = 2.821, $p > 0.05$). Thus, a b_{SMA} of 2.62 (95% CI [2.514; 2.732], R^2 = 0.92, $p < 0.001$) was used as the scaling factor to calculate the SMI of the frogs from South Africa and a b_{SMA} of 2.84 (95% CI [2.767; 2.918], R^2 = 0.98, $p < 0.001$) was employed in the case of the frogs from France. The SMI was standardised to the mean SVL of the French sample (L_0 = 66 mm) as arbitrarily chosen value. The obtained SMI was uncorrelated with SVL in frogs from South Africa (Spearman's ρ = -0.088, $p > 0.05$) and France (Spearman's ρ = -0.064, $p > 0.05$).

5.2.4 Habitat classification in the native range

Habitats at the respective collection sites in South Africa were categorised into four main groups based upon both observations at the site at the time of capture, as well as an assessment of the predominant land cover in a 1 km buffer around each site, derived via zonal statistics in QGIS *version* 3.10.2-A Coruña (QGIS Development Team, 2018) from the 2018 South African National Land Cover (SANLC) dataset (https://egis.environment.gov.za/gis_data_downloads). These categories are (1) Peri-urban: water bodies within 1 km of urban settlements, (2) Unvegetated artificial: artificial water bodies with negligible vegetation cover and (3) Vegetated artificial: high vegetation cover and (4) Natural: natural or established artificial water bodies in natural river systems.

5.2.5 Calculation of least cost path from introduction site in invasive range

Position on the invasion wave was identified as a potential predictor of parasitism in the invasive range. Thus, collection sites in France were specifically chosen to represent a range of distances from the introduction point of *X. laevis* – a municipal pond adjacent to the closed *X. laevis* breeding facility near the town of Bouillé-Saint-Paul (Fouquet, 2001). Thus, it was not possible to classify sites into range core and edge sites as was done in previous *X. laevis* studies from the region (Courant *et al.*, 2017, 2018, 2019a,b; Louppe *et al.*, 2017, 2018). Historical dispersal from the introduction point by the frog had also not taken place evenly in all directions, with greater expansion to the northwest (Vimercati *et al.*, 2020). In the light of this uneven spread, we calculated least cost paths ("as the frog hops") from the introduction point to each collection site rather than to make use of physical distance ("as the crow flies").

Least cost path analysis (LCPA) was based upon a species-specific cost of locomotion raster of *X. laevis* in western France. A spatial grid of the predominant land cover of every 25 m^2 quadrant in the area from 35° 16' 33.894"N to 46° 46' 20.261" N and 1° 42' 26.803" W to 6° 51' 34.615" E, encompassing the whole of the invasive range of *X. laevis* in western France, was obtained from Vimercati *et al.* (2020) (Figure 5.1). Standardised

resistance costs of *X. laevis* for each land cover type, obtained from Vimercati *et al.* (2021), were superimposed on the grid to create a cost raster necessary for the LCPA. Accordingly, rivers and water bodies were assigned a standardised resistance cost of 1.5, asphalt and bare soil a cost of 5, forest and leaf litter a cost of 7.5, grass a cost of 11 and buildings and other impassable infrastructure a cost of 999.

As a first step in the LCPA, the cost raster was converted to a transition matrix containing conductance values. These were calculated as the inverse of the arithmetic mean of the cost values of adjacent cells in a Moore neighbourhood. Matrix values were corrected for distance distortion in the East-West direction and across diagonal connections between grid cells. The calculation of the least cost distances from the introduction point to each of the 11 collection sites were computed with Dijkstra's (1959) algorithm. All steps of the LCPA were executed with the R package *gdistance* (van Etten, 2017) that relies on the R package *igraph* (Csárdi & Nepusz, 2006) for underlying calculations.

5.2.6 Quantification of parasitism

In order to identify the factors influencing overall parasitism of a single host, each host's infracommunity was reduced to a single absolute measure that portrays both species richness and evenness. The infracommunity crowding (ICr) index, as defined by Ferrari *et al.* (2016), expands a concept of crowding previously proposed by Lloyd (1967). Crowding, according to Lloyd (1967), quantifies the number of individual parasites experienced by a single parasite individual of the same species. The ICr index extends this basic idea to the interspecific level (Ferrari *et al.*, 2016). Essentially, the ICr index averages the crowding each parasite species experiences from the individuals of other parasite species present in a host over the total number of individual parasites. This yields the crowding experienced by an average parasite species in a given host's infracommunity according to the following formula:

$$ICr = \frac{2 \cdot \sum_{j=1}^{S-1} \left(x_j \cdot \sum_{i=j+1}^{S} x_i \right)}{N}$$

Here, x_j is the abundance of the j-th parasite species, S is the metazoan parasite species richness and N is the total metazoan parasite abundance. Since impoverished infracommunities are found in both native and invasive *X. laevis* populations (Schoeman *et al.*, 2019), we encountered a few hosts with zero parasites, resulting in an undefined ICr index for some. To counter this in the analyses, we added a single dummy parasite individual to the total parasite abundance of each host. The ICr index without and with the dummy exhibited a near perfect correlation in both the South African (Spearman's ρ =

0.999, $p < 0.001$) and the French survey (Spearman's ρ = 0.998, $p < 0.001$), justifying the addition of the dummy.

5.2.7 Selection of predictors

Prior to analysis, we carefully considered our available predictors to reflect hypotheses about the study system (Harrison *et al.*, 2018). Thus, only predictors that were relevant to the problem at hand were included, rather than all available variables (Burnham & Anderson, 2002; Harrison *et al.*, 2018). This is particularly important for smaller data sets where there is a risk for overparameterisation. Furthermore, we ensured that the selected predictors contributed independently to the variance in the response variable (Zuur *et al.*, 2010). In cases where variables were collinear, we selected the most biologically meaningful variable (Zuur *et al.*, 2010).

For the models implemented on the South African data set, we considered only SMI and SVL as fixed effects. We did not include mass, since mass was correlated with both SMI (Spearman's ρ = 0.175, p = 0.02) and SVL (Spearman's ρ = 0.957, $p < 0.001$). Sex was also not considered, since both SVL (W = 5974.5, $p < 0.001$) and SMI (W = 2862, $p <$ 0.001) differed significantly between males and females. As a result, the effect of sex could not be separated from dimorphism in body size and condition.

In the invasive population in western France, the mass of all measured frogs correlated with SVL (Spearman's ρ = 0.987, $p < 0.001$) and was not included as predictor in any models. There was a significant correlation between distance from the introduction point and both SVL (Spearman's ρ = -0.249, p = 0.008) and SMI (Spearman's ρ = -0.191, p = 0.04). Since distance from introduction point is our predictor of interest, we considered only distance from the introduction point as a fixed effect in the models implemented on the French dataset to avoid possible multicollinearity and overfitting (Harrison *et al.*, 2018).

We included collection site as a random effect in all models implemented on both the South African and French data sets. The inclusion of locality as a random effect allowed us to account for the inherent nestedness of our data sets and small group sizes (Gelman & Hill, 2006; Zuur & Ieno, 2016). Moreover, we were also interested in the variation among the localities in our data sets, since this represents unmeasured environmental or demographic heterogeneity (Harrison *et al.*, 2018).

5.2.8 Statistical analyses

All continuous predictors were scaled and centered to mean zero and a standard deviation of one prior to analyses (Schielzeth, 2010). Moreover, observations with missing values

were removed from both the South African and French data sets. The resulting two data sets included 176 frogs from 31 sites in the native range (113 females and 63 males) and 105 frogs from 10 sites in the invasive range (59 females and 54 males). We employed six generalised linear mixed models (GLMMs) to explore the relationships between the parasite burdens experienced by individual *X. laevis* in both the native and invasive range as response variables and intrinsic and extrinsic factors as predictor variables.

The ICr index is a combination of discrete exact zeros and a right-skewed continuous distribution of positive values, a situation commonly encountered in density and relative abundance data of organisms, also that of parasites (e.g. Canel *et al.*, 2019). When sampling conditions vary between sites, this situation is most appropriately approximated by a specific case of the Tweedie family of distributions (Jørgensen, 1997) called the Poisson-Gamma with an index term in the mean-variance relationship $V(\mu) = \phi\mu^p$ of $1 < p < 2$ (Dunn & Smyth, 2005; Jørgensen, 1997; Smyth, 1996). However, in cases where sampling volume variability is small, the hurdle-Gamma approach provides comparable results and is much simpler to implement (Lecomte *et al.*, 2013). Thus, to model the number of intraspecific interactions in each parasite infracommunity (ICr index) as a function of SMI and SVL as fixed effects and collection locality as random effect in South Africa and a function of distance from the introduction point as fixed effect and collection locality as random effect in France, two hurdle-Gamma LMMs were implemented with a log link function.

Overdispersed count data with variance greater than the mean is well-approximated by the negative binomial distribution. Thus, *P. xenopodis* and *C. namaquensis* abundance values from western France were modelled in two GLMMs according to the negative binomial response distribution with a log link function. In both these GLMMs, distance from the introduction point was included as fixed effect and collection locality as random effect.

Since these parasites were not detected at all localities in South Africa, zeros could theoretically arise in the data set because of true absence of a parasite at a locality, or because the surveyed hosts were not infected at a locality where the parasite actually occurred. Thus, to account for both true and false zeros in this data set, *P. xenopodis* and *C. namaquensis* abundances in South Africa were modelled with a zero-inflated negative binomial distribution in two more GLMMs (Martin *et al.*, 2005). As mentioned before, SMI and SVL were included as fixed effects and collection locality was modelled as a random effect. The resulting posterior distributions of the random effect of collection locality were interpreted in the light of habitat type to investigate possible spatial patterns in the abundance of *P. xenopodis* and *C. namaquensis* across the native range.

For the GLMMs, a Bayesian approach was preferred, which elegantly incorporates the uncertainty associated with the random effects in overall parameter estimation (Bolker *et al.*, 2009; Ellison, 2004; Gelman & Hill, 2006). Furthermore, the inclusion of weakly informative

priors has a regularising effect on the parameters, shrinking parameter estimates to zero unless the data strongly demonstrate an effect (Lemoine, 2019; McElreath, 2020). This implicitly takes into account the fact that ecological data are noisy and that effects are generally small. The inclusion of weakly regularising prior information can increase confidence in the outcomes (McCarthy & Masters, 2005) whilst providing similar estimates as frequentist methods (Bolker *et al.*, 2009).

Prior distributions were chosen based upon the recommendations of Bolker *et al.* (2009), Evans & Jang (2011), Gelman (2006), Gelman *et al.* (2008), Lemoine (2019), Polson & Scott (2012), Simpson *et al.* (2017) and Zuur *et al.* (2015). We applied a Student's *t* (3,0,1) prior distribution to the model intercepts, a normal (0,1) prior distribution to the fixed effects and a half-Cauchy (0,1) distribution to the random effect. For the family-specific parameters, we kept the default prior distributions as recommended in Bürkner (2017).

The Bayesian GLMMs were fit with the Markov chain Monte Carlo (MCMC) algorithm (Gilks *et al.*, 1996) in the R package *brms* (Bürkner, 2017), which is an interface for the C++ package *Stan* (Carpenter *et al.*, 2017). This package implements the Hamiltonian MCMC method (Duane *et al.*, 1987; Neal, 2011) and its extention, the No-U-Turn Sampler (NUTS) (Hoffman & Gelman, 2014). Model convergence was achieved with five chains of 100 000 iterations each, of which the first 15 000 were discarded as burn-in. To remedy divergent transitions, the behaviour of the NUTS sampler was adjusted by decreasing initial step size to 0.001, increasing the target acceptance rate to 0.999 and increasing the tree depth to 20. Chains were thinned hundredfold prior to the summary of the posterior distributions.

To confirm model convergence, we consulted potential scale reduction factors (Brooks & Gelman, 1998) and diagnostic plots produced by the R package *bayesplot* (Gabry *et al.*, 2019). Absence of multicollinearity was confirmed via variance inflation factors with the R package *performance* (Lüdecke *et al.*, 2020). The estimates of the effects sizes were taken from the posterior distribution of the model parameters with the help of the R package *bayestestR* (Makowski *et al.*, 2019). The 89% credible intervals around the means were used to evaluate support for the effect of each parameter, since these are deemed to be more stable than, say, 95% credible intervals (Kruschke, 2015; McElreath, 2020). If these intervals did not overlap zero, support for an effect was inferred. Model goodness-of-fit was evaluated with the Bayesian R^2 (Gelman *et al.*, 2019) in *performance* (Lüdecke *et al.*, 2020), which calculates both the conditional and marginal R^2 (Nakagawa & Schielzeth, 2013).

All statistical analyses were performed in R *version* 4.0.2 (R Core Team, 2020) using the above-mentioned packages and Wickham *et al.*'s (2019) *tidyverse* and Mangiafico's (2020) *rcompanion* for data carpentry and calculation of summary statistics.

5.3 Results

5.3.1 Parasite assemblages of *X. laevis* in the native and invasive range

In total, 25 metazoan parasite species were recovered in association with *X. laevis* in South Africa during the present survey. These included two cestode, two monogenean, ten nematode, nine digenean, one mite and one leech species. The cestode *C. namaquensis* from the intestine and the monogenean *P. xenopodis* from the bladder were present at 29 and 27 of the 31 localties and in 61% and 52% of all hosts, respectively.

Component community metazoan parasite species richness across the 31 South African collection localities ranged from zero to eleven with a median of six species at a site. On the infracommunity level, if at least one metazoan parasite was present in a host, the average metazoan parasite species in South Africa interacted with 3.8 $\pm$ 95% CI [2.50; 6.42] parasites from other species, the median of the ICr index calculated without the addition of a dummy parasite. As is typical of parasite distribution in hosts, many hosts harboured uncrowded communities. A third (33%) of hosts either harboured no metazoan parasites or a single metazoan parasite species.

Five metazoan parasites were recovered from *X. laevis* in western France during the present survey. The two most common parasites across the region were both co-invaders of southern African origin, namely *C. namaquensis* and *P. xenopodis*. Both of these parasites were recovered from all 11 sites, infecting 85% of hosts in the case of the cestode and 71% in the case of the monogenean. Together, the other three metazoan parasite species, one species of Nematoda and two of Digenea (both present as metacercariae), were recovered from only 8% of all hosts. The *ITS* region of one of the digenean species was identical to a species recovered in the same stage from some hosts in South Africa. Comparison of the 1 239 bp obtained of the *ITS* region of these specimens with sequences available on Genbank (KP721422–39 from Caffara *et al.* (2016) and KC894798–801 from Senapin *et al.* (2014)) revealed that this species belongs to the family Clinostomidae and is probably a member of the genus *Euclinostomum* Travassos, 1928. This suggests a third co-introduction of a parasite of African origin along with *X. laevis* in western France.

In cases where there was at least one parasite present in a host, the average metazoan parasite species in a parasite infracommunity of *X. laevis* in western France experienced median crowding of 1.6 $\pm$ 95% CI [0.00, 1.71] parasites. This value was obtained from the ICr index calculated without the addition of a dummy parasite. The parasites revealed a typically aggregated distribution across all the hosts, where 38% of *X. laevis* harboured parasite infracommunities characterised by zero to one parasite species.

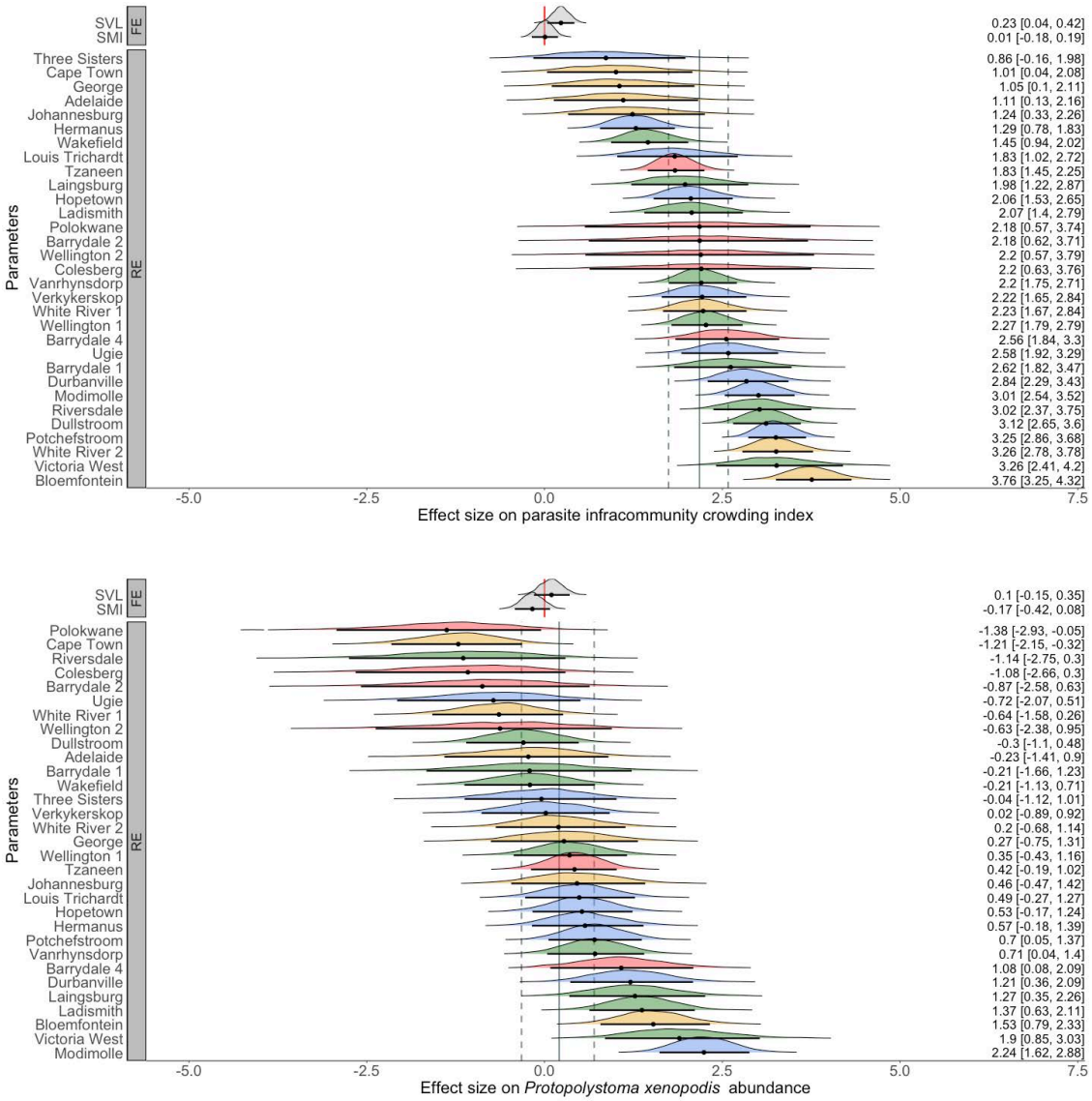

Figure 5.2: Summaries of the estimated posterior distributions for the fixed effects (FE) of host length from snout to urostyle (SVL) and host scaled mass index (SMI) and the random effect (RE) of collection locality from the three Bayesian generalised linear mixed models with measures of parasitism of *Xenopus laevis* in South Africa as response. Black dots show posterior means and bars indicate 89% confidence intervals (CI), of which the values are indicated to the right of each distribution. A positive effect size (to the right of the red line) for a fixed effect indicates an increased potential for parasitism in relation to an increase in that fixed effect. In the case of the random effects, a positive deviation from the mean effect size (solid grey line) with 89% CI (dashed grey line) indicates above-average potential for parasitism at that particular locality. Width of 89% CI indicates confidence in estimates. Collection localities are coloured according to habitat type, namely natural (green), vegetated artificial (blue), unvegetated artificial (red) and peri-urban (yellow) water bodies, and are named after the nearest town.

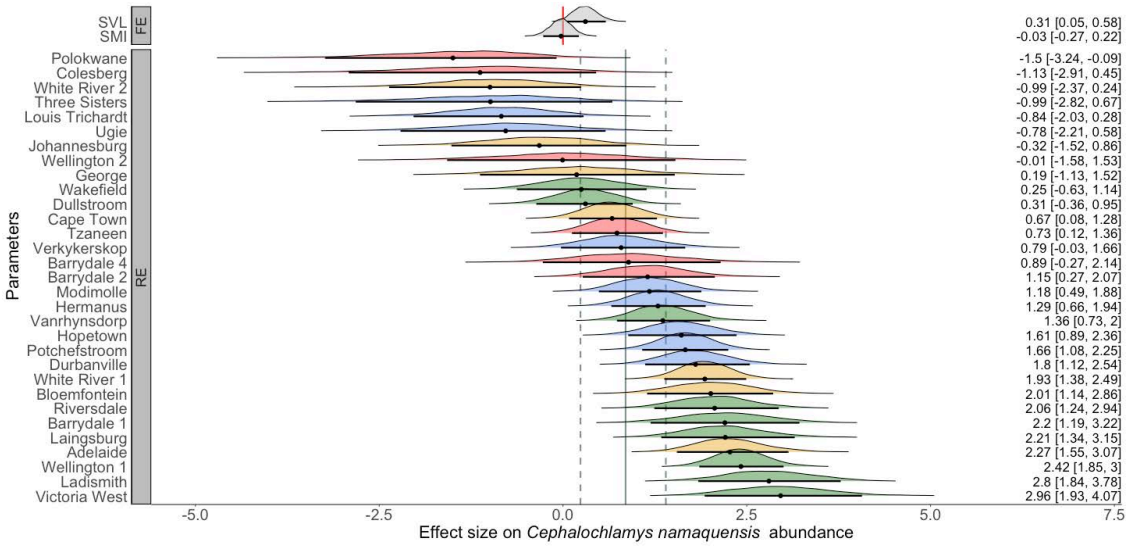

Figure 5.2: Summaries of the estimated posterior distributions for the fixed and random effects from the three Bayesian generalised linear mixed models with measures of parasitism of *Xenopus laevis* in South Africa as response (*continued*).

5.3.2 Intrinsic and extrinsic factors affecting parasitism in the native range

In the native range, hosts with greater SVL harboured more crowded parasite infracommunities than smaller hosts and were also infected with more *C. namaquensis* (Figure 5.2). Conversely, the *P. xenopodis* burden did not vary with host SVL (Figure 5.2). As for SMI, there was no effect of body condition on ICr or *C. namaquensis* and *P. xenopodis* abundance (Figure 5.2). In all cases, the random effect of collection locality explained considerably more of the variability in parasitism in the native range than the fixed effects, as evidenced by the the considerable discrepancy between the marginal and conditional R^2 of each of the models (Table 5.1).

Specifically, a notably greater proportion of the variability in *C. namaquensis* abundance could be ascribed to site-level variance than in the case of ICr and *P. xenopodis* abundance (Table 5.1). A closer look at the posterior distributions of the various localities confirmed that hosts from localities with natural habitats had a higher potential for infection with *C. namaquensis* than those from localities with vegetated and unvegetated artificial water bodies or localities from a peri-urban environment (Figure 5.2). The confidence intervals of the estimates for the unvegetated artificial water bodies were generally much wider that for the other habitat types (Figure 5.2). Nonetheless, infracommunity crowding was not consistently lower than expected in these water bodies (Figure 5.2).

Table 5.1: Bayesian R^2 values (Nakagawa & Schielzeth, 2013) of the six generalised linear mixed models where infracommunity crowding (ICr) and *Cephalochlamys namaquensis* (Ceph) and *Protopolystoma xenopodis* (Prot) abundance in both the native (ZA) and invasive (FR) range of *Xenopus laevis* were modelled as response variables. Fixed effects could be any of host length (*SVL*), host body condition (*SMI*), or least cost path of collection locality from introduction point in France (*distance*). Collection locality (*site*) was included as a random effect. Marginal R^2 gives the proportion of the variability explained by the fixed effects alone, whilst the conditional R^2 is the proportion of the total variance explained through both fixed and random effects.

Model terms	Marginal R^2	Conditional R^2
$ICr_{za} \sim SVL + SMI + (1\|site)$	0.8% ± 0.8 SE	30.5% ± 8.9 SE
$Ceph_{za} \sim SVL + SMI + (1\|site)$	1.2% ± 1.4 SE	48.4% ± 8.9 SE
$Prot_{za} \sim SVL + SMI + (1\|site)$	0.5% ± 0.5 SE	24.7% ± 10.5 SE
$ICr_{fr} \sim distance + (1\|site)$	1.0% ± 1.2 SE	5.6% ± 2.9 SE
$Ceph_{fr} \sim distance + (1\|site)$	0.9% ± 0.9 SE	4.4% ± 2.8 SE
$Prot_{fr} \sim distance + (1\|site)$	1.1% ± 1.4 SE	13.7% ± 6.1 SE

5.3.3 Effect of range expansion on parasitism in the invasive range

Among the *X. laevis* collected from the invasive population in western France, distance from the introduction point did not affect all parasites in equal measure (Figure 5.3). The abundance of *C. namaquensis* decreased towards the range edge (Figure 5.3), whilst this effect did not differ markedly from zero in the case of *P. xenopodis* abundance and infracommunity crowding. Site-level differences had the greatest effect on *P. xenopodis* abundance when compared to infracommunity crowding or *C. namaquensis* abundance (Table 5.1).

Overall, the Bayesian R^2 indicated that neither the fixed effect of distance from introduction point, nor the random effect of collection locality could explain much of the heterogeneity in parasitism observed in *X. laevis* from western France (Table 5.1). Inspection of the confidence intervals of the posterior distributions of the localities revealed the lowest confidence in the estimates for Chalonnes-sur-Loire, the site furthest from the introduction point, across all three GLMMs (Figure 5.3). Moreover, across all three GLMMs, the locality of La Coudray-Macouard was the only locality that consistently exhibited lower than expected levels of parasitism. This was also the only collection locality where invasive crayfish *Procambarus clarkii* (Girard, 1852) was present (Jean Secondi, personal communication).

5.4 Discussion

The reaction of parasites to biological invasions is many-sided (Dunn & Hatcher, 2015). In the present study, the dynamic interplay between the range expansion of the amphibian host *X. laevis* and its metazoan parasites observed in both its native and invasive ranges

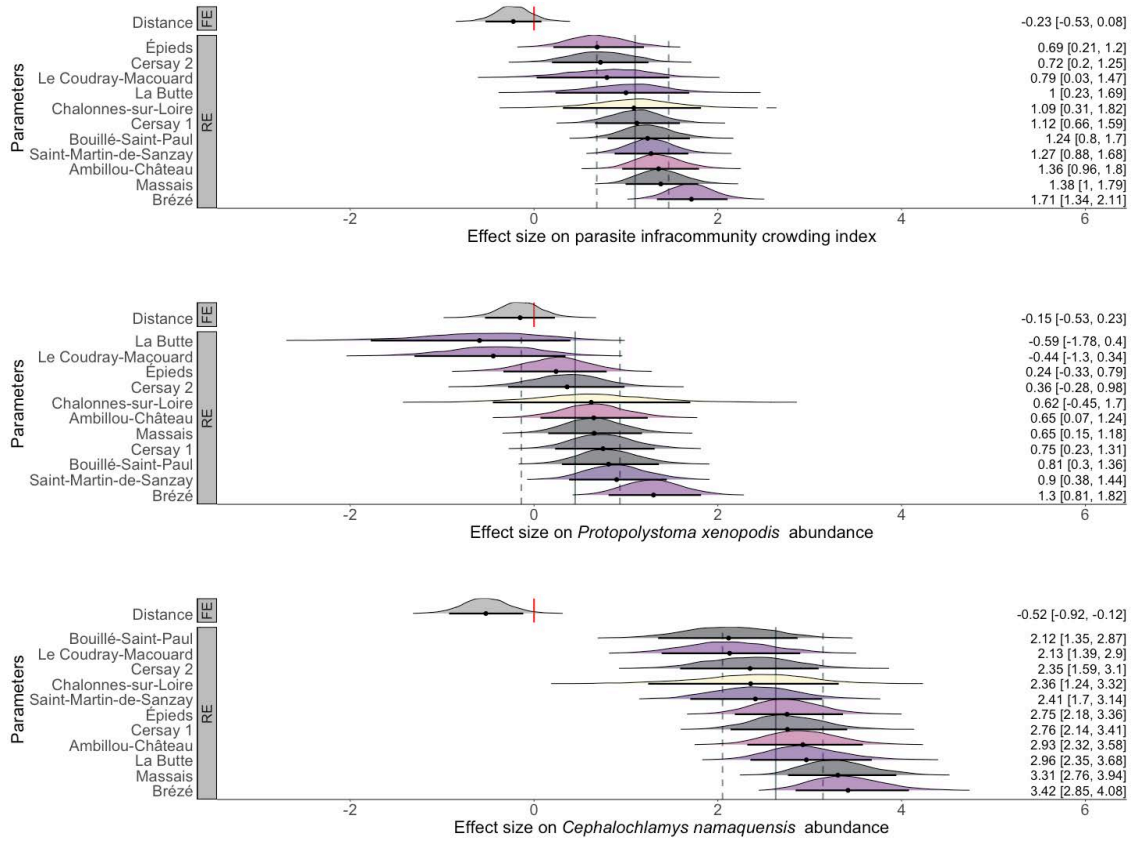

Figure 5.3: Summaries of the estimated posterior distributions for the fixed effect (FE) of least cost distance from the introduction point and the random effect (RE) of collection locality from the three Bayesian generalised linear mixed models of three measures of parasitism of *Xenopus laevis* in western France as response. Black dots show posterior means and bars indicate 89% confidence intervals (CI), also indicated to the right of each distribution. A positive effect size (to the right of the red line) for the fixed effect indicates an increased potential for parasitism in relation to an increase in that fixed effect. In the case of the random effects, a positive deviation from the mean effect size (solid grey line) with 89% CI (dashed grey line) indicates above-average potential for parasitism at that particular locality. Width of 89% CI indicates confidence in estimates. Collection localities are coloured according to distance with the lightest colour indicating the locality furthest from the introduction point, and are named after the nearest town.

demonstrates the multifaceted response of host-parasite systems to a changing world. Moreover, the concurrent investigation of host-parasite dynamics in both the native and invasive range allows us to identify processes that are repeated across space.

5.4.1 Host body size has some effect on crowding and cestode, but not monogenean, abundance of native *Xenopus laevis*

Body size of the host has been regarded as a somewhat recurring determinant of parasite dynamics in many host taxa (Kamiya *et al.*, 2014). This is true of a number of frog species, where parasite communities are more diverse or parasite species are more

abundant in large, and therefore older, frogs (see Bolek & Coggins, 2001; Campião *et al.*, 2015; Hamann *et al.*, 2006). In our analysis of native *X. laevis*, we noticed a positive correlation between host body size and some measures of parasitism. There is an increase in parasite infracommunity crowding and the abundance of one of the dominant infracommunity members, the cestode *C. namaquensis*, in relation to body size, a trend that is not observed in the common monogenean parasite *P. xenopodis*.

Tellingly, the effect of host size on parasitism might be directly linked to host diet in terms of both diet breadth and the number of prey items ingested (Poulin & Morand, 2004). This is simply because larger hosts will eat more, thereby increasing their chances to encounter trophically transmitted parasites (Leung & Koprivnikar, 2019). This is a possible explanation for why the correlation between host body size and the abundance of the cestode, a heteroxenous parasite that enters the host via invertebrate prey (Thurston, 1967), is more marked than the correlation between host body size and abundance of the monogenean, a monoxenous parasite that enters the host as a free-swimming larva (Theunissen *et al.*, 2014).

On the other hand, acquired immunity against parasite infections can counter the effects of parasite accumulation with age, of which host body size is a proxy. Acquired immunity in *X. laevis* against secondary *P. xenopodis* infections has been demonstrated before (Jackson & Tinsley, 2001b), albeit not for *C. namaquensis*. Thus, the connection between host body size, immunity and parasite life history merits further investigation in the present host-parasite system.

Some of the variation in body size seen in the current data set can be ascribed to the observed significant sexual dimorphism in body size in *X. laevis*. Although we did not explicitly test the effect of sex on parasite crowding and abundance, the significant size difference implies that female *X. laevis* might harbour more crowded parasite communities with a higher abundance of *C. namaquensis* than males. Differences in parasite infections between males and females, if observed, can therefore be ascribed to the effect of body size, rather than differences in host behaviour or immune responses that affect chances of infection. Differential infection between the sexes of a North American frog species was found for some, but not all, parasite species (Bolek & Coggins, 2001). Males harboured more of some species of parasites due to more time spent in aquatic habitats during the breeding season compared to females (Bolek & Coggins, 2001). Conversely, terrestrial-based parasites had reached higher levels of parasitism in female frogs due to ecological differences in habitat preference throughout the year (Bolek & Coggins, 2001). Generally, this is a more distinct trend in mammals where different social organisation between males and females is more common than in amphibians (see Bertolino *et al.*, 2003; Perkins *et al.*, 2017; Stuart *et al.*, 2020).

An intrinsic factor that was not included in the current analysis is that of host density. For

example, host density correlates with presence of protozoan parasites in red squirrels (Bertolino *et al.*, 2003). Similarly, the surprisingly low parasite prevalence and diversity of the parasite communities of a newt host were explained by the fact that this host occurs at naturally low densities for long periods of the year (Comas & Ribas, 2013). More broadly, the population density of fish, bird and mammal hosts served as a seemingly universal predictor of parasite species richness at any geographical scale (Kamiya *et al.*, 2014).

With all this being said, the demonstrated effect of host factors on both parasite infracommunity crowding and individual species abundance is overshadowed by the magnitude of the heterogeneity in parasitism explained by site-level variance. Overall, in the native range of *X. laevis*, the host traits of body condition and size manage to explain very little of the observed variation in how metazoan parasites are distributed among hosts.

5.4.2 Extrinsic factors primarily shape parasitism of native *Xenopus laevis*

The predominant portion of the variance in the metazoan parasite dynamics of *X. laevis* in its native range is related to the variation among the South African collection localities, which represent a continuous range of collection seasons, sampling years and habitat types. However, it is specifically the presumed differences in habitat disturbance, which vary from peri-urban or unvegetated artificial water bodies to highly pristine aquatic systems, that differentiate the sites from one another. Similarly, locally operating biotic and abiotic factors, shaped by land use, is the major driver in the differences observed between parasite communities of other frog species (Campião *et al.*, 2012; Hartson *et al.*, 2011).

Be that as it may, our analyses demonstrate that the overall direction of the effect of habitat type and disturbance levels on parasitism is not uniform. Across all three analyses in the native range, hosts collected from unvegetated artificial water bodies, which represent the most anthropogenically disturbed collection localities in our data set, harboured the most aggregated and variable parasite infracommunities, as evidenced by the wide confidence intervals for random effect size for these populations. These wide confidence intervals can be interpreted as the existence of more extreme outcomes of parasitism in hosts from these disturbed water bodies, from completely uncrowded parasite infracommunities where the two dominant parasites might be absent, to highly crowded parasite infracommunities with high maximum parasite loads.

Consequently, we see that habitat disturbance can have many and somewhat opposing effects on parasitism. Frog populations from altered landscapes may well experience lower mean infections yet exhibit greater variance in infection levels, coupled with higher maximum infections (Hartson *et al.*, 2011). As in our study, previous work on amphibian parasite communities has shown that intensive forms of human land use, such as agri-

cultural development, may actually enhance variation in parasite infection, from parasite absence in some cases to infection epizootics in others (Hartson *et al.*, 2011). Chemicals in agricultural run-off and other pollutants may act as immunosuppressants in Amphibia, which in turn may even boost parasitism (Christin *et al.*, 2003; Pochini & Hoverman, 2017; Rohr *et al.*, 2008).

On the other end of the spectrum, the parasites of some frog species are very sensitive to the combination of intensive agriculture and pesticides and respond to environmental disturbance with lowered richness and diversity (King *et al.*, 2007, 2010). What is more, the lowered habitat complexity of intensely disturbed sites will lead to a decrease in the availability of invertebrate, bird and mammal hosts, which will in turn hinder the completion of parasite life cycles (King *et al.*, 2007). This would lead one to expect an upwards trend in parasitism at more pristine sites, as has been postulated before for the metazoan parasites of *X. laevis* (Mbokane *et al.*, 2020; Svitin *et al.*, 2018). Yet, in our study the parasite infracommunities of hosts from pristine localities are not consistently more crowded than those from disturbed localities, suggesting that habitat disturbance is not the only factor at play.

A slightly different picture emerges if we consider the pronounced site-level variance in the abundance of *C. namaquensis*. Hosts from the most pristine localities have a higher potential for infection with this heteroxenous parasite. This goes to show that the conflicting influences of drivers of change such as eutrophication, pesticides and overall changes in water quality are exacerbated when invertebrate intermediate stages are involved (Hartson *et al.*, 2011). The abundance of intermediate hosts can be increased in polluted water, caused by an increase in food sources, as well as a decrease in predator abundance (Rumschlag *et al.*, 2019). In turn, the presence and identity of intermediate hosts can have a notable influence on parasite community composition in amphibian hosts (Mihaljevic *et al.*, 2017). This was also found in a comparison of two populations of a South American frog species with different levels of habitat disturbance where the frogs from the more disturbed area had higher parasite richness, yet harboured less species that require invertebrates as intermediate hosts (Aguiar *et al.*, 2015).

Conversely, another study showed that frogs in disturbed wetlands actually harboured higher levels of direct life cycle parasites (King *et al.*, 2010). Direct life cycle parasites are usually least affected by such environmental changes (King *et al.*, 2010), which would explain why *P. xenopodis* abundance is not necessarily higher in more natural water bodies. Nonetheless, although *P. xenopodis* abundance displays higher variability among hosts from the most disturbed habitats, they were not generally more abundant at these localities.

When looking at the bigger picture of the domestic translocation of *X. laevis* in its native range of South Africa, both past and current (de Villiers & Measey, 2017; Measey, 2016;

Measey *et al.*, 2017; van Sittert & Measey, 2016; Weldon *et al.*, 2007), it is important to realise that the habitats in our data set are more than just water bodies along a disturbance gradient. Previous studies have demonstrated that *X. laevis* readily moves overland in search of new water bodies (Measey, 2016) and that it is also extensively translocated by the many role players to stock dams for recreational fishing and other purposes (van Sittert & Measey, 2016; Weldon *et al.*, 2007). Unvegetated artificial and temporary water bodies will of course be more susceptible to colonisation by pioneers and thus possibly harbour *X. laevis* that have recently dispersed from another habitat. Thus, the net effect of habitat disturbance on parasite dynamics should further be interpreted in the light of the widespread and frequent dispersal of *X. laevis* in its native range, a characteristic of this frog that makes some of its native populations not unlike its rapidly expanding populations in the invasive range.

5.4.3 Cestode abundance decreases with distance from the introduction point in invasive *Xenopus laevis*

The actively expanding population of *X. laevis* in its invasive range in western France exhibits markedly less among-site variation in parasitism than in the native range. Of course, this is to be expected of parasite infracommunities that were all sampled within one season from very similar habitats. Moreover, despite some observed differences between the sites in terms of host demography, we now know from our analyses in the native range that these differences will have but a weak effect on overall variability in parasitism. The site-level variance was most pronounced for *P. xenopodis* abundance, which can be explained by some sites with overall low mean *P. xenopodis* abundance yet high variability, as was found for the disturbed sites in the native range.

Remarkably, the locality that was the furthest from the introduction point consistently presented with *X. laevis* with the most variable parasite infracommunities and cestode and monogenean abundances. As was seen for the disturbed localities in the native range, a pattern such as this is often the hallmark of a recently established, pioneer host-parasite assemblage, which is to be expected of the locality furthest from the introduction point. Our approach of the concurrent examination of these patterns in the native and invasive range thus identifies the footprint of an invasive host-parasite system not simply as an impoverished parasite community (Schoeman *et al.*, 2019; Torchin *et al.*, 2003), but rather as a more variable and thus unpredictable parasite dynamic.

There is reason to believe that the abundance of the cestode, but not the two other investigated measures of parasitism, might decay with distance from the introduction site in the expanding population of *X. laevis* in western France. The phenomenon of lowered parasitism (lower abundance, prevalence and diversity) at the range edge of an expanding invasive population has been found in invasive birds (Coon & Martin, 2014),

small mammals (Stuart *et al.*, 2020) and reptiles (Barnett *et al.*, 2018; Coates *et al.*, 2017). Moreover, this has also been extensively studied in the invasive cane toad population in Australia (see Brown *et al.*, 2015; Mayer *et al.*, 2021; Phillips *et al.*, 2010).

Population density might be the most likely explanation for this effect, since the density of *X. laevis* has been documented to be low at the range edge of the invasive population in western France (Vimercati *et al.*, 2020). Low population density of frogs has been linked with lowered transmission rates of parasites at the range edge before, although serial founding effects might also play a role (Cronin & Reeve, 2005; Kelehear *et al.*, 2012; Phillips *et al.*, 2010).

However, the effect of range expansion demonstrated in our study might actually be confounded by the effect of host body size. Distance from the introduction site and host body size are correlated in the current data set, which is not surprising given the spatial sorting of dispersal traits in this host population (Courant *et al.*, 2019b). Our analyses of native parasite assemblages have pointed out that both parasite infracommunity crowding and *C. namaquensis* abundance increase with body size. The decrease in body size towards the range edge points towards the mechanism behind the observed decrease in parasite abundance. Compellingly, the coupling of the spatial sorting of the two traits – that of enhanced body size for dispersal and lowered parasite burdens – could enhance invasion success even further. In this, it should be kept in mind that the loss of parasites during invasion is almost inevitable (Torchin *et al.*, 2003) but its role as driver of invasion success is debatable (Blackburn & Ewen, 2017). For example, the release from parasitic worms in invasive frogs does not significantly contribute to invasiveness (Roznik *et al.*, 2020). In the light of this, slightly lowered cestode burdens might give their host an edge during range expansion, but more likely it is just an artefact of spatial sorting that maximises dispersal traits over large body size.

A final factor that might contribute to differences in parasitism along localities in the invasive range is the co-occurrence of the invasive crayfish *P. clarkii* at one of the sites. Across all three analyses conducted on the data set of invasive hosts, the *X. laevis* hosts at this particular site consistently displayed lower than expected parasite infracommunity crowding, as well as lower than expected cestode and monogenean abundances. Where these two species co-occur in western France, *P. clarkii* is possibly a predator of *X. laevis* (Kruger *et al.*, 2019). Its presence might therefore control *X. laevis* numbers and lower its overall density at this locality, as is the effect of *P. clarkii* on other Amphibia elsewhere (Cruz *et al.*, 2006; Souty-Grosset *et al.*, 2016). As already mentioned, lowered host densities negatively affect parasite numbers (Bertolino *et al.*, 2003; Comas & Ribas, 2013; Kamiya *et al.*, 2014). This points towards the influence of locality-specific stochastic effects that shape the parasite infection of *X. laevis* in western France.

5.4.4 Implications for the domestic and global invasion of host-parasite systems

In a rapidly changing world that is characterised by the large scale movement of organisms, it is important to not just describe the parasite dynamics of range expansions, but also to make predictions about the future distributions of species and their symbionts. Our study attempted to uncover general responses to range expansion in the parasites associated with a globally invasive amphibian by investigating the factors that determine the make-up of its parasite assemblages in both its native and invasive range.

We see that anthropogenic disturbance and host translocation simultaneously have positive and negative effects on parasite transmission. Clearly, the idea of speciose native parasite communities versus impoverished non-native parasite communities (Schoeman *et al.*, 2019; Torchin *et al.*, 2003) is an oversimplification of the actual dynamics. Host populations that are recently established do not necessarily carry fewer parasites or facilitate fewer parasite infracommunity interactions. Rather, these assemblages are characterised by their variability, which is in essence a perfect storm for parasite outbreaks that can cause these newly established populations to collapse, as has been observed before in captive *X. laevis* (Brayton, 1992; Cohen *et al.*, 1984; Elkan & Murray, 1952; Nigrelli & Maraventano, 1944).

The often opposing responses of the two dominant parasites species to the predictors underscore the importance of studying parasite dynamics on a species-by-species basis, as opposed to pooling parasite species (Poulin, 2019). Our incomplete understanding of these differing dynamics also highlights the need for elegant and detailed natural history experiments that can provide invasion ecologists with a deeper understanding of the co-introduced parasites they encounter (Valenzuela-Sánchez *et al.*, 2021). Despite years of study (reviewed in Tinsley, 1996), the parasite assemblage of *X. laevis* holds many mysteries, with unanswered questions about host immune response, parasite life cycles, especially when it comes to hosts other than *X. laevis*, and even basic taxonomy.

An improved understanding of the parasite ecology of a widespread amphibian such as *X. laevis* will have a number of applications. With a well-described, widespread model host-parasite system at our disposal, invasion biologists can use *X. laevis* and its parasites as bioindicators of disturbance. Since *X. laevis* harbours a parasite assemblage with species that also make use of invertebrate, reptile, fish and bird hosts in their life cycle (Schoeman *et al.*, 2020), the decline or absence of certain parasite species can be an even more useful indicator of ecosystem health than amphibian species themselves. Ultimately, a thorough understanding of the telltale parasite assemblage of a recently established population of a host can be a useful tool to determine the maturity of the establishment of invasive hosts in an ecosystem, as well as enable us to better predict the impacts complex, multispecies invasion packages in an ever-changing world.

Chapter 6

A forgotten introduction reveals a hidden one: co-phylogeography of the African Clawed Frog and its monogenean parasite sheds new light on their shared introduction history

6.1 Introduction

The Anthropocene is characterised by the unparalleled human-mediated passage of organisms from their natural ranges to ecosystems across the world (Capinha *et al.*, 2015; Ricciardi, 2007). This reshuffling of the world's biota is a decisive agent of global change, as evidenced by the fact that invasive species are implicated as the cause of a third of recent animal extinctions (Blackburn *et al.*, 2019). With this in mind, the development of methods to trace both the origin and expansion of biological invaders has never been more urgent.

Alien organisms are regarded as *invasive* if they manage to disperse from their initial introduction point and seed new populations in their non-native range (Blackburn *et al.*, 2011; Richardson *et al.*, 2011b). What is more, organisms can be both native and invasive within the borders of their country of origin, especially in large countries with high climatic and habitat diversity (van Wilgen *et al.*, 2020). These so-called *domestic exotics* occur outside their native range, yet remain within one administrative region, a feature which

hinders their detection and management (Guo & Ricklefs, 2010). Along the same line are what are known as *intraspecific cryptic invasives*. This describes the process where one lineage of a species spreads into parts of the species' native range where another lineage is already present, often with human help (Morais & Reichard, 2018).

The African Clawed Frog *Xenopus laevis* (Daudin, 1802) (Anura: Pipidae) is arguably the world's most widely distributed and well-studied amphibian (Measey *et al.*, 2012; van Sittert & Measey, 2016). As large scale exports of *X. laevis* from South Africa bore this frog to laboratories on all continents except Antarctica, subsequent accidental and deliberate releases led to its introduction and invasion in areas outside its native southern Africa (Measey *et al.*, 2012).

The ability to trace the native origins of the invasive populations of *X. laevis* is brought about by the high levels of phylogeographic structuring of this frog in its native range of southern Africa (de Busschere *et al.*, 2016; Furman *et al.*, 2015). Previous studies on the morphology and genetics of *X. laevis* have identified several differentiated populations in South Africa that are segregated by large mountain ranges and different climatic regions (de Busschere *et al.*, 2016; du Preez *et al.*, 2009; Furman *et al.*, 2015; Measey & Channing, 2003). Conversely, invasive frog populations exhibit markedly less genetic diversity, consisting almost entirely of individuals with a genetic make-up similar to native *X. laevis* populations from the winter rainfall region to the southwest of South Africa (de Busschere *et al.*, 2016; Lillo *et al.*, 2013; Lobos *et al.*, 2014).

The behaviour and genetics of *X. laevis* from the native range of the southwestern lineages have suggested the occurrence of both natural and human-mediated translocation in the region, leading some authors to advocate for its recognition as a domestic exotic (Measey & Davies, 2011; Measey *et al.*, 2017). However, the translocation of lineages of *X. laevis* likely extends beyond the southwestern winter rainfall region, based upon the fact that the bulk of exports was dispatched to the domestic market, including many research and higher learning institutions in the native range of the northeastern lineage (van Sittert & Measey, 2016). Regardless, the cryptic invasion of *X. laevis* from the southwestern lineages into the native range of the northeastern lineage has not been confirmed in previous phylogeographic studies of this frog (de Busschere *et al.*, 2016; du Preez *et al.*, 2009; Furman *et al.*, 2015; Measey & Channing, 2003).

The phylogeographic analyses of invasive species can be highly informative for the reconstruction of invasion histories, the prediction of potential range expansion and invasion success and the development of control strategies (e.g. de Busschere *et al.*, 2016; Dufresnes *et al.*, 2017; Dlugosch & Parker, 2008; Hiller & Lessios, 2017; Lee & Gelembiuk, 2008; Prentis *et al.*, 2009; Stouthamer *et al.*, 2017; Zahiri *et al.*, 2019). Nonetheless, in many cases the available molecular data are of insufficient resolution by themselves to trace the movement of species (e.g. Ahyong *et al.*, 2017; Criscione *et al.*, 2006). In fact, the

use of molecular population genetics at the short timescales and coarse-grained genomic resolution of most biological invasions seems to be applicable only in rare instances (Fitzpatrick *et al.*, 2012).

A more holistic approach to solving the origin and range shifts of invasive species may involve molecular data from co-introduced parasites. Such an integrative approach has been proposed to investigate invasions that are difficult to trace (Clavero *et al.*, 2016) but is applied only rarely. For example, the long-debated cryptogenic history of the European marine snail was solved with the help of an associated digenean parasite (Blakeslee *et al.*, 2008). Likewise, intraspecific morphometric variation of monogenean parasites identified both the origin and introduced life stage of invasive clupeid fish in Africa (Kmentová *et al.*, 2019), shed light on the history of an invasive population of odontobutid fish in Europe (Ondračková *et al.*, 2012) and provided information on the introduction route of an invasive goby in Europe (Huyse *et al.*, 2015).

In general, monogenean parasites exhibit sufficient levels of phylogeographic structuring at the level of population to assess intraspecific spatial patterns in their hosts (Baldwin *et al.*, 2012; Hahn *et al.*, 2015; Huyse *et al.*, 2017; Kmentová *et al.*, 2018, 2020). At the very least, the phylogeographic structuring of monogenean lineages can support evidence revealed by the host data set or historic records, such as the well-documented anthropogenic introduction of salmonid fish host stocks across Europe that is reflected in the phylogeography of their gyrodactylid monogenean lineages (Hahn *et al.*, 2015). In particular, monogenean parasites are regarded as ideal tags of host genealogy due to their short generations, direct life cycles and generally high host-specificity (Nieberding & Olivieri, 2007).

Thus, we posit that the bladder polystomatid *Protopolystoma xenopodis* (Price, 1943) Bychowsky, 1957 (Monogenea: Polystomatidae) is the ideal tool to trace the hitherto unconfirmed contact between different lineages of its host *X. laevis* across its native southern Africa. In natural populations across Africa, *P. xenopodis*, the most widely distributed of the species of *Protopolystoma*, is restricted to a single host species complex, *X. laevis sensu lato*, even in sympatry with other *Xenopus* species (Tinsley & Jackson, 1998a,b). Patterns of host-specificity and speciation within *Protopolystoma* reflect the phylogenetic relationships among their hosts, hinting at a very close co-evolutionary association (Tinsley & Jackson, 1998a). Furthermore, in *P. xenopodis*, notable morphological variation exists between populations of the polystomatid in southern Africa and those infecting more northerly host subspecies (Tinsley & Jackson, 1998b), as well as between polystomatids from *X. laevis* from the southwestern and northeastern lineages in South Africa (see Appendix B for analysis). These factors suggest that the phylogeny *P. xenopodis* might mirror that of *X. laevis* also on an intraspecific level, meaning that this host-parasite system is a good candidate for a co-phylogeographic study.

All things considered, the well-studied, widely distributed and intimately associated *X. laevis* and *P. xenopodis* system may act as a proof of concept that intraspecific parasite phylogeography can reveal cryptic introductions of host lineages. In the present study, we assessed the performance of this integrative approach in the detection of intraspecific cryptic invasions by determining whether the phylogeography of *P. xenopodis* in its native range (1) mirrors the documented intraspecific divergence of its host *X. laevis* and (2) may identify recent human-mediated contact between distinct lineages of *X. laevis*.

6.2 Methods

6.2.1 Host and parasite sampling

During a parasite survey of *X. laevis* that ran from 2017 to 2019, total of 59 adult *X. laevis* and their corresponding 59 *P. xenopodis* parasites were collected in southern Africa, France and Portugal (see Appendix A for detailed information). In the native range of southern Africa, 46 adult frogs, captured from March 2017 to April 2019 in liver baited funnel traps from 30 localities across the region, were surveyed (Figure 6.1). These sampling localities were selected based upon the geographic distribution of the phylogeographic lineages of *X. laevis* in South Africa proposed by de Busschere *et al.* (2016), namely SA1–3 and SA7 in the winter rainfall region to the southwest and SA4–6 in the summer rainfall region to the northeast (Figure 6.1). Accordingly, *X. laevis* collected along the coast to the southwest of the Cape Fold Mountains were assigned to SA1, or SA2 if these coastal localities were more to the east. The SA3 *X. laevis* were captured among the Cape Fold Mountains near Laingsburg between the southwestern coast and the Great Escarpment to the northeast, with SA4 *X. laevis* captured further northward in the lowland Karoo semi-desert in the summer rainfall region near the plateau edge of the Great Escarpment. The *X. laevis* captured to the north of the Cape Fold Mountains near the western coast in the winter rainfall region were designated SA7. Finally, *X. laevis* from the summer rainfall region to the northeast were classified as SA5 if they were captured on the inland plateau of the Great Escarpment or as SA6 if they were captured at the edge of the Great Escarpment along the eastern seaboard.

In the invasive range, 13 adult *X. laevis*, collected from 12 localities in western France and one locality near Lisbon, Portugal, during the summers of 2017, 2018 and 2019, were included. In France, frogs were captured in baited traps by members of the EU LIFE CROAA team as part of the regional eradication programme for invasive amphibians. The adult frog in Portugal was obtained from the locally captured laboratory stock of the University of Lisbon.

Prior to dissection, all frogs underwent double euthanasia with anaesthesia in 6% ethyl-

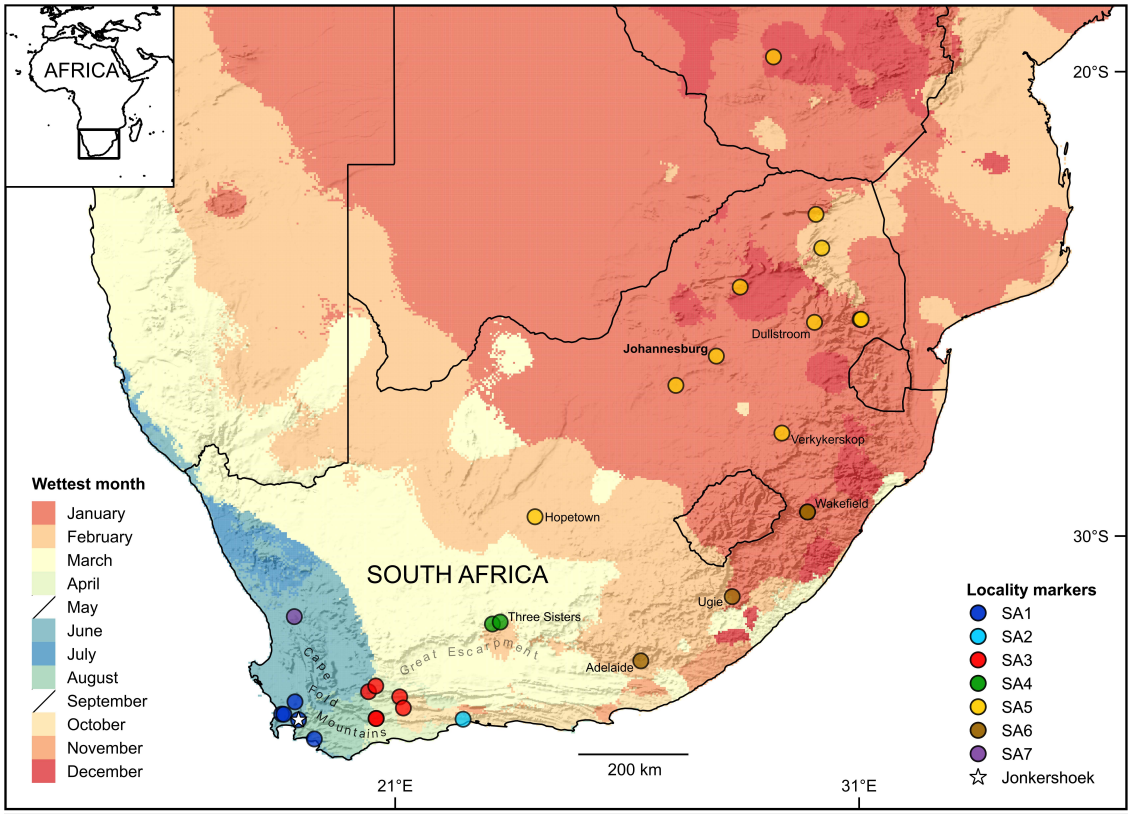

Figure 6.1: Localities in southern Africa where 46 adult *Xenopus laevis* were collected along with the flatworm parasite *Protopolystoma xenopodis*. Localities are classified according to the geographic extent of the native phylogeographic lineages of *X. laevis* in the region (SA1–7), following (de Busschere *et al.*, 2016). Key localities are named according to the closest town or city (in the case of Johannesburg) and Jonkershoek, the source locality of the majority of historic *X. laevis* exports, is indicated. Mountain ranges are indicated with shaded relief and rainfall seasonality is represented by the wettest month of each 25 km^2 grid cell, with summer months (October–March) in shades of red and winter months (April–August) in shades of blue. Monthly mean precipitation data, obtained from the WorldClim 2.1 database at a spatial resolution of 2.5 arc-minutes (Fick & Hijmans, 2017), were used to identify the months with the highest historical mean precipitation from 1970 to 2000 for each grid cell. Elevation data were obtained from the Natural Earth database. The map was constructed in QGIS *version* 3.10.2-A Coruña (QGIS Development Team, 2018) with the Mercator projection. Data manipulation of precipitation means was conducted in R *version* 4.0.2 (R Core Team, 2020).

3-aminobenzoate methanesulfonate (MS222) (Sigma-Aldrich Co., Steinheim, Germany) followed by pithing. Euthanised frogs were examined for the presence of ecto- and endoparasites. In total, 59 polystomatids (one per each host individual) retrieved from the bladder were included in the present study. Parasites and aliquots of liver tissue from the corresponding 59 frog hosts were preserved in 70% ethanol. Relevant institutional, national and international guidelines for the care and use of animals were followed under the North-West University AnimCare ethics number NWU-0380-16-A5-01.

Table 6.1: Primers used for DNA amplification and sequencing of the *COX1* and *rrnS* genes of *Xenopus laevis* and *Protopolystoma xenopodis* with information on gene targets, orientation (forward [F] and reverse [R]) and sequences.

Gene target	Primer	Sequence (5' to 3')
X. laevis COX1	'LCO1490' [F] (Folmer *et al.*, 1994)	GGTCAACAAATCATAAAGATATTGG
	'HCO2198' [R] (Folmer *et al.*, 1994)	TAAACTTCAGGGTGACCAAAAAATCA
	'VF1' [F] (Ivanova *et al.*, 2006)	TTCTCAACCAACCACAAAGACATTGG
	'VR1' [R] (Ward *et al.*, 2005)	TAGACTTCTGGGTGGCCAAAGAATC
P. xenopodis COX1	'L-CO1p' [F] (Littlewood *et al.*, 1997)	TTTTTTGGGCATCCTGAGGTTTAT
	'H-Cox1p2' [R] (Littlewood *et al.*, 1997)	TAAAGAAAGAACATAATGAAAATG
	'H-Cox1R' [R] (Héritier *et al.*, 2015)	AACAACAAACCAAGAATCATG
X. laevis rrnS	'12SA-F' [F] (Kocher *et al.*, 1989)	CTGGGATTAGATACCCCACTA
	'12SB-R' [R] (Kocher *et al.*, 1989)	TGAGGAGGGTGACGGGCGGT
P. xenopodis rrnS	'12SpolF1' [F] (Héritier *et al.*, 2015)	YVGTGMCAGCMRYCGCGGYYA
	'12SpolR1' [R] (Héritier *et al.*, 2015)	TACCRTGTTACGACTTRHCTC
	'12SpolR9' [R] (Héritier *et al.*, 2015)	TCGAAGATGACGGGCGATGTG

6.2.2 Molecular data collection

The preserved host and parasite tissue underwent DNA extraction with either the PCRBIO Rapid Extract PCR kit (PCR Biosystems Ltd., London, United Kingdom) or the *Quick*-DNA™ Miniprep Plus kit (Zymo Research, United States). Subsequently, amplification reactions were performed with 2 to 5 μL extracted genomic DNA, 1.25 μL forward primer, 1.25 μL reverse primer, 12.5 μL master mix and PCR-grade water to the final volume of 25 μL. The employed master mixes of PCR reagents were either the PCRBIO HS Taq Mix Red (PCR Biosystems Ltd., London, United Kingdom) or the OneTaq® 2X Master Mix with Standard Buffer (New England Biolabs Ltd., Massachusetts, United States). Various primer combinations were employed to amplify the partial *COX1* and *rrnS* genes of the 59 frog-polystomatid pairs (Table 6.1).

The thermocycling profile implemented for the each of the amplification reactions depended upon the primer pair and the master mix used. Across all reactions, the temperature for elongation was determined by the master mix used as per supplier instructions. The 'LCO1490'/'HCO2198' and 'VF1'/'VR1' primer pairs were implemented with the following general thermocycling profile: initial denaturation at 95°C for 2 min, followed by 35 cycles of denaturation at 95°C for 30 s, annealing for 30 s at 50°C for the first primer pair and 54°C for the second and elongation for 2 min, terminated by one cycle of elongation for 7 min. In the case of the '12SA-F'/'12SB-R' primer pair, the proposed thermocycling profile of Amaro *et al.* (2013) was followed. For the amplification of the two polystomatid genes, the thermocycling profile recommended by Héritier *et al.* (2015) was implemented for all primer pairs.

For purification and sequencing, all PCR products were sent to a commercial company

(Inqaba Biotec, Pretoria, South Africa) that used the ExoSAP protocol (New England Biolabs Ltd., Massachusetts, United States) for purification and obtained the sequences with BigDye® Terminator *version* 3.1 Cycle Sequencing, utilising the corresponding primer pairs used in the PCR, on an ABI3500XL analyser. Sequences were assembled and manually edited in Geneious Prime *version* 2021.0.3 (www.geneious.com).

6.2.3 Haplotype networks

The intraspecific phylogeography of both *X. laevis* and *P. xenopodis* were analysed as haplotype networks. Each of the four sets of sequences, namely the frog *COX1* and *rrnS* and the polystomatid *COX1* and *rrnS* genes, were aligned using the Clustal Omega algorithm (Sievers & Higgins, 2017) implemented in Geneious Prime. For the protein-coding genes, translation alignment was implemented under the vertebrate mitochondrial genetic code (table 2) for the frogs' *COX1* and the echinoderm and flatworm mitochondrial genetic code (table 9) for the polystomatids' *COX1*. The separate gene alignments were trimmed to the length of the shortest sequence to remove end gaps since gaps are masked during analysis in any case (Leigh & Bryant, 2015). The aligned genes were concatenated by individual in Geneious Prime, resulting in one frog and one polystomatid alignment. Minimum spanning networks (MSN) of the concatenated partial *COX1* and *rrnS* gene data sets were inferred for 59 *X. laevis* and 59 *P. xenopodis* individuals separately in PopART *version* 1.7.2 (Bandelt *et al.*, 1999; Leigh & Bryant, 2015).

6.2.4 Phylogenetic analyses

For the phylogenetic analyses, duplicate sequences were identified with the help of the CD-HIT programme (Fu *et al.*, 2012; Li & Godzik, 2006) implemented on its online web server (Huang *et al.*, 2010). Host and parasite specimens with a unique *COX1* or *rrnS* gene haplotype were retained for the analysis. The *COX1* and *rrnS* gene sequences of the congeneric Müller's clawed frog *X. muelleri* (Peters, 1844) (accession numbers EU599031 and AY581657; Evans *et al.*, 2004 and Evans *et al.*, 2008) and the polystomatid *P. occidentalis* Tinsley *et* Jackson, 1998 (accession numbers KR856179 and KR856121; Héritier *et al.*, 2015) were obtained from GenBank and added as outgroups. This polystomatid only infects *X. muelleri*-like species, even in sympatry with *X. laevis* (Tinsley & Jackson, 1998b). Furthermore, its host *X. muelleri* reportedly reproduces sterile offspring when hybridisation occurs between this species and its sympatric congener *X. laevis* (Fischer *et al.*, 2000). Therefore, the selected outgroups are applicable in an intraspecific analysis of the *X. laevis* and *P. xenopodis* host-parasite system.

The resulting data sets, after removal of duplicates and addition of the outgroups, were aligned as for the haplotype networks with the exception that gaps in the alignment were

not trimmed. Descriptive statistics of the two alignments were derived in DnaSP *version* 6.12.03 (Rozas *et al.*, 2017).

Initially, the concatenated alignments comprised four partitions, namely the three codon positions of the partial *COX1* gene and the *rrnS* gene. The ModelFinder selection routine (Kalyaanamoorthy *et al.*, 2017), in conjunction with the FreeRate heterogeneity model (Soubrier *et al.*, 2012), implemented in IQ-TREE *version* 2.1.2 (Minh *et al.*, 2020), was employed to select the optimal model of molecular evolution for each partition. To reveal the optimal partitioning scheme and most suitable evolutionary models for each alignment, the initial partitions were sequentially merged (Chernomor *et al.*, 2016) until model fit, as evaluated by the Bayesian Information Criterion (BIC), ceased to improve.

Consequently, the maximum likelihood (ML) phylogeny of the host was inferred under the TIM2 model (Posada, 2003) for all partitions merged as one with edge-unlinked FreeRate heterogeneity models (Soubrier *et al.*, 2012), proportions of invariant sites (Gu *et al.*, 1995) and discrete gamma models (Yang, 1994) for each initial partition. Similarly, the ML tree of the polystomatid was inferred under the TPM3 model (Kimura, 1981) with a FreeRate heterogeneity model (Soubrier *et al.*, 2012) for each of the initial partitions merged as one. The analyses were performed in IQ-TREE *version* 2.1.2 (Minh *et al.*, 2020), with the assessment of branch support through ultrafast bootstrapping (UFboot2; Hoang *et al.*, 2018) and the Shimodaira-Hasegawa approximate likelihood ratio test (SH-aLRT; Guindon *et al.*, 2010), each with 10 000 replicates.

The resulting topologies were rooted with respect to the outgroups in TreeGraph2 *version* 2.15.0-877 *beta* (Stöver & Müller, 2010). Clades with UFboot2 support lower than 95% or SH-aLRT lower than 80% were collapsed to polytomies in the same programme.

6.2.5 Co-phylogenetic analyses

The resulting phylogenies formed the basis of a global fit approach to the co-phylogenetic analysis of *X. laevis* and *P. xenopodis*. The global congruence of the phylogenies of *X. laevis* and *P. xenopodis* was assessed by the implementation of both Procrustean Approach to Co-phylogeny (PACo) (Balbuena *et al.*, 2013) and the fourth-corner statistical approach of ParaFit (Legendre *et al.*, 2002). Going further than other global fit methods, PACo and ParaFit can also make co-evolutionary inferences at the level of species interactions, allowing for a more direct inference of the process (Balbuena *et al.*, 2013; Legendre *et al.*, 2002; Poisot & Stouffer, 2015). Moreover, both these methods can accommodate trees that are not fully resolved and support instances of uneven numbers of terminal nodes of hosts and parasites, as was the case for our phylogenies.

In PACo, we specifically assessed the dependency of the parasite phylogeny upon that of

the host through asymmetrical Procrustean superimposition of host and parasite distance matrices, whilst ParaFit tested the dependence of both phylogenies upon one another (Balbuena *et al.*, 2013; Legendre *et al.*, 2002). Prior to analyses, the outgroups were removed from the ML phylogenies to assess congruence at the intraspecific scale. These phylogenies of the host and parasite were converted to matrices of patristic distances by the package *ape* (Paradis & Schliep, 2019) in R *version* 4.0.2 (R Core Team, 2020). These matrices served as input for both analyses, along with the corresponding host-parasite association matrix, where the polystomatids were assigned to their original host individuals, or to a host with an identical gene sequence to the original host individual.

The principal coordinates for PACo were derived with the R package *paco* (Hutchinson *et al.*, 2017) for the Procrustes superimposition in conjunction with the Cailliez correction (Cailliez, 1983) of non-Euclidean distances. The PACo analysis was performed, using the asymmetric Procrustes statistic, in the same R package with 10 000 permutations, with conserved row sums and number of interactions (Hutchinson *et al.*, 2017). The potential co-evolutionary dynamics of the interacting clades were further explored by identifying those interactions that most contribute to the possible concordance between the two phylogenies through a jackknife procedure in the R package *paco* (Hutchinson *et al.*, 2017). Those interactions with the smallest residual distances were interpreted as stronger supporters of overall congruence.

The ParaFit analysis (Legendre *et al.*, 2002) was carried out with the R package *ape* (Paradis & Schliep, 2019) based upon the patristic distance matrices, using 10 000 permutations with the Cailliez correction (Cailliez, 1983) for negative eigenvalues. Both the ParaFitLink tests were employed to assess the significance of the individual links (Legendre *et al.*, 2002).

A tanglegram of the host and parasite ML phylogenies with a weighted interaction network, based upon the residuals yielded by the PACo jackknife procedure, was constructed with the R package *phytools* (Revell, 2012) with the function `cophylo`, which has an internal algorithm that rotates nodes to optimally match tips. Due to the removal of duplicate sequences, certain host and parasite terminal nodes could be involved in multiple interactions.

6.3 Results

6.3.1 Sequence diversity

The trimmed and concatenated alignment of the two hosts genes used for the network analysis, namely *COX1* (trimmed to 641 bp) and *rrnS* (trimmed to 369 bp), was 1010 bp in

length. The final alignment contained no gaps, thus all the sites were used for inference. In the case of the two parasite genes, a total alignment of length 901 bp, which included seven sites with gaps that were not included in inference, was comprised of *COX1* of 416 bp and *rrnS* of 485 bp.

Analysis of redundancy identified 30 unique sequence combinations in the concatenated *X. laevis* data set with 23 unique haplotypes of *COX1* and 10 of *rrnS*. Including the outgroup *X. muelleri*, 31 haplotypes were aligned for the ML analysis to a total of 1153 bp of 717 bp *COX1* and 436 bp *rrnS* containing 189 sites with missing data and 183 variable sites, of which 88 were parsimony informative. Similarly, after removal of duplicates, the concatenated parasite alignment contained 44 unique *P. xenopodis* sequences, a combination of 34 unique haplotypes of *COX1* and 35 of *rrnS*. Along with the outgroup *P. occidentalis*, the 45 aligned *COX1* sequences of 423 bp and the *rrnS* sequences of 511 bp resulted in a concatenated alignment of 934 bp in length that was used to obtain the ML phylogeny of the parasite. Of these sites, the 799 complete sites contained 225 sites that were polymorphic with a subset of 174 parsimony informative sites.

6.3.2 Host and parasite phylogeographic clustering

The frog haplotypes were visualised in a MSN (Figure 6.2). Frog specimens from the SA5–6 localities in the summer rainfall region were represented by seven unique haplotypes, whilst the specimens from the winter rainfall region were represented by 15 unique haplotypes. The invasive frog populations from France and Portugal were represented by five unique haplotypes.

The MSN of the frog host supported the existence of three major phylogeographic clades that roughly coincide with the summer and winter rainfall regions in the native range (NE and SW clusters in Figure 6.2). The northeastern frog cluster corresponded with NE in the frog ML tree (refer to Figure 6.3) and included frog specimens from SA4–6 and France. This cluster exhibited a star-like topology with two dominant native haplotypes and four satellite haplotypes that were separated from the dominant haplotypes by one to seven mutations. Frog specimens from Wakefield and Ugie had similar haplotypes that fell between the two major clusters, separated from the nearest northeastern haplotype by 29 mutations and the nearest southwestern haplotype by 45 mutations. The southwestern frog cluster included frogs from SA1–4, SA7, France and Portugal and corresponded with SW_{coast} and SW_{inland} from the frog ML tree. One central dominant haplotype in the southwestern cluster represented specimens from SA1 and SA4, as well as France and Portugal. Satellite haplotypes fanned out from the dominant southwestern haplotype with a star-like topology and, with the exception of a cluster of four highly divergent haplotypes that differed from the most frequent haplotype by 36 to 50 mutations, the rest were separated from the central haplotype by one to seven mutations. The specimens in the

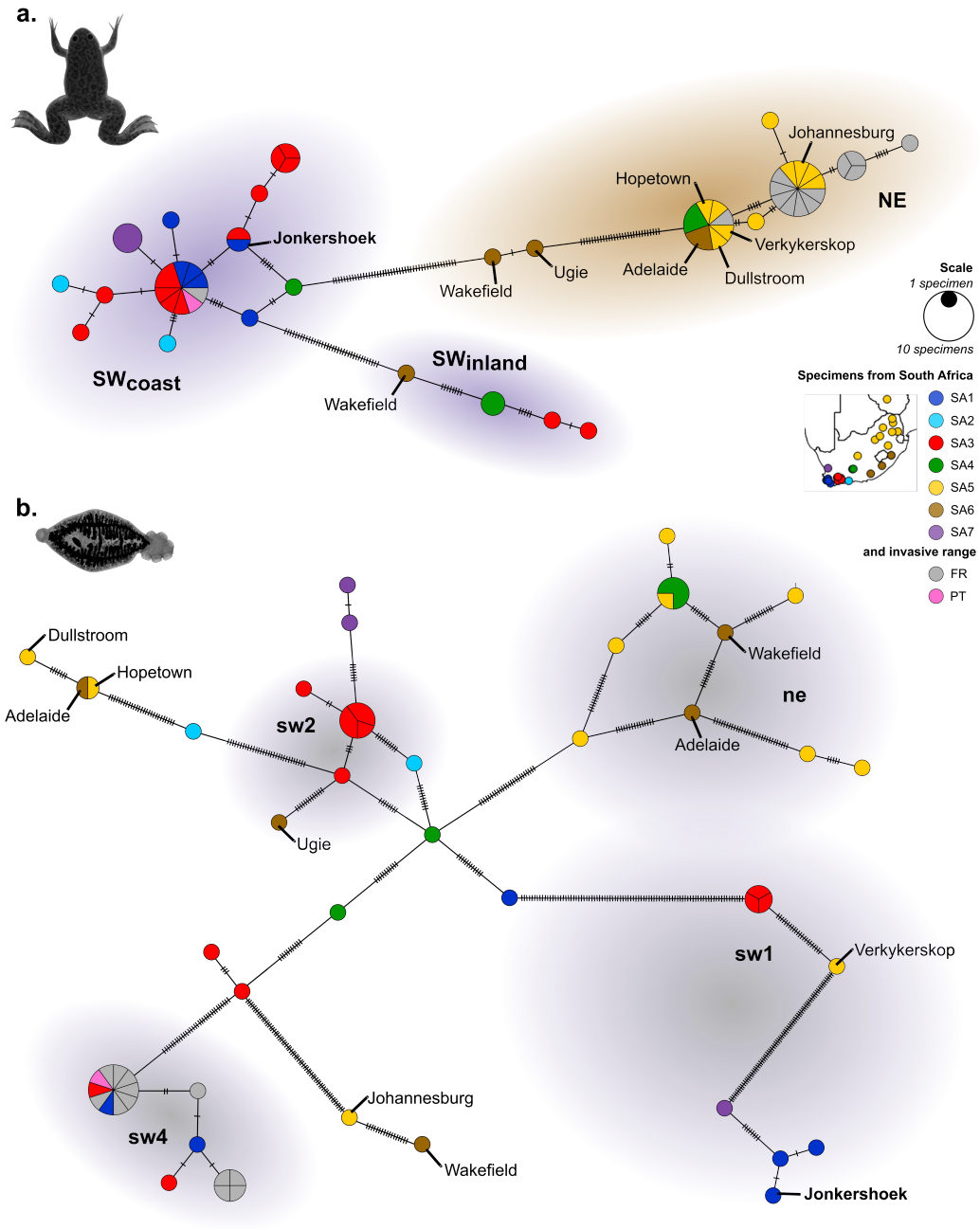

Figure 6.2: Median spanning haplotype networks of the concatenated partial *COX1* and *rrnS* genes of: **a** – 59 *Xenopus laevis* specimens; **b** – and their corresponding 59 *Protopolystoma xenopodis* parasites from their native and invasive range. For *X. laevis* and their polystomatids collected at 30 localities in the native southern Africa (see inset map), the colours refer to the seven phylogeographic lineages of the host, following de Busschere *et al.* (2016). Co-introduced *X. laevis* and their polystomatids from France (grey) and Portugal (pink) are also included. Clusters that correspond to the clades revealed by the ML analyses (see Figure 6.3) are the northeastern host (NE) and parasite (ne) clades and the southwestern host (SW) and parasite (sw) clades and are highlighted. Key localities where host switches were detected are named, along with the haplotype from the source locality of most of the *X. laevis* exports, Jonkershoek. The sizes of the circles are proportional to haplotype frequencies (see legend). The number of mutations is marked on the connecting branches.

divergent southwestern cluster corresponded to SW_{inland} of the host ML tree and also included a specimen collected from Wakefield (SA6). Frog specimens from Three Sisters (SA4) were present in the NE, SW_{coast} and SW_{inland} clusters.

The phylogeographic lineages uncovered in the host ML tree was broadly reflected in the structure of the polystomatid MSN, with the exception of **sw3** that was dispersed across the network (see clusters **ne**, **sw1–2,4** in Figure 6.2). This echoed the many unresolved relationships among polystomatids colected from SA1–4 and SA7 localities in the winter rainfall region uncovered in the ML tree.

A cluster of polystomatid specimens from NE hosts that corresponds to **ne** in the polystomatid ML tree represented twelve of the specimens collected from SA4–6. The rest of the polystomatids from SA4–6 localities were spread across the remainder of the network, therefore clustering with polystomatids from SW hosts. These specimens are the same as those identified as indications of host switches in the tanglegram analysis, namely polystomatids collected in Adelaide, Dullstroom, Hopetown, Johannesburg, Ugie, Verkykerskop and Wakefield. Moreover, polystomatids collected near Three Sisters (SA4) were spread across the entire network.

The polystomatids from France and Portugal clustered together as a peripheral dominant haplotype that included frogs from SA1 and SA3 with two satellite haplotypes that differed by two or four mutations, respectively. This haplogroup of polystomatid specimens from the invasive localities, which corresponds to **sw4** of the polystomatid ML tree, was separated from the specimen from Jonkerhoek by 255 to 260 mutations. Polystomatids co-introduced to the invasive range mainly clustered in the opposite phylogeographic lineages as their hosts, with all but one of the invasive frogs from France clustering with their native counterparts from the northeastern region (NE) and their polystomatids clustering with native polystomatids in the southwestern haplotype clusters (**sw4**). This suggests the occurrence of repeated host switching by the polystomatid from one clade of the host to others.

6.3.3 Host and parasite phylogeny and congruence

Tree reconstruction showed that frogs from the northeastern localities in the native range (SA4–6) form a well-supported clade (clade NE in Figure 6.3 with UFboot2 = 95% / SH-aLRT = 95.8%). The geographic origin of this clade coincides with the summer rainfall region in southern Africa. In addition, two clades with unresolved relationships to one another and to NE could be identified among sampled frogs from the southwestern localities in the native range of *X. laevis* (clades SW_{coast} with UFboot2 = 81% / SH-aLRT = 86.1% and SW_{inland} with UFboot2 = 98% / SH-aLRT = 99.7% in Figure 6.3). These two clades both hail from the winter rainfall region, with members of the first clade originating

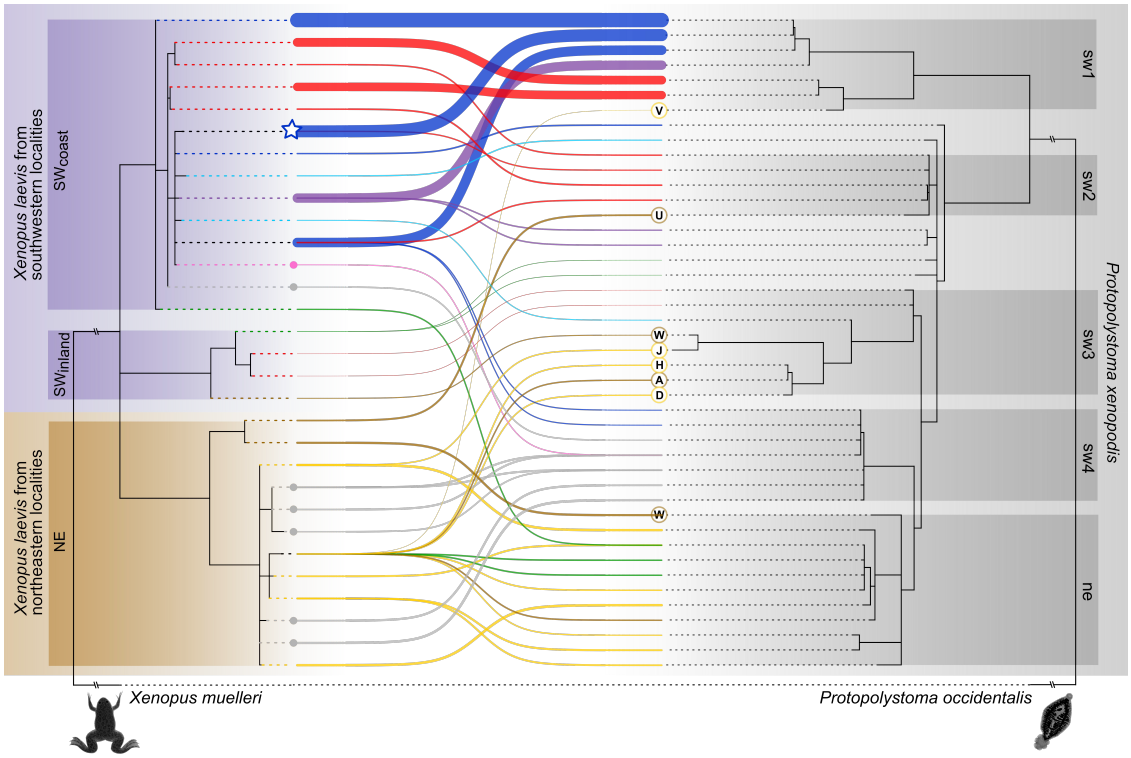

Figure 6.3: The interaction network and phylogenies of the frog *Xenopus laevis* (left) and its polystomatid *Protopolystoma xenopodis* (right) with closely related *X. muelleri* and *P. occidentalis* as outgroups. Topologies are based on the maximum likelihood analyses of the concatenated *COX1* and *rrnS* gene alignments of 31 hosts and 45 parasites with low support clades (UFboot2 $<$ 95% or SH-alrt $<$ 80%) collapsed. Coloured lines indicate the observed host-parasite associations and are weighted according to the contribution of each interaction to the overall phylogenetic congruence with thicker lines corresponding to greater support. Line colours refer to the geographic origin of the representative specimen of each unique sequence, following the phylogeographic lineages of de Busschere *et al.* (2016): SA1 (dark blue), SA2 (light blue), SA3 (red), SA4 (green), SA5 (yellow), SA6 (brown) and SA7 (purple) (see Figure 6.1) with the main lineages highlighted. Well-supported host clades from the northeast (NE) and southwest (SW) and parasite clades from the northeast (ne) and southwest (sw1–4) are indicated. Invasive *X. laevis* and co-introduced *P. xenopodis* from France (grey) and Portugal (pink) are also included. Key localities are Adelaide (A), Dullstroom (D), Hopetown (H), Johannesburg (J), Ugie (U), Verkykerskop (V) and Wakefield (W). Jonkershoek (☆) is the origin of the majority of *X. laevis* exports to date.

from localities closer to the coastline (clade SW_{coast} in Figure 6.3 from SA1–3, SA7 localities) than the second one (clade SW_{inland} in Figure 6.3 from SA3–4, SA6 localities).

The two localities near Three Sisters in the Karoo (SA4) are suggested as a contact zone between NE, SW_{coast} and SW_{inland}, with sampled individuals from these localities present in all three host lineages. Likewise, frogs from Wakefield (SA6) near Lesotho were also present in both NE and SW_{inland}.

The non-native frog from the invasive population in Portugal, along with one of the non-native frogs from western France, grouped together with the native frogs from SW_{coast} in South Africa in the host phylogeny, thus placing these exotic frogs in the same clade as

the frog from Jonkershoek. Nonetheless, the invasive population of *X. laevis* in France also harboured several frogs from the native northeastern clade (see Figure 6.3).

In the same manner as the host phylogeny, the ML inference of the *P. xenopodis* tree revealed a single, well-supported clade of polystomatids from hosts from the northeastern localities (clade **ne** in Figure 6.3 from the SA4–6 localities with UFboot2 = 97% / SH-aLRT = 87.6%). Several clades basal to the northeastern group emerged among the polystomatids from hosts collected in the southwestern region (clades **sw1–4** from the SA1–4 and SA7 localities in Figure 6.3). The earliest diverging clade was a well-supported grouping of polystomatids collected from SA1, SA3 and SA7 (clade **sw1** in Figure 6.3 with UFboot2 = 94%/SH-alrt = 88.1%). Two other native southwestern clades included a clade of polystomatids from the SA3 localities (clade **sw2** in Figure 6.3 with UFboot2 = 53%/SH-alrt = 90.7%) and another clade from a combination of SA2 and SA3 localities (clade **sw3** in Figure 6.3 with UFboot2 = 61% / SH-aLRT = 86.6%). Another well-supported clade, the sister clade to **ne** contained polystomatids from SA1, France and Portugal (clade **sw4** in Figure 6.3 with UFboot2 = 100% / SH-aLRT = 100%). However, overall low support values of many internal nodes in the parasite ML tree hampered the interpretation of phylogenetic clustering among some of the polystomatids collected from the winter rainfall region (SA1–4 and SA7).

The phylogeny of *X. laevis* exhibited significant overall congruence with that of *P. xenopodis* (PACo m^2_{xy} = 0.1034, p = 0.0018, n = 10000; ParaFitGlobal = 0.0202, $p < 0.0001$, n = 10000), with the PACo analysis suggesting that the phylogeny of *P. xenopodis* tracked that of *X. laevis*. According to PACo, links between frogs from SW_{coast} and their corresponding polystomatids that fall within **sw1** in the parasite phylogeny, generally contributed the most to the overall phylogenetic congruence. The PACo jackknife procedure further identified the interactions between frog–polystomatid pairs from the invasive range in France and Portugal as links conveying low support to congruence. Moreover, interactions between frogs and polystomatids from the contact zone near Three Sisters (SA4) and Wakefield (SA6) demonstrate low support to overall congruence, illustrating that host switches happened at localities where divergent host clades came into contact. The ParaFitLink tests reported 30 out of 48 links as significant at a level of 0.05. Out of the 18 links that did not significantly support congruence, 11 signified host switches by parasites to another host lineage that occurred in the invasive range of France and Portugal and near Johannesburg, Three Sisters, Ugie and Wakefield in the native range.

A few links represented mismatches between the host and parasite phylogenies that could be explained host switches originating from long distance translocation of the SW host lineages into the summer rainfall region followed by spill-over of polystomatids to hosts within NE. These indications of host switching were identified in frog–polystomatid pairs from Dullstroom, Hopetown, Johannesburg and Verkykerskop from SA5 and Adelaide, Ugie and Wakefield from SA6. Of these, polystomatids from Adelaide, Dullstroom, Hopetown,

Johannesburg and Wakefield clustered together with reasonable support (UFboot2 = 54% / SH-aLRT = 81.3%) in **sw3** along with polystomatids collected from hosts from SA2 and SA3 localities.

6.4 Discussion

In the present study, the co-phylogeographic analysis of a globally invasive host-parasite system reveals significant congruence between the intraspecific phylogeny the frog *X. laevis* and its polystomatid *P. xenopodis*. As a result, the *X. laevis* and *P. xenopodis* host-parasite system is eminently suited to a comparative phylogeographic study (Nieberding & Olivieri, 2007) in a context of intraspecific cryptic invasions.

6.4.1 Parasite clustering mirrors the intraspecific phylogeography of the host

The phylogeographic analysis of the parasite *P. xenopodis* reveals marked intraspecific geographic structuring across the native range of the species. This is an independent line of evidence that corroborates and expounds upon the findings of the phylogeographic analysis of the host *X. laevis* which also shows notable phylogeographic clustering across its native range (de Busschere *et al.*, 2016; du Preez *et al.*, 2009; Furman *et al.*, 2015; Grohovaz *et al.*, 1996; Measey & Channing, 2003).

The genetically distinct host-parasite clusters display distributions that are roughly shaped by the two climatic regimes in the region, namely the summer rainfall region to the northeast and the winter rainfall region to the southwest, with the plateau edge of the Great Escarpment as an assumed geographical barrier to dispersal (Furman *et al.*, 2015). The more pronounced clustering among hosts and parasites that hail from the winter rainfall region to the southwest of the Great Escarpment revealed by our analyses ($SW_{\text{inland \& coast}}$ and **sw1–4**) is likely brought about by the presence of the many ridges of the Cape Fold Mountains (de Busschere *et al.*, 2016; du Preez *et al.*, 2009; Furman *et al.*, 2015; Grohovaz *et al.*, 1996; Measey & Channing, 2003). However, well-documented human-mediated translocation of *X. laevis* in the Cape (van Sittert & Measey, 2016; Weldon *et al.*, 2007), in conjunction with widespread overland migration of the frog with the help of the many interconnected artificial water bodies in the region (de Villiers & Measey, 2017; Measey, 2016), might obscure clear phylogeographic delineation in this area at our level of sampling effort.

6.4.2 Parasite spill-over is an indication of contact between divergent host lineages

Parasite phylogeography offers a tool to recover historical insights of host dispersal pathways since they reflect past interactions between host organisms at both more recent and deeper time scales (e.g. Galbreath *et al.*, 2020). The usefulness of parasite species in reflecting the introduction pathways of their hosts has been demonstrated for fish hosts and their monogenean parasites on a few occasions (Huyse *et al.*, 2015; Kmentová *et al.*, 2019; Ondračková *et al.*, 2012). In our study, multiple instances of host lineage switches revealed by the phylogeographic analyses of *P. xenopodis* acts as an indicator for contact between phylogeographically distinct *X. laevis* lineages, even if these contact zones cannot be identified by the analysis of host phylogeography. To our knowledge, this is the first use of parasite tags to trace intraspecific cryptic invasions, although multipronged approaches to this problem have been successful before (e.g. Clavero *et al.*, 2016).

Thus far, genetic evidence for the admixture of the lineages of *X. laevis* with native ranges on opposite sides of the Great Escarpment has not been found, despite historical records pointing towards large scale exports from the winter rainfall region to the rest of southern Africa (van Sittert & Measey, 2016; Weldon *et al.*, 2007). In our study, the host phylogeographic analyses suggest the presence of contact zones between the northeastern (NE) and southwestern lineages ($SW_{inland\ \&\ coast}$) at two localities in the summer rainfall region to the north of the Great Escarpment. Since these zones are situated to the north of a predicted geographical barrier (Furman *et al.*, 2015), one could surmise that anthropogenic translocation had a hand in bringing about this sympatry of multiple clades of *X. laevis*.

More evidence for the recent anthropogenic translocation of *X. laevis* across southern Africa is provided by the presence of southwestern parasite lineages (**sw1–3**) at seven localities in the summer rainfall region. In these cases, hosts from localities in the northeastern summer rainfall region belong to the expected NE clade, yet their parasites fall within the southwestern parasite clades (**sw1–3**). The sympatry of different host lineages is a prerequisite for host lineage switching. In these instances, parasite lineages that are translocated along with their respective host lineages (locally non-native) may spill over to other host lineages (locally native) when these divergent, previously allopatric host lineages come into contact. This provides us with the means of recognising recent contact between *X. laevis* lineages even in cases where the original locally non-native host lineage may have gone extinct after the introduction event or where they are not detected at a certain sampling effort.

Differential survival between locally native and non-native *X. laevis* lineages in southern Africa can partially explain the fewer observed instances of establishment by non-native *X. laevis* lineages when compared to its co-introduced polystomatid. In translocation

experiments of different lineages in the native range, *X. laevis* tadpoles and metamorphs exhibited remarkable phenotypic plasticity when translocated between rainfall regimes at the cost of longterm survival (Kruger, 2020). Under these circumstances, the locally native *X. laevis* lineage would outcompete the non-native lineage, preventing successful local invasion. Thus, the employment of host phylogeography alone to trace long range translocation of *X. laevis* in southern Africa would mask introduction events.

Upon arrival in the new area, the co-introduced *P. xenopodis* lineage may rapidly spread in a population of locally native and therefore naive *X. laevis*. It has been shown that primary infections by *P. xenopodis* in previously uninfected *X. laevis* hosts elicit strong long term immunological responses against secondary infections by the same parasite species (Jackson & Tinsley, 2001b). Correspondingly, a cross-infectivity experiment between sympatric and allopatric *X. laevis* and *P. xenopodis* lineages further suggested that *X. laevis* lineages in their native ranges might be more susceptible to infection by the locally co-introduced *P. xenopodis* lineage than to their corresponding locally native parasite lineage (Jackson & Tinsley, 2005). Not only will *P. xenopodis* more readily infect naive *X. laevis*, but multiple worm infestations in a single frog enhances initial reproductive rate of the polystomatid (Jackson & Tinsley, 1988). In turn, this effect will boost the nascent spread of co-introduced *P. xenopodis* in the locally native lineage of *X. laevis*.

The indications of parasite spill-over revealed by our analyses of polystomatid phylogeography suggest that smaller scale human-mediated dispersal events, as opposed to large official consignments from the summer rainfall region to centers of higher learning across South Africa, have far-reaching effects. The role of recreational fishing across South Africa in the dispersal of *X. laevis*, and by extension, *P. xenopodis*, has been recognised before (Weldon *et al.*, 2007). Previously documented interviews with local anglers and suppliers exposed the use of *X. laevis*, frequently bought from pet shops and local breeders, as live bait for predominantly catfish angling (Weldon *et al.*, 2007). Our own informal discussions with local anglers at the localities where we collected *X. laevis* affirm the widespread use of *X. laevis* as live bait for the capture of both black bass and catfish.

In terms of sheer numbers, the impact of these translocation events on the domestic dispersal of *X. laevis* has been deemed negligible when compared to exports from Jonkershoek and other official suppliers to the domestic market (van Sittert & Measey, 2016; Weldon *et al.*, 2007). Nonetheless, previous studies have pointed out that the use of live bait in angling is an important pathway for introductions, even if the market might be small in economic terms (Kalous *et al.*, 2013; Kilian *et al.*, 2012). Therefore, the impact of anglers on the spread of *X. laevis* to more remote areas, as opposed to the bigger centra that received the documented official consignments, should not be underestimated. Our informal interviews identified a myriad of ways for *X. laevis* to be released in new environments by anglers, from escapees *en route*, to the deliberate release of surplus bait, to the intentional stocking of water bodies for future use. All the evidence point towards a

widespread undocumented dispersal network of *X. laevis* in South Africa.

6.4.3 Parasite phylogeography as an underutilised tool in invasion biology

As shown above, the present study acts as a proof of concept for the potential of the co-phylogeographic approach to the clarification of patterns in intraspecific host divergence and dispersal. In turn, this independent line of evidence can provide additional insight on invasion pathways and inform management strategies in profound ways.

Our approach was able to provide a new perspective on the origin of the relatively high haplotype diversity of the invasive population in France, recovered in our analysis and others, when compared to other invasive populations in Portugal, Sicily and Chile (de Busschere *et al.*, 2016; Lillo *et al.*, 2013; Lobos *et al.*, 2014). The idea of multiple introduction events from various source populations in South Africa has been offered before as the most parsimonious explanation for this genetic diversity (de Busschere *et al.*, 2016). Since we found evidence for host switches in the native range, an event that necessarily involves the sympatry of divergent host lineages, it is a certainty that multiple host lineages can co-occur at certain localities in the native range. In this, our results build upon the evidence provided by historical export records (van Sittert & Measey, 2016; Weldon *et al.*, 2007), dispersal patterns (de Villiers & Measey, 2017; Measey, 2016) and anecdotal information (Weldon *et al.*, 2007). Thus, the mixing of lineages most likely already happened in the source populations in South Africa prior to the co-introduction of *X. laevis* and *P. xenopodis* to western France in addition to mixing brought about by multiple introduction events from a number of exporters across South Africa (van Sittert & Measey, 2016; Weldon *et al.*, 2007).

The novel insights provided by the addition of the parasite data set has implications for both the conservation of *X. laevis* and its host-specific parasites. The widespread anthropogenic translocation of this host-parasite system disrupts interactions between *X. laevis* lineages and the *P. xenopodis* lineages that tracked their phylogenetic divergence, ancient interactions that deserve to be targets of conservation in themselves (Gómez & Nichols, 2013). Especially in the case of host-specific parasites, translocation of lineages within the native range of a species may be more detrimental than translocation to non-native ecosystems where close relatives of the original host will probably not be encountered to facilitate host switches (Blackburn & Ewen, 2017). Host-parasite interactions is also something to keep in mind when conducting conservation reintroduction programmes, where captive-bred or locally non-native individuals of a species are used to restock locally extinct populations of endangered species (Britt *et al.*, 2004).

This approach also holds great promise in the management of invasive species. In risk assessment, anthropogenic translocations in the native range that may have already

altered the source populations of invasive species, as is the case of *X. laevis*, need to be taken into account to adequately monitor the course of an invasion or the novel interactions that may arise. Parasites as passengers or invaders themselves easily slip under the radar in invasion biology (Blackburn & Ewen, 2017; Solarz & Najberek, 2017). Yet, the role of parasites on the move in emerging infectious diseases and habitat transformation via indirect density-mediated effects cannot be overemphasised (Amundsen *et al.*, 2013; Bobadilla-Suarez *et al.*, 2017; Daszak, 2000; Dunn *et al.*, 2012; Lymbery *et al.*, 2014; Roy & Lawson Handley, 2012; Sures *et al.*, 2017).

6.4.4 Conclusions and recommendations

All in all, our findings agree with the necessity of a more holistic approach to data collection in invasion biology (Clavero *et al.*, 2016). The idea of the ”holistic specimen” has recently gained some traction (Cook *et al.*, 2017). This approach to the collection and study of organisms advocates for the integrated specimen-based studies of animals and their associated parasites and pathogens. The present study demonstrates that the documentation of the parasite diversity of native and non-native populations of hosts can clearly lead to more information to address questions in invasion biology. The optimisation of sampling effort is crucial to improve the allocation of resources, both in terms of funding and specimen use, especially when working with endangered species or specimens that require considerable effort to obtain, or in view of other ethical concerns. Moreover, the deposition of voucher material of both host and parasite can be vital for later studies (Thompson *et al.*, 2021).

Ultimately, this study serves as a proof of concept that the use of parasite data sets will add value to investigations in invasion biology, especially in the case of intraspecific cryptic invasions. In fact, we show that the utility of parasite data sets can go beyond the provision of supporting evidence and provide greater resolution that may lead to elucidation of patterns that went undetected in the host data set. In this study, the widespread, yet previously hidden, domestic expansion of *X. laevis* with the aid of the angling community as a major role player, is brought to light by the phylogeography of its co-invasive parasite, *P. xenopodis*, an element of the invasion history that was largely forgotten to date. Looking forward, we advocate that the inclusion of co-introduced parasites in the study of invasive species already at the phase of specimen collection will enhance inference prospects without a doubling of sampling effort.

Chapter 7

Room for manoeuvre: the compact mitochondrial genome of the invasive flatworm *Protopolystoma xenopodis* (Monogenea: Polystomatidae) displays high intraspecific variability

7.1 Introduction

When it comes to addressing questions in taxonomy, evolution and even ecology, mitochondrial DNA is usually the molecular marker of choice. The versatility of mitochondrial markers is showcased in the recent scientific investigations of the monogenean flatworm family Polystomatidae Gamble, 1896. Specifically, the mitochondrial *COX1* gene, in conjunction with two discriminant morphological traits, was proposed as an efficient procedure for polystomatid identification (Héritier *et al.*, 2018). Divergence in the *COX1* gene is commonly employed to differentiate between closely related polystomatid species and genera (Berthier *et al.*, 2014; Chaabane *et al.*, 2019; du Preez *et al.*, 2017, 2019; Landman *et al.*, 2021; Rahariveloloniaina *et al.*, 2011). Similarly, the *COX1* gene, along with the mitochondrial *rrnS* gene and two nuclear markers, helped resolve taxonomic issues among genera within the Polystomatidae (Chaabane *et al.*, 2019; du Preez *et al.*, 2017; du Preez & Verneau, 2020).

The Polystomatidae's unique affiliation with tetrapod hosts within the largely fish-parasi-

tising Monogenea makes it a compelling subject of phylogenetic, co-phylogenetic and phylogeographic studies. Phylogenetic investigations of members of the Polystomatidae based upon both mitochondrial and nuclear markers confirmed a long co-evolutionary history between these monogeneans and their hosts (Héritier *et al.*, 2015), even providing information on the colonisation and diversification of their highly endangered anuran hosts on Madagascar (Verneau *et al.*, 2009). Likewise, these markers were used to infer ancestral host switches by polystomatids from amphibians to other aquatic tetrapods, emphasising the link between polystomatid evolution and key events in tetrapod evolution (Héritier *et al.*, 2015). Moreover, phylogeny based upon the concatenated mitochondrial *COX1* and nuclear *28S rRNA* genes demonstrated that host switches more likely drove speciation in this family than within-host duplication (Littlewood *et al.*, 1997).

Shifting towards the present, mitochondrial markers have also illuminated the role of polystomatids as biological invaders. For instance, the *COX1* gene emerged as an invaluable molecular barcode to identify and discriminate local parasite fauna from the polystomatids co-introduced with the notoriously invasive turtle *Trachemys scripta elegans* (Wied, 1838), some of which have become co-invaders during parasite spill-over events to native hosts (Héritier *et al.*, 2017; Meyer *et al.*, 2015; Verneau *et al.*, 2011). The fact that *COX1* barcodes can be used to identify polystomatid species based simply upon screening for polystomatid eggs without the necessity of dissecting endangered host species, makes mitochondrial markers a particularly appealing avenue of species identification in studies of biological invasions where polystomatids are involved (Héritier *et al.*, 2017; Meyer *et al.*, 2015; Verneau *et al.*, 2011). The same can be said of instances where the soft tissue of the retrieved parasites may be damaged by collection techniques, as was the case for the co-introduced polystomatid *Protopolystoma xenopodis* (Price, 1943) Bychowsky, 1957 of the globally invasive African Clawed Frog *Xenopus laevis* (Daudin, 1802) which was identified via the *COX1* barcode in the invasive region of western France (Schoeman *et al.*, 2019).

Going further than mere identification, the phylogeographic analysis of the mitochondrial *COX1* and *rrnS* genes of *P. xenopodis* revealed the cryptic introductions of locally invasive lineages of the host *X. leavis* in its native range of southern Africa (Chapter 6 of this thesis). Prior to this analysis, the status of *X. laevis* as domestic invader was suggested (Measey & Davies, 2011; Measey *et al.*, 2017; van Sittert & Measey, 2016), yet phylogeographic analyses of the host across the native range could not provide genetic proof for the dispersal of non-native lineages of the host (de Busschere *et al.*, 2016; Furman *et al.*, 2015). It was only with the additional line of evidence provided by the intraspecific analysis of the polystomatid's mitochondrial markers that recent contact between divergent lineages of *X. laevis* in its native range, followed by spill-over of locally non-native *P. xenopodis* to naive *X. laevis* hosts, was identified (Chapter 6 of this thesis).

In this co-phylogeographic study (Chapter 6 of this thesis), the two mitochondrial markers

were chosen based upon availability of primers, rather than prior knowledge of population-level variability. Although there was marked divergence in these mitochondrial markers of *P. xenopodis* in South Africa, populations could not be discriminated on the finer regional scale (Chapter 6 of this thesis). The interspecific comparison of the mitochondrial genomes (mitogenomes) of diplozoid, gyrodactylid and dactylogyrid monogeneans have indicated that other genes might be more suitable for species identification or even population-level studies within these families (Huyse *et al.*, 2008; Vanhove *et al.*, 2018; Zhang *et al.*, 2018b). At the same time, the variation in nucleotide diversity within monogenean mitogenomes on the intraspecific level has not received much attention (exceptions are Huyse *et al.*, 2008; Solá *et al.*, 2015). Thus, the characterisation of the complete mitogenome of *P. xenopodis*, followed by the intraspecific comparison of nucleotide diversity, will inform the choice of mitochondrial markers that can allow us to better identify the origin and dispersal of invasive polystomatids.

The past four decades has seen the rise of mitochondrial genomics, from the sequencing of the first two complete mitogenomes in 1981 (Anderson *et al.*, 1981; Bibb *et al.*, 1981) to the availability of over 12 000 complete mitogenomes on the public repository GenBank as of March 2021 (National Center for Biotechnology Information, 2021). Despite the deluge of available mitochondrial data (Smith, 2015), flatworms are currently represented by a mere 152 entries (National Center for Biotechnology Information, 2021). Of these, the first three complete monogenean mitogenomes were sequenced and annotated in 2007 (Huyse *et al.*, 2007; Park *et al.*, 2007; Plaisance *et al.*, 2007) but this class remains underrepresented as a whole (Wey-Fabrizius *et al.*, 2013). Within the Polystomatidae, there is only one incomplete draft mitogenome available on GenBank, that of the frog-parasitising *Diplorchis hangzhouensis* Zhang *et* Long, 1987 from Asia (Zhang *et al.*, unpubl.).

The diverse and apomorphic host associations of the Polystomatidae (Héritier *et al.*, 2015), coupled with the basal position of this family in the polyopisthocotylean phylogeny (Mollaret *et al.*, 2000), highlight their evolutionary importance within the Monogenea. Together with the fact that many of the Polystomatidae are co-introduced and even co-invasive parasites (Héritier *et al.*, 2017; Meyer *et al.*, 2015; Schoeman *et al.*, 2019; Verneau *et al.*, 2011, Chapter 6 of this thesis), it is clear that a complete mitogenome of a representative of this family will be of great use to future investigators. Specifically, there is a need for mitochondrial markers that exhibit greater intraspecific discriminant power than the currently employed *COX1* and *rrnS* genes, which will allow us to track the dispersal of the invasive amphibian and chelonian hosts of polystomatids at finer geographic scales.

Thus, we present the first complete mitogenome of the globally distributed polystomatid monogenean *P. xenopodis*. The mitogenomes of two specimens were sequenced, assembled and characterised, whereupon they were compared to the mitogenomes of other parasitic flatworms of the subclass Polyopisthocotylea Ohdner, 1912. As a preliminary

intraspecific analysis, we compared the mitogenome sequences of two specimens of *P. xenopodis* from the same population of hosts in the summer rainfall region of South Africa.

7.2 Methods

Six adult *X. laevis* were captured in liver baited funnel traps from two connected water bodies near Bloemfontein, South Africa (29.06363°S; 26.21881°E) in November 2019. This locality is situated near the campus of the University of the Free State, an institution that regularly imported *X. laevis* for teaching and research purposes from both the summer (Lydenburg fish farm, Mpumalanga Province) and winter (supplier in Vishoek area, Western Cape Province) rainfall lineages of South Africa (Louis du Preez, personal communication). From these stocks, *X. laevis* often escaped or were supplied directly to pet shops and local anglers, which could in turn could seed water bodies nearby (Louis du Preez, personal communication).

The frogs were captured, euthanised according to internationally accepted standard operating procedures and internally and externally examined for parasites under the North-West University AnimCare ethics number NWU-0380-16-A5-01. Eighteen specimens of *P. xenopodis* were retrieved from the bladders of these hosts and fixed in 70% ethanol for further molecular analyses.

Total genomic DNA was extracted from two whole specimens using an optimised protocol for low input DNA samples. Initial digestion was performed in 195 μl of TNES buffer (400 mM NaCl, 20 mM EDTA, 50 mM Tris pH 8, 0.5% SDS) and 5 μl of proteinase K (20 mg/ml) incubated at 55°C for $\sim$30–60 minutes. DNA was precipitated in a mixture of 65 μl 5 M NaCl and 290 μl 96% ethanol with yeast tRNA as a carrier, stored in -20°C for 1 hour and purified with three runs of 1 ml chilled 70% ethanol. Purified DNA was eluted in 100 μl of 0.1X TE buffer with 0.02% tween-20. NGS libraries of each specimen were prepared with a Nextera DNA Flex. Simultaneous paired-end sequencing (2 $\times$ 151 bp) on Illumina HiSeq X Ten system was outsourced.

The obtained reads were trimmed of adapters using fastp (Chen *et al.*, 2018) and minimum length of 40 bp with Trimmomatic (Bolger *et al.*, 2014). The mitogenomes were assembled from the two sets of trimmed paired reads for each specimen in NOVOPlasty *version* 3.7.2 (Dierckxsens *et al.*, 2017) with the partial *COX1* gene of *P. xenopodis* (MK342938; Schoeman *et al.*, 2019) as seed. Expected assembly length was adjusted from 13 000 to 20 000 bp and k-mer values from 21 to 39 bp in a stepwise fashion. Read length was set at 151 bp and insert size at 390 bp, with all other assembly parameters set at default. Ultimately, the longest circularisable contigs were selected to represent the assembled mitochondrial sequences of the two specimens of *P. xenopodis*.

To identify possible gaps in coverage or misassembled regions, the two sets of trimmed reads were remapped to their respective assembled contigs in Geneious Prime *version* 2021.0.3 (www.geneious.com) using the software's built-in mapping algorithm at medium sensitivity.

Circularisation of the assembled contigs was performed manually in Geneious Prime by searching for duplicated regions on the 5' and 3' ends of the assembled contigs.

The composition of the two complete circular mitochondrial sequences was quantified through GC content and the GC and AT skew indices (Perna & Kocher, 1995). The skew indices were calculated with the formulas $[(G - C)/(G + C)]$ and $[(A - T)/(A + T)]$ derived from the nucleotide composition of the coding strands of each mitochondrial sequence obtained in Geneious Prime.

Annotation of the two *P. xenopodis* mitogenome sequences was initiated using the online servers of Arwen *version* 1.2 (Laslett & Canbäck, 2008), MITOS1 (Bernt *et al.*, 2013), MITOS2 (*beta* version) and tRNAscan-SE *version* 2.0 (Chan & Lowe, 2019; Lowe & Chan, 2016). The suggestions for protein-coding genes (PCGs) were compared to open reading frames which were identified in Geneious Prime under default settings and the echinoderm and flatworm mitochondrial code (table 9). The tentatively identified PCGs and tRNA and rRNA genes were fine-tuned based upon their alignment with other polyopisthocotylean mitochondrial genes available from GenBank (Table 7.1) and the principles of minimum gene overlap and maximum mitogenome density.

Sequence alignments for mitogenome annotation, calculation of nucleotide diversity and phylogenetic analyses were all conducted in a similar manner, albeit with different sets of taxa. Codon-based alignment of all the obtained PCGs was performed under the echinoderm and flatworm mitochondrial genetic code (table 9) using the Clustal Omega algorithm (Sievers & Higgins, 2017) in Geneious Prime. The rRNA genes were aligned online (Katoh *et al.*, 2017) by MAFFT *version* 7 (Katoh & Standley, 2013) in the Q-INS-i mode (Katoh & Toh, 2008), which considers the secondary structure of RNA based upon the McCaskill routine from the *ViennaRNA* package (Hofacker *et al.*, 2002) and MXSCARNA (Tabei *et al.*, 2008). The rest of the mitogenome, including the tRNA genes and non-coding regions (NCRs), was aligned with the Clustal Omega algorithm (Sievers & Higgins, 2017) implemented in Geneious Prime.

In the case of tRNA genes, the predicted secondary structures of MiTFi (Jühling *et al.*, 2012), Arwen (Laslett & Canbäck, 2008) and tRNAscan-SE (Chan & Lowe, 2019; Lowe & Chan, 2016) were also considered. We gave preference to the proposed tRNA genes of which the secondary structure had a 7 bp acceptor stem and a low minimum free energy (MFE) level. Free energy of the secondary structures was calculated online with RNAeval (Gruber *et al.*, 2008), a tool in the ViennaRNA *package version* 2.4 (Lorenz *et al.*, 2011), under 20 ℃, the optimal water temperature for *P. xenopodis* egg development (Jackson

Table 7.1: Polyopisthocotylean species, their available mitochondrial genes, corresponding GenBank accession numbers and associated publications that were used to align genes for the purpose of mitogenome annotation and phylogenetic analyses.

Species	Available genes	Accession number
Microcotylidae		
Microcotyle sebastis Goto, 1894	All	DQ412044 (Park *et al.*, 2007)
Polylabris halichoeres Wang *et* Zhang, 1998	All	JF505509 (Zhang *et al.*, 2011)
Polylabroides guangdongensis Zhang *et* Yang, 2000	All except *COX3*, *NAD6*, $tRNA^{Leu1\ \&\ Lys}$	JQ038230 (Zhang *et al.*, unpubl.)
Mazocraeidae		
Neomazocraes dorosomatis (Yamaguti, 1938) Price, 1943	All except *COX3*, *NAD6*, $tRNA^{Leu1,\ Leu2\ \&\ Lys}$	JQ038229 (Zhang *et al.*, unpubl.)
Chauhaneidae		
Pseudochauhanea macrorchis Lin, Liu *et* Zhang, 2001	All	JN592039 (Zhang *et al.*, 2012)
Diclidophoridae		
Heterobothrium okamotoi Ogawa, 1991	All	MK948930 (Li *et al.*, 2019)
Diplozoidae		
Eudiplozoon Khotenovsky, 1984, sp.	All	MG458328 (Zhang *et al.*, 2018b)
Paradiplozoon opsariichthydis (Jiang, Wu *et* Wang, 1984) Jiang, Wu *et* Wang, 1989	All	MG458327 (Zhang *et al.*, 2018b)
Sindiplozoon Khotenovsky, 1981, sp.	All	MG458326 (Zhang *et al.*, 2018b)
Polystomatidae		
Diplorchis hangzhouensis Zhang *et* Long, 1987	All except *NAD2*	JQ038227 (Zhang *et al.*, unpubl.)

& Tinsley, 1988). The intraspecific polymorphic sites in the mitochondrial tRNA genes of *P. xenopodis*, as identified via the Clustal Omega alignment, were added to the secondary structures for visualisation of intraspecific diversity.

The annotated mitogenome of *P. xenopodis*, along with its GC content, was visualised in OrganellarGenomeDRAW (Greiner *et al.*, 2019). The Relative Synonymous Codon Usage (RSCU) across the 12 PCGs in the two variants of the mitogenome of *P. xenopodis* was calculated on the CAIcal web server (http://genomes.urv.es/CAIcal; Puigbò *et al.*, 2008) following Sharp *et al.* (1986). Codon frequency and amino acid usage statistics were derived in Geneious Prime.

Based upon the same principles as outlined above, we examined the available annotated polyopisthocotylean mitogenomes (Table 7.1) to ameliorate the original annotations. The subsequent phylogenetic analyses were based upon our proposed re-annotations.

Alignment was performed on all the genes and NCRs in the two sequences of the *P. xenopodis* mitogenome with the methods detailed above. The separately aligned sections, including the PCGs, rRNA and tRNA genes and NCRs, were concatenated in Geneious Prime in the order they appeared in the mitogenome. The resulting alignment, amounting to 13 768 bp, was used to visualise variability in the *P. xenopodis* mitogenome by a sliding window analysis of nucleotide diversity (π). The analysis was performed with a window size of 300 bp and step size of 10 bp in DnaSP *version* 6.12.03 (Rozas *et al.*, 2017).

The most parsimonious mitochondrial genetic rearrangements within Polyopisthocotylea, along with pairwise comparisons of the mitochondrial gene order, were inferred with the CREx online server (Bernt *et al.*, 2007). The common intervals parameter was applied for distance measurement. All available polyopisthocotylean mitogenomes, aside from those of *Neomazocraes dorosomatis* (Yamaguti, 1938) Price, 1943 and *Polylabroides guangdongensis* Zhang *et* Yang, 2000 that had more than one gene missing, were considered in the analysis (Table 7.1).

Alignments for the phylogenetic analyses were performed for all the polyopisthocotylean mitogenomes available on GenBank (Table 7.1). The mitogenome sequences of the fish-parasitic monopisthocotyleans *Paratetraonchoides inermis* Bychowsky, Gussev *et* Nagibina, 1965 (Monogenea: Tetraonchoidae) (accession number KY856918; Zhang *et al.*, 2017) and *Dactylogyrus lamellatus* Achmerov, 1952 (Monogenea: Dactylodyridae) (accession number KR871673; Zhang *et al.*, 2018c) were included as outgroups. Gene alignments were performed separately, as outlined above, on 12 PCGs and on the rRNA genes (*rrnS* and *rrnL*). Subsequently, all 14 gene alignments were concatenated in Geneious Prime.

The concatenated alignment was initially partitioned based upon genes and also codon positions in the case of PCGs. The optimal models of molecular evolution for the partitions were selected with the ModelFinder selection routine (Kalyaanamoorthy *et al.*, 2017) implemented in IQ-TREE *version* 2.1.2 (Minh *et al.*, 2020), which employed the FreeRate heterogeneity model during model selection (Soubrier *et al.*, 2012). The initial partitions were then sequentially merged (Chernomor *et al.*, 2016) until model fit, as evaluated with the Bayesian Information Criterion (BIC), no longer improved. The resulting optimal partitioning scheme and most suitable evolutionary models for each subset were specified in the subsequent phylogenetic analyses (Table 7.2). For tree reconstruction, both maximum likelihood (ML) analysis and Bayesian inference of phylogeny (BI) were performed to increase confidence in the resulting topology.

The ML phylogeny was inferred under the six partitions suggested by the ModelFinder selection routine (Table 7.2). During the analysis, the partitions were unlinked at the edges. The analysis was performed in IQ-TREE *version* 2.1.2 (Minh *et al.*, 2020), with the assessment of branch support through ultrafast bootstrapping (UFboot2; Hoang *et al.*,

Table 7.2: Best partitioning scheme for the concatenated alignment of 14 mitochondrial genes from 14 monogenean flatworm species, evaluated according to the Bayesian Information Criterion. The optimal evolutionary models for each partition is presented as the output of the ModelFinder selection routine (Kalyaanamoorthy *et al.*, 2017) implemented in IQ-TREE2 (Minh *et al.*, 2020) with sequential merging (Chernomor *et al.*, 2016) utilised for the maximum likelihood (ML) analysis, with the adapted nucleotide substitution models chosen for the Bayesian inference (BI).

Partition	Model for ML	Model for BI
rrnS, *rrnL*	TPM3 + F + I + G4	`nst = 6 rates = invgamma`
1st codon positions of *NAD4–6* and *NAD4L*	HKY + F + R3	`nst = 2 rates = equal`
1st codon positions of *ATP6*, *COX3*, *cytb*, *NAD1* and *NAD3*; 2nd of *ATP6*	HKY + F + G4	`nst = 2 rates = gamma`
1st codon positions of *COX1*; 2nd of *COX1*, *COX3*, *cytb*, *NAD1* and *NAD4L*	GTR + F + I + G4	`nst = 6 rates = invgamma`
1st codon positions of *COX2* and *NAD2*; 2nd of *COX2* and *NAD2–6*	GTR + F + I + G4	`nst = 6 rates = invgamma`
3rd codon positions of *ATP6*, *COX1–3*, *cytb*, *NAD1–6* and *NAD4L*	TIM2 + F + R3	`nst = 6 rates = equal`

DNA models: HKY (Hasegawa *et al.*, 1985), TPM ("3-parameter model") (Kimura, 1981), TIM ("transitional model") (Posada, 2003) and GTR ("general time-reversible model") (Tavaré, 1986); Rate heterogeneity across sites: F (empirical base frequencies), G (discrete Gamma model) (Yang, 1994), I (allowing for a proportion of invariable sites) (Gu *et al.*, 1995) and R (FreeRate model) (Soubrier *et al.*, 2012)

2018) and the Shimodaira-Hasegawa approximate likelihood ratio test (SH-aLRT; Guindon *et al.*, 2010), each with 10 000 replicates.

The BI was performed in MrBayes *version* 3.2.6 (Ronquist *et al.*, 2012) implemented in XSEDE on the CIPRES Science Gateway *version* 3.3 (Miller *et al.*, 2010). The substitution models implemented in MrBayes were adapted from the selection of ModelFinder as the next more complex model under the BIC in terms of substitution rates available in MrBayes (Table 7.2). Posterior probabilities were calculated with four different Metropolis-coupled Markov chains over 10 000 000 generations, with sampling of the Markov chain every 1 000 generations. The first quarter of the samples was discarded as burn-in. All parameter estimates were unlinked for the partitions. Stationarity of the Markov chains was reached, as indicated by a deviation of split frequencies of 0.001, by a potential scale reduction factor converging to 1 and by the absence of a trend in the plot of log-probabilities as function of generations.

The resulting topologies were rooted with respect to the monopisthocotylean outgroups, *Da. lamellatus* and *Pt. inermis*, in FigTree *version* 1.4.4 (Rambaut, 2018).

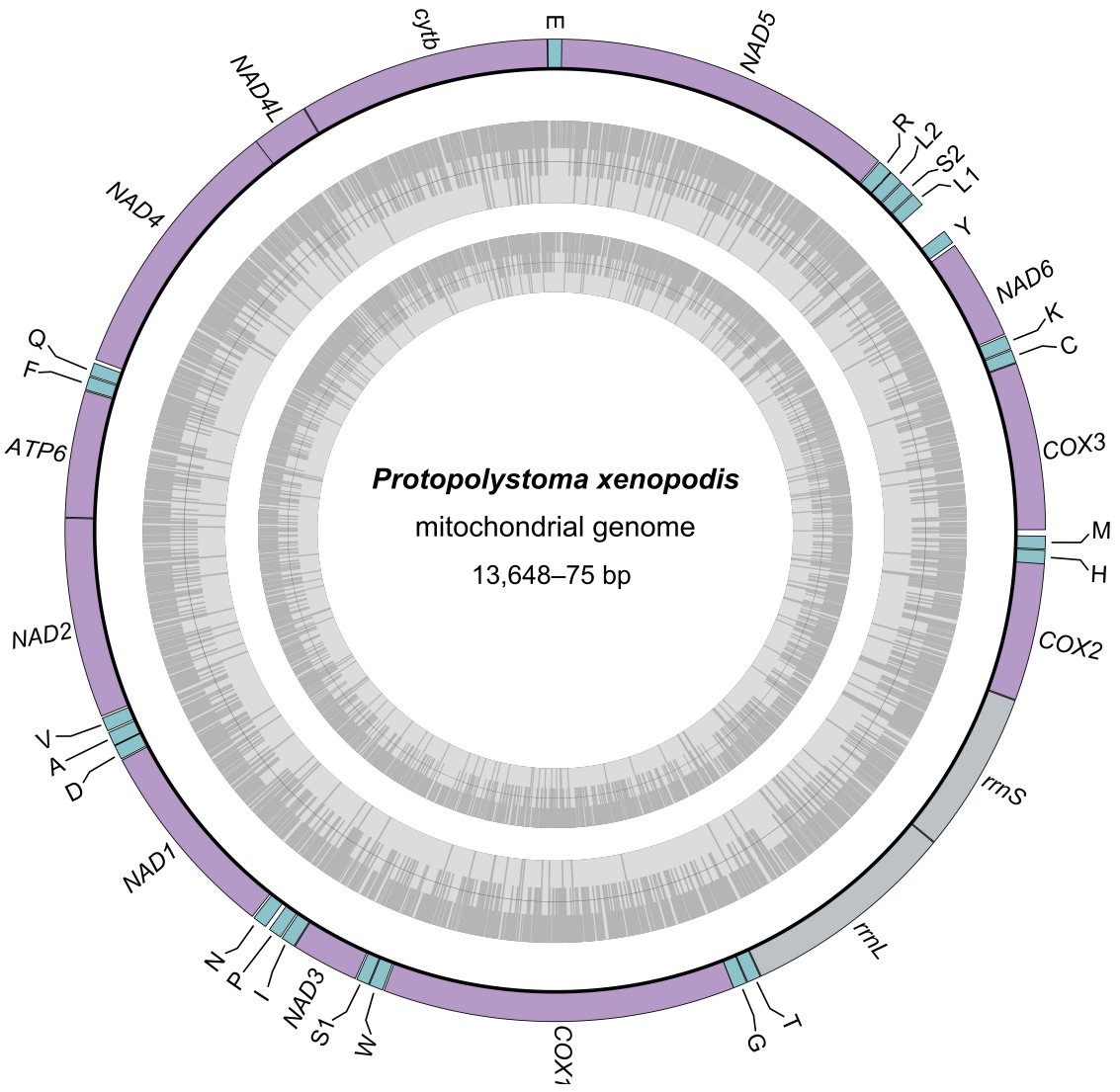

Figure 7.1: Mitochondrial genome of the polystomatid flatworm *Protopolystoma xenopodis*, as constructed in OGDraw. GC content of the first specimen is displayed in the inner ring, GC content of the second specimen in the middle ring and gene arrangement in the outer ring. One-letter abbreviations are used for the transfer RNA genes.

7.3 Results

Two complete mitogenome sequences of *P. xenopodis* were assembled (Figure 7.1). The draft annotation of *D. hangzhouensis* was ameliorated. Moreover, some changes were proposed to the mitogenomes of *Microcotyle sebastis* Goto, 1894, *N. dorosomatis*, *Pseudochauhanea macrorchis* Lin, Lui *et* Zhang, 2001 and *Sindiplozoon* Khotenovsky, 1981, sp.

Table 7.3: GC content and compositional asymmetry in the two newly assembled sequences of *Protopolystoma xenopodis* and the re-annotated draft mitogenome of *Diplorchis hangzhouensis*. Skew values were calculated manually following the formulas [(G - C)/(G + C)] and [(A - T)/(A + T)].

	P. xenopodis specimen 1	*P. xenopodis* specimen 2	*D. hangzhouensis*
GC%	31.8	30.0	27.9
GC skew	0.354	0.372	0.479
AT skew	-0.276	-0.277	-0.377

7.3.1 Sequencing and assembly

The assembled mitogenome sequence from the first *P. xenopodis* specimen was obtained from 86 588 420 raw reads (59 466 598 paired and 10 846 698 unpaired reads) trimmed by Trimmomatic (Bolger *et al.*, 2014), with k-mer length set at 37 bp and expected length of the sequence set between 15 000 and 20 000 bp. Average coverage was 611$\times$ and 35 912 out of a total of 39 202 788 trimmed reads (0.092%) were assembled into a single contig of length 20 019 bp.

In the case of the assembled sequence from the second specimen, 70 980 916 raw reads (70 256 538 paired and 353 680 unpaired reads) were trimmed by fastp (Chen *et al.*, 2018) and k-mer length was set at 39 bp, with an expected genome size between 13 000 and 16 000 bp. Assembly resulted in four overlapping contigs of lengths 1 518, 4 945, 5 051 and 9 867 bp, which aligned to form a continuous sequence of length 15 335 bp. Average coverage was 3927$\times$, with a total of 301 606 out of 54 221 376 trimmed reads (0.556%) participating in the final assembly.

Re-mapping of the reads indicated no areas of low coverage or misassembly in either of the sequences. Circularisation notably reduced the length of the NCR between *NAD5* and *NAD6*, including eliminating one or possibly two stretches of tandem repeats from the draft assemblies. This agreed with the draft mitogenome of *D. hangzhouensis*, which also had a relatively short NCR between these two genes that does not include any tandem repeats. The linear draft mitogenome of *D. hangzhouensis* was circularised through alignment with the obtained *P. xenopodis* mitogenome.

The complete circular mitogenome of *P. xenopodis* is between 13 648 and 13 675 bp in size, whilst the circular draft mitogenome of *D. hangzhouensis* is longer at 13 918 bp. Moreover, the mitogenomes of both polystomatid species were AT-rich with A $<$ T and G $>$ C on the coding strand (Table 7.3).

Table 7.4: Localisation of genes and non-coding regions in the mitochondrial genome of *Protopolystoma xenopodis*.

	P. xenopodis specimen 1		*P. xenopodis* specimen 2	
Genes	Position (Length)	Start & Stop/Anticodon	Position (Length)	Start & Stop/Anticodon
COX3	1–757 (757)	ATG & T(TA)	1–754 (754)	ATG & T(TA)
trnC	758–819 (62)	GCA	755–816 (62)	GCA
trnK	822–888 (67)	CTT	824–890 (67)	CTT
NAD6	893–1348 (456)	ATG & TAG	895–1350 (456)	ATG & TAG
trnY	1360–1426 (67)	GTA	1353–1419 (67)	GTA
trnL1	1576–1640 (65)	TAG	1570–1633 (64)	TAG
trnS1	1643–1710 (68)	TGA	1636–1705 (70)	TGA
trnL2	1713–1778 (66)	TAA	1707–1772 (66)	TAA
trnR	1778–1846 (69)	TCG	1772–1841 (70)	TCG
NAD5	1850–3397 (1548)	GTG & TAG	1845–3392 (1548)	GTG & TAG
trnE	3388–3454 (67)	TTC	3383–3451 (69)	TTC
cytb	3453–4589 (1137)	GTG & TAG	3450–4586 (1137)	GTG & TAG
NAD4L	4590–4850 (261)	GTG & TAG	4587–4847 (261)	GTG & TAG
NAD4	4811–6066 (1256)	GTG & TA(A)	4808–6057 (1250)	ATG & TA(G)
trnQ	6080–6141 (62)	TTG	6069–6129 (61)	TTG
trnF	6144–6207 (64)	GAA	6132–6194 (63)	GAA
ATP6	6209–6781 (573)	ATG & TAG	6195–6767 (573)	ATG & TAG
NAD2	6782–7684 (903)	GTG & TAG	6768–7670 (903)	GTG & TAG
trnV	7690–7755 (66)	TAC	7676–7740 (65)	TAC
trnA	7760–7825 (66)	TGC	7744–7807 (64)	TGC
trnD	7825–7893 (69)	GTC	7807–7875 (69)	GTC
NAD1	7896–8808 (913)	ATG & T(CG)	7878–8790 (913)	ATG & T(CA)
trnN	8814–8882 (69)	GTT	8796–8864 (69)	GTT
trnP	8900–8963 (64)	TGG	8875–8937 (63)	TGG
trnI	8968–9035 (68)	GAT	8942–9008 (67)	GAT
NAD3	9036–9343 (308)	GTG & TA(A)	9009–9319 (311)	GTG & TA(G)
trnS1	9347–9407 (61)	GCT	9324–9382 (59)	GCT
trnW	9408–9474 (67)	TCA	9384–9450 (67)	TCA
COX1	9478–11068 (1591)	ATG & T(CA)	9454–11044 (1591)	ATG & T(AA)
trnG	11065–11131 (67)	TCC	11037–11103 (67)	TCC
trnT	11132–11197 (66)	TGT	11104–11169 (66)	TGT
rrnL	11198–12177 (980)		11170-12151 (982)	
rrnS	12178–12906 (729)		12152–12875 (724)	
COX2	12907–13530 (624)	GTG & TAA	12876–13494 (619)	GTG & T(GG)
trnH	13524–13588 (65)	GTG	13495–13560 (66)	GTG
trnM	13590–13651 (62)	CAT	13563–13624 (62)	CAT

7.3.2 Annotation

We were able to identify the positions of all 36 expected genes in the two mitogenome sequences of *P. xenopodis* (Table 7.4). For the most part, the genes could be annotated based upon software predictions and gene alignments. However, there were a few cases where the final annotation decisions deserve special mention.

The stop codons of a number of PCGs seemingly differed between the two sequences of the mitogenome of *P. xenopodis*. In the *COX1*, *NAD1*, *NAD3* and *NAD4* genes the stop codons were, respectively, T(CA/AA), T(CG/CA), TA(G/A) and TA(G/A). These were annotated as truncated stop codons but might represent cases of population-level heterozygosity if we were to assume that these are complete rather than abbreviated stop codons.

A frame shift indel of 2 bp at the 3' end of the *COX2* gene in one of the sequences caused a new stop codon position to appear 1 aa sooner than in the other sequence. This led to an intraspecific length difference (619 *vs* 624) and variable stop position (619 *vs* 622) and codon (T(GG) *vs* TAA) in *COX2* of this gene. In the alignment of 116 469 trimmed reads to the sequence containing the longer variant of the *COX2* gene, less than 2% of the participating reads contained a 2 bp insertion at this point that was omitted from the final assembly. We assumed that this is a sequencing error and not an indication that this mitogenome may also contain the extra 2 bp.

We proposed a truncated T stop codon for the *COX3* gene in *P. xenopodis*, rather than the non-canonical TTA that was present at this position in both sequences, since this removed the overlap with the following *trnC*.

We chose a canonical TAG start codon for the *NAD5* gene in *P. xenopodis* over a truncated T(TC) stop codon 9 bp upstream from this position in view of the gene's alignment with those of the other polyopisthocotyleans. This termination position resulted in a 10 bp overlap with the following *trnE*, the longest region of gene overlap in this mitogenome aside from the expected *NAD4L* and *NAD4* overlap of 40 bp.

In the case of *rrnL* in the *P. xenopodis* mitogenome, the software predictions were revealed to be inaccurate when these predictions were aligned with the same gene in the other polyopisthocotyleans. Nonetheless, the nucleotide sequence between the 3' end of *trnT* and the 5' end of *rrnS* aligned well with the gene of other polyopisthocotyleans, which enabled us to annotate this gene.

There is only one case where our annotation of a tRNA gene deviated from the software predictions. The predictions for *trnR* in the first *P. xenopodis* sequence all differed from one another in length and none predicted a 7 bp acceptor arm. These predictions were also shorter than the proposed *trnR* gene in the second *P. xenopodis* sequence. We added 1 bp on either end of the longest prediction (the Arwen prediction) of the gene in the first sequence to bring the gene into alignment with the gene in the second sequence. This caused the acceptor arm to be 7 bp in length and resulted in a negligible increase in the free energy level of the gene ($+$ 0.19 kcal/mol).

In addition to our annotation of the mitogenome of *P. xenopodis*, we proposed seven changes to the mitogenome annotation of *D. hangzhouensis* (Table 7.5), for which a

Table 7.5: Proposed changes in gene position, length and start, stop and anticodons to the annotations in some of the polyopisthocotylean mitogenomes available on GenBank. Genes which could not be annotated are indicated with 'n/a'.

Species	Genes	Position (Length)	Start & Stop/Anticodon
Diplorchis hangzhouensis	*NAD6*	1009–1458 (450)	GTT & TAG
	NAD4L	4823–5063 (261)	TTG & TAA
	ATP6	6446–7016 (571)	ATG & TAG
	NAD2	n/a	n/a
	trnV	7898–7964 (67)	TAC
	trnA	7965–8033 (69)	TGC
	trnS1	9563–19620 (58)	GCT
Microcotyle sebastis	*NAD4*	3008–4243 (1236)	ATG & TAA
Neomazocraes dorosomatis	*NAD5*	185–1729 (1545)	TTG & TAA
	COX1	7797–9380 (1584)	TTG & TAA
Pseudochauhanea macrorchis	*NAD4*	6154–7278 (1125)	ATG & TAG
Sindiplozoon sp.	*NAD5*	3032–4559 (1528)	TTG & T(AT)
	ATP6	7535–8140 (606)	TTG & TAG
	NAD2	8143–9033 (891)	TTG & TAG
	NAD3	10411–10698 (288)	TTG & TAG
	COX2	14448–15077 (630)	TTG & TAG

draft annotation is available on GenBank (Zhang *et al.*, unpubl.). Based upon software predictions and alignment with the same genes in other polyopsithocotyleans, we proposed changing the initiation of the gene for *ATP6* to 24 bp downstream of the originally predicted position at an ATG start codon, *NAD4L* to 7 bp upstream at a TTG start codon and *NAD6* to 42 bp upstream to a non-canonical GTT start codon. Two tRNA genes that were missing from the original annotation, namely those for *trnA* and *trnV*, were added based upon the positions proposed by the tRNA annotation software. Another tRNA gene, that for *trnS1*, was moved 6 bp downstream from its original position. Finally, we called the annotation of the *NAD2* gene into question, although we failed to provide a better annotation. None of the software predictions, nor any alignments of this region of the mitogenome with the orthologous region in the other polyopisthocotylean mitogenomes, could identify the start and stop positions or the correct reading frame for this gene beyond reasonable doubt. Therefore, we question the *NAD2* gene annotated by Zhang *et al.* (unpubl.).

Furthermore, some annotation adjustments were proposed for the other polyopsthocotylean mitogenomes based upon the same principles as those outlined above (Table 7.5). We proposed that the start codon of *NAD4* in *M. sebastis* should move 36 bp upstream to an ATG start codon (as opposed to the annotation by Park *et al.*, 2007). This facilitated an overlap of 40 bp between *NAD4L* and *NAD4*, which corresponds with relatives. The addition of 60 bp to the 5' end of the *COX1* gene in *N. dorosomatis* brought its starting position into alignment with that of the other polyopisthocotyleans and reduced the gap between this gene and the preceding *trnW*. Likewise, shifting the starting position of the *NAD5* gene of this species 135 bp upstream also improved alignment. In the

case of *Ps. macrorchis*, a shift of the starting position 9 bp downstream caused a better alignment of its *NAD4* with relatives and a more typical overlap length of 40 bp with the *NAD4L* gene (as opposed to the annotation by Zhang *et al.*, 2012). In the mitogenome of *Sindiplozoon* sp., we proposed shifting the starting positions of the *ATP6*, the *COX2* and the *NAD5* genes 30 and 39 bp upstream and 30 bp downstream, respectively, from the original positions (as opposed to the annotation by Zhang *et al.*, 2018b). For the start codon in the *NAD2* gene, we rejected Zhang *et al.*'s (2018b) working hypothesis of a TTG start codon and proposed the neighbouring TTG codon 3 bp upstream to bring the start position closer to the 3' end of the *ATP6* gene. Similarly, we rejected the tentatively assigned start position of the *NAD3* gene and propose a start codon 9 bp upstream from this point. Finally, we concurred with the tentatively assigned start codons and positions of the *NAD5* gene in *Eudiplozoon* Khotenovsky, 1984, sp., the *ATP6* and *NAD2* genes in *Paradiplozoon opsariichthydis* (Jiang, Wu *et* Wang,1984) Jiang, Wu *et* Wang, 1989, the *COX1*, *cytb* and *NAD1* genes in *Sindiplozoon* sp. (in agreement with Zhang *et al.*, 2018b).

7.3.3 Mitogenome architecture, gene content and intraspecific variation

The *P. xenopodis* mitogenome encoded all 36 genes expected for the neodermatan mitogenome, namely 12 PCGs, 22 tRNA genes and two rRNA genes (Figure 7.1; Table 7.4). All genes were transcribed from the same strand.

The mitogenome was highly compact, with bases that do not participate in coding accounting for only 1.80–1.87% of the total length of the *P. xenopodis* mitogenome. The mitogenome of *P. xenopodis* contained 20 NCRs in total, ranging from 1 to 150 bp in length with a mean length of 13 bp. The longest NCR (149–150 bp in total) lay between the *trnY* and *trnL1* genes and contained sets of mononucleotide repeats ($A_{4–5}$, $C_{6–12}$, $G_{7–10}$, $T_{4–5}$) as well as a TA-rich region ($TA_{10–14}$). Pairwise identity of this region between the two mitogenome sequences of *P. xenopodis* was not high at 65.8%. MITOS2 (*beta* version) proposed this region to be the origin of replication in the mitogenome of both specimens. According to the RNAfold algorithm (Gruber *et al.*, 2008) in the *ViennaRNA* package *version* 2.4 (Lorenz *et al.*, 2011), these NCRs were capable of forming stem-loop secondary structures. No stretches of tandem repeats could be identified in either of the *P. xenopodis* sequences. Moreover, none of the prediction software programmes indicated the presence of tRNA-like genes in this region.

The *NAD4L* gene presented the only instance of one PCG overlapping with another, namely *NAD4*. There were three instances of major overlap between a PCG and the tRNA gene following it in the mitogenome of *P. xenopodis*, namely *COX1–trnG* (4–8 bp), *COX2–trnH* (0–7 bp) and *NAD5–trnE* (10 bp). Furthermore, there were several cases of tRNA genes overlapping one another, or PCGs, by one or two bases.

The PCGs were arranged in the order *COX3–NAD6–NAD5–cytb–NAD4L–NAD4–ATP6–NAD2–NAD1–NAD3–COX1–COX2* (Figure 7.1). A total of 10 276–10 287 bp participated in protein coding, comprising 75.2–75.3% of the mitogenome. The PCGs encoded for 286 amino acids on average and ranged from 261 (86 aa) to 1 591 (530 aa) bp in length. Intraspecific length differences in PCGs between the first and second *P. xenopodis* mitogenome sequences were noted. Differences in length by one or two amino acids were observed in the *COX1* (1 aa), *COX2* (1 aa), *COX3* (1 aa), *NAD3* (1 aa) and the *NAD4* (2 aa) genes. In *COX2*, this length difference resulted in a variable stop position for the gene.

The start codons ATG and GTG were employed at similar frequencies. Both start codons were employed to initiate the *NAD4* gene, representing a case of population-level heterozygosity. Likewise, TAG was utilised as a stop in the majority of cases but TAA and the truncated stop codons T and TA were also present. In some instances where we proposed the use of a truncated stop codon, non-canonical stop codons or population-level heterozygosity in stop codons could also be a possibility. This is true for the *COX3* gene, where a TTA stop codon could terminate the gene, rather than a truncated T. However, we chose the truncated stop to eliminate overlap with the following *trnC*. Likewise, variable stop codons could be used to terminate the *NAD1* (TCG *vs* TCA), *NAD3* (TAA *vs* TAG) and *NAD4* (TAA *vs* TAG) genes, as opposed to abbreviated stops, since the 3' ends of none of these genes overlap with the 5' ends of their following tRNA genes regardless of whether an abbreviated or complete stop codon is assigned. Lastly, the 3' end of the *COX1* gene overlapped with the following *trnG* gene whether we assigned an abbreviated T stop codon or assumed population-level heterozygosity in the stop codon (TCA *vs* TAA).

Together, phenylalanine, leucine, serine and valine were the amino acids most frequently encoded by the PCGs, representing roughly 50% of all amino acids used. To encode these amino acids, the generally AT-rich triplets of AGT, TCA, TCT, TTA, TTG, TTT, GTG and GTT were preferred (Table 7.6). Conversely, glutamic acid, histidine, lysine, glutamine and arginine, most frequently encoded by the triplets GAA, GAG, CAC, CAT, AAG, CAA and CGT (Table 7.6), were the amino acids used most infrequently. Codon usage was roughly similar in the PCGs of both *P. xenopodis* sequences (Table 7.6), with discrepancies in the most frequently used codon only occurring for amino acids with overall low usage, such as glutamic acid (1.9%), histidine (1.6%), asparagine (4.1–4.2%) and tryptophan (2.7–2.8%).

The two rRNA genes were situated adjacent to each other flanked by the *trnT* and *COX2* genes with no intergenic gaps. The two genes were not the same length in the two *P. xenopodis* mitogenome sequences, with a pairwise identity of 87.4% in the case of the *rrnS* gene pair and 89.2% in the case of the *rrnL* gene pair. In total, the two rRNA genes comprised 12.5% of the mitogenome of *P. xenopodis*.

Table 7.6: Codon frequency in the mitochondrial protein-coding genes of *Protopolystoma xenopodis* expressed as a fraction of occurrences in each synonymous codon family and as relative codon usage (RSCU). GTG and ATG can operate as start codons and are marked with (i). Most frequently used codons per mitogenome are indicated in bold for each amino acid.

		P. xenopodis specimen 1		*P. xenopodis* specimen 2	
Amino acid	Triplet	Fraction	RSCU	Fraction	RSCU
A	GCA	0.344	1.38	0.323	1.29
	GCC	0.118	0.47	0.065	0.26
	GCG	0.097	0.39	0.075	0.30
	GCT	**0.441**	1.76	**0.538**	2.15
C	TGC	0.093	0.19	0.071	0.14
	TGT	**0.907**	1.181	**0.929**	1.86
D	GAC	0.095	0.19	0.068	0.14
	GAT	**0.905**	1.81	**0.932**	1.86
E	GAA	**0.516**	1.03	0.455	0.91
	GAG	0.484	0.97	**0.545**	1.09
F	TTC	0.033	0.07	0.027	0.05
	TTT	**0.968**	1.94	**0.973**	1.95
G	GGA	0.152	0.61	0.185	0.74
	GGC	0.097	0.39	0.040	0.16
	GGG	0.218	0.87	0.165	0.66
	GGT	**0.533**	2.13	**0.610**	2.44
H	CAC	**0.589**	1.18	0.375	0.75
	CAT	0.411	0.82	**0.625**	1.25
I	ATA	0.431	1.29	0.423	1.27
	ATC	0.037	0.11	0.033	0.10
	ATT	**0.532**	1.60	**0.544**	1.63
K	AAG	**1.000**	1.00	**1.000**	10.00
L	CTA	0.082	0.49	0.053	0.32
	CTC	0.018	0.11	0.006	0.04
	CTG	0.031	0.18	0.018	0.11
	CTT	0.100	0.60	0.103	0.62
	TTA	**0.420**	2.52	**0.513**	3.08
	TTG	0.349	2.09	0.307	1.84
M	ATG (i)	**1.000**	1.00	**1.000**	1.00
N	AAA	**0.531**	1.59	0.454	1.36
	AAC	0.126	0.38	0.028	0.09
	AAT	0.343	1.03	**0.518**	1.55
P	CCA	**0.473**	1.89	**0.565**	2.26
	CCC	0.121	0.48	0.129	0.52
	CCG	0.187	0.75	0.082	0.33
	CCT	0.220	0.88	0.224	0.89
Q	CAA	**0.724**	1.45	**0.889**	1.78
	CAG	0.276	0.55	0.111	0.22
R	CGA	0.296	1.19	0.327	1.31
	CGC	0.019	0.07	0.091	0.36
	CGG	0.148	0.59	0.055	0.22
	CGT	**0.537**	2.15	**0.527**	2.11
S	AGA	0.094	0.75	0.075	0.61
	AGC	0.036	0.29	0.030	0.24
	AGG	0.094	0.75	0.114	0.91
	AGT	0.251	2.01	0.254	2.03
	TCA	0.157	1.26	0.165	1.32
	TCC	0.047	0.37	0.035	0.28
	TCG	0.063	0.51	0.065	0.52
	TCT	**0.259**	2.07	**0.262**	2.10
T	ACA	**0.438**	1.75	**0.385**	1.54
	ACC	0.171	0.69	0.137	0.55
	ACG	0.114	0.46	0.120	0.48
	ACT	0.276	1.10	0.359	1.44
V	GTA	0.175	0.70	0.167	0.67
	GTC	0.017	0.07	0.008	0.03
	GTG (i)	0.259	1.03	0.221	1.89
	GTT	**0.549**	2.20	**0.604**	2.42
W	TGA	0.478	0.96	**0.589**	1.18
	TGG	**0.522**	1.04	0.411	0.82
Y	TAC	0.150	0.30	0.061	0.12
	TAT	**0.850**	1.70	**0.939**	1.88
Stop	TAA	0.083	0.25	0.000	0.00
	TAG	**0.500**	1.50	**0.500**	1.50
	T– –	0.417	1.25	0.500	1.50

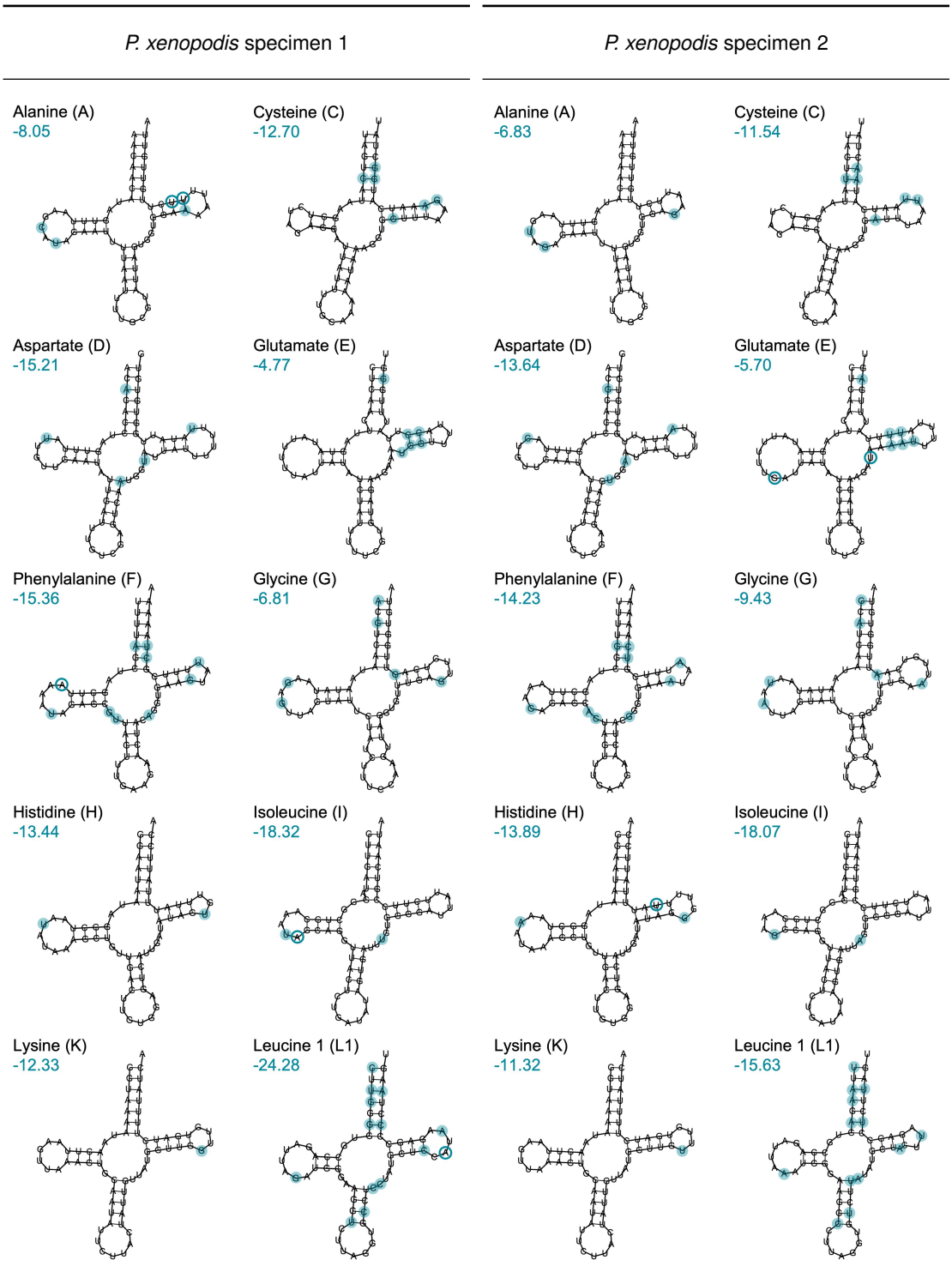

Figure 7.2: Predicted secondary structures of transfer RNAs encoded by the two newly annotated mitochondrial sequences of *Protopolystoma xenopodis*, as visualised by MiTFi. Values in blue represent free energy levels of the structures expressed in kcal/mol. Intraspecific nucleotide differences in the tRNA genes between the two specimens, as identified via Clustal Omega alignment, are indicated as blue circles. Filled circles denote nucleotide substitutions and blank circles denote insertions.

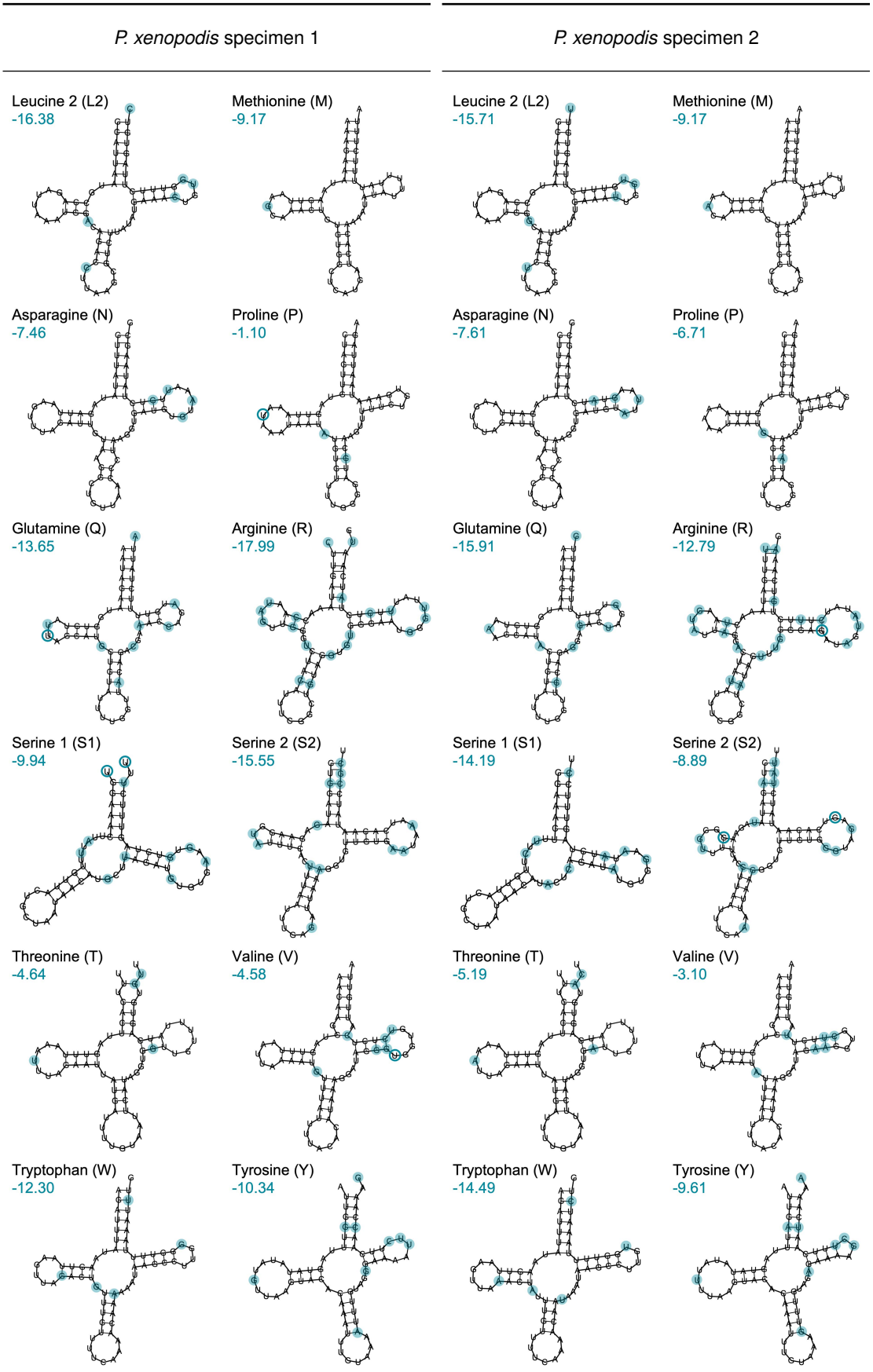

Figure 7.2: Predicted secondary structures of tRNAs encoded by the two newly annotated mitochondrial sequences of *Protopolystoma xenopodis* (*continued*).

The mitogenome of *P. xenopodis* encoded 22 tRNA genes (Figure 7.1). The genes ranged from 59 to 70 bp in length (Table 7.4). Except for *trnS1*, which lacked the dihydrouridine (DHU) arm, all of the tRNAs were predicted to exhibit the typical cloverleaf structure when folded (Figure 7.2). When comparing the tRNA genes in the two *P. xenopodis* mitogenome sequences, nucleotide substitutions were much more commonly observed than differences in tRNA gene length (Figure 7.2). The nucleotide differences in the tRNA genes between the two sequences of the *P. xenopodis* mitogenome were mainly found in the TΨC loop (substitutions and indels observed in 16 out of 22 tRNA genes) and stem (in 13 tRNA genes), the acceptor stem (in 15 tRNA genes) and the DHU loop (in 14 tRNA genes). Base differences in the DHU stem were less common (in 5 tRNA genes), likewise in the anticodon stem (in 10 tRNA genes) and the variable loop (in 8 tRNA genes). Notably, the substitutions found in the stems of all four arms were not compensatory base changes in the majority of cases, meaning that mismatched base pairings were common. Nucleotide substitutions in the anticodon loop itself were only observed in the *trnL1* and *trnS2* genes.

An unmatched A base insertion was observed in the acceptor stem of the *trnI* gene's secondary structure of both *P. xenopodis* mitogenome sequences. Secondary loops formed by unmatched base pairs were present in the acceptor, DHU or anticodon stems of several of the tRNA genes' secondary structures. Notably, in the case of an unmatched base pair in the DHU stem of the secondary structure of the *trnE* gene, this structure was only present in one of the two *P. xenopodis* mitogenome sequences.

In our study, nucleotide diversity in the *P. xenopodis* mitogenome was only determined based upon two sequences, not averaged over a representative sample of sequences of the mitogenome of *P. xenopodis*. These two sequences were remarkably different, with an overall pairwise identity of 84.2%. Differences were more noticeable in certain regions of the mitogenome (Figure 7.3). In particular, the highest peaks in variability were found in the longest NCR in the mitogenome and the 5' and 3' ends of the *NAD5* gene.

Genes with the highest nucleotide diversity per unit length were those for *ATP6*, *COX2*, *NAD2*, *NAD4–5* and *rrnL*. This corresponded with a pairwise identities of 78.1%, 80.2%, 82.2%, 82.3%, 89.2% and 81.2%, respectively, for these genes which are generally lower than the global mean identity. The genes for *COX1*, *NAD3* and *NAD4L* and the 3' ends of both the rRNA genes were amongst the most conserved regions in the two sequences with pairwise identities of 93.9%, 86.8% and 89.3% for the three PCGs. Likewise, the variability in some tRNA genes was low, with the genes for *trnK*, *trnP*, *trnI*, *trnH* and *trnM* exhibiting pairwise identities of 98.5%, 95.3%, 95.6%, 95.5% and 98.4%, respectively.

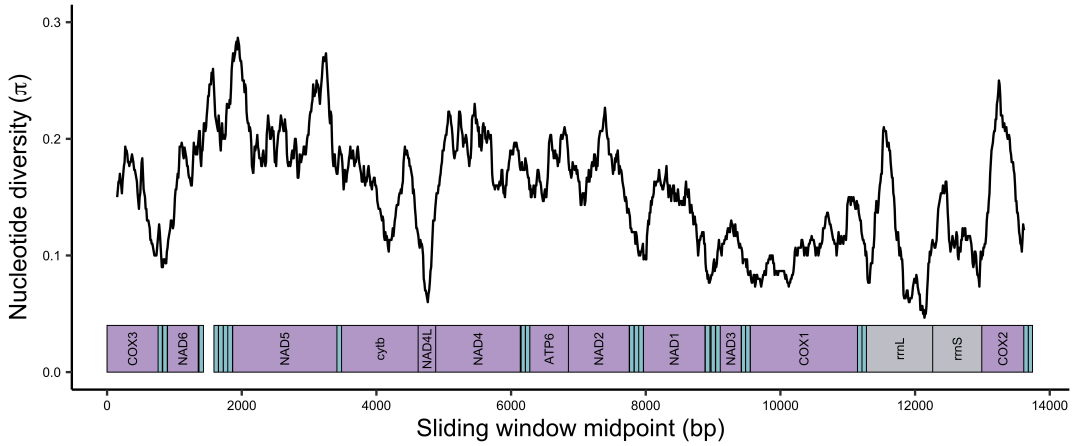

Figure 7.3: Nucleotide diversity (π) between the two newly annotated *Protopolystoma xenopodis* mitochondrial sequences calculated from a sliding window analysis (window size 300 bp, step size 10 bp) of the concatenated alignments of all genes and non-coding regions. The boundaries of the aligned genes are indicated below the map.

7.3.4 Comparison with other polyopisthocotylean mitogenomes

Based upon the two available *P. xenopodis* mitogenome sequences, we assumed that gene order was conserved within the species. Moreover, three gene blocks were conserved across all available polyopisthocotylean mitogenomes, namely the five genes from *NAD5* to *NAD4*, the thirteen genes from *ATP6* to *COX1* and the four genes from *trnT* to *COX2* (Figure 7.4). A gene rearrangement hot spot within the Polyopsthocotylea was found between the *COX3* and *NAD5* genes, meaning that the tRNA genes *trnC*, *trnK*, *trnL1*, *trnL2*, *R*, *trnS2* and *trnY* were often involved in transpositions or tandem duplication random loss (TDRL) events.

In terms of the pairwise comparisons, two transpositions involving the tRNA genes differentiated the two polystomatid mitogenomes of *P. xenopodis* and *D. hangzhouensis*. Two other tRNA gene transpositions commonly explained the differences between the mitogenomes of *P. xenopodis* and some of the other eight polyopisthocotylean species. Two more tRNA gene transpositions differentiated the mitogenomes of *P. xenopodis* and *Heterobothrium okamotoi* Ogawa, 1991. In addition to these tRNA transpositions, a long range transposition of another tRNA gene explained the difference in mitochondrial gene order between *P. xenopodis* and *Pa. opsariichthydis*. The TDRL of two tRNA genes further differentiated the mitogenomes of *P. xenopodis* and *H. okamotoi*. Finally, the TDRL of the *NAD6* gene and its surrounding tRNA genes, coupled with a transposition in the case of *Polylabris halichoeres* Wang *et* Zhang, 1998 and a second TDRL scenario in the case of *Ps. macrorchis*, was the only instance of a PCG being involved in gene order rearrangements.

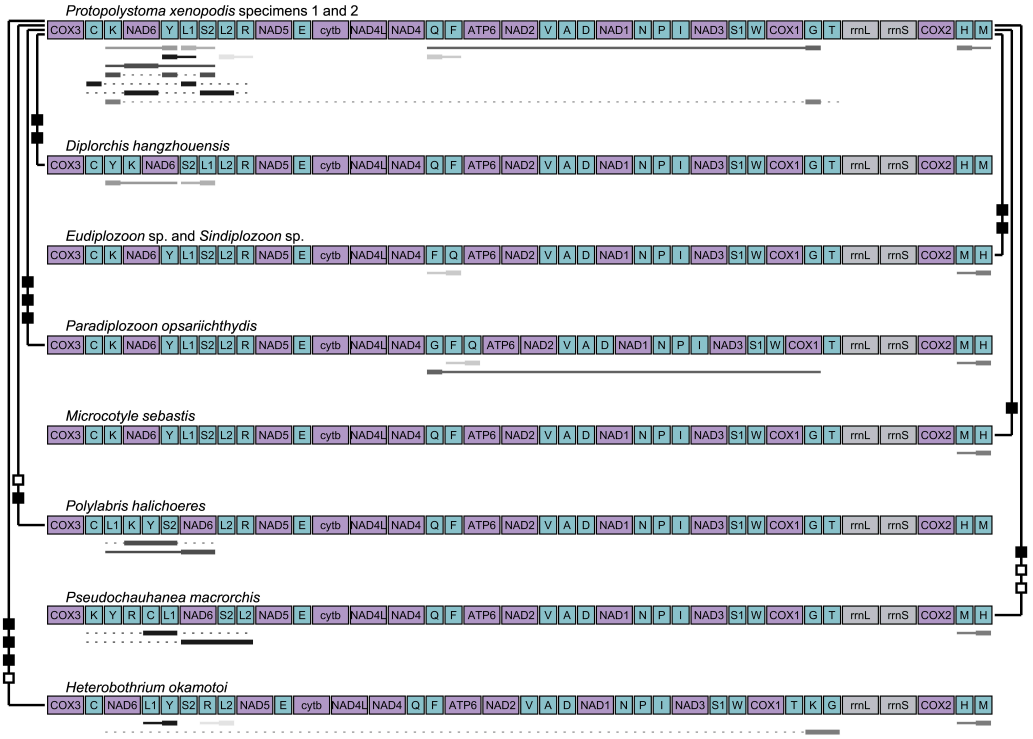

Figure 7.4: Gene order rearrangement scenarios, as identified by CREx, among nine polyopisthocotylean mitogenomes based upon the pairwise comparison of seven complete mitogenomes to the newly annotated sequences of *Propopolystoma xenopodis*. Black squares on the lines connecting the pairs and solid lines below the rearranged gene blocks indicate instances of transposition, whilst white squares and dotted lines indicate scenarios of tandem duplication random loss. Thicker sections of the lines below the gene blocks show the translocated gene(s) in the pairwise comparisons with *P. xenopodis*. Linearised sequences are displayed. Gene and genome sizes are not to scale and non-coding regions are omitted.

Among available polyopisthocotylean mitogenomes, that of *P. xenopodis* was the shortest (Table 7.7), which tied in with its high genome density. Although comparable in terms of number of NCRs, the longest intergenic region in the mitogenome of *P. xenopodis* was much shorter (149–150 bp) than the longest intergenic region in any of the other Polyopisthocotylea (314–2000+ bp). Moreover, no regions with tandem repeats were identified in the mitogenome of *P. xenopodis*. Uniquely, the major NCRs in the mitogenomes of both *D. hangzhouensis* and *P. xenopodis* were broadly situated between the *NAD6* and *NAD5* genes, whilst the longest NCRs of all other examined complete polyopisthocotylean mitogenomes lay before the *NAD6* gene and after *COX3*.

7.3.5 Mitogenome phylogeny

The concatenated alignment of the 14 mitochondrial genes from 12 available polyopisthocotylean species and two monopisthocotylean species as outgroups amounted to 13 346

Table 7.7: Comparison of the general features of all previously published complete polyopisthocotylean mitochondrial genomes with the newly annotated mitogenome sequences of *Protopolystoma xenopodis*. Based upon the original notations of these mitogenomes, we report mitogenome length, A + T content, the codons that initiate and terminate the 12 protein-coding genes with their frequency in brackets and exceptions on the typical cloverleaf secondary structure of folded transfer RNA for each mitogenome, along with the number and minimum and maximum length of non-coding regions (NCRs) and the number and length of the repeating units in, or the total length of, the highly repetitive regions (HRRs), if the information was made available.

Polyopistho-cotylean species	Reference	Length (bp)	A+T (%)	Start codons	Stop codons	tRNA exceptions	NCRs and HRRs
Microcotylidae							
Microcotyle caudata	MT180126 (Nam *et al.*, 2020)	14 267	70.8	ATA(1); ATG(10); ATT(1)	TAA(8); TAG(2); TAT(1); TTA(1)	*trnS1* no DHU arm	numerous NCRs; 1 HRR (349 bp in total)
Microcotyle sebastis	DQ412044 (Park *et al.*, 2007)	14 407	70.5	ATA(1); ATG(10); ATT(1)	TAA(7); TAG(3); TA(1); T(1)	*trnS1* & *trnS2* no DHU arm	21 NCRs (1–472 bp); 1 HRR (7.9 (53 bp) units)
Polylabris halichoeres	JF505509 (Zhang *et al.*, 2011)	15 527	72.6	ATG(10); GTG(2)	TAA(5); TAG(7)	not investigated	22 NCRs (1–1939 bp); 1 HRR (17.8 (94 bp) units)
Mazocraeidae							
Mazocraeoides gonialosae Tripathi, 1959	MT015514 (Kim *et al.*, 2020b)	15 106	73.4	ATG(8); ATT(1); GTG(3)	TAA(8); TAG(4)	*trnS1* no DHU arm	numerous NCRs; 1 HRR (1039 bp in total)
Chauhaneidae							
Pseudochauhanea macrorchis	JN592039 (Zhang *et al.*, 2012)	15 031	71.5	ATA(2); ATG(10)	TAA(6); TAG(6)	*trnS1* & *trnS2* no DHU arm	24 NCRs (1–1200 bp); 1 HRR (6.9 (88 bp) and 5.2 (107 bp) units)
Diclidophoridae							
Heterobothrium okamotoi	MK948930 (Li *et al.*, 2019)	14 643		ATG(10); GTA(1); GTG(1)	TAA(7); TAG(5)	not investigated	19 NCRs (1–796 bp); HRRs not investigated
Neoheterobothrium hirame Ogawa, 1999	MN984338 (Kim *et al.*, 2020a)	14 588	70.8	ATA(1); ATG(11)	TAA(7); TAG(5)	*trnS1* no DHU arm	numerous NCRs; 1 HRR (885 bp in total)
Diplozoidae							
Eudiplozoon sp.	MG458328 (Zhang *et al.*, 2018b)	14 334	70.7	ATG(7); GTG(4); TTG(1)	TAA(4); TAG (7); T (1)	*trnS1* & *trnS2* no DHU arm	25 NCRs (1–586 bp); no HRRs
Paradiplozoon opsariichthydis	MG458327 (Zhang *et al.*, 2018b)	15 385 (NCR incomplete)	67.4	ATG(10); ATT(2)	TAA(4); TAG (7); T (1)	*trnS1* & *trnS2* no DHU arm	21 NCRs (1–2000+ bp); 1 HRR (>1 (197 bp) and >1 (244 bp) units)
Sindiplozoon sp.	MG458326 (Zhang *et al.*, 2018b)	15 254	68.0	ATG(3); GTG(4); GTT(1); TTG(4)	TAA(1); TAG(8); T(3)	*trnS1* & *trnS2* no DHU arm	29 NCRs (1–1205 bp); 1 HRR (7 (11–16 bp) units)
Polystomatidae							
Diplorchis hangzhouensis	JQ038227 (Zhang *et al.*, unpubl.)	13 918 (draft)	72.1	ATG(9); GTT(1); TTG(1)	TAA(4); TAG(6); T(1)	*trnS1* no DHU arm	>23 NCRs (2–314 bp); no HRRs
Protopolystoma xenopodis		13 648–13 675	68.2–70	ATG(5–6); GTG(6–7)	TAA(0–1); TAG(6); TA(2); T(3–4)	*trnS1* no DHU arm	20 NCRs (1–150 bp); no HRRs

nucleotides. The topologies yielded by the ML and BI analyses were identical (Figure 7.5). Both analyses indicated that the polystomatids are basal to the other available polyopisthocotyleans. Notably, the number of nucleotide substitutions per site between the two *P. xenopodis* sequences were higher than the intergeneric differences between some other polyopisthocotylean species.

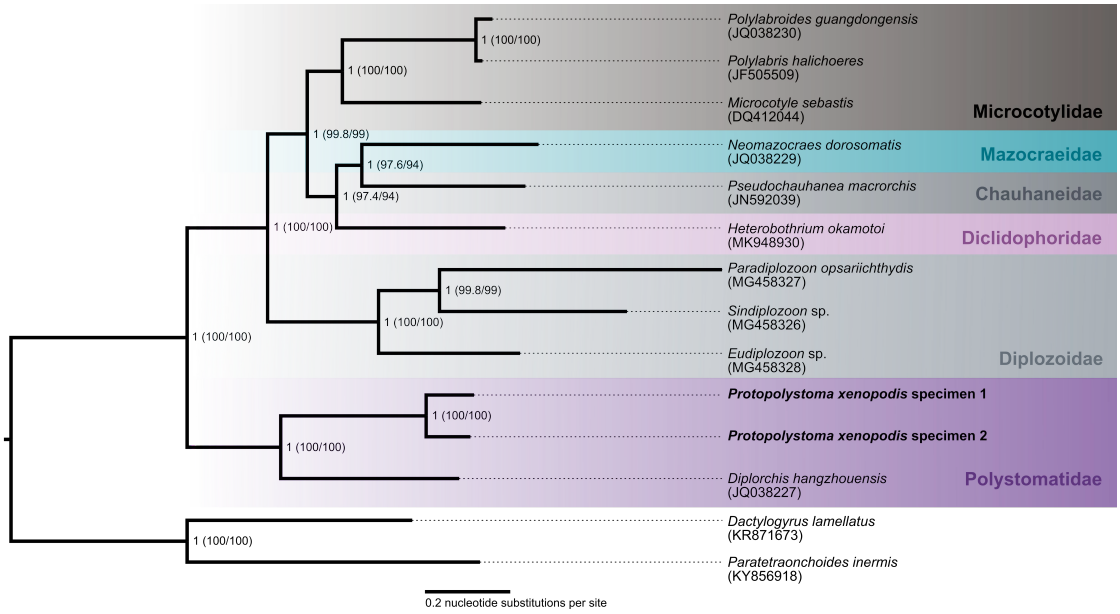

Figure 7.5: Majority-rule consensus tree from the Bayesian inference (BI) of phylogeny of 14 mitochondrial genes from 12 polyopisthocotylean species, including two sequences of the newly annotated *Protopolystoma xenopodis*, and *Dactylogyrus lamellatus* and *Paratetraonchoides inermis*, monopisthocotylean species, which served as outgroups. Node support, in order of posterior probability, SH-like approximated likelihood ratio and ulfra-fast bootstrap, is indicated to the right of nodes. The topology of the maximum likelihood (ML) tree is identical to the BI tree. Polyopisthocotylean families are indicated in colour. Branch lengths indicate the expected number of nucleotide substitutions per site.

7.4 Discussion

We present and compare the complete mitogenome sequences of two specimens of *P. xenopodis*, a polystomatid parasite of the African Clawed Frog *X. laevis*, hereby adding the first fully annotated mitogenome of the family Polystomatidae to the body of available monogenean mitogenomes. Prior to the present study, an incomplete draft mitogenome of the polystomatid *D. hangzhouensis* was the only representative mitogenome of the family (Zhang *et al.*, unpubl.). What is more, this is also the first mitogenome-wide intraspecific comparison conducted within Polyopisthocotylea and one of very few such comparisons within the class Monogenea.

Polystomatidae is regarded as the earliest diverging polyopisthocotylean clade (Mollaret *et al.*, 2000), a position that is confirmed by the phylogenetic analyses of the available polyopisthocotylean mitogenomes conducted in this study and others (Kim *et al.*, 2020a,b; Nam *et al.*, 2020). Moreover, the genus *Protopolystoma* is also the sister group of all remaining polystomatids that parasitise amphibian hosts, likely diverging from other polystomatids in this clade around 275 million years ago (Héritier *et al.*, 2015). Consequently, the newly characterised mitogenome of *P. xenopodis* provides a unique addition to the available mitogenomic data of Polyopisthocotylea in particular and Monogenea in general, enabling us to compare the mitogenome architecture of earlier diverging and more derived clades

of this group.

One feature shared by the mitogenomes of both the studied polystomatids is the apparent lack of a highly repetitive region, a phenomenon that has only been found in one other polyopisthocotylean mitogenome thus far (Zhang *et al.*, 2018b). The complexity and length of the repetitive regions recovered in the earliest annotated polyopisthocotylean mitogenomes has led investigators to hypothesise that the major NCRs in these mitogenomes contain longer and more repeating units than those in monopisthocotylean mitogenomes (Zhang *et al.*, 2011, 2012). This hypothesis has been refuted by the discovery of comparable major NCRs in more recently assembled monopisthocotylean mitogenomes (Ye *et al.*, 2014; Zhang *et al.*, 2018c, 2019b, 2020).

Across all the monogenean mitogenomes sequenced to date, only the major NCRs of the monopisthocotylean capsalids *Benedenia seriolae* (Yamaguti, 1934) Meserve, 1938 and *Neobenedenia melleni* (MacCallum, 1927) Yamaguti, 1963 are shorter than the major NCR of *P. xenopodis* (see Perkins *et al.*, 2010; Zhang *et al.*, 2014). Nonetheless, the approximately 150 bp situated between the *trnY* and *trnL1* genes in the mitogenome of *P. xenopodis* exhibit certain features that suggest that the function of the major NCR might not be impaired despite the relatively short length. This includes microsatellite-like TA• regions, mononucleotide repeats and the capability to form stem-loop structures. These features have all been suggested as indicative of the presence of a control region that plays a role in the initiation of replication in metazoan mitogenomes (Cameron, 2014; Fumagalli *et al.*, 1996; Kuhn *et al.*, 2008; Li *et al.*, 2016; Shui *et al.*, 2008; Zhang *et al.*, 1995; Zhang & Hewitt, 1997). That this has the same role in monogenean mitogenomes has been suggested but remains to be demonstrated (Le *et al.*, 2002a; Park *et al.*, 2007).

With its relatively short intergenic regions, it comes as no surprise that the mitogenome of *P. xenopodis* is the shortest and most compact of all the polyopisthocotylean mitogenomes reported thus far (Kim *et al.*, 2020a,b; Li *et al.*, 2019; Nam *et al.*, 2020; Park *et al.*, 2007; Zhang *et al.*, 2011, 2012, 2018b). Even when compared to the available monopisthocotylean mitogenomes, this mitogenome is shorter than most, with the exception of the mitogenomes of the four capsalids *B. hoshinai* Ogawa, 1984, *B. humboldti* Baeza, Sepúlveda *et* González, 2019, *B. seriolae* and *N. melleni* and the ancyrocephalid *Tetrancistrum nebulosi* Young, 1967 (see Baeza *et al.*, 2019; Kang *et al.*, 2012; Kawato *et al.*, 2019; Perkins *et al.*, 2010; Zhang *et al.*, 2014, 2016). Interestingly, all five these mitogenomes have relatively short major NCRs that lack long tandem repeats but contain the telltale signs of a putative invertebrate mitogenome control region also found in the major NCR of *P. xenopodis*.

The comparably high density and short length of the other available polystomatid mitogenome, that of *D. hangzhouensis*, suggests that low complexity of NCRs could be a synapomorphy in this basal clade of the Polyopisthocotylea. Tandem repeats in the major

NCRs of more recently diverging clades are a consequence of strand slippage during replication (Levinson & Gutman, 1987; Macey *et al.*, 1998; Okada *et al.*, 2010) and might therefore be a derived characteristic of certain polyopisthocotylean species rather than a synapomorphy for the group (as opposed to the hypothesis of Zhang *et al.*, 2011, 2012).

The major NCR in Polyopisthocotylea is situated in the identified gene rearrangement hot spot of this subclass, which involves the tRNA genes that lie between *COX3–NAD6–NAD5*. This supports the connection between NCRs and gene rearrangement (Macey *et al.*, 1998; Okada *et al.*, 2010), where rearranged parts of the mitogenome are often adjacent to the control region where secondary structure may facilitate recombination and rearrangement (Cameron, 2014; Erpenbeck *et al.*, 2009; Le *et al.*, 2002a). This notion is further supported by the fact that NCRs sometimes contain copies of pseudo-genes in monogenean mitochondria, that is defunct copies of genes that have duplicates in other parts of the genome (Zhang *et al.*, 2011, 2017, 2018a).

However, the assembly of highly repetitive regions can be challenging, especially if the length of the repeating unit exceeds that of the read length during assembly (e.g. Vanhove *et al.*, 2018; Zhang *et al.*, 2018b). Uncertainty regarding the true length of the major NCR is heightened if manual circularisation of the mitogenome has to be implemented in this region, as was the case for our *P. xenopodis* sequences. Although our choice of cicularisation point was quite self-evident, the assembly issues in this region is still a factor to keep in mind. Furthermore, the available mitogenome of *D. hangzhouensis* is a linear draft for which no assembly information has been made available. For these reasons, we interpret the issue of NCR length and complexity in polyopisthocotylean mitogenomes with caution.

Upon consideration of the genes present (36 in total, no *ATP8* gene), the predicted tRNA secondary structures (cloverleaf, except for *trnS1*) and the most frequent stop and start codons utilised in the PCGs (ATG and GTG for initiation and TAA and TAG for termination), we can conclude that the polystomatid mitogenome architecture does not deviate from that of the standard neodermatan (Le *et al.*, 2002a; Wey-Fabrizius *et al.*, 2013). An exception is the *NAD6* gene of *D. hangzhouensis*, where we propose the non-canonical GTT start codon. In the Platyhelminthes, the GTT codon has also been suggested as start for the *COX1* genes of the cestodes *Echinococcus granulosus* (Batsch, 1786) and *Hymenolepis diminuta* (Rudolphi, 1819) and for the *ATP6* gene of another cestode *Taenia pisiformes* Bloch, 1780 (see Jia *et al.*, 2010; Le *et al.*, 2001; von Nickisch-Rosenegk *et al.*, 2001). Moreover, Zhang *et al.* (2018b) tentatively proposed GTT as the presumptive start codon of the *NAD3* gene of the polyopisthocotylean *Sindiplozoon* sp. based upon the alignment with orthologous genes of other monogeneans. However, we should note that based upon our alignment with the orthologs of more recently published polyopisthocotylean mitogenomes (Li *et al.*, 2019; Zhang *et al.*, unpubl.; present study), we call this starting position into question and propose a TTG start codon 9 bp upstream.

Across all the available polyopisthocotylean mitogenomes (Kim *et al.*, 2020a,b; Li *et al.*, 2019; Nam *et al.*, 2020; Park *et al.*, 2007; Zhang *et al.*, 2011, 2012, 2018b), TAA and TAG are predominantly used as stop codons. In addition, instances of abbreviated stop codons (TA or T) are reported (Park *et al.*, 2007; Zhang *et al.*, 2018b) and are also encountered in our newly annotated polystomatid mitogenomes. These codons are presumably completed via polyadenylation after transcription (Nakao *et al.*, 2003; Ojala *et al.*, 1981).

When looking at the overall structure of polyopisthocotylean mitogenomes, the reshuffling of tRNA genes leads to remarkable variation in gene order between species when compared with some other flatworm groups (Le *et al.*, 2002a; Wey-Fabrizius *et al.*, 2013; Ross *et al.*, 2016), especially in the gene rearrangement hot spot situated between the *COX3* and *NAD5* genes (Zhang *et al.*, 2012). Even within the family Polystomatidae, the mitogenomes of *D. hangzhouensis* and *P. xenopodis* can be distinguished by no less than two tRNA transpositions in this area. Recent comparisons of the gene order of available monogenean mitogenomes suggests that the evolution of mitogenome gene order might be discontinuous, with some families exhibiting higher levels of gene reshuffling than others (Zhang *et al.*, 2017, 2018a,b, 2019a). Even though Polyopisthocotylea is the earliest diverging branch in the neodermatan phylogeny, the gene order of none of the available mitogenomes of this group conforms to the proposed ancestral gene order of neodermatans (Zhang *et al.*, 2019a). Moreover, our comparison illustrates a common gene order of the PCGs and rRNA genes across the available polyopisthocotylean mitogenomes that represent five families. Interpreted in the light of the gene order of *P. xenopodis*, a species in the earliest diverging clade of Polyopisthocotylea (Mollaret *et al.*, 2000), this implies a scenario where the common ancestor of all Polyopisthocotylea underwent rearrangement of the *NAD6–NAD5* gene block when compared to the proposed ancestral neodermatan gene order (Zhang *et al.*, 2019a).

Going further than most of the previous studies on the mitogenomes of monogeneans that retrieved their sequences from a single individual (with regards to Polyopisthocotylea see Kim *et al.*, 2020a,b; Li *et al.*, 2019; Nam *et al.*, 2020; Park *et al.*, 2007; Zhang *et al.*, 2011, 2012, 2018b), the present study compared the mitogenome sequences of two specimens of *P. xenopodis*. This comparison reveals marked intraspecific variability in the mitogenome of this polystomatid in terms of overall sequence length and pairwise identity, as well as the length and structure of single genes and NCRs. This variability is all the more striking given the fact that these specimens were collected during a single parasite survey from one water body.

Within Monogenea, the intraspecific comparison of whole mitogenomes was only conducted for the monopisthocotyleans *B. seriolae* and *Gyrodactylus salaris*/*thymalli* Malmberg, 1957 (Huyse *et al.*, 2008; Solá *et al.*, 2015). The observed intraspecific variation in the *P. xenopodis* mitogenome is much higher than for the mitogenome of the *G. salaris*-/*thymalli* complex (Huyse *et al.*, 2008). In the two *P. xenopodis* sequences, 15.8% of sites

are not identical and overall length differs with 27 bp *vs* a 2.2% identity and 1 bp length difference between the two *Gyrodactylus* von Nordmann, 1832 mitogenomes (Huyse *et al.*, 2008). The same could be said of the mitogenome sequences of the capsalid *B. seriolae* (see Kawato *et al.*, 2019). Among 12 specimens collected from four prefectures across Japan, the mitogenome sequences differed only at 1% of sites with an overall 1 bp length difference (Kawato *et al.*, 2019), although there was a steep decline in identity when these were compared to the same species from Australia (Perkins *et al.*, 2010). All in all, the sequence differentiation observed within the mitogenome of *P. xenopodis* is noteworthy when compared with other flatworms (Le *et al.*, 2002a).

Delving deeper, the mitogenome sequences of *P. xenopodis* exhibit five PCGs of variable length (*COX1–3*, *NAD3–4*), one that employed two variations of start codon (*NAD4*) and another with a variable stop position due to a frame-shift mutation (*COX2*). Occasional differences at the protein-coding level has been reported before among different populations of a species of triclad flatworms (Kenny *et al.*, 2019) and cestodes (Le *et al.*, 2001). The mitogenome of *P. xenopodis* demonstrates that in the case of three PCGs, *NAD1*, *NAD3* and *NAD4*, there is also a possibility for variable stop codons, although we tentatively assigned truncated T stop codons to err on the side of caution. In flatworms, this has been suggested for the free-living planariid *Crenobia alpina* (Dana, 1766), where the *COX2* gene might have a TAR stop codon, indicative of the presence of two possible stop codons in the population (Solá *et al.*, 2015). Nonetheless, Solá *et al.* (2015) also opted to assign a truncated TA stop codon. In the *rrnS* and *rrnL* genes there are noteworthy nucleotide differences between the two specimens of *P. xenopodis*, both in terms of length and pairwise identity. The rRNA genes are generally regarded as more conserved among related taxa (Vanhove *et al.*, 2013) but there are exceptions among the Platyhelminthes (e.g. Le *et al.*, 2002b).

We acknowledge that the intraspecific differences noted here only reflect the comparison of two sequences, which limits the inferences we can make to advise future population genetic analyses. Be that as it may, the sliding window analysis of nucleotide diversity of the two sequences identified many of the same genes as those identified as the most variable among the mitogenomes of the polyopisthocotylean family Diplozoidae and the monopisthocotylean families Dactylogyridae, Gyrodactylidae and Diplectanidae (Huyse *et al.*, 2008; Vanhove *et al.*, 2018; Zhang *et al.*, 2018a,b). These include the *ATP6*, *NAD2* and *NAD5* genes as the most variable markers in the Diplozoidae, with the frequently used barcoding gene *COX1* as the among the least variable (Zhang *et al.*, 2018b). In a similar intergeneric comparison of monogenean *Gyrdicotylus* mitogenome sequences, *NAD2* and *NAD5* once again emerge as the most variable, along with *NAD1*, *NAD4* and *COX3* (Plaisance *et al.*, 2007; Huyse *et al.*, 2008). In this comparison, *COX1* was identified as one of the most conserved regions (Huyse *et al.*, 2008). Likewise, Vanhove *et al.* (2018) suggested *NAD2* as the best marker to study population-level processes in African monopisthocotyleans. As for diplectanids, the fast-evolving *NAD2*, *NAD4–6* are

suggested as better markers than *COX1* (Zhang *et al.*, 2018a).

It is therefore interesting to note that the regions of high intraspecific divergence in the two *P. xenopodis* mitogenome sequences, namely *ATP6*, *COX2*, *NAD2*, *NAD4*, *NAD5* and *rrnL*, are shown as fast-evolving markers in Monogenea as a whole. This points towards non-random population-level heterozygosity in the mitogenome of *P. xenopodis* that may be a sign of incipient speciation of different lineages within the species. Recent analyses (Chapter 6 of this thesis) of *P. xenopodis* from many populations across southern Africa have indicated the presence of multiple diverged lineages within the species. What is more, due to extensive human-mediated movement of the host *X. laevis* across the the region (van Sittert & Measey, 2016; Weldon *et al.*, 2007), many populations of the locally native hosts may harbour both locally native and locally invasive lineages of *P. xenopodis* (Chapter 6 of this thesis). Thus, the high divergence between the two studied mitogenome sequences in the present study might also reflect this recent contact between different host lineages followed by spill-over of parasites as opposed to a reflection of high levels of genetic divergence within a natural, locally native population. This is particularly likely for this population in Bloemfontein, which is situated near a tertiary institution that imported many consignments of locally non-native *X. laevis* from localities across South Africa for the purpose of teaching and research (van Sittert & Measey, 2016; Weldon *et al.*, 2007). The deliberate and accidental release of these frogs and subsequent small scale dispersal by local fishermen, events that occurred regularly (Louis du Preez, personal communication), could bring these locally non-native *X. laevis* into contact with the native *X. laevis*. In turn, this could facilitate the persistence of a genetically divergent population of *P. xenopodis* in the water bodies in Bloemfontein and surrounds.

Previously, the *COX1* and *rrnS* genes were the only two mitochondrial markers for which primers were available for polystomatid flatworms. These markers were used along with the nuclear markers *18S* and *28S* to investigate patterns of speciation and evolutionary relationships within the Polystomatidae (e.g. Héritier *et al.*, 2015; Verneau *et al.*, 2009). More recently, these two markers were also used in a co-phylogeographic study of *P. xenopodis* and *X. laevis* (Chapter 6 of this thesis). Our analysis suggests that *ATP6*, *COX2*, *NAD2*, *NAD4*, *NAD5* and *rrnL* might be more suitable to discriminate different lineages of *P. xenopodis* and the complete mitogenome provides future investigators with the means to develop suitable primers. Particularly, *COX2*, *NAD2* and *rrnL* might be well suited to the task, since these genes are flanked by relatively conservative stretches where primers may be designed. Naturally, our preliminary investigation should be followed by an investigation with a greater sample size. A useful application of next generation sequencing methods, namely the sequencing of pooled samples, can be a cost-effective approach to compare the mitogenomic data from more *P. xenopodis* specimens from the same population and identify mitochondrial gene regions suitable for population-level studies (Karlsen *et al.*, 2014; Mimee *et al.*, 2015; Schlötterer *et al.*, 2014).

These investigations are particularly crucial in the light of the invasive status of not only the host, *X. laevis*, but also its parasite, *P. xenopodis*. The ability to develop high resolution markers to trace the origin and spread of invasive species is an important tool in any invasion biologist's toolkit. The complete and annotated mitogenome sequence of *P. xenopodis* provides us with the opportunity to study the mechanisms of incipient speciation on the intraspecific level with the added complication of a species on the move.

Chapter 8

General discussion and future perspectives: the marriage of invasion biology and parasitology

The current study has demonstrated the value of incorporating data from co-introduced parasites into the study of invasive species. In this study, approximately 350 specimens of African Clawed Frog *Xenopus laevis* (Daudin, 1802) (Anura: Pipidae) and their metazoan parasite assemblages from more than 45 localities in the native and invasive range are used as a model co-invasive host-parasite system. This addition of parasite data brings us to a number of insights that would otherwise have remained obscured.

Firstly, the study shows the importance of the integrative approach to taxonomy to the description and clarification of native parasite dynamics. In turn, the more robust identification of the native parasite fauna of *X. laevis* can inform management of the host-parasite system in the invasive range.

Secondly, the global replicates of the parasitological surveys of this invasive amphibian are put to use to test long-standing hypotheses in invasion biology and illuminate unifying patterns within host-parasite systems during range expansion. These analyses attest to the fact that biological invasion events should be regarded as the translocation of species packages – hosts with an assemblage of co-introduced and even co-invasive parasites. What is more, these events bring about complex host-parasite dynamics.

Thirdly, the utility of parasite data sets as independent line of evidence in studying the origin and pathways of biological invasions is demonstrated by the first ever application of intraspecific co-phylogeographic analyses to invasion biology. This approach highlights the need for holistic sampling in invasion biology. As a first-of-its-kind resource, the complete mitogenome of the co-introduced monogenean parasite *Protopolystoma xenopodis* (Price,

1943) Bychowsky, 1957 (Monogenea: Polystomatidae) is provided to aid future investigators in the development of molecular markers suited to their level of co-phylogeographic analyses.

8.1 The role of integrative taxonomy in invasion biology

Species identification forms the basis of all investigations in ecology (Ferris & Ferris, 1989). In modern times, the framework of integrative taxonomy has expanded the toolkit of taxonomists and ecologists alike (Schlick-Steiner *et al.*, 2010). For instance, the incorporation of molecular data in the systematics of different groups of nematodes demonstrated that morphological characters may appear independently in different lineages and are often not suitable interspecific discriminants (Carreno & Nadler, 2003; Tkach *et al.*, 2014). Nonetheless, molecular data that can inform phylogenetics are still conspicuously absent for many families within the Nematoda (Svitin *et al.*, 2018). The approach of both Svitin *et al.* (2018) and Schoeman *et al.* (2020) (Chapters 2 and 3) provides a blueprint for how one may go about to address gaps in taxonomic information in the age of advanced imaging and molecular techniques. Especially the use of molecular barcoding can be a shortcut for species identification in studies with ecological applications (such as Schoeman *et al.* (2019) and Chapter 5 of this thesis). This tool is only applicable to parasites for which molecular data are already available, which underlines the necessity of incorporating both morphological and molecular data in species descriptions.

On one level, the pluralistic approach to the systematics of these nematode species reveal previously undocumented host-parasite associations and the central role of *X. laevis* as parasite reservoir in aquatic habitats in its native range (brought to light in Chapter 3). A surprisingly high number of novel parasite associations is reported despite more than 100 years of investigations of the parasites of *X. laevis* (see parasitological surveys in Cosgrove & Jared, 1974; Macnae *et al.*, 1973; Pritchard, 1964; Southwell & Kirshner, 1937; Thurston, 1970; Tinsley, 1996; Vercammen-Grandjean, 1960). In addition to emphasising the role of *X. laevis* as a versatile host for a multitude of nematode parasites, the newly documented parasite associations serves as an indicator of trophic interactions between *X. laevis* and several aquatic and semi-aquatic animal species, demonstrating how parasite taxonomy might inform our understanding of ecological interactions. Armed with this information, future investigators may now develop more targeted natural history studies of *X. laevis* and its parasites, a field of study that has been neglected in an era of fast science and big data (Valenzuela-Sánchez *et al.*, 2021).

On another level, we see how a lack of clear descriptions and molecular data in previous investigations of the parasites of *X. laevis* in both its native and invasive range may lead to false assumptions regarding the origin of the parasites that associate themselves with

X. laevis in the invasive range. In the current study, nematode larvae from *X. laevis* in its native range are uncovered that belong to genera that have also been reported in association with this frog in the invasive range (Castillo *et al.*, 2017; Kuperman *et al.*, 2004). However, because no molecular data were incorporated in previous investigations and since third stage nematode larvae are impossible to identify based upon morphology alone, it was generally assumed that these species represent novel parasite associations in the invasive range, an idea that might be refuted when more molecular data become available.

As a demonstration of the framework outlined above, the molecular approach was also applied to distinguish among digenean species in the conducted parasite surveys (Chapters 4 and 5). Digenean metacercariae present with similar taxonomic challenges as larval nematodes, yet the barcoding of the *ITS* gene of the recovered digeneans in South Africa and France revealed a *Euclinostomum* Travassos, 1928, sp. that accompanied *X. laevis* from the native to the invasive range (Chapter 5). Specimens of *Euclinostomum* sp. have also been recovered in feral *X. laevis* from California (Kuperman *et al.*, 2004). However, without an integrated taxonomic approach to the species identification of the digenean metacercariae in this population, we will remain in the dark as to whether this also represents a co-introduction.

In the case of heteroxenous Digenea and Nematoda, the co-introduction of taxa that utilise other species as final hosts may have far-reaching effects. The integrative taxonomic approach to the nematode parasites of *X. laevis* in its native range has emphasised the role of this host as parasite reservoir, linking all manner of aquatic and semi-aquatic organisms via shared parasites (Chapter 3). The associations of *X. laevis* with heteroxenous parasites that originate from the native fauna of its invasive range (Castillo *et al.*, 2017; Kuperman *et al.*, 2004; Rodrigues, 2014), demonstrates that this frog plays a like role in its new environments. In the light of these risks, parasitological studies in modern times have no excuse not to incorporate molecular data, even if the taxonomic expertise might be lacking to conduct detailed morphological descriptions.

As a recommendation for future investigations, the current study identifies the systematics of the Digenea of *X. laevis*, the most speciose parasite taxon of the *X. laevis* native parasite assemblage, as a neglected taxonomic group. In addition, the protozoan parasite taxa of *X. laevis* are greatly in need of taxonomic revisions. Due to the lack of taxonomic knowledge on the protozoan parasites of *X. laevis*, the investigations of the current study focused entirely on the metazoan parasite dynamics of *X. laevis*, hampering the inference of unifying trends across all parasite groups of this globally invasive frog.

8.2 Discerning patterns in invasion biology with global replicates of co-introduced host-parasite systems

Moving from the level of species to the community scale, this project seized the opportunity provided by the many available parasitological surveys of *X. laevis*, both in the native and invasive ranges (Castillo *et al.*, 2017; Kuperman *et al.*, 2004; Rodrigues, 2014; Schoeman *et al.*, 2019), to identify general trends in the parasite dynamics of a species on the move. Using this approach, we see repeated parasite loss in globally invasive *X. laevis* irrespective of continent, climate, mechanism of parasite loss, or invasion history (Schoeman *et al.*, 2019). However, despite this overall trend of parasite loss, the picture that emerges on the infracommunity level is one of a complex interplay of intrinsic and extrinsic factors that shape co-introduced parasite dynamics (Chapter 5).

A closer look at the parasite dynamics across these geographic replicates demonstrates that host range expansion may have opposing effects on the transmission of different parasite species. Thus, the oversimplified idea of depauperate non-native parasite assemblages is supplanted by a unifying pattern of increased variability in the parasite dynamics of host populations that recently underwent range expansion. In this view of the typical parasite assemblage of hosts in expanding populations, we expect more extreme dynamics, ranging from highly infected host individuals to near absence of some parasite groups coupled with an upsurge in the abundance of yet other parasite species. This pattern is found at the range edge of an invasive population, as well as at highly disturbed localities in the native range where one would expect pioneer populations of the host to be present.

When trying to find explanations for the divergent responses of different parasite species to the range expansion of their host, we are confronted with aspects of the parasite dynamics of *X. laevis* where our knowledge is patchy. Elegant and detailed natural history experiments conducted in both the native and invasive ranges of this host can provide invasion ecologists with a deeper understanding of the co-introduced parasites they may encounter (Valenzuela-Sánchez *et al.*, 2021). Specifically, investigators should direct their focus towards host immune responses and the other host species that interact with these parasites as intermediate or final hosts during their life cycles.

With a well-described, widespread model host-parasite system at our disposal, invasion biologists can use *X. laevis* and its parasites as bioindicators of disturbance. Since *X. laevis* harbours a parasite assemblage with species that make use of a wide variety of other hosts in their life cycle (Schoeman *et al.*, 2020), the decline or absence of certain parasite species can be a useful indicator of ecosystem health and the maturity of the establishment of invasive hosts in an ecosystem.

8.3 Parasites as supporting evidence in bio-invasion research

The final application of this host-parasite model is a comparative phylogeographic study that managed to neatly identify both the intraspecific cryptic introduction of *X. laevis* in its native range and the dispersal networks that facilitate this widespread translocation (Chapter 6). This approach reveals multiple instances of host lineage switches by its polystomatid parasite *P. xenopodis*, which acts as a tag for contact between phylogeographically distinct *X. laevis* lineages. Despite the availability of a host data set of equal size that consists of orthologous mitochondrial markers, the parasite data set acts as an independent line of evidence that uncovers trends that remain obscured in host phylogeography alone.

Thus, the use of the model in this way acts as a proof of concept for the potential of the co-phylogeographic approach to the clarification of patterns in intraspecific host divergence and dispersal. In turn, this provides additional insight on invasion pathways and informs management and conservation strategies. Based upon the success of this approach, it becomes clear that studies in invasion biology will benefit from the incorporation of ”holistic specimens” (Cook *et al.*, 2017). This relatively new approach to sampling advocates for the collection of the target species along with their symbionts (Cook *et al.*, 2017). Even if these symbionts cannot be processed directly, their preservation as voucher specimens in natural history collections will be a treasure trove for future investigations (Thompson *et al.*, 2021).

The above proof of concept shows that the development of high resolution markers to trace the origin and spread of invasive species is an important tool in the invasion biologist’s toolkit. The monogenean family Polystomatidae emerges as an excellent tag for host movement on the intraspecific level, as has been found for other monogeneans (Huyse *et al.*, 2015; Kmentová *et al.*, 2019; Ondračková *et al.*, 2012). This is all the more promising given the co-invasive status of several polystomatid species (Héritier *et al.*, 2017; Meyer *et al.*, 2015; Schoeman *et al.*, 2019; Verneau *et al.*, 2011). To streamline the use of polystomatid monogeneans as tags for host movement in future investigations, the first complete mitochondrial genome of a polystomatid flatworm was sequenced and annotated, namely that of *P. xenopodis* (Chapter 7). A preliminary analysis revealed areas of the mitogenome that could be more suitable markers for intraspecific phylogeographic studies than the currently employed *COX1* and *rrnS*. This finding will be confirmed by an investigation with a greater sample size, possibly via the cost-effective sequencing of pooled samples (Karlsen *et al.*, 2014; Mimee *et al.*, 2015; Schlötterer *et al.*, 2014).

8.4 The future of invasion biology from the perspective of a parasitologist

It is a given that the movement of wildlife will continue to rock our world (Capinha *et al.*, 2015; Chinchio *et al.*, 2020; Morens *et al.*, 2020). As free-living species navigate new environments, associations with their parasites will shift in time and space, giving rise to novel interactions that can have far-reaching effects (Amundsen *et al.*, 2013; Dunn *et al.*, 2012; Dunn & Hatcher, 2015; Roy & Lawson Handley, 2012; Telfer & Bown, 2012). From the perspective of a parasitologist, this provides us with the prime opportunity to tease apart the mechanisms that shape host-parasite associations, especially when hosts are experiencing range expansion. From the viewpoint of an invasion biologist, parasites can be incorporated in investigations from the stage of project inception as an independent line of evidence. With the marriage of these two fields, this study demonstrates the application of a multidisciplinary approach to the dynamics of range expansion with the aid of a well-studied model system of a globally invasive amphibian host and its metazoan parasites.

Bibliography

Aguiar, A., Toledo, G. M., Anjos, L. A. & Silva, R. J. 2015. Helminth parasite communities of two *Physalaemus cuvieri* Fitzinger, 1826 (Anura: Leiuperidae) populations under different conditions of habitat integrity in the Atlantic Rain Forest of Brazil. *Brazilian Journal of Biology*, 75:963–968. https://doi.org/10.1590/1519-6984.03614

Ahyong, S. T., Kupriyanova, E., Burghardt, I., Sun, Y., Hutchings, P. A., Capa, M. & Cox, S. L. 2017. Phylogeography of the invasive Mediterranean fan worm, *Sabella spallanzanii* (Gmelin, 1791), in Australia and New Zealand. *Journal of the Marine Biological Association of the United Kingdom*, 97:985–991. https://doi.org/10.1017/S0025315417000261

Aisien, S. O., Ayeni, F. & Ilechie, I. 2004. Helminth fauna of anurans from the Guinea savanna at New Bussa, Nigeria. *African Zoology*, 39:133–136

Altschul, S. F., Gish, W., Miller, W., Myers, E. W. & Lipman, D. J. 1990. Basic local alignment search tool. *Journal of Molecular Biology*, 215:403–410

Amaro, R. C., Nunes, I., Canedo, C., Napoli, M. F., Junca, F. A., Verdade, V. K., ... Rodrigues, M. T. 2013. A molecular phylogeny recovers *Strabomantis aramunha* Cassimiro, Verdade and Rodrigues, 2008 and *Haddadus binotatus* (Spix, 1824) (Anura: Terrarana) as sister taxa. *Zootaxa*, 3741:S569–S582. https://doi.org/10.11646/zootaxa.3741.4.7

Amundsen, P. A., Lafferty, K. D., Knudsen, R., Primicerio, R., Kristoffersen, R., Klemetsen, A. & Kuris, A. M. 2013. New parasites and predators follow the introduction of two fish species to a subarctic lake: implications for food-web structure and functioning. *Oecologia*, 171:993–1002. https://doi.org/10.1007/s00442-012-2461-2

Anderson, R. C. 2000. *Nematode parasites of vertebrates. Their development and transmission*. 2nd ed. Wallongford, UK: CABI Publishing.

Anderson, S., Bankier, A. T., Barrell, B. G., de Bruijn, M. H. L., Coulson, A. R., Drouin, J., ... Young, I. G. 1981. Sequence and organization of the human mitochondrial genome. *Nature*, 290:457–465. https://doi.org/10.1038/290457a0

Avery, R. A. 1971. A preliminary list of parasites collected from reptiles and amphibians in northern Nigeria. *British Journal of Herpetology*, 4:217–219

Baeza, J. A., Sepúlveda, F. A. & González, M. T. 2019. The complete mitochondrial genome and description of a new cryptic species of *Benedenia* Diesing, 1858 (Monogenea: Capsalidae), a major pathogen infecting the yellowtail kingfish *Seriola lalandi* Valenciennes in the South-East Pacific. *Parasites & Vectors*, 12, art. 490. https://doi.org/10.1186/s13071-019-3711-5

Baker, M. R. 1983. Nematode parasites of the turtle *Pelusios sinuatus* (Pelomedusidae: Pleurodira) from southern Africa. *Systematic Parasitology*, 5:161–167. https://doi.org/10.1007/bf00009348

Balbuena, J. A., Miguez-Lozano, R. & Blasco-Costa, I. 2013. PACo: a novel procrustes application to cophylogenetic analysis. *PLOS One*, 8, e61048. https://doi.org/10.1371/journal.pone.0061048

Baldwin, R. E., Banks, M. A. & Jacobson, K. C. 2012. Interating fish and parasite data as a holistic solution for identifying the elusive stock structure of Pacific sardines (*Sardinops sagax*). *Reviews in Fish Biology and Fisheries*, 22:137–156. https://doi.org/10.1007/s11160-011-9227-5

Bandelt, H.-J., Forster, P. & Röhl, A. 1999. Median-joining networks for inferring intraspecific phylogenies. *Molecular Biology and Evolution*, 16:37–48. https://doi.org/10.1093/oxfordjournals.molbev.a026036

Bar-On, Y. M., Phillips, R. & Milo, R. 2018. The biomass distribution on Earth. *Proceedings of the National Academy of Sciences USA*, 115:6506–6511. https://doi.org/10.1073/pnas.1711842115

Barnett, L. K., Phillips, B. L., Heath, A. C. G., Coates, A. & Hoskin, C. J. 2018. The impact of parasites during range expansion of an invasive gecko. *Parasitology*, 145:1400–1409. https://doi.org/10.1017/s003118201800015x

Barson, M. 2004. The occurrence of *Contracaecum* sp. larvae (Nematoda: Anisakidae) in the catfish *Clarias gariepinus* (Burchell) from Lake Chivero, Zimbabwe. *Onderstepoort Journal of Veterinary Research*, 71:35–39. https://doi.org/10.4102/ojvr.v71i1.283

Barson, M. & Avenant-Oldewage, A. 2006. Nematode parasites of *Clarias gariepinus* (Burchell, 1822) from the Rietvlei Dam, South Africa. *Onderstepoort Journal of Veterinary Research*, 73:87–94. https://doi.org/10.4102/ojvr.v73i2.152

Barson, M., Bray, R., Ollevier, F. & Huyse, T. 2008. Taxonomy and faunistics of the helminth parasites of *Clarias gariepinus* (Burchell, 1822), and *Oreochromis mossambicus* (Peters, 1852) from temporary pans and pools in the Save-Runde river floodplain, Zimbabwe. *Comparative Parasitology*, 75:228–240. https://doi.org/10.1654/4337.1

Baylis, H. A. 1934. A little known nematode parasite of the eel. *Annals and Magazine of Natural History, Series 10*, 13:235–240

Baylis, H. A. 1939. Some parasitic worms from the Belgian Congo. *Annals and Magazine of Natural History, Series 11*, 4:401–404

Bellard, C., Genovesi, P. & Jeschke, J. M. 2016. Global patterns in threats to vertebrates by biological invasions. *Proceedings of the Royal Society B: Biological Sciences*, 283, art. 20152454. https://doi.org/10.1098/rspb.2015.2454

Bernt, M., Donath, A., Jühling, F., Externbrink, F., Florentz, C., Fritzsch, G., ... Stadler, P. F. 2013. MITOS: improved *de novo* metazoan mitochondiral genome annotation. *Molecular Phylogenetics and Evolution*, 69:313–319. https://doi.org/10.1016/j.ympev.2012.08.023

Bernt, M., Merkle, D., Ramsch, K., Fritzsch, G., Perseke, M., Bernhart, D., ... Middendorf, M. 2007. CREx: inferring genomic rearrangements based on common intervals. *Bioinformatics*, 23:2957–2958. https://doi.org/10.1093/bioinformatics/btm468

Berthier, P., du Preez, L. H., Raharivololoniana, L., Vences, M. & Verneau, O. 2014. Two new species of polystomes (Monogenea: Polystomatidae) from the anuran host *Guibemantis liber*. *Parasitology International*, 63:108–119. https://doi.org/10.1016/j.parint.2013.09.014

Bertolino, S., Wauters, L. A., De Bruyn, L. & Canestri-Trotti, G. 2003. Prevalence of coccidia parasites (Protozoa) in red squirrels (*Sciurus vulgaris*): effects of host phenotype and environmental factors. *Oecologia*, 137:286–295. https://doi.org/10.1007/s00442-003-1345-x

Beverley-Burton, M. 1963. Some digenetic trematodes from amphibians and reptiles in Southern Rhodesia including two new species and a new genus: *Sarumitrema hystatorchis* n.gen., n.sp. (Plagiorchiidae) and *Halipegus rhodiensis* n.sp. (Halipegidae). *Proceedings of the Helminthological Society of Washington*, 30:49–59

Bibb, M. J., van Etten, R. A., Wright, C. T., Walberg, M. W. & Clayton, D. A. 1981. Sequence and gene organization of mouse mitochondrial DNA. *Cell*, 26:167–180. https://doi.org/10.1016/0092-8674(81)90300-7

Blackburn, T. M. 2008. Using aliens to explore how our planet works. *Proceedings of the National Academy of Sciences USA*, 105:9–10. https://doi.org/10.1073/pnas.0711228105

Blackburn, T. M., Bellard, C. & Ricciardi, A. 2019. Alien versus native species as drivers of recent extinctions. *Frontiers in Ecology and the Environment*, 17:203–207. https://doi.org/10.1002/fee.2020

Blackburn, T. M. & Ewen, J. G. 2017. Parasites as drivers and passengers of human-mediated biological invasions. *EcoHealth*, 14:61–73. https://doi.org/10.1007/s10393-015-1092-6

Blackburn, T. M., Pyšek, P., Bacher, S., Carlton, J. T., Duncan, R. P., Jarošík, V., ... Richardson, D. M. 2011. A proposed unified framework for biological invasions. *Trends in Ecology & Evolution*, 26:333–339. https://doi.org/10.1016/j.tree.2011.03.023

Blakeslee, A. M. H., Byers, J. E. & Lesser, M. P. 2008. Solving cryptogenic histories using host and parasite molecular genetics: the resolution of *Littorina littorea*'s North American origin. *Molecular Ecology*, 17:3684–3696. https://doi.org/10.1111/j.1365-294x.2008.03865.x

Boane, C., Cruz, C. & Saraiva, A. 2008. Metazoan parasites of *Cyprinus carpio* L. (Cyprinidae) from Mozambique. *Aquaculture*, 284:59–61. https://doi.org/10.1016/j.aquaculture.2008.07.037

Bobadilla-Suarez, M., Ewen, J. G., Groombridge, J. J., Beckmann, K., Shotton, J., Masters, N., ... Sainsbury, A. W. 2017. Using qualitative disease risk analysis for herpetofauna conservation translocations transgressing ecological and geographical barriers. *EcoHealth*, 14:47–60. https://doi.org/10.1007/s10393-015-1086-4

Bolek, M. G. & Coggins, J. R. 2001. Seasonal occurrence and community structure of helminth parasites in green frogs, *Rana clamitans melanota*, from southeastern Wisconsin, USA. *Comparative Parasitology*, 68:164–172

Bolger, A. M., Lohse, M. & Usadel, B. 2014. Trimmomatic: a flexible trimmer for Illumina sequence data. *Bioinformatics*, 30:2114–2120. https://doi.org/10.1093/bioinformatics/btu170

Bolker, B. M., Brooks, M. E., Clark, C. J., Geange, S. W., Poulsen, J. R., Stevens, M. H. & White, J. S. 2009. Generalized linear mixed models: a practical guide for ecology and evolution. *Trends in Ecology and Evolution*, 24:127–135. https://doi.org/10.1016/j.tree.2008.10.008

Boomker, J. 1982. Parasites of South African freshwater fish. I. Some nematodes of the catfish [*Clarias gariepinus* (Burchell, 1822)] from the Hartbeespoort Dam. *Onderstepoort Journal of Veterinary Research*, 49:41–51

Boomker, J. 1994a. Parasites of South African freshwater fish. VI. Nematode parasites of some fish species in the Kruger National Park. *Onderstepoort Journal of Veterinary Research*, 61:35–43

Boomker, J. 1994b. Parasites of Southern African freshwater fish. VII. Nematodes of some scaled fishes from the Hartbeespoort Dam, Transvaal. *Onderstepoort Journal of Veterinary Research*, 61:197–199

Brayton, C. 1992. Wasting disease associated with cutaneous and renal nematodes in commercially obtained *Xenopus laevis*. *Annals of the New York Academy of Sciences*, 653:197–201

Britt, A., Welch, C., Katz, A., Iambana, B., Porton, I., Junge, R., ... Haring, D. 2004. The re-stocking of captive-bred ruffed lemurs (*Varecia variegata variegata*) into the Betampona Reserve, Madagascar: methodology and recommendations. *Biodiversity and Conservation*, 13:635–657. https://doi.org/10.1023/b:bioc.0000009497.24917.ae

Brodeur, J. C., Damonte, M. J., Vera Candioti, J., Poliserpi, M. B., D'Andrea, M. F. & Bahl, M. F. 2020. Frog body condition: basic assumptions, comparison of methods and characterization of natural variability with field data from *Leptodactylus latrans*. *Ecological Indicators*, 112, art. 106098. https://doi.org/10.1016/j.ecolind.2020.106098

Brooks, S. P. & Gelman, A. 1998. General methods for monitoring convergence of iterative simulations. *Journal of Computational and Graphical Statistics*, 7:434–455. https://doi.org/10.2307/1390675

Brown, G. P., Kelehear, C., Shilton, C. M., Phillips, B. L. & Shine, R. 2015. Stress and immunity at the invasion front: a comparison across cane toad (*Rhinella marina*) populations. *Biological Journal of the Linnean Society*, 116:748–760. https://doi.org/10.1111/bij.12623

Bruňanská, M., Matey, V. & Nebesářová, J. 2012. Ultrastructure of the spermatozoon of the diphyllobothriidean cestode *Cephalochlamys namaquensis* (Cohn, 1906). *Parasitology Research*, 111:1037–1043. https://doi.org/10.1007/s00436-012-2928-4

Bürkner, P.-C. 2017. brms: an R package for Bayesian multilevel models using Stan. *Journal of Statistical Software*, 80:1–28. https://doi.org/10.18637/jss.v080.i01

Burnham, K. P. & Anderson, D. R. 2002. *Model selection and multi-model inference: A practical information-theoretic approach*. 2nd ed. New York, USA: Springer-Verlag.

Bursey, C. R., Goldberg, S. R., Kusamba, C. & Greenbaum, E. 2018. New species of *Falcaustra* (Nematoda: Kathlaniidae) and other helminths in *Amietia nutti* (Anura: Pyxicephalidae) from the Democratic Republic of Congo. *Comparative Parasitology*, 85:177–181. https://doi.org/10.1654/1525-2647-85.2.177

Bush, A. O., Lafferty, K. D., Lotz, J. M. & Shostak, A. W. 1997. Parasitology meets ecology on its own terms: Margolis et al. revisited. *The Journal of Parasitology*, 83:575–583. https://doi.org/10.2307/3284227

Caffara, M., Locke, S. A., Cristanini, C., Davidovich, N., Markovich, M. P. & Fioravanti, M. L. 2016. A combined morphometric and molecular approach to identifying metacercariae of *Euclinostomum heterostomum* (Digenea: Clinostomidae). *The Journal of Parasitology*, 102:239–248. https://doi.org/10.1645/15-823

Cailliez, F. 1983. The analytical solution of the additive constant problem. *Psychometrika*, 48:305–310. https://doi.org/10.1007/bf02294026

Cameron, S. L. 2014. Insect mitochondrial genomics: implications for evolution and phylogeny. *Annual Review of Entomology*, 59:95–117. https://doi.org/10.1146/annurev-ento-011613-162007

Campião, K., da Silva, R. & Ferreira, V. 2012. Helminth parasite communities of allopatric populations of the frog *Leptodactylus podicipinus* from Pantanal, Brazil. *Journal of Helminthology*, 88:13–19. https://doi.org/10.1017/s0022149x12000557

Campião, K. M., de Aquino Ribas, A. C., Morais, D. H., da Silva, R. J. & Tavares, L. E. R. 2015. How many parasites species a frog might have? Determinants of parasite diversity in South American anurans. *PLOS One*, 10, e0140577. https://doi.org/10.1371/journal.pone.0140577

Canel, D., Levy, E., Alarcos, A. J., Braicovich, P. E., Cantatore, D. M. P., Irigoitia, M. M., ... Timi, J. T. 2019. Distribution patterns of two species of *Corynosoma* (Acanthocephala: Polymorphidae) in fishes from Southwestern Atlantic. *Parasitology Research*, 118:2831–2841. https://doi.org/10.1007/s00436-019-06440-5

Capinha, C., Essl, F., Seebens, H., Moser, D. & Pereira, H. M. 2015. The dispersal of alien species redefines biogeography in the Anthropocene. *Science*, 348:1248–1251. https://doi.org/10.1126/science.aaa8913

Carpenter, B., Gelman, A., Hoffman, M., Lee, D., Goodrich, B., Betancourt, M., ... Ridell, A. 2017. Stan: a probabilistic programming language. *Journal of Statistical Software*, 76:1–32. https://doi.org/10.18637/jss.v076.i01

Carreno, R. & Nadler, S. A. 2003. Phylogenetic analysis of the Metastrongyloidea (Nematoda: Strongylida) inferred from ribosomal RNA gene sequences. *Journal of Parasitology*, 89:965–973. https://doi.org/10.1645/ge-76r

Castillo, C., Lobos, G., González-Acuña, D., Moreno, L., González, C. E. & Landaeta-Aqueveque, C. 2017. First parasitological study of the African clawed frog (*Xenopus laevis*, Amphibia) in Chile. *Revista Brasileira de Parasitologia Veterinária*, 26:243–247. https://doi.org/10.1590/s1984-29612017029

Ceballos, G., Ehrlich, P. R., Barnosky, A. D., García, A., Pringle, R. M. & Palmer, T. M. 2015. Accelerated modern human-induced species losses: entering the sixth mass extinction. *Science Advances*, 1, e1400253. https://doi.org/10.1126/sciadv.1400253

Chaabane, A., Verneau, O. & du Preez, L. H. 2019. *Indopolystoma* n. gen. (Monogenea, Polystomatidae) with the description of three new species and reassignment of eight known *Polystoma* species from Asian frogs (Anura, Rhacophoridae). *Parasite*, 26, art. 67. https://doi.org/10.1051/parasite/2019067

Chan, P. P. & Lowe, T. M. 2019. tRNAscan-SE: searching for tRNA genes in genomic sequences. *Methods in Molecular Biology*, 1962:1–14. https://doi.org/10.1007/978-1-4939-9173-0_1

Chen, S., Zhou, Y., Chen, Y. & Gu, J. 2018. fastp: an ultra-fast aill-in-one FASTQ preprocessor. *Bioinformatics*, 34:i884–i890. https://doi.org/10.1093/bioinformatics/bty560

Chernomor, O., von Haeseler, A. & Minh, B. Q. 2016. Terrace aware data structure for phylogenomic inference from supermatrices. *Systematic Biology*, 65:997–1008. https://doi.org/10.1093/sysbio/syw037

Chinchio, E., Crotta, M., Romeo, C., Drewe, J. A., Guitian, J. & Ferrari, N. 2020. Invasive alien species and disease risk: an open challenge in public and animal health. *PLOS Pathogens*, 16, e1008922. https://doi.org/10.1371/journal.ppat.1008922

Christin, M.-S., Gendron, A. D., Brousseau, P., Ménard, L., Marcogliese, D. J., Cyr, D., ... Fournier, M. 2003. Effects of agricultural pesticides on the immune system of *Rana pipiens* and on its resistance to parasitic infection. *Environmental Toxicology and Chemistry*, 22:1127–1133. https://doi.org/10.1002/etc.5620220522

Clarke, K. R., Somerfield, P. J. & Chapman, M. G. 2006. On resemblance measures for ecological studies, including taxonomic dissimilarities and a zero-adjusted Bray–Curtis coefficient for denuded assemblages. *Journal of Experimental Marine Biology and Ecology*, 330:55–80. https://doi.org/10.1016/j.jembe.2005.12.017

Clavero, M., Nores, C., Kubersky-Piredda, S., & Centeno-Cuadros, A. 2016. Interdisciplinarity to reconstruct historical introductions: solving the status of cryptogenic crayfish. *Biological Reviews*, 91:1036–1049. https://doi.org/10.1111/brv.12205

Coates, A., Barnett, L. K., Hoskin, C. & Phillips, B. L. 2017. Living on the edge: parasite prevalence changes dramatically across a range edge in an invasive gecko. *The American Naturalist*, 189:178–183. https://doi.org/10.1086/689820

Cohen, N., Effridge, N. J., Parsons, S. C. V., Rollins-Smith, L. A., Nagata, S. & Albright, D. 1984. Identification and treatment of a lethal nematode (*Capillaria xenopodis*) infestation in the South African frog, *Xenopus laevis*. *Developmental and Comparative Immunology*, 8:739–741

Cohn, L. 1906. Zur Anatomie zweier Cestoden. *Zentralblatt für Bakteriologie, Parasitenkunde und Infektionskrankheiten*, 40:362–367

Comas, M. & Ribas, A. 2013. Why are the prevalence and diversity of helminths in the endemic Pyrenean brook newt *Calotriton asper* (Amphibia, Salamandridae) so low? *Journal of Helminthology*, 89:175–181. https://doi.org/10.1017/s0022149x13000710

Cone, D. K., Marcogliese, D. J. & Watt, W. D. 1993. Metazoan parasite communities of yellow eels (*Anguilla rostrata*) in acidic and limed rivers of Nova Scotia. *Canadian Journal of Zoology*, 71:177–184. https://doi.org/10.1139/z93-024

Cook, J. A., Galbreath, K. E., Bell, K. C., Campbell, M. L., Carrière, S., Colella, J. P., ... Hoberg, E. P. 2017. The Beringian Coevolution Project: holistic collections of mammals and associated parasites reveal novel perspectives on evolutionary and environmental change in the North. *Arctic Science*, 3:585–617. https://doi.org/10.1139/as-2016-0042

Coon, C. A. C. & Martin, L. B. 2014. Patterns of haemosporidian prevalence along a range expansion in introduced Kenyan house sparrows *Passer domesticus*. *Journal of Avian Biology*, 45:34–42. https://doi.org/10.1111/j.1600-048X.2013.00235.x

Cosgrove, G. E. & Jared, D. W. 1974. Diseases and parasites of *Xenopus*, the Clawed Toad. In: Amborski, R. L., Hood, M. A. & Miller, R. R., eds. *Conference proceedings*. Gulf Coast Regional Symposium on Diseases of Aquatic Animals, Center for Wetland Resources. Baton Rouge, LA: Louisiana State University. pp. 225–242.

Cosgrove, G. E. & Jared, D. W. 1977. Treatment of skin-invading capillariid nematode in a colony of South African Clawed Frog (*Xenopus laevis*). *Laboratory Animal Science*, 27:526–526

Courant, J., Adil, L., de Kegel, B., Adriaens, D. & Herrel, A. 2019a. Conserved growth rate and age structure of *Xenopus laevis* in the edge and core of an expanding population. *Biological Journal of the Linnean Society*, 128:122–129. https://doi.org/10.1093/biolinnean/blz088

Courant, J., Secondi, J., Bereiziat, V. & Herrel, A. 2017. Resources allocated to reproduction decrease at the range edge of an expanding population of an invasive amphibian. *Biological Journal of the Linnean Society*, 122:157–165. https://doi.org/10.1093/biolinnean/blx048

Courant, J., Secondi, J., Guillemet, L., Vollette, E. & Herrel, A. 2019b. Rapid changes in dispersal on a small spatial scale at the range edge of an expanding population. *Evolutionary Ecology*, 33:599–612. https://doi.org/10.1007/s10682-019-09996-x

Courant, J., Vollette, E., Secondi, J. & Herrel, A. 2018. Changes in the aquatic macroinvertebrate communities throughout the expanding range of an invasive anuran. *Food Webs*, 17, e00098. https://doi.org/10.1016/j.fooweb.2018.e00098

Crayon, J. J. 2005. Species account: *Xenopus laevis*. In: Lannoo, M. J., ed. *Amphibian declines: the conservation status of United States species*. Berkeley: University of California Press. pp. 522–525.

Criscione, C. D., Cooper, B. & Blouin, M. S. 2006. Parasite genotypes identify source populations of migratory fish more accurately than fish genotypes. *Ecology*, 87:823–828. https://doi.org/10.1890/0012-9658(2006)87[823:pgispo]2.0.co;2

Cronin, J. T. & Reeve, J. D. 2005. Host-parasitoid spatial ecology: a plea for a landscape-level synthesis. *Proceedings of the Royal Society B: Biological Sciences*, 272:2225–2235. https://doi.org/10.1098/rspb.2005.3286

Crous, H. P. & du Preez, L. H. 1997. Morphology of *Gyrdicotylus gallieni* Vercammen-Grandjean, 1960 (Monogenea: Gyrodactylidae) from *Xenopus laevis* (Daudin, 1803). *Proceedings of the Microscopy Society of Southern Africa*, 27:117

Cruz, M. J., Rebelo, R. & Crespo, E. G. 2006. Effects of an introduced crayfish, *Procambarus clarkii*, on the distribution of south-western Iberian amphibians in their breeding habitats. *Ecography*, 29:329–338. https://doi.org/10.1111/j.2006.0906-7590.04333.x

Crystal-Ornelas, R. & Lockwood, J. L. 2020. The 'known unknowns' of invasive species impact measurement. *Biological Invasions*, 22:1513–1525. https://doi.org/10.1007/s10530-020-02200-0

Csárdi, G. & Nepusz, T. 2006. The igraph software package for complex network research. *InterJournal Complex Systems*, 1695:1–9

Daszak, P. 2000. Emerging infectious diseases of wildlife – threats to biodiversity and human health. *Science*, 287:443–449. https://doi.org/10.1126/science.287.5452.443

de Busschere, C., Courant, J., Herrel, A., Rebelo, R., Rödder, D., Measey, G. J. & Backeljau, T. 2016. Unequal contribution of native South African phylogeographic lineages to the invasion of the African clawed frog, *Xenopus laevis*, in Europe. *PeerJ*, 4, e1659. https://doi.org/10.7717/peerj.1659

de Puytorac, P. D. & Grain, J. 1965. Structure et ultrastructure de *Balantidium xenopi* sp. nov. Cilié trichostome parasite du batracien *Xenopus fraseri* Boul. *Protistologica*, 1:29–36

de Villiers, F. A. & Measey, G. J. 2017. Overland movement in African clawed frogs (*Xenopus laevis*): empirical dispersal data from within their native range. *PeerJ*, 5, e4039. https://doi.org/10.7717/peerj.4039

Dick, R. I. 1959. Preliminary notes on the relationships existing between the leech, *Marsupiobdella africana*, the river-crab, *Potamon perlatus*, and the platanna, *Xenopus laevis*, as observed in specimens taken from the Kromboom River in the Cape Province of the Union of South Africa. *Journal of the Scientific Society of Cape Town*, 2:47–49

Dierckxsens, N., Mardulyn, P. & Smits, G. 2017. NOVOPlasty: *de novo* assembly of organelle genomes from whole genome data. *Nuclei Acids Research*, 45, e18. https://doi.org/10.1093/nar/gkw955

Dijkstra, E. W. 1959. A note on two problems in connexion with graphs. *Numerische Mathematik*, 1:269–271. https://doi.org/10.1007/bf01386390

Dlugosch, K. M. & Parker, I. M. 2008. Founding events in species invasions: genetic variation, adaptive evolution, and the role of multiple introductions. *Molecular Ecology*, 17:431–449. https://doi.org/10.1111/j.1365-294X.2007.03538.x

Dollfus, R. P. 1968. Presence insolité chez un urodele et en Afrique du nord d'un *Cephalochlamys* (Cestoda: Pseudophyllidea). *Bulletin du Muséum National d'Histoire Naturelle*, 39:1192–1201

du Preez, L. H., Badets, M., Héritier, L. & Verneau, O. 2017. Tracking platyhelminth parasite diversity from freshwater turtles in French Guiana: first report of *Neopolystoma* Price, 1939 (Monogenea: Polystomatidae) with the description of three new species. *Parasites & Vectors*, 10, art. 53. https://doi.org/10.1186/s13071-017-1986-y

du Preez, L. H., Crous, H. P. & Kok, D. J. 1996. Morphology of an unknown cyclophyllidean cysticercoid found in the Clawed Frog, *Xenopus laevis*. *Proceedings of the Microscopy Society of Southern Africa*, 26:111

du Preez, L. H., Kunene, N., Hanner, R., Giesy, J. P., Solomon, K. R., Hosmer, A. & van der Kraak, G. J. 2009. Population-specific incidence of testicular ovarian follicles in *Xenopus laevis* from South Africa: a potential issue in endocrine testing. *Aquatic Toxicology*, 95:10–16. https://doi.org/10.1016/j.aquatox.2009.07.018

du Preez, L. H., Rahariviololoniaina, L., Verneau, O. & Vences, M. 2019. A new genus of polystomatid parasitic flatworm (Monogenea: Polystomatidae) without free-swimming life stage from the Malagasy poison frogs. *Zootaxa*, 2722:54–68. https://doi.org/10.11646/zootaxa.2722.1.2

du Preez, L. H. & van Wyk, A. 2007. *Bios: an integrated approach to life sciences teaching and learning*. Pretoria: Mediakor.

du Preez, L. H. & Verneau, O. 2020. Eye to eye: classification of conjunctival sac polystomes (Monogenea: Polystomatidae) revisited with the description of three new genera *Apaloneotrema* n. g., *Aussietrema* n. g. and *Fornixtrema* n. g. *Parasitology Research*, 119:4017–4031. https://doi.org/10.1007/s00436-020-06888-w

Duane, S., Kennedy, A. D., Pendleton, B. J. & Roweth, D. 1987. Hybrid Monte Carlo. *Physics Letters B*, 195:216–222. https://doi.org/10.1016/0370-2693(87)91197-x

Dufresnes, C., Santo, L. D., Leuenberger, J., Schuerch, J., Mazepa, G., Grandjean, N., ... Dubey, S. 2017. Cryptic invasion of Italian pool frogs (*Pelophylax bergeri*) across Western Europe unraveled by multilocus phylogeography. *Biological Invasions*, 19:1407–1420. https://doi.org/10.1007/s10530-016-1359-z

Dunn, A. M. & Hatcher, M. J. 2015. Parasites and biological invasions: parallels, interactions, and control. *Trends in Parasitology*, 31:189–199. https://doi.org/10.1016/j.pt.2014.12.003

Dunn, A. M., Torchin, M. E., Hatcher, M. J., Kotanen, P. M., Blumenthal, D. M., Byers, J. E., ... Fox, C. 2012. Indirect effects of parasites in invasions. *Functional Ecology*, 26:1262–1274. https://doi.org/10.1111/j.1365-2435.2012.02041.x

Dunn, P. K. & Smyth, G. K. 2005. Series evaluation of Tweedie exponential dispersion models densities. *Statistics and Computing*, 15:267–280. https://doi.org/10.1007/s11222-005-4070-y

Elephandt, A., Eistetter, I., Fleig, A., Günther, E., Hainich, M., Hepperle, S. & Traub, B. 2000. Hearing threshold and frequency discrimination in the purely aquatic frog *Xenopus laevis* (Pipidae): measurement by means of conditioning. *The Journal of Experimental Biology*, 203:3621–3629

Elkan, E. & Murray, R. W. 1952. A larval trematode infection of the lateral line system of the Toad *Xenopus laevis* (Daudin). *Proceedings of the Zoological Society of London*, 122:121–126. https://doi.org/10.1111/j.1469-7998.1952.tb06314.x

Ellis, E. C., Antill, E. C. & Kreft, H. 2012. All is not loss: plant biodiversity in the Anthropocene. *PLOS One*, 7, e30535. https://doi.org/10.1371/journal.pone.0030535

Ellison, A. M. 2004. Bayesian inference in ecology. *Ecology Letters*, 7:509–520. https://doi.org/10.1111/j.1461-0248.2004.00603.x

Elton, C. 1958. *The ecology of invasions by animals and plants*. London, UK: Methuen.

Engemann, K., Enquist, B. J., Sandel, B., Boyle, B., Jørgensen, P. M., Morueta-Holme, N., ... Svenning, J. C. 2015. Limited sampling hampers ”big data” estimation of species richness in a tropical biodiversity hotspot. *Ecology and Evolution*, 5:807–820. https://doi.org/10.1002/ece3.1405

Erpenbeck, D., Voigt, O., Wörheide, G. & Lavrov, D. V. 2009. The mitochondrial genomes of sponges provide evidence for multiple invasions by Repetitive Hairpin-forming Elements (RHE). *BMC Genomics*, 10, art. 591. https://doi.org/10.1186/1471-2164-10-591

Evans, B. J., Carter, T. F., Tobias, M. L., Kelley, D. B., Hanner, R. & Tinsley, R. C. 2008. A new species of clawed frog (genus *Xenopus*) from the Itombwe Massif, Democratic Republic of the Congo: implications for DNA barcodes and biodiversity conservation. *Zootaxa*, 1780:55–68. https://doi.org/10.11646/zootaxa.1780.1.2

Evans, B. J., Kelley, D. B., Tinsley, R. C., Melnick, D. J. & Cannatella, D. C. 2004. A mitochondrial DNA phylogeny of African clawed frogs: phylogeography and implications for polyploid evolution. *Molecular Phylogenetics and Evolution*, 33:197–213. https://doi.org/10.1016/j.ympev.2004.04.018

Evans, M. & Jang, G. H. 2011. Weak informativity and the information in one prior relative to another. *Statistical Science*, 26:423–439. https://doi.org/10.1214/11-sts357

Feldman, S. H. & Ramirez, M. P. 2014. Molecular phylogeny of *Pseudocapillaroides xenopi* (Moravec *et* Cosgrove, 1982) and development of a quantitative PCR assay for its detection in aquarium sediment. *Journal of the American Association for Laboratory Animal Science*, 53:668–674

Ferguson, R. R. & Appleton, C. C. 1988a. Some aspects of the morphology, population structure and larval biology of *Cephalochlamys namaquensis* (Cestoda: Diphyllidea), a parasite of the Clawed Toad, *Xenopus laevis*. *South African Journal of Zoology*, 23:117–123. https://doi.org/10.1080/02541858.1988.11448087

Ferguson, R. R. & Appleton, C. C. 1988b. The tapeworm *Cephalochlamys namaquensis* (Pseudophyllidea) in a population of Clawed Toad, *Xenopus laevis*, in Natal. *South African Journal of Science*, 84:140

Ferrari, N., Citterio, C. V. & Lanfranchi, P. 2016. Infracommunity crowding as an individual measure of interactive-isolationist degree of parasite communities: disclosing the effects of extrinsic and host factors. *Parasites & Vectors*, 9, art. 88. https://doi.org/10.1186/s13071-016-1371-2

Ferris, V. R. & Ferris, J. M. 1989. Why ecologists need systematics: importance of systematics to ecological research. *Journal of Nematology*, 21, art. 308

Fick, S. E. & Hijmans, R. J. 2017. WorldClim 2: new 1-km spatial resolution climate surfaces for global land areas. *International Journal of Climatology*, 37:4302–4315. https://doi.org/10.1002/joc.5086

Fischer, W., Koch, W. & Elepfandt, A. 2000. Sympatry and hybridization between the clawed frogs *Xenopus laevis laevis* and *Xenopus muelleri* (Pipidae). *Journal of Zoology*, 252:99–107. https://doi.org/10.1111/j.1469-7998.2000.tb00824.x

Fischthal, J. H. & Thomas, J. D. 1968. Digenetic trematodes of amphibians and reptiles from Ghana. *Proceedings of the Helminthological Society of Washington*, 35:1–15

Fitzpatrick, B., Fordyce, J., Niemiller, M. & Reynolds, R. G. 2012. What can DNA tell us about biological invasions? *Biological Invasions*, 14:245–253. https://doi.org/10.1007/s10530-011-0064-1

Folmer, O., Black, M., Hoeh, W., Lutz, R. & Vrijenhoek, R. 1994. DNA primers for amplification of mitochondrial cytochrome *c* oxidase subunit I from diverse metazoan invertebrates. *Molecular Marine Biology and Biotechnology*, 3:294–299

Fouquet, A. 2001. Des clandestins aquatiques. *Zamenis*, 6:10–11

Fouquet, A. & Measey, G. J. 2006. Plotting the course of an African clawed frog invasion in Western France. *Animal Biology*, 56:95–102. https://doi.org/10.1163/157075606775904722

Fu, L., Niu, B., Zhu, Z., Wu, S. & Li, W. 2012. CD-HIT: accelerated for clustering the next generation sequencing data. *Bioinformatics*, 28:3150–3152. https://doi.org/10.1093/bioinformatics/bts565

Fumagalli, L., Taberlet, P., Favre, L. & Hausser, J. 1996. Origin and evolution of homologous repeated sequences in the mitochondrial DNA control region of shrews. *Molecular Biology and Evolution*, 13:31–46. https://doi.org/10.1093/oxfordjournals.molbev.a025568

Furman, B. L., Bewick, A. J., Harrison, T. L., Greenbaum, E., Gvozdik, V., Kusamba, C. & Evans, B. J. 2015. Pan-African phylogeography of a model organism, the African clawed frog *Xenopus laevis*. *Molecular Ecology*, 24:909–925. https://doi.org/10.1111/mec.13076

Gabry, J., Simpson, D., Vehtari, A., Betancourt, M. & Gelman, A. 2019. Visualization in Bayesian workflow. *Journal of the Royal Statictical Society: Series A*, 182:389–402. https://doi.org/10.1111/rssa.12378

Galazzo, D. E., Dayanandan, S., Marcogliese, D. J. & McLaughlin, J. D. 2002. Molecular systematics of some North American species of *Diplostomum* (Digenea) based on rDNA sequence data and comparisons with European congeners. *Canadian Journal of Zoology*, 80:2207–2217. https://doi.org/10.1139/Z02-198

Galbreath, K. E., Toman, H. M., Li, C. & Hoberg, E. P. 2020. When parasites persist: tapeworms survive host extinction and reveal waves of dispersal across Beringia. *Proceedings of the Royal Society B: Biological Sciences*, 287, art. 20201825. https://doi.org/10.1098/rspb.2020.1825

Gelman, A. 2006. Prior distributions for variance parameters in hierarchical models. *Bayesian Analysis*, 1:515–533. https://doi.org/10.1214/06-ba117a

Gelman, A., Goodrich, B., Gabry, J. & Vehtari, A. 2019. R-squared for Bayesian regression models. *The American Statistician*, 73:307–309. https://doi.org/10.1080/00031305.2018.1549100

Gelman, A. & Hill, J. K. 2006. *Data Analysis Using Regression and Multilevel/Hierarchical Models*. New York: Cambridge University Press.

Gelman, A., Jakulin, A., Pittau, M. G. & Su, Y.-S. 2008. A weakly informative default prior distribution for logistic and other regression models. *The Annals of Applied Statistics*, 2:1360–1383. https://doi.org/10.1214/08-aoas191

Gilks, W. R., Richardson, S. & Spiegelhalter, D. J., eds. 1996. *Markov Chain Monte Carlo in Practice*. London: Chapman & Hall.

Gómez, A. & Nichols, E. 2013. Neglected wild life: parasitic biodiversity as a conservation target. *International Journal for Parasitology: Parasites and Wildlife*, 2:222–227. https://doi.org/10.1016/j.ijppaw.2013.07.002

Greiner, S., Lehwark, P. & Bock, R. 2019. OrganellarGenomeDRAW (OGDRAW) version 1.3.1: expanded toolkit for the graphical visualization of organellar genomes. *Nucleic Acids Research*, 47:W59–W64. https://doi.org/10.1093/nar/gkz238

Grohovaz, G. S., Harley, E. & Fabian, B. 1996. Significant mitochondrial DNA sequence divergence in natural populations of *Xenopus laevis* (Pipidae) from South Africa. *Herpetologica*, 52:247–253. https://doi.org/10.1080/11250003.2013.847502

Gruber, A. R., Lorenz, R., Bernhart, S. H., Neuböck, R. & Hofacker, I. L. 2008. The Vienna RNA Websuite. *Nucleic Acids Research*, 36:W70–W74. https://doi.org/10.1093/nar/gkn188

Gu, X., Fu, Y. X. & Li, W. H. 1995. Maximum likelihood estimation of the heterogeneity of substitution rate among nucleotide sites. *Molecular Biology and Evolution*, 12:546–557. https://doi.org/10.1093/oxfordjournals.molbev.a040235

Guindon, S., Dufayard, J. F., Lefort, V., Anisimova, M., Hordijk, W. & Gascuel, O. 2010. New algorithms and methods to estimate maximum-likelihood phylogenies: assessing the performance of PhyML 3.0. *Systematic Biology*, 59:307–321. https://doi.org/10.1093/sysbio/syq010

Gundale, M. J., Pauchard, A., Langdon, B., Peltzer, D. A., Maxwell, B. D. & Nuñez, M. A. 2014. Can model species be used to advance the field of invasion ecology? *Biological Invasions*, 16:591–607. https://doi.org/10.1007/s10530-013-0610-0

Guo, Q. & Ricklefs, R. E. 2010. Domestic exotics and the perception of invasibility. *Diversity and Distributions*, 16:1034–1039. https://doi.org/10.1111/j.1472-4642.2010.00708.x

Gupta, V. & Bakshi, R. 1984. Nematode parasites of fishes IV. On two new ascarids, *Ascaridia seenghali* n. sp. and *Paraquimperia xenentodonia* n. sp., from freshwater fishes of India. *Indian Journal of Helminthology*, 36:55–60

Gurdon, J. B. & Hopwood, N. 2000. The introduction of *Xenopus laevis* into developmental biology: of empire, pregnancy testing and ribosomal genes. *The International Journal of Developmental Biology*, 44:43–50 http://www.ijdb.ehu.es/web/descarga/paper/10761846

Hahn, C., Bakke, T. A., Bachmann, L., Weiss, S. & Harris, P. D. 2011. Morphometric and molecular characterization of *Gyrodactylus teuchis* Lautraite, Blanc, Thiery, Daniel & Vigneulle, 1999 (Monogenea: Gyrodactylidae) from an Austrian brown trout population. *Parasitology International*, 60:480–487. https://doi.org/10.1016/j.parint.2011.08.016

Hahn, C., Weiss, S. J., Stojanovski, S. & Bachmann, L. 2015. Co-speciation of the ectoparasite *Gyrodactylus teuchis* (Monogenea, Platyhelminthes) and its salmonid hosts. *PLOS One*, 10, e0127340. https://doi.org/10.1371/journal.pone.0127340

Halajian, A., Bursey, C. R., Goldberg, S. R. & Luus-Powell, W. 2013. Helminths of six species of anurans from the Republic of South Africa: *Amietophrynus garmani*, *Amietophrynus gutturalis*, *Amietophrynus maculatus*, *Schismaderma carens* (Bufonidae), *Amietia angolensis*, and *Strongylopus grayii* (Pyxicephalidae), with a review of South African anuran helminths. *Comparative Parasitology*, 80:80–95. https://doi.org/10.1654/4599.1

Hamann, M., González, C. & Kehr, A. 2006. Helminth community structure of the oven frog *Leptodactylus latinasus* (Anura, Leptodactylidae) from Corrientes, Argentina. *Acta Parasitologica*, 51:294–299. https://doi.org/10.2478/s11686-006-0045-1

Hanek, G. & Molnar, K. 1974. Parasites of freshwater and anadromous fishes from Matamek River system, Quebec. *Journal of the Fisheries Research Board of Canada*, 31:1135–1139

Hanek, G. & Threlfall, W. 1970. Metazoan parasites of the American eel (*Anguilla rostrata* (LeSueur)) in Newfoundland and Labrador. *Canadian Journal of Zoology*, 48:597–600

Harris, P. & Tinsley, R. C. 1987. The biology of *Gyrdicotylus gallieni* (Gyrodactylidea), an unusual vivparous monogenean from the African Clawed Toad, *Xenopus laevis*. *Proceedings of the Zoological Society of London*, 212:325–346. https://doi.org/10.1111/j.1469-7998.1987.tb05993.x

Harrison, X. A., Donaldson, L., Correa-Cano, M. E., Evans, J., Fisher, D. N., Goodwin, C. E., ... Inger, R. 2018. A brief introduction to mixed effects modelling and multi-model inference in ecology. *PeerJ*, 6, e4794. https://doi.org/10.7717/peerj.4794

Hartson, R. B., Orlofske, S. A., Melin, V. E., Dillon, R. T. & Johnson, P. T. J. 2011. Land use and wetland spatial position jointly determine amphibian parasite communities. *EcoHealth*, 8:485–500. https://doi.org/10.1007/s10393-011-0715-9

Hasegawa, M., Kishino, H. & Yano, T. 1985. Dating of the human-ape splitting by a molecular clock of mitochondrial DNA. *Journal of Molecular Evolution*, 22:160–174. https://doi.org/10.1007/BF02101694

Heger, T. & Jeschke, J. M. 2014. The enemy release hypothesis as a hierarchy of hypotheses. *Oikos*, 123:741–750. https://doi.org/10.1111/j.1600-0706.2013.01263.x

Hering-Hagenbeck, S. F. B. N. & Boomker, J. 2000. A check-list on the nematode parasites of South African Serpentes (snakes) and Sauria (lizards). *Onderstepoort Journal of Veterinary Research*, 67:1–13

Héritier, L., Badets, M., du Preez, L. H., Aisien, M. S., Lixian, F., Combes, C. & Verneau, O. 2015. Evolutionary processes involved in the diversification of chelonian and mammal polystomatid parasites (Platyhelminthes, Monogenea, Polystomatidae) revealed by palaeoecology of their hosts. *Molecular Phylogenetics and Evolution*, 92:1–10. https://doi.org/10.1016/j.ympev.2015.05.026

Héritier, L., Valdeón, A., Sadaoui, A., Gendre, T., Ficheux, S., Bouamer, S., ... Verneau, O. 2017. Introduction and invasion of the red-eared slider and its parasites in freshwater ecosystems of Southern Europe: risk assessment for the European pond turtle in wild environments. *Biodiversity and Conservation*, 26:1817–1843. https://doi.org/10.1007/s10531-017-1331-y

Héritier, L., Verneau, O., Smith, K. G., Coetzer, C. & du Preez, L. H. 2018. Demonstrating the value and importance of combining DNA barcodes and discriminant morphological characters for polystome taxonomy (Platyhelminthes, Monogenea). *Parasitology International*, 67:38–46. https://doi.org/10.1016/j.parint.2017.03.002

Hill, J. E., Lawson, K. M. & Tuckett, Q. M. 2017. First record of a reproducing population of the African clawed frog *Xenopus laevis* Daudin, 1802 in Florida (USA). *BioInvasions Records*, 6:87–94. https://doi.org/10.3391/bir.2017.6.1.14

Hiller, A. & Lessios, H. A. 2017. Phylogeography of *Petrolisthes armatus*, an invasive species with low dispersal ability. *Scientific Reports*, 7, 3359. https://doi.org/10.1038/s41598-017-03410-8

Hoang, D. T., Chernomor, O., von Haeseler, A., Minh, B. Q. & Vinh, L. S. 2018. UFBoot2: improving the ultrafast bootstrap approximation. *Molecular Biology and Evolution*, 35:518–522. https://doi.org/10.1093/molbev/msx281

Hofacker, I. L., Fekete, M. & Stadler, P. F. 2002. Secondary structure prediction for aligned RNA sequences. *Journal of Molecular Biology*, 319:1059–1066. https://doi.org/10.1016/S0022-2836(02)00308-X

Hoffman, M. D. & Gelman, A. 2014. The No-U-Turn Sampler: adaptively setting path lengths in Hamiltonian Monte Carlo. *The Journal of Machine Learning Research*, 15:1593–1623

Hope, R. M. 2013. Rmisc: Ryan Miscellaneous. R Package version 1.5. https://doi.org/https://CRAN.R-project.org/package=Rmisc

Huang, Y., Niu, B., Gao, Y., Fu, L. & Li, W. 2010. CD-HIT Suite: a web server for clustering and comparing biological sequences. *Bioinformatics*, 26:680–682. https://doi.org/10.1093/bioinformatics/btq003

Hutchinson, M. C., Cagua, E. F., Balbuena, J. A., Stouffer, D. B., Poisot, T. & Fitzjohn, R. 2017. paco: implementing Procrustean approach to cophylogeny in R. *Methods in Ecology and Evolution*, 8:932–940. https://doi.org/10.1111/2041-210x.12736

Huyse, T., Buchmann, K. & Littlewood, D. T. J. 2008. The mitochondrial genome of *Gyrodactylus derjavinoides* (Platyhelminthes: Monogenea): a mitogenomic approach for *Gyrodactylus* species and strain identification. *Gene*, 417:27–34. https://doi.org/10.1016/j.gene.2008.03.008

Huyse, T., Oeyen, M., Larmuseau, M. H. D. & Volckaert, F. A. M. 2017. Co-phylogeographic study of the flatworm *Gyrodactylus gondae* and its goby host *Pomatoschistus minutus*. *Parasitology International*, 66:119–125. https://doi.org/10.1016/j.parint.2016.12.008

Huyse, T., Plaisance, L., Webster, B. L., Mo, T. A., Bachmann, L. & Littlewood, D. T. J. 2007. The mitochondrial genome of *Gyrodactylus salaris* (Platyhelminthes: Monogenea), a pathogen of Atlantic salmon (*Salmo salar*). *Parasitology*, 134:739–747. https://doi.org/10.1017/S0031182006002010

Huyse, T., Vanhove, M. P. M., Mombaerts, M., Volckaert, F. A. M. & Verreycken, H. 2015. Parasite introduction with an invasive goby in Belgium: double trouble? *Parasitology Research*, 114:2789–2793. https://doi.org/10.1007/s00436-015-4544-6

Ihlow, F., Courant, J., Secondi, J., Herrel, A., Rebelo, R., Measey, G. J., ... Rödder, D. 2016. Impacts of climate change on the global invasion potential of the African clawed frog *Xenopus laevis*. *PLOS One*, 11, e0154869. https://doi.org/10.1371/journal.pone.0154869

Ivanova, N. V., Dewaard, J. R. & Hebert, P. D. N. 2006. An inexpensive, automation-friendly protocol for recovering high-quality DNA. *Molecular Ecology Notes*, 6:998–1002. https://doi.org/10.1111/j.1471-8286.2006.01428.x

Ivashkin, V. M. & Khromova, L. A. 1976. Cucullanata and Gnathostomata of animals and man and the diseases caused by them. Vol. 27, *Osnovy Nematodologii*. Moskow: Nauka. pp. 436.

Jabbar, A., Fong, R. W. J., Kok, K. W., Lopata, A. L., Gasser, R. B. & Beveridge, I. 2013. Molecular characterization of anisakid nematode larvae from 13 species of fish from Western Australia. *International Journal of Food Microbiology*, 161:247–253. https://doi.org/10.1016/j.ijfoodmicro.2012.12.012

Jackson, H. C. & Tinsley, R. C. 1988. Environmental influences on egg production by the monogenean *Protopolystoma xenopodis*. *Parasitology*, 97:115–128. https://doi.org/10.1017/S0031182000066798

Jackson, J. A. 2000. Two new *Falcaustra* Lane, 1915 species (Nematoda: Kathlaniidae) from African pipids (Anura). *Journal of Natural History*, 34:663–677. https://doi.org/10.1080/002229300299336

Jackson, J. A. & Tinsley, R. C. 1995a. Evolutionary relationships, host range and geographical distribution of *Camallanus* Railliet & Henry, 1915 species (Nematoda: Camallaninae) from clawed toads of the genus *Xenopus* (Anura: Pipidae). *Systematic Parasitology*, 32:1–21. https://doi.org/10.1007/BF00009463

Jackson, J. A. & Tinsley, R. C. 1995b. Representatives of *Batrachocamallanus* n. g. (Nematoda: Procamallaninae) from *Xenopus* spp. (Anura: Pipidae): geographical

distribution, host range and evolutionary relationships. *Systematic Parasitology*, 31:159–188. https://doi.org/10.1007/BF00009115

Jackson, J. A. & Tinsley, R. C. 1997. The taxonomic status, host range and geographic distribution of *Dollfuschella* Vercammen-Grandjean, 1960 (Digenea: Halipeginae) from *Xenopus* spp. (Anura: Pipidae). *Systematic Parasitology*, 36:1–11. https://doi.org/10.1023/A:1005716503218

Jackson, J. A. & Tinsley, R. C. 1998a. Incompatibility of *Protopolystoma xenopodis* (Monogenea: Polystomatidae) with an octoploid *Xenopus* species from southern Rwanda. *International Journal for Parasitology*, 28:1195–1199. https://doi.org/10.1016/s0020-7519(98)00065-4

Jackson, J. A. & Tinsley, R. C. 1998b. Paramphistome digeneans from *Xenopus* species (Pipidae) in Africa: taxonomy, host-specificity and biogeography. *Systematic Parasitology*, 40:143–160. https://doi.org/10.1023/A:1005936429562

Jackson, J. A. & Tinsley, R. C. 2001a. Host-specificity and distribution of cephalochlamydid cestodes: correlation with allopolyploid evolution of pipid anuran hosts. *Journal of Zoology*, 254:405–419. https://doi.org/10.1017/S0952836901000905

Jackson, J. A. & Tinsley, R. C. 2001b. *Protopolystoma xenopodis* (Monogenea) primary and secondary infections in *Xenopus laevis*. *Parasitology*, 123:455–463. https://doi.org/10.1017/s0031182001008745

Jackson, J. A. & Tinsley, R. C. 2005. Geographic and within-population structure in variable resistance to parasite species and strains in a vertebrate host. *International Journal for Parasitology*, 25:29–37. https://doi.org/10.1016/j.ijpara.2004.10.017

Jackson, P. B. B. 1978. Health and disease in aquaculture. *Journal of the South African Veterinary Association*, 49:57–59

Jakob, E. M., Marshall, S. D. & Uetz, G. W. 1996. Estimating fitness: a comparison of body condition indices. *Oikos*, 77:61–67. https://doi.org/10.2307/3545585

Jeschke, J. M. 2014. General hypotheses in invasion ecology. *Diversity and Distributions*, 20:1229–1234. https://doi.org/10.1111/ddi.12258

Jia, W.-Z., Yan, H.-B., Guo, A.-J., Zhu, X.-Q., Wang, Y.-C., Shi, W.-G., ... Cai, X.-P. 2010. Complete mitochondrial genomes of *Taenia multiceps*, *T. hydatigena* and *T. pisiformis*: additional molecular markers for a tapeworm genus of human and animal health significance. *BMC Genomics*, 11, art. 447. https://doi.org/10.1186/1471-2164-11-447

Jørgensen, B. 1997. *The Theory of Dispersion Models*. London: Chapman & Hall.

Jovani, R. & Tella, J. L. 2006. Parasite prevalence and sample size: misconceptions and solutions. *Trends in Parasitology*, 22:214–218. https://doi.org/10.1016/j.pt.2006.02.011

Jühling, F., Pütz, J., Bernt, M., Donath, A., M., M., Florentz, C. & Stadler, P. F. 2012. Improved systematic tRNA gene annotation allows new insights into the evolution of mitochondrial tRNA structures and into the mechanisms of mitochondrial genome rearrangements. *Nucleic Acids Research*, 40:2833–2845. https://doi.org/10.1093/nar/gkr1131

Junker, K., Boomker, J., Govender, D. & Mutafchiev, Y. 2019. Nematodes found in Nile crocodiles in the Kruger National Park, South Africa, with redescriptions of *Multicaecum agile* (Wedl, 1861) (Heterocheilidae) and *Camallanus kaapstaadi* Southwell & Kirshner, 1937 (Camallanidae). *Systematic Parasitology*, 96:381–398. https://doi.org/10.1007/s11230-019-09856-w

Kalous, L., Musil, J., Petrtỳl, M., Vajglová, T., Romočuskỳ, Š. & Bušta, L. 2013. The danger in the anglers' bucket: qualitative and quantitative insight into bait fish market in Prague (Czech Republic). *Acta Societatis Zoologicae Bohemicae*, 77:27–35

Kalyaanamoorthy, S., Minh, B. Q., Wong, T. K. F., von Haeseler, A. & Jermiin, L. S. 2017. ModelFinder: fast model selection for accurate phylogenetic estimates. *Nature Methods*, 14:587–589. https://doi.org/10.1038/nmeth.4285

Kamiya, T., O'Dwyer, K., Nakagawa, S. & Poulin, R. 2014. What determines species richness of parasitic organisms? A meta-analysis across animal, plant and fungal hosts. *Biological Reviews*, 89:123–134. https://doi.org/10.1111/brv.12046

Kang, S., Kim, J., Lee, J., Kim, S., Min, G.-S. & Park, J.-K. 2012. The complete mitochondrial genome of an ectoparasitic monopisthocotylean fluke *Benedenia hoshinai* (Monogenea: Platyhelminthes). *Mitochondrial DNA*, 23:176–178. https://doi.org/10.3109/19401736.2012.668900

Karlsen, B. O., Emblem, Å., Jørgensen, T. E., Klingan, K. A., Nordeide, J. T., Moum, T. & Johansen, S. D. 2014. Mitogenome sequence variation in migratory and stationary ecotypes of North-east Atlantic cod. *Marine Genomics*, 15:103–108. https://doi.org/10.1016/j.margen.2014.01.001

Karve, J. N. 1941. Some parasitic nematodes of fishes. I. *Journal of the University of Bombay*, 10:9–42

Katoh, K., Rozewicki, J. & Yamada, K. D. 2017. MAFFT online service: multiple sequence alignment, interactive sequence choice and visualization. *Briefings in Bioinformatics*, 20:1160–1166. https://doi.org/10.1093/bib/bbx108

Katoh, K. & Standley, D. M. 2013. MAFFT multiple sequence alignment software version 7: improvements in performance and usability. *Molecular Biology and Evolution*, 30:772–780. https://doi.org/10.1093/molbev/mst010

Katoh, K. & Toh, H. 2008. Improved accuracy of multiple ncRNA alignment by incorporation structural information into a MAFFT-based framework. *BMC Bioinformatics*, 9, art. 212. https://doi.org/10.1186/1471-2105-9-212

Kawato, S., Kobayashi, K., Shirakashi, S., Yanagi, S., Fukuda, Y., Yamashita, H., ... Kondo, H. 2019. Phylogenetic analysis with complete mitochondrial genome sequences of *Benedenia seriolae* specimens derived from Japanese *Seriola* spp. *Fish Pathology*, 54:27–33. https://doi.org/10.3147/jsfp.54.27

Keane, R. M. & Crawley, M. J. 2002. Exotic plant invasions and the enemy release hypothesis. *Trends in Ecology and Evolution*, 17:164–170. https://doi.org/10.1016/S0169-5347(02)02499-0

Kelehear, C., Brown, G. P. & Shine, R. 2012. Rapid evolution of parasite life history traits on an expanding range-edge. *Ecology Letters*, 15:329–337. https://doi.org/10.1111/j.1461-0248.2012.01742.x

Kenny, N. J., Noreña, C., Damborenea, C. & and, C. G. 2019. Probing recalcitrant problems in polyclad evolution and systematics with novel mitochondrial genome resources. *Genomics*, 111:343–355. https://doi.org/10.1016/j.ygeno.2018.02.009

Kilian, J. V., Klauda, R. J., Widman, S., Kashiwagi, M., Bourquin, R., Weglein, S. & Schuster, J. 2012. An assessment of a bait industry and angler behavior as a vector of invasive species. *Biological Invasions*, 14:1469–1481. https://doi.org/10.1007/s10530-012-0173-5

Kim, J.-H., Lee, B.-S. & Jung, S.-J. 2020a. The complete mitochondrial genome of *Neoheterobothrium hirame* (Platyhelminthes: Monogenea) from olive flounder (*Paralichthys olivaceus*). *Mitochondrial DNA Part B*, 5:1408–1409. https://doi.org/10.1080/23802359.2020.1735953

Kim, K.-H., Nam, U.-H., Kim, H. & Whang, I. 2020b. The complete mitochondrial genome of *Mazocraeoides gonialosae* (Platyhelminthes: Monogenea) from dotted gizzard shad, *Konosirus punctatus*. *Mitochondrial DNA Part B*, 5:1570–1572. https://doi.org/10.1080/23802359.2020.1742606

Kimura, M. 1981. Estimation of evolutionary distances between homologous nucleotide sequences. *Proceedings of the National Academy of Sciences USA*, 78:454–458. https://doi.org/10.1073/pnas.78.1.454

King, K. C., McLaughlin, J. D., Boily, M. & Marcogliese, D. J. 2010. Effects of agricultural landscape and pesticides on parasitism in native bullfrogs. *Biological Conservation*, 143:302–310. https://doi.org/10.1016/j.biocon.2009.10.011

King, K. C., McLaughlin, J. D., Gendron, A. D., Pauli, B. D., Giroux, I., Rondeau, B., ... Marcogliese, D. J. 2007. Impacts of agriculture on the parasite communities of

northern leopard frogs (*Rana pipiens*) in southern Quebec, Canada. *Parasitology*, 134:2063–2080. https://doi.org/10.1017/s0031182007003277

King, P. H. & van As, J. G. 1992. Scanning electron microscopy of *Diplostomum* (*Tylodelphys*) *xenopodis* (Southwell & Kirshner, 1937) (Trematoda: Diplostomatidae). *Electron Microscopy Society of Southern Africa*, 22:127–128

King, P. H. & van As, J. G. 1997. Description of the adult and larval stages of *Tylodelphys xenopi* (Trematoda: Diplostomidae) from Southern Africa. *The Journal of Parasitology*, 83:287–295. https://doi.org/10.2307/3284458

King, P. H. & van As, J. G. 2000. Morphology and life history of *Petasiger variospinosus* (Trematoda: Echinostomatidae) in the Free State, South Africa. *The Journal of Parasitology*, 86:312–318. https://doi.org/10.1645/0022-3395(2000)086[0312:MALHOP]2.0.CO;2

Kmentová, N., Koblmüller, S., Van Steenberge, M., Raeymaekers, J. A., Artois, T., De Keyzer, E. L. R., ... Vanhove, M. P. 2020. Weak population structure and recent demographic expansion of the monogenean parasite *Kapentagyrus* spp. infecting clupeid fishes of Lake Tanganyika, East Africa. *International Journal for Parasitology*, 50:471–486. https://doi.org/10.1016/j.ijpara.2020.02.002

Kmentová, N., Van Steenberge, M., Raeymaekers, J. A. M., Kolbmüller, S., Hablützel, P., Bukinga, F. M., ... Vanhove, M. P. 2018. Monogenean parasites of sardines in Lake Tanganyika: diversity, origin and intraspecific variability. *Contributions to Zoology*, 87:105–132. https://doi.org/10.1163/18759866-08702004

Kmentová, N., Van Steenberge, M., van den Audenaerde, D. F. E. T., Nhiwatiwa, T., Bukinga, F. M., N'sibula, T. M., ... Vanhove, M. P. M. 2019. Co-introduction success of monogeneans infecting the fisheries target *Limnothrissa miodon* differs between two non-native areas: the potential of parasites as a tag for introduction pathway. *Biological Invasions*, 21:757–773. https://doi.org/10.1007/s10530-018-1856-3

Kocher, T. D., Thomas, W. K., Meyer, A., Edwards, S. V., Pääbo, S., Villablanca, F. X. & Wilson, A. C. 1989. Dynamics of mitochondrial DNA evolution in animals: amplification and sequencing with conserved primers. *Proceedings of the National Academy of Sciences USA*, 86:6196–6200

Køie, M. 1988. Parasites in European eel *Anguilla anguilla* (L.) from Danish freshwater, brackish and marine localities. *Ophelia*, 29:93–118

Kołodziej-Sobocińska, M., Brzeziński, M., Niemczynowicz, A. & Zalewski, A. 2018. High parasite infection level in non-native invasive species: it is just a matter of time. *Ecography*, 41:1283–1294. https://doi.org/10.1111/ecog.03362

Kruger, J., Basson, L. & van As, J. G. 1991. Redescription of *Trichodina xenopodos* Fantham, 1924 (Ciliophora: Peritrichida), a urinary bladder parasite of *Xenopus laevis laevis* Daudin, 1802, with notes on transmission. *Systematic Parasitology*, 19:43–50. https://doi.org/10.1007/BF00010301

Kruger, N. 2020. *Do vulnerable life stages of Xenopus laevis reduce its invasion potential?* Stellenbosch: Stellenbosch University and Université Claude Bernard Lyon 1. (Thesis – PhD).

Kruger, N. & du Preez, L. H. 2015. Reproductive strategies of the kangaroo leech, *Marsupiobdella africana* (Glossiphoniidae). *International Journal for Parasitology: Parasites and Wildlife*, 4:142–147. https://doi.org/10.1016/j.ijppaw.2015.01.005

Kruger, N., Measey, J., Herrel, A. & Secondi, J. 2019. Anti-predator strategies of the invasive African clawed frog, *Xenopus laevis*, to native and invasive predators in western France. *Aquatic Invasions*, 14:433–443. https://doi.org/10.3391/ai.2019.14.3.03

Kruschke, J. K. 2015. *Doing Bayesian Data Analysis: A Tutorial with R, JAGS, and Stan*. 2nd ed. London: Academic Press.

Kuhn, K., Streit, B. & Schwenk, K. 2008. Conservation of structural elements in the mitochondrial control region of *Daphnia*. *Gene*, 420:107–112. https://doi.org/10.1016/j.gene.2008.05.020

Kung, C. C. 1948. On some new species of spirurids from terrestrial vertebrates, with notes on *Habronema mansioni*, *Physaloptera paradoxa* and *Hartertia zuluensis*. *Journal of Helminthology*, 22:141–161

Kuperman, B. I., Matey, V. E., Fisher, R. N., Ervin, E. L., Warburton, M. L., Bakhireva, L. & Lehman, C. A. 2004. Parasites of the African Clawed Frog, *Xenopus laevis*, in Southern California, U.S.A. *Comparative Parasitology*, 71:229–232. https://doi.org/10.1654/4112

Kuzmin, Y., Tkach, V. V., Snyder, S. D. & Bell, J. A. 2011. *Camallanus* Railliet *et* Henry, 1915 (Nematoda, Camallanidae) from Australian freshwater turtles with descriptions of two new species and molecular differentiation of known taxa. *Acta Parasitologica*, 56:213–226. https://doi.org/10.2478/s11686-011-0015-0

Laetsch, D. R., Heitlinger, E. G., Taraschewski, H., Nadler, S. A. & Blaxter, M. L. 2012. The phylogenetics of Anguillicolidae (Nematoda: Anguillicoloidea), swimbladder parasites of eels. *BMC Evolutionary Biology*, 12:60. https://doi.org/10.1186/1471-2148-12-60

Lafferty, K. D. & Page, C. J. 1997. Predation on the endangered tidewater goby, *Eucyclogobius newberryi*, by the introduced African clawed frog, *Xenopus laevis*, with notes on the frog's parasites. *Copeia*, 1997:589–592. https://doi.org/10.2307/1447564

Landman, W. J., Verneau, O., Raharivololoniaina, L. & du Preez, L. H. 2021. First record of *Metapolystoma* (Monogenea: Polystomatidae) from *Boophis* tree frogs in Madagascar,

with the description of five new species. *International Journal for Parasitology: Parasites and Wildlife*, 14:161–178. https://doi.org/10.1016/j.ijppaw.2021.01.012

Laslett, D. & Canbäck, B. 2008. ARWEN: a program to detect tRNA genes in metazoan mitochondiral nucleotide sequences. *Bioinformatics*, 24:172–175. https://doi.org/10.1093/bioinformatics/btm573

Le, T. H., Blair, D. & McManus, D. P. 2001. Complete DNA sequence and gene organization of the mitochondrial genome of the liverfluke, *Fasciola hepatica* L. (Platyhelminthes; Trematoda). *Parasitology*, 123:609–612. https://doi.org/10.1017/s0031182001008733

Le, T. H., Blair, D. & McManus, D. P. 2002a. Mitochondrial genomes of parasitic flatworms. *Trends in Parasitology*, 18:206–213. https://doi.org/10.1016/s1471-4922(02)02252-3

Le, T. H., Pearson, M. S., Blair, D., Dai, N., Zhang, L. H. & McManus, D. P. 2002b. Complete mitochondrial genomes confirm the distinctiveness of the horse-dog and sheep-dog strains of *Echinococcus granulosus*. *Parasitology*, 124:97–112. https://doi.org/10.1017/s0031182001008976

Lecomte, J.-B., Benoît, H. P., Ancelet, S., Etienne, M.-P., Bel, L. & Parent, E. 2013. Compound Poisson-gamma vs. delta-gamma to handle zero-inflated continuous data under a variable sampling volume. *Methods in Ecology and Evolution*, 4:1159–1166. https://doi.org/10.1111/2041-210X.12122

Lee, C. E. & Gelembiuk, G. W. 2008. Evolutionary origins of invasive populations. *Evolutionary Applications*, 1:427–448. https://doi.org/10.1111/j.1752-4571.2008.00039.x

Lefoulon, E., Bain, O., Bourret, J., Junker, K., Guerrero, R., Cañizales, I., ... Martin, C. 2015. Shaking the tree: multi-locus sequence typing usurps current onchocercid (filarial nematode) phylogeny. *PLOS Neglected Tropical Diseases*, 9, e0004233. https://doi.org/10.1371/journal.pntd.0004233

Legendre, P., Desdevises, Y. & Bazin, E. 2002. A statistical test for host-parasite coevolution. *Systematic Biology*, 51:217–234. https://doi.org/10.1080/10635150252899734

Legendre, P. & Gallagher, E. D. 2001. Ecologically meaningful transformations for ordination of species data. *Oecologia*, 129:271–280. https://doi.org/10.1007/s004420100716

Leigh, J. W. & Bryant, D. 2015. PopART: full-feature software for haplotype network construction. *Methods in Ecology and Evolution*, 6:1110–1116. https://doi.org/10.1111/2041-210x.12410

Leiper, R. T. 1908. An account of some helminths contained in Dr. C.M. Wenyon's collection from the Sudan. *Report of the Wellcome Tropical Research Laboratories at the Gordon Memorial College, Khartoum*, 3:187–199

Lemoine, N. P. 2019. Moving beyond noninformative priors: why and how to choose weakly informative priors in Bayesian analyses. *Oikos*, 128:912–928. https://doi.org/10.1111/oik.05985

Lester, P. J., Bosch, P. J., Gruber, M. A., Kapp, E. A., Peng, L., Brenton-Rule, E. C., ... Wenseleers, T. 2015. No evidence of enemy release in pathogen and microbial communities of common wasps (*Vespula vulgaris*) in their native and introduced range. *PLOS One*, 10, e0121358. https://doi.org/10.1371/journal.pone.0121358

Leung, T. L. F. & Koprivnikar, J. 2019. Your infections are what you eat: how host ecology shapes the helminth parasite communities of lizards. *Journal of Animal Ecology*, 88:416–426. https://doi.org/10.1111/1365-2656.12934

Levinson, G. & Gutman, G. A. 1987. Slipped-strand mispairing: a major mechanism for DNA sequence evolution. *Molecular Biology and Evolution*, 4:203–221. https://doi.org/10.1093/oxfordjournals.molbev.a040442

Li, R., Zhou, C., Ye, S., Men, L., Lui, Y. & Fu, S. 2019. Mitochondrial genome sequencing of the monogenean *Heterobothrium okamotoi* isolated from the tiger puffer *Takifugu rubripes* in North China. *Mitochondrial DNA Part B*, 4:3051–3052. https://doi.org/10.1080/23802359.2019.1666671

Li, T., Yang, J., Li, Y., Cui, Y., Xie, Q., Bu, W. & Hillis, D. M. 2016. A mitochondrial genome of Rhyparochromidae (Hemiptera: Heteroptera) and a comparative analysis of related mitochondrial genomes. *Scientific Reports*, 6, art. 35175. https://doi.org/10.1038/srep35175

Li, W. & Godzik, A. 2006. Cd-hit: a fast program for clustering and comparing large sets of protein or nucleotide sequences. *Bioinformatics*, 22:1658–1659. https://doi.org/10.1093/bioinformatics/btl158

Lillo, F., Dufresnes, C., Faraone, F. P., Lo Valvo, M. & Stöck, M. 2013. Identification and potential origin of invasive clawed frogs *Xenopus* (Anura: Pipidae) in Sicily based on mitochondrial and nuclear DNA. *Italian Journal of Zoology*, 80:566–573. https://doi.org/10.1080/11250003.2013.847502

Lin, Y.-J., Jessop, B. M., Weyl, O. L. F., Iizuka, Y., Lin, S.-H. & Tzeng, W.-N. 2015. Migratory history of African longfinned eel *Anguilla mossambica* from Maningory River, Madagascar: discovery of a unique pattern in otolith Sr:Ca ratios. *Environmental Biology of Fishes*, 98:457–468. https://doi.org/10.1007/s10641-014-0275-2

Littlewood, D. T. J., Rohde, K. & Clough, K. A. 1997. Parasite speciation within or between host species? – Phylogenetic evidence from site-specific polystome monogeneans. *International Journal for Parasitology*, 27:1289–1297. https://doi.org/10.1016/S0020-7519(97)00086-6

Lloyd, M. 1967. Mean crowding. *Journal of Animal Ecology*, 36:1–30. https://doi.org/10.2307/3012

Lobos, G., Cattan, P., Estades, C. & Jaksic, F. M. 2013. Invasive African clawed frog *Xenopus laevis* in southern South America: key factors and predictions. *Studies on Neotropical Fauna and Environment*, 48:1–12. https://doi.org/10.1080/01650521.2012.746050

Lobos, G. & Measey, G. J. 2002. Invasive populations of *Xenopus laevis* (Daudin) in Chile. *Herpetological Journal*, 12:163–168

Lobos, G., Mendez, M. A., Cattan, P. & Jaksic, F. 2014. Low genetic diversity of the successful invasive African clawed frog *Xenopus laevis* (Pipidae) in Chile. *Studies on Neotropical Fauna and Environment*, 49:50–60. https://doi.org/10.1080/01650521.2014.912865

Locke, S. A., Levy, M. S., Marcogliese, D. J., Ackerman, S. & McLaughlin, J. D. 2012. The decay of parasite community similarity in ring-billed gulls *Larus delawarensis* and other hosts. *Ecography*, 35:530–538. https://doi.org/10.1111/j.1600-0587.2011.07244.x

Lorenz, R., Bernhart, S. H., Höner zu Siederdissen, C., Tafer, H., Flamm, C. Stadler, P. F. & Hofacker, I. L. 2011. ViennaRNA package 2.0. *Algorithms for Molecular Biology*, 6, art. 26. https://doi.org/10.1186/1748-7188-6-26

Louppe, V., Courant, J. & Herrel, A. 2017. Differences in mobility at the range edge of an expanding invasive population of *Xenopus laevis* in the west of France. *Journal of Experimental Biology*, 220:278–283. https://doi.org/10.1242/jeb.146589

Louppe, V., Courant, J., Videlier, M. & Herrel, A. 2018. Differences in standard metabolic rate at the range edge versus the center of an expanding invasive population of *Xenopus laevis* in the West of France. *Journal of Zoology*, 305:163–172. https://doi.org/10.1111/jzo.12548

Lowe, T. M. & Chan, P. P. 2016. tRNAscan-SE On-line: integrating search and context for analysis of transfer RNA genes. *Nucleic Acids Research*, 44:W54–W77. https://doi.org/10.1093/nar/gkw413

Lüdecke, D., Makowski, D., Waggoner, P. & Patil, I. 2020. performance: assessment of regression models performance. *CRAN*. https://doi.org/10.5281/zenodo.3952174

Lui, H. & Stiling, P. 2006. Testing the enemy release hypothesis: a review and meta-analysis. *Biological Invasions*, 8:1535–1545. https://doi.org/10.1007/s10530-005-5845-y

Luque, J. L. & Poulin, R. 2007. Metazoan parasite species richness in Neotropical fishes: hotspots and the geography of biodiversity. *Parasitology*, 134:865–878. https://doi.org/10.1017/S0031182007002272

Lymbery, A. J., Morine, M., Kanani, H. G., Beatty, S. J. & Morgan, D. L. 2014. Co-invaders: the effects of alien parasites on native hosts. *International Journal for Parasitology: Parasites and Wildlife*, 3:171–177. https://doi.org/10.1016/j.ijppaw.2014.04.002

MacCracken, J. G. & Stebbings, J. L. 2012. Test of a body condition index with amphibians. *Journal of Herpetology*, 46:346–350. https://doi.org/10.2307/23326905

Macey, J. R., Schulte, J. A., Larson, A. & Papenfuss, T. 1998. Tandem duplication via light-strand synthesis may provide a precursor for mitochondrial genomic rearrangement. *Molecular Biology and Evolution*, 15:71–75

Macnae, W., Rock, L. & Makowski, M. 1973. Platyhelminths from the South African Clawed Toad, or Platanna (*Xenopus laevis*). *Journal of Helminthology*, 47:199–235. https://doi.org/10.1017/S0022149X00023890

Madanire-Moyo, G. N., Luus-Powell, W. J. & Olivier, P. A. S. 2010. Ecology of metazoan parasites of *Clarias gariepinus* (Osteichthyes: Clariidae) from the Nwanedi-Luphephe Dams of the Limpopo River System, South Africa. *African Zoology*, 45:233–243. https://doi.org/10.3377/004.045.0202

Makowski, D., Ben-Shachar, M. & Lüdecke, D. 2019. bayestestR: describing effects and their uncertainty, existence and significance within the Bayesian framework. *Journal of Open Source Software*, 4, art. 1541. https://doi.org/10.21105/joss.01541

Mangiafico, S. 2020. rcompanion: functions to support extension education program evaluation. R package version 2.3.25. https://CRAN.R-project.org/package=rcompanion

Manter, H. W. & Pritchard, M. H. 1964. Mission de zoologie médicale au Maniema (Congo, Leopoldville). *Annales du Musée Royal de l'Afrique Centrale*, 132:75–101

Marcogliese, D. J. & Cone, D. K. 1996. On the distribution and abundance of eel parasites in Nova Scotia: influence of pH. *The Journal of Parasitology*, 82:389–399. https://doi.org/10.2307/3284074

Marr, S. R., Mautz, W. J. & Hara, A. H. 2008. Parasite loss and introduced species: a comparison of the parasites of the Puerto Rican tree frog, (*Eleutherodactylus coqui*), in its native and introduced ranges. *Biological Invasions*, 10:1289–1298. https://doi.org/10.1007/s10530-007-9203-0

Marra, G. & Wood, S. N. 2011. Practical variable selection for generalized additive models. *Computational Statistics & Data Analysis*, 55:2372–2387. https://doi.org/10.1016/j.csda.2011.02.004

Martin, T. G., Wintle, B. A., Rhodes, J. R., Kuhnert, P. M., Field, S. A., Low-Choy, S. J., ... Possingham, H. P. 2005. Zero tolerance ecology: improving ecological inference by modelling the source of zero observations. *Ecology Letters*, 8:1235–1246. https://doi.org/10.1111/j.1461-0248.2005.00826.x

Marzal, A., Ricklefs, R. E., Valkiunas, G., Albayrak, T., Arriero, E., Bonneaud, C., ... Bensch, S. 2011. Diversity, loss, and gain of malaria parasites in a globally invasive bird. *PLOS One*, 6, e21905. https://doi.org/10.1371/journal.pone.0021905

Mashego, S. N. 1989. Nematode parasites of *Barbus species* in Lebowa and Venda, South Africa. *South African Journal of Wildlife Research*, 19:35–37

Mashego, S. N. & Saayman, J. E. 1981. Observations on the prevalence of nematode parasites of the catfish, *Clarias gariepinus* (Burchell, 1822), in Lebowa, South Africa. *South African Journal of Wildlife Research*, 11:46–48

Mayer, M., Shine, R. & Brown, G. P. 2021. Rapid divergence of parasite infectivity and host resistance during a biological invasion. *Biological Journal of the Linnean Society*, 132:861–871. https://doi.org/10.1093/biolinnean/blaa229

Mazzamuto, M. V., Galimberti, A., Cremonesi, G., Pisanu, B., Chapuis, J.-L., Stuyck, J., ... Martinoli, A. 2016. Preventing species invasion: a role for integrative taxonomy? *Integrative Zoology*, 11:214–228. https://doi.org/10.1111/1749-4877.12185

Mbokane, E. M., Theron, J. & Luus-Powel, W. J. 2020. Diversity of parasites from *Xenopus laevis* (Amphibia: Pipidae) and their seasonal rate of infection in selected habitats in the Limpopo Province, South Africa. *Helminthologia*, 57:252–267. https://doi.org/10.2478/helm-2020-0027

Mbokane, E. M., Theron, J. & Luus-Powell, W. J. 2015. Seasonal occurrence of some larval stages of endoparasites in three cyprinids from the Nwanedi-Luphephe dams, the Limpopo River System, South Africa. *Helminthologia*, 52:229–235. https://doi.org/10.1515/helmin-2015-0037

McCarthy, M. A. & Masters, P. 2005. Profiting from prior information in Bayesian analyses of ecological data. *Journal of Applied Ecology*, 42:1012–1019. https://doi.org/10.1111/j.1365-2664.2005.01101.x

McElreath, R. 2020. *Statistical Rethinking: A Bayesian Course with Examples in R and Stan*. 2nd ed. New York: Chapman & Hall/CRC.

McHugh, K. J., Weyl, O. L. F. & Smit, N. J. 2016. Parasites of fishes in the recently inundated ephemeral Lake Liambezi, Namibia. *African Journal of Aquatic Science*, 41:505–509. https://doi.org/10.2989/16085914.2016.1238338

Measey, G. J. 2004. *Xenopus laevis*. In: Minter, L., Burger, M., Harrison, J., Braack, H., Bishop, P. & Knoepfer, D., eds. *Atlas and Red Data Book of the Frogs of South Africa, Lesotho and Swaziland*. Washington, DC: Smithsonian Institution Press. pp. 264–265.

Measey, G. J. 2016. Overland movement in African clawed frogs (*Xenopus laevis*): a systematic review. *PeerJ*, 4, e2474. https://doi.org/10.7717/peerj.2474

Measey, G. J. & Channing, A. 2003. Phylogeography of the genus *Xenopus* in southern Africa. *Amphibia-Reptilia*, 24:321–330. https://doi.org/10.1163/156853803322440781

Measey, G. J. & Davies, S. J. 2011. Struggling against domestic exotics at the southern end of Africa. *Froglog*, 97:28–30

Measey, G. J., Davies, S. J., Vimercati, G., Rebelo, A., Schmidt, W. & Turner, A. 2017. Invasive amphibians in southern Africa: a review of invasion pathways. *Bothalia*, 47, a2117. https://doi.org/10.4102/abc.v47i2.2117

Measey, G. J., Rödder, D., Green, S. L., Kobayashi, R., Lillo, F., Lobos, G., ... Thirion, J. M. 2012. Ongoing invasions of the African clawed frog, *Xenopus laevis*: a global review. *Biological Invasions*, 14:2255–2270. https://doi.org/10.1007/s10530-012-0227-8

Metcalf, M. M. 1923. The opalinid ciliate infusorians. *Bulletin of the United States National Museum*, 120:1–484

Mettrick, D. F. 1963. Some cestodes of reptiles and amphibians from the Rhodesias. *Proceedings of the Zoological Society of London*, 141:239–250. https://doi.org/10.1111/j.1469-7998.1963.tb01610.x

Meyer, L., du Preez, L. H., Bonneau, E., Héritier, L., Quintana, M., Valdeón, A., ... Verneau, O. 2015. Parasite host-switching from the invasive American red-eared slider, *Trachemys scripta elegans*, to the native Mediterranean pond turtle, *Mauremys leprosa*, in natural environments. *Aquatic Invasions*, 10:79–91. https://doi.org/10.3391/ai.2015.10.1.08

Mihaljevic, J. R., Hoye, B. J. & Johnson, P. T. J. 2017. Parasite metacommunities: evaluating the roles of host community composition and environmental gradients in structuring symbiont communities within amphibians. *Journal of Animal Ecology*, 87:354–368. https://doi.org/10.1111/1365-2656.12735

Miller, M. A., Pfeiffer, W. & Schwartz, T. 2010. Creating the CIPRES Science Gateway for inference of large phylogenetic trees. *Conference proceedings*. 2010 Gateway Computing Environments Workshop (GCE): Institute of Electrical and Electronics Engineers.

Mimee, B., Duceppe, M.-O., Véronneau, P.-Y., Lafond-Lapalme, J., Jean, M., Belzile, F. & Bélair, G. 2015. A new method for studying population genetics of cyst nematodes based on Pool-Seq and genomewide allele frequency analysis. *Molecular Ecology Resources*, 15:1356–1365. https://doi.org/10.1111/1755-0998.12412

Minh, B. Q. Schmidt, H. A., Chernomor, O., Schrempf, D., Woodhams, M. D., von Haeseler A. & Lanfear, R. 2020. IQ-TREE 2: new models and efficient methods for phylogenetic inference in the genomic era. *Molocular Biology and Evolution*, 37:1530–1534. https://doi.org/10.1093/molbev/msaa015

Mollaret, I., Jamieson, B. G. M. & Justine, J.-L. 2000. Phylogeny of the Monopisthocotylea and Polyopisthocotylea (Platyhelminthes) inferred from 28S rDNA sequences. *International Journal for Parasitology*, 30:171–185. https://doi.org/10.1016/s0020-7519(99)00197-6

Morais, P. & Reichard, M. 2018. Cryptic invasions: a review. *Science of the Total Environment*, 613–614:1438–1448. https://doi.org/10.1016/j.scitotenv.2017.06.133

Morand, S., Bordes, F., Chen, H. W., Claude, J., Cosson, J. F., Galan, M., ... Ribas, A. 2015. Global parasite and *Rattus* rodent invasions: the consequences for rodent-borne diseases. *Integrative Zoology*, 10:409–423. https://doi.org/10.1111/1749-4877.12143

Moravec, F. 1966a. The finding of the nematode *Paraquimperia tenerrima* (v. Linstow, 1878) from eels *Anguilla anguilla* (L.) in Czechoslovakia. *Folia Parasitologica*, 13:182–186

Moravec, F. 1966b. On the systematics of the genus *Paraquimperia* Baylis, 1934 (Nematoda: Quimperiidae). *Helminthologia*, 7:353–364

Moravec, F. 1994. *Parasitic Nematodes of Freshwater Fishes of Europe*. Prague and Dordrecht, Boston, London: Academia and Kluwer Academic Publishers.

Moravec, F. 2007. Some aspects of the taxonomy and biology of adult spirurine nematodes parasitic in fishes: a review. *Folia Parasitologica*, 54:239–257. https://doi.org/10.14411/fp.2007.033

Moravec, F., Boomker, J. & Taraschewski, H. 2000. *Paraquimperia africana* n. sp. (Nematoda: Quimperiidae), a new intestinal parasite of the eel *Anguilla mossambica* Peters, in South Africa. *The Journal of Parasitology*, 86:113–117. https://doi.org/10.2307/3284919

Moravec, F. & Cosgrove, G. E. 1982. *Pseudocapillaroides xenopi* gen. *et* sp. nov. from the skin of the South African Clawed Frog *Xenopus laevis* Daud. (Nematoda: Capillariidae). *Revue de Zoologie Africaine*, 96:129–137

Moravec, F., Jansen van Rensburg, C. & van As, L. L. 2016. Larvae of *Contracaecum* sp. (Nematoda: Anisakidae) in the threatened freshwater fish *Sandelia capensis* (Anabantidae) in South Africa. *Diseases of Aquatic Organisms*, 120:251–254. https://doi.org/10.3354/dao03033

Moravec, F. & Justine, J.-L. 2006. *Camallanus cotti* (Nematoda: Camallanidae), an introduced parasite of fishes in New Caledonia. *Folia Parasitologica*, 53:287–296. https://doi.org/10.14411/fp.2006.035

Moravec, F., Justine, J.-L., Würzt, J., Taraschewski, H. & Sasal, P. 2006. A new species of *Procamallanus* (Nematoda: Camallanidae) from Pacific eels (*Anguilla* spp.). *The Journal of Parasitology*, 92:130–137. https://doi.org/10.1645/ge-3509.1

Moravec, F., Nie, P. & Guitang, W. 2004. Redescription of *Camallanus hypophthalmichthys* Dogel and Akhmerov, 1959 (Nematoda: Camallanidae) and its first record from fishes in China. *Journal of Parasitology*, 90:1463–1467. https://doi.org/10.1645/ge-3391

Moravec, F., Prokopic, J. & Schlikas, A. V. 1987. The biology of the nematodes of the family Capillariidae, Neveu-Lemaire, 1936. *Folia Parasitologica*, 34:39–56

Moravec, F. & Scholtz, T. 2017. Some nematodes, including two new species, from freshwater fishes in the Sudan and Ethiopia. *Folia Parasitologica*, 64, art. 010. https://doi.org/10.14411/fp.2017.010

Moravec, F. & van As, L. L. 2015. Studies on ascaridid, oxyurid and enoplid nematodes (Nematoda) from fishes of the Okavango River, Botswana. *Folia Parasitologica*, 62, art. 039. https://doi.org/10.14411/fp.2015.039

Morens, D. M., Daszak, P., Markel, H. & Taubenberger, J. K. 2020. Pandemic COVID-19 joins history's pandemic legion. *mBio*, 11, e00812–20. https://doi.org/10.1128/mbio.00812-20

Moyo, D. Z., Chimbira, C. & Yalala, P. 2009. Observations on the helminth parasites of fish in Insukamini dam, Zimbabwe. *Research Journal of Agriculture and Biological Sciences*, 5:782–785

Mueller, J. F. 1934. Parasites of Oneida Lake fishes. Part 4. Additional notes on parasites of Oneida Lake fishes, including descriptions of new species. *Roosevelt Wildlife Annals*, 3:335–373

Nadler, S. A., D'Amelio, S., Fagerholm, H. P., Berland, B. & Paggi, L. 2000. Phylogenetic relationships among species of *Contracaecum* Railliet & Henry, 1912 and *Phocascaris* Høst, 1932 (Nematoda: Ascaridoidea) based on nuclear rDNA sequence data. *Parasitology*, 121:455–463. https://doi.org/10.1017/s0031182099006423

Naidu, T. S. V. 1983. Records of some nematode parasites of fishes of Vidarbha region, Maharashtra State, India. *Rivista di Parassitologia*, 44:143–146

Nakagawa, S. & Schielzeth, H. 2013. A general and simple method for obtaining R^2 from generalized linear mixed-effects models. *Methods in Ecology and Evolution*, 4:133–142. https://doi.org/10.1111/j.2041-210x.2012.00261.x

Nakao, M., Sako, Y. & Ito, A. 2003. The mitochondrial genome of the tapeworm *Taenia solium*: a finding of the abbreviated stop codon U. *Journal of Parasitology*, 89:633–635. https://doi.org/10.1645/0022-3395(2003)089[0633:tmgott]2.0.co;2

Nam, U.-H., Whang, I. & Kim, J.-H. 2020. The complete mitochondrial genome sequence of *Microcotyle caudata* (Platyhelminthes: Monogenea) from dark-banded rockfish (*Sebastes inermis*) in Korea. *Mitochondrial DNA Part B*, 5:1817–1819. https://doi.org/10.1080/23802359.2020.1750986

National Center for Biotechnology Information 2021. Organelle Genome Resources. https://www.ncbi.nlm.nih.gov/genome/browse#!/organelles/. Date of access: 19 March 2021.

Neal, R. M. 2011. MCMC Using Hamiltonian Dynamics. Vol. 2, *Handbook of Markov Chain Monte Carlo*. New York: CRC Press.

Nelson, F. B., Brown, G. P., Shilton, C. M. & Shine, R. 2015. Helpful invaders: can cane toads reduce the parasite burdens of native frogs? *International Journal for Parasitology: Parasites and Wildlife*, 4:295–300. https://doi.org/10.1016/j.ijppaw.2015.05.004

Nie, P. & Kennedy, C. R. 1991. Seasonal population dynamics of *Paraquimperia tenerrima* (Linstow) (Nematoda) in the European eel *Anguilla anguilla* (Linnaeus) in three localities of southwest England. *Journal of Fish Biology*, 39:441–449. https://doi.org/10.1111/j.1095-8649.1991.tb04375.x

Nieberding, C. M. & Olivieri, I. 2007. Parasites: proxies for host genealogy and ecology? *Trends in Ecology and Evolution*, 22:156–165. https://doi.org/10.1016/j.tree.2006.11.012

Nigrelli, R. F. & Maraventano, L. W. 1944. Pericarditis in *Xenopus laevis* caused by *Diplostomulum xenopi* sp. nov., a larval strigeid. *The Journal of Parasitology*, 30:184–190. https://doi.org/10.2307/3272796

Ojala, D., Montoya, J. & Attardi, G. 1981. tRNA punctuation model of RNA processing in human mitochondria. *Nature*, 290:470–474. https://doi.org/10.1038/290470a0

Okada, K., Yamazaki, Y., Yokobori, S. & Wada, H. 2010. Repetitive sequences in the lamprey mitochondrial DNA control region and speciation of *Lethenteron*. *Gene*, 465:45–52. https://doi.org/10.1016/j.gene.2010.06.009

Oksanen, J., Blanchet, G., Friendly, M., Kindt, R., Legendre, P., McGlinn, D., ... Wagner, H. 2019. vegan: community ecology package. R package version 2.5-6. https://CRAN.R-project.org/package=vegan

Ondračková, M., Matějusová, I. & Grabowska, J. 2012. Introduction of *Gyrodactylus percotti* (Monogenea) into Europe on its invasive fish host, Amur sleeper (*Perccottus glenii*, Dybowski 1877). *Helminthologia*, 49:21–26. https://doi.org/10.2478/s11687-012-0004-3

Ortega, N., Price, W., Campbell, T. & Rohr, J. 2015. Acquired and introduced macroparasites of the invasive Cuban treefrog, *Osteopilus septentrionalis*. *International Journal for Parasitology: Parasites and Wildlife*, 4:379–384. https://doi.org/10.1016/j.ijppaw.2015.10.002

Paradis, E. & Schliep, K. 2019. ape 5.0: an environment for modern phylogenetics and evolutionary analyses in R. *Bioinformatics*, 35:526–528. https://doi.org/10.1093/bioinformatics/bty633

Park, J.-K., Kim, K.-H., Kang, S., Kim, W., Eom, K. S. & Littlewood, D. T. J. 2007. A common origin of complex life cycles in parasitic flatworms: evidence from the complete mitochondrial genome of *Microcotyle sebastis* (Monogenea: Platyhelminthes). *BMC Evolutionary Biology*, 7, art. 11. https://doi.org/10.1186/1471-2148-7-11

Peig, J. & Green, A. J. 2009. New perspectives for estimating body condition from mass/length data: the scaled mass index as an alternative method. *Oikos*, 118:1883–1891. https://doi.org/10.1111/j.1600-0706.2009.17643.x

Peig, J. & Green, A. J. 2010. The paradigm of body condition: a critical reappraisal of current methods based on mass and length. *Functional Ecology*, 24:1323–1332. https://doi.org/10.1111/j.1365-2435.2010.01751.x

Perkins, E. M., Donnellan, S. C., Bertozzi, T. & Whittington, I. D. 2010. Closing the mitochondrial circle on paraphyly of the Monogenea (Platyhelminthes) infers evolution in the diet of parasitic flatworms. *International Journal for Parasitology*, 40:1237–1245. https://doi.org/10.1016/j.ijpara.2010.02.017

Perkins, S. E., White, T. A., Pascoe, E. L. & Gillingham, E. L. 2017. Parasite community dynamics in an invasive vole: from focal introduction to wave front. *International Journal for Parasitology: Parasites and Wildlife*, 6:412–419. https://doi.org/10.1016/j.ijppaw.2017.07.005

Perna, N. T. & Kocher, T. D. 1995. Patterns of nucleotide composition at fourfold degenerate site of animal mitochondrial genomes. *Journal of Molecular Evolution*, 41:353–358. https://doi.org/10.1007/bf00186547

Phillips, B. L., Kelehear, C., Pizzatto, L., Brown, G. P., Barton, D. & Shine, R. 2010. Parasites and pathogens lag behind their host during periods of host range advance. *Ecology*, 91:872–881. https://doi.org/10.1890/09-0530.1

Plaisance, L., Huyse, T., Littlewood, D. T. J., Bakke, T. A. & Bachmann, L. 2007. The complete mitochondrial DNA sequence of the monogenean *Gyrodactylus thymalli* (Platyhelminthes: Monogenea), a parasite of grayling (*Thymallus thymallus*). *Molecular and Biochemical Parasitology*, 154:190–194. https://doi.org/0.1016/j.molbiopara.2007.04.012

Pochini, K. M. & Hoverman, J. T. 2017. Immediate and lag effects of pesticide exposure on parasite resistance in larval amphibians. *Parasitology*, 144:817–822. https://doi.org/10.1017/s0031182016002560

Poisot, T. & Stouffer, D. 2015. When is cophylogeny evidence of coevolution? In: Morand, B. R., Krasnov, S. & Littlewood, D. T., eds. *Parasite Diversity and Diversification*. Cambridge, UK: Cambridge University Press. pp. 420–434.

Polson, N. G. & Scott, J. G. 2012. On the half-Cauchy prior for a global scale parameter. *Bayesian Analysis*, 7:887–902. https://doi.org/10.1214/12-BA730

Porter, A. 1938. The larval trematodes found in certain South African Mollusca with special reference to schistosomiasis (bilharziasis). *Publications of the South African Institution of Medical Research*, 42:682–683. https://doi.org/10.1001/jama.1940.02810080054030

Posada, D. 2003. Using MODELTEST and PAUP$*$ to select a model of nucleotide substitution. *Current Protocols in Bioinformatics*, 00:6.5.1–6.5.14. https://doi.org/10.1002/0471250953.bi0605s00

Poulin, R. 2007. The structure of parasite communities in fish hosts: ecology meets geography and climate. *Parassitologia*, 49:169–172

Poulin, R. 2019. Best practice guidelines for studies of parasite community ecology. *Journal of Helminthology*, 93:8–11. https://doi.org/10.1017/s0022149x18000767

Poulin, R. & Morand, S. 2004. *Parasite Biodiversity*. Washington D.C.: Smithsonian Institution Books.

Prentis, P. J., Sigg, D. P., Raghu, S., Dhileepan, K., Pavasovic, A. & Lowe, A. J. 2009. Understanding invasion history: genetic structure and diversity of two globally invasive plants and implications for their management. *Diversity and Distributions*, 15:822–830. https://doi.org/10.1111/j.1472-4642.2009.00592.x

Price, E. W. 1943. A new trematode of the genus *Polystoma* (Monogenea: Polystomatidae) from *Xenopus laevis* Daud. *Proceedings of the Helminthological Society of Washington*, 10:83–85

Prior, K. M. & Hellmann, J. J. 2015. Does enemy release contribute to the success of invasive species? A review of the enemy release hypothesis. In: Keller, R., Cadotte, M. & Sandiford, G., eds. *Invasive Species in a Globalized World*. Chicago: University of Chicago Press.

Prior, K. M., Powell, T. H. Q., Joseph, A. L. & Hellmann, J. J. 2015. Insight from community ecology into the role of enemy release in causing invasion success: the importance of native enemy effects. *Biological Invasions*, 17:1283–1297. https://doi.org/10.1007/s10530-014-0800-4

Pritchard, M. H. 1964. Notes on four helminths from the Clawed Toad, *Xenopus laevis* (Daudin), in South Africa. *Proceedings of the Helminthological Society of Washington*, 31:121–128

Prudhoe, S. & Bray, R. A. 1982. *Platyhelminth parasites of the Amphibia*. Oxford: Oxford University Press.

Puigbò, P., Bravo, I. G. & Garcia-Vallve, S. 2008. CAIcal: a combined set of tools to assess codon usage adaptation. *Biology Direct*, 3, art. 38. https://doi.org/10.1186/1745-6150-3-38

QGIS Development Team. 2018. *QGIS Geographic Information System*. Oregon, United States of America: Open Source Geospatial Foundation Project. http://qgis.osgeo.org/

R Core Team. 2018. *R: A language and environment for statistical computing*. Vienna, Austria: R Foundation for Statistical Computing. https://www.R-project.org/

R Core Team. 2020. *R: a language and environment for statistical computing*. Vienna, Austria: R Foundation for Statistical Computing. https://www.R-project.org/

Raharivololoniaina, L., Verneau, O., Berthier, P., Vences, M. & du Preez, L. H. 2011. First monogenean flatworm from a microhylid frog host: *Kankana*, a new polystome genus from Madagascar. *Parasitology International*, 60:465–473. https://doi.org/10.1016/j.parint.2011.08.001

Rambaut, A. 2018. FigTree *version* 1.4.4 http://tree.bio.ed.ac.uk/software/figtree/

Řehulková, E., Baruš, V. & Gelnar, M. 2005. Two remarkable nematodes from the African reedfish *Erpetoichthys calabaricus* (Polypteriformes: Polypteridae). *Helminthologia*, 42:149–153

Revell, L. J. 2012. phytools: an R package for phylogenetic comparative biology (and other things). *Methods in Ecology and Evolution*, 3:217–223. https://doi.org/10.1111/j.2041-210X.2011.00169.x

Ricciardi, A. 2007. Are modern biological invasions an unprecedented form of global change? *Conservation Biology*, 21:329–336. https://doi.org/10.1111/j.1523-1739.2006.00615.x

Richardson, D. M., Carruthers, J., Hui, C., Impson, F. A. C., Miller, J. T., Robertson, M. P., ... Wilson, J. R. U. 2011a. Human-mediated introductions of Australian acacias: a global experiment in biogeography. *Diversity and Distributions*, 17:771–787. https://doi.org/10.1111/j.1472-4642.2011.00824.x

Richardson, D. M., Pyšek, P. & Carlton, J. T. 2011b. A compendium of essential concepts and terminology in invasion ecology. In: Richardson, D. M., ed. *Fifty years of invasion ecology: the legacy of Charles Elton*. Oxford: Wiley-Blackwell.

Richardson, D. M. & Ricciardi, A. 2013. Misleading criticisms of invasion science: a field guide. *Diversity and Distributions*, 19:1461–1467. https://doi.org/10.1111/ddi.12150

Ricklefs, R. E. 2010. Host-pathogen coevolution, secondary sympatry and species diversification. *Philosophical Transactions of the Royal Society of London B*, 365:1139–1147. https://doi.org/10.1098/rstb.2009.0279

Ricotta, C. & Podani, J. 2017. On some properties of the Bray-Curtis dissimilarity and their ecological meaning. *Ecological Complexity*, 31:201–205. https://doi.org/10.1016/j.ecocom.2017.07.003

Rödder, D., Ihlow, F., Courant, J., Secondi, J., Herrel, A., Rebelo, R., ... Backeljau, T. 2017. Global realized niche divergence in the African clawed frog *Xenopus laevis*. *Ecology and Evolution*, 7:4044–4058. https://doi.org/10.1002/ece3.3010

Rodrigues, R. A. E. 2014. *Macroparasites of invasive Xenopus laevis (Amphibia: Anura): characterization and assessment of possible exchanges with native Pelophylax perezi in Oeiras streams, Portugal*. Lisbon: University of Lisboa. (Dissertation – MSc).

Rohr, J. R., Raffel, T. R., Sessions, S. K. & Hudson, P. J. 2008. Understanding the net effects of pesticides on amphibian trematode infections. *Ecological Applications*, 18:1743–1753. https://doi.org/10.1890/07-1429.1

Ronquist, F., Teslenko, M., van der Mark, P., Ayres, D. L., Darling, A., Hohna, S., ... Huelsenbeck, J. P. 2012. MrBayes 3.2: efficient Bayesian phylogenetic inference and model choice across a large model space. *Systematic Biology*, 61:539–542. https://doi.org/10.1093/sysbio/sys029

Ross, E., Blair, D., Guerrero-Hernández, C. & Alvarado, A. S. 2016. Comparative and transcriptome analyses uncover key aspects of coding and long noncoding RNAs in flatworm mitochondrial genomes. *G3: Genes|Genomes|Genetics*, 6:1191–1200. https://doi.org/10.1534/g3.116.028175

Roy, H. E. & Lawson Handley, L.-J. 2012. Networking: a community approach to invaders and their parasites. *Functional Ecology*, 26:1238–1248. https://doi.org/10.1111/j.1365-2435.2012.02032.x

Rozas, J., Ferrer-Mata, A., Sánchez-DelBarrio, J., Guirao-Rico, S., Librado, P., Ramos-Onsins, S. & Sánchez-Gracia, A. 2017. DnaSP 6: DNA sequence polymorphism analysis of large datasets. *Molecular Biology and Evolution*, 34:3299–3302. https://doi.org/10.1093/molbev/msx248

Roznik, E. A., Surbaugh, K. L., Cano, N. & Rohr, J. R. 2020. Elucidating mechanisms of invasion success: effects of parasite removal on growth and survival rates of invasive and native frogs. *Journal of Applied Ecology*, 57:1078–1088. https://doi.org/10.1111/1365-2664.13634

Rumschlag, S. L., Halstead, N. T., Hoverman, J. T., Raffel, T. R., Carrick, H. J., Hudson, P. J. & Rohr, J. R. 2019. Effects of pesticides on exposure and susceptibility to parasites can be generalised to pesticide class and type in aquatic communities. *Ecology Letters*, 22:962–972. https://doi.org/10.1111/ele.13253

Sandon, H. 1941. Studies on South African endozoic ciliates I. *Paranyctotherus* (*Balantidium*) *kirbyi* (Rodriquez) emend., gen. nov. from the rectum of the clawed toad, *Xenopus laevis*. *South African Journal of Medical Science*, 6:116–127

Sara, J. R., Smit, W. J., Erasmus, L. J. C., Ramalepe, T. P., Mogashoa, M. E., Raphahlelo, M. E., ... Luus-Powell, W. J. 2014. Ecological status of Hout River Dam, Limpopo province, South Africa, using fish condition and health assessment index protocols: a preliminary investigation. *African Journal of Aquatic Science*, 39:35–43. https://doi.org/10.2989/16085914.2013.848181

Saraiva, A. & Chubb, J. C. 1989. Preliminary observations on the parasites of *Anguilla anguilla* (L.) from Portugal. *Bulletin of the European Association of Fish Parasitologists*, 9:88–89

Sasal, P., Taraschewski, H., Valade, P., Grondin, H., Wielgoss, S. & Moravec, F. 2008. Parasite communities in eels of the Island of Reunion (Indian Ocean): a lesson in parasite introduction. *Parasitology Research*, 102:1343–1350. https://doi.org/10.1007/s00436-008-0916-5

Schielzeth, H. 2010. Simple means to improve the interpretability of regression coefficients. *Methods in Ecology and Evolution*, 1:103–113. https://doi.org/10.1111/j.2041-210X.2010.00012.x

Schlick-Steiner, B. C., Steiner, F. M., Seifert, B., Stauffer, C., Christian, E. & Crozier, R. H. 2010. Integrative taxonomy: a multisource approach to exploring biodiversity. *Annual Review of Entomology*, 55:421–438. https://doi.org/10.1146/annurev-ento-112408-085432

Schlötterer, C., Tobler, R., Kofler, R. & Nolte, V. 2014. Sequencing pools of individuals — mining genome-wide polymorphism data without big funding. *Nature Reviews Genetics*, 15:749–763. https://doi.org/10.1038/nrg3803

Schoeman, A. L., Joubert, T.-L., du Preez, L. H. & Svitin, R. 2020. *Xenopus laevis* as UberXL for nematodes. *African Zoology*, 55:7–24. https://doi.org/10.1080/15627020.2019.1681295

Schoeman, A. L., Kruger, N., Secondi, J. & du Preez, L. H. 2019. Repeated reduction in parasite diversity in invasive populations of *Xenopus laevis*: a global experiment in enemy release. *Biological Invasions*, 21:1323–1338. https://doi.org/10.1007/s10530-018-1902-1

Schultheis, E. H., Berardi, A. E. & Lau, J. A. 2015. No release for the wicked: enemy release is dynamic and not associated with invasiveness. *Ecology*, 96:2446–2457. https://doi.org/10.1890/14-2158.1

Selechnik, D., Rollins, L. A., Brown, G. P., Kelehear, C. & Shine, R. 2017. The things they carried: the pathogenic effects of old and new parasites following intercontinental invasion of the Australian cane toad (*Rhinella marina*). *International Journal for Parasitology: Parasites and Wildlife*, 6:375–385. https://doi.org/10.1016/j.ijppaw.2016.12.001

Senapin, S., Phiwsaiya, K., Laosinchai, P., Kowasupat, C., Ruenwongsa, P. & Panijpan, B. 2014. Phylogenetic analysis of parasitic trematodes of the genus *Euclinostomum*

found in *Trichopsis* and *Betta* fish. *The Journal of Parasitology*, 100:368–371. https://doi.org/10.1645/13-285.1

Shamsi, S., Norman, R., Gasser, R. B. & Beveridge, I. 2009. Redescription and genetic characterization of selected *Contracaecum* spp.(Nematoda: Anisakidae) from various hosts in Australia. *Parasitology Research*, 104:1507–1525. https://doi.org/10.1007/s00436-009-1357-5

Shapiro, H. A. & Zwarenstein, H. 1934. A rapid test for pregnancy of *Xenopus laevis*. *Nature*, 133:762. https://doi.org/10.1038/133762a0

Sharp, P. M., Tuohy, T. M. & Mosurski, K. R. 1986. Codon usage in yeast: cluster analysis clearly differentiates highly and lowly expressed genes. *Nucleic Acids Research*, 14:5125–5143. https://doi.org/10.1093/nar/14.13.5125

Shui, B. N., Han, Z. Q., Gao, T. X. & Miao, Z. Q. 2008. Tandemly repeated sequence in 5' end of mtDNA control region of Japanese Spanish mackerel *Scomberomorus niphonius*. *African Journal of Biotechnology*, 7:4415–4422

Sievers, F. & Higgins, D. G. 2017. Clustal Omega for making accurate alignments of many protein sequences. *Tools for Protein Science*, 27:135–145. https://doi.org/10.1002/pro.3290

Simberloff, D. 2011. How common are invasion-induced ecosystem impacts? *Biological Invasions*, 13:1255–1268. https://doi.org/10.1007/s10530-011-9956-3

Simpson, D., Rue, H., Riebler, A., Martins, T. G. & Sørbye, S. H. 2017. Penalising model component complexity: a principled, practical approach to constructing priors. *Statistical Science*, 32:1–28. https://doi.org/10.1214/16-sts576

Skrjabin, K. I., Shikhobalovna, P. & Lagodovskaey, A. A. 1964. Oxyurata of animals and man. In: Skrjabin, K. I., ed. *Essentials of Nematology, Part 3, Volume 13*. Moscow: Academy of Sciences of the USSR.

Smit, W. J. & Luus-Powell, W. J. 2012. The occurrence of metazoan endoparasites of *Schilbe intermedius* Rüppell, 1832 from the Nwanedi-Luphephe Dams in the Limpopo River System, South Africa. *African Zoology*, 47:35–41. https://doi.org/10.1080/15627020.2012.11407520

Smith, D. R. 2015. The past, present and future of mitochondrial genomics: have we sequenced enough mtDNAs? *Briefings in Functional Genomics*, 15, 47–54. https://doi.org/10.1093/bfgp/elv027

Smyth, G. K. 1996. Regression analysis of quantity data with exact zeros. *Conference proceedings*. Second Australia-Japan Workshop on Stochastic Models in Engineering, Technology and Management. Brisbane: Technology Management Centre, University of Queensland. pp. 572–580.

Snyder, S. D. & Clopton, R. E. 2005. New methods for the collection and preservation of spirorchiid trematodes and polystomatid monogeneans from turtles. *Comparative Parasitology*, 72:102–107. https://doi.org/10.1654/4155

Solá, E., Álvarez Presas, M., Frías-López, C., Littlewood, D. T. J., Rozas, J. & Riutort, M. 2015. Evolutionary analysis of mitogenomes from parasitic and free-living flatworms. *PLOS One*, 10, art. 30120081. https://doi.org/10.1371/journal.pone.0120081

Solarz, W. & Najberek, K. 2017. Alien parasites may survive even if their original hosts do not. *EcoHealth*, 14, art. 3. https://doi.org/10.1007/s10393-015-1092-6

Soubrier, J., Steel, M., Lee, M. S., Der Sarkissian, C., Guindon, S., Ho, S. Y. & Cooper, A. 2012. The influence of rate heterogeneity among sites on the time dependence of molecular rates. *Molecular Biology and Evolution*, 29:3345–3358. https://doi.org/10.1093/molbev/mss140

Southwell, T. & Kirshner, A. 1937. On some parasitic worms found in *Xenopus laevis*, the South African Clawed Toad. *Annals of Tropical Medicine and Parasitology*, 31:245–265. https://doi.org/10.1080/00034983.1937.11684979

Souty-Grosset, C., Anastácio, P. M., Aquiloni, L., Banha, F., Choquer, J., Chucholl, C. & Tricarico, E. 2016. The red swamp crayfish *Procambarus clarkii* in Europe: impacts on aquatic ecosystems and human well-being. *Limnologica*, 58:78–93. https://doi.org/10.1016/j.limno.2016.03.003

Šrámek, A. 1901. Helminthen der an der zoologische Station in Podiebrad (Böhmen) untersuchten Fische. *Archiv für naturwissenschaftliche Landesfurchforschung Böhmens*, 11:94–118

Stekhoven, D. J. 2013. missForest: nonparametric missing value imputation using random forest. R package *version* 1.4

Stekhoven, D. J. & Bühlmann, P. 2012. MissForest: non-parametric missing value imputation for mixed-type data. *Bioinformatics*, 28:112–118. https://doi.org/10.1093/bioinformatics/btr597

Stephens, L. C., Cromeens, D. M., Robbins, V. W., Stromberg, P. C. & Jardine, J. H. 1987. Epidermal capillariasis in South African clawed frogs (*Xenopus laevis*). *Laboratory Animal Science*, 37:341–344

Stouthamer, R., Rugman-Jones, P., Thu, P. Q., Eskalen, A., Thibault, T., Hulcr, J., ... Zong, S. 2017. Tracing the origin of a cryptic invader: phylogeography of the *Euwallacea fornicatus* (Coleoptera: Curculionidae: Scolytinae) species complex. *Agricultural and Forest Entomology*, 19:366–375. https://doi.org/10.1111/afe.12215

Stöver, B. C. & Müller, K. F. 2010. TreeGraph 2: combining and visualizing evidence from different phylogenetic analyses. *BMC Bioinformatics*, 11, art. 7. https://doi.org/10.1186/1471-2105-11-7

Stromberg, P. C. & Crites, J. L. 1974. Specialization, body volume, and geographical distribution of Camallanidae (Nematoda). *Systematic Zoology*, 23:189–201. https://doi.org/10.2307/2412131

Stuart, P., Paredis, L., Henttonen, H., Lawton, C., Ochoa Torre, C. A. & Holland, C. V. 2020. The hidden faces of a biological invasion: parasite dynamics of invaders and natives. *International Journal for Parasitology*, 50:111–123. https://doi.org/10.1016/j.ijpara.2019.11.003

Sures, B., Nachev, M., Pahl, M., Grabner, D. & Selbach, C. 2017. Parasites as drivers of key processes in aquatic ecosystems: facts and future directions. *Experimental Parasitology*, 180:141–147. https://doi.org/10.1016/j.exppara.2017.03.011

Svitin, R., Schoeman, A. L. & du Preez, L. H. 2018. New information on morphology and molecular data of camallanid nematodes parasitising *Xenopus laevis* (Anura: Pipidae) in South Africa. *Folia Parasitologica*, 65, art. 003. https://doi.org/10.14411/fp.2018.003

Tabei, Y., Kiryu, H., Kin, T. & Asai, K. 2008. A fast structural multiple alignment method for long RNA sequences. *BMC Bioinformatics*, 9, art. 33. https://doi.org/10.1186/1471-2105-9-33

Taskinen, S. & Warton, D. I. 2011. Robust estimation and inference for bivariate line-fitting in allometry. *Biometrical Journal*, 53:652–672. https://doi.org/10.1002/bimj.201000018

Tavakol, S., Smit, W. J., Sara, J. R., Halajian, A. & Luus-Powell, W. J. 2015. Distribution of *Contracaecum* (Nematoda: Anasakidae) larvae in freshwater fish from the northern regions of South Africa. *African Zoology*, 50:133–139. https://doi.org/10.1080/15627020.2015.1052302

Tavaré, S. 1986. Some probabalistic and statistical problems in the analysis of DNA sequences. *Lectures on Mathematics in the Life Sciences*, 17:56–86

Telfer, S. & Bown, K. 2012. The effects of invasion on parasite dynamics and communities. *Functional Ecology*, 26:1288–1299. https://doi.org/10.1111/j.1365-2435.2012.02049.x

Theunissen, M., Tiedt, L. & du Preez, L. H. 2014. The morphology and attachment of *Protopolystoma xenopodis* (Monogenea: Polystomatidae) infecting the African clawed frog *Xenopus laevis*. *Parasite*, 21, art. 20. https://doi.org/10.1051/parasite/2014020

Thielin, F., Münderle, M., Taraschewski, H. & Sures, B. 2007. Do eel parasites reflect the local crustacean community? A case study from the Rhine river system. *Journal of Helminthology*, 81:179–189. https://doi.org/10.1017/S0022149X07753725

Thompson, C. W., Phelps, K. L., Allard, M. W., Cook, J. A., Dunnum, J. L., Ferguson, A. W., ... Kilpatrick, C. W. 2021. Preserve a voucher specimen! The critical need for integrating natural history collections in infectious disease studies. *mBio*, 12, e02698–20. https://doi.org/10.1128/mbio.02698-20

Thorpe, R. S. 1981. A comparative study of ordination techniques in numerical taxonomy in relation to racial variation in the ringed snake *Natrix natrix* (L.). *Biological Journal of the Linnean Society*, 13:7–40. https://doi.org/10.1111/j.1095-8312.1980.tb00067.x

Thurston, J. P. 1967. The morphology and life-cycle of *Cephalochlamys namaquensis* (Cohn, 1906) (Cestoda: Pseudophyllidea) from *Xenopus muelleri* and *X. laevis*. *Parasitology*, 57:187–200. https://doi.org/10.1017/S0031182000072000

Thurston, J. P. 1970. Studies on some Protozoa and helminth parasites of *Xenopus*, the African Clawed Toad. *Revue de Zoologie et de Botanique Africaines*, 82:349–368

Tinsley, R. C. 1972. The adaptation of attachment by the Polystomatidae (Monogenoidea). *Conference proceedings*. Comptes-Rendus Multicolloque Europeen de Parasitologie. pp. 65–68.

Tinsley, R. C. 1996. Parasites of *Xenopus*. In: Tinsley, R. C. & Kobel, H. R., eds. Vol. 1, *The Biology of Xenopus*. Oxford: Clarendon Press. pp. 233–261.

Tinsley, R. C. & Jackson, J. A. 1995. The genus *Oligolecithus* Vercammen-Grandjean (Digenea: Telorchiidae) from *Xenopus* spp. (Anura: Pipidae), with a description of *O. siluranae* n. sp. from *X. tropicalis* (Gray) in Ghana. *Systematic Parasitology*, 32:131–140. https://doi.org/10.1007/BF00009512

Tinsley, R. C. & Jackson, J. A. 1998a. Correlation of parasite speciation and specificity with host evolutionary relationships. *International Journal for Parasitology*, 28:1573–1582. https://doi.org/10.1016/s0020-7519(98)00085-x

Tinsley, R. C. & Jackson, J. A. 1998b. Speciation of *Protopolystoma* Bychowsky, 1957 (Monogenea: Polystomatidae) in hosts of the genus *Xenopus* (Anura: Pipidae). *Systematic Parasitology*, 40:93–141. https://doi.org/10.1023/B:SYPA.0000004047.41228.a6

Tinsley, R. C., Kobel, H. R. & Fischberg, M. 1979. The biology and systematics of a new species of *Xenopus* (Anura: Pipidae) from the highlands of Central Africa. *Journal of Zoology*, 188:69–102

Tinsley, R. C., Stott, L. C., Viney, M. E., Mable, B. K. & Tinsley, M. C. 2015. Extinction of an introduced warm-climate alien species, *Xenopus laevis*, by extreme weather events. *Biological Invasions*, 17:3183–3195. https://doi.org/10.1007/s10530-015-0944-x

Tinsley, R. C. & Sweeting, R. A. 1974. Studies on the biology and taxonomy of *Diplostomulum* (*Tylodelphylus*) *xenopodis* from the African Clawed Toad, *Xenopus laevis*. *Journal of Helminthology*, 48:247–263. https://doi.org/10.1017/S0022149X00022938

Tinsley, R. C. & Whitear, M. 1980. The surface fauna of *Xenopus* skin. *Proceedings of the Royal Society of Edinburgh*, 79:127–129. https://doi.org/10.1017/S026972700001037X

Tinsley, R. C. & Wynne Owen, R. 1975. Studies on the biology of *Protopolystoma xenopodis* (Monogenoidea): the oncomiracidium and life-cycle. *Parasitology*, 71:445–463. https://doi.org/10.1017/s0031182000047211

Tinsley, R. C. & Wynne Owen, R. 1979. The morphology and biology of *Xenopodistomum xenopodis* from the gall bladder of the African Clawed Toad, *Xenopus laevis*. *Journal of Helmintology*, 53:307–316. https://doi.org/10.1017/S0022149X00006155

Tkach, V. V., Kuzmin, Y. & Snyder, S. D. 2014. Molecular insight into systematics, host associations, life cycles and geographic distribution of the nematode family Rhabdiasidae. *International Journal for Parasitology*, 44:273–298. https://doi.org/10.1016/j.ijpara.2013.12.005

Torchin, M. E., Lafferty, K. D., Dobson, A. P., McKenzie, V. J. & Kuris, A. M. 2003. Introduced species and their missing parasites. *Nature*, 421:628–630. https://doi.org/10.1038/nature01346

Torchin, M. E., Lafferty, K. D. & Kuris, A. M. 2001. Release from parasites as natural enemies: increased performance of a globally introduced marine crab. *Biological Invasions*, 3:333–345. https://doi.org/10.1023/A:1015855019360

Torchin, M. E. & Mitchell, C. E. 2004. Parasites, pathogens, and invasions by plants and animals. *Frontiers in Ecology and the Environment*, 2:183–190. https://doi.org/10.1890/1540-9295(2004)002[0183:PPAIBP]2.0.CO;2

Valenzuela-Sánchez, A., Wilber, M. Q., Canessa, S., Bacigalupe, L. D., Muths, E., Schmidt, B. R., ... Cayuela, H. 2021. Why disease ecology needs life-history theory: a host perspective. *Ecology Letters*, 24:876–890. https://doi.org/10.1111/ele.13681

van As, J. G. & Basson, L. 1984. Checklist of freshwater fish parasites from southern Africa. *South African Journal of Wildlife Research*, 14:49–61

van der Lande, V. M. & Tinsley, R. C. 1976. Studies on the anatomy, life history and behaviour of *Marsupiobdella africana* (Hirudinea: Glossiphoniidae). *Journal of Zoology*, 180:537–563. https://doi.org/10.1111/j.1469-7998.1976.tb04703.x

van Etten, J. 2017. R package gdistance: distances and routes on geographical grids. *Journal of Statistical Software*, 76:1–21. https://doi.org/10.18637/jss.v076.i13

van Sittert, L. & Measey, G. J. 2016. Historical perspectives on global exports and research of African clawed frogs (*Xenopus laevis*). *Transactions of the Royal Society of South Africa*, 71:157–166. https://doi.org/10.1080/0035919x.2016.1158747

van Wilgen, B. W., Measey, J., Richardson, D. M., Wilson, J. R. & Zengeya, T. A. 2020. Biological invasions in South Africa: an overview. In: van Wilgen, B., Measey, J., Richardson, D., Wilson, J. & Zengeya, T., eds. *Biological Invasions in South Africa*. Springer International Publishing. pp. 3–31.

Vanhove, M., Tessens, B., Schoelinck, C., Jondelius, U., Littlewood, T., Artois, T. & Huyse, T. 2013. Problematic barcoding in flatworms: a case-study on monogeneans and rhabdocoels (Platyhelminthes). *ZooKeys*, 365:355–379. https://doi.org/10.3897/zookeys.365.5776

Vanhove, M. P. M., Briscoe, A. G., Jorissen, M. W. P., Littlewood, D. T. J. & Huyse, T. 2018. The first next-generation sequencing approach to the mitochondrial phylogeny of African monogenean parasites (Platyhelminthes: Gyrodactylidae and Dactylogyridae). *BMC Genomics*, 19, art. 520. https://doi.org/10.1186/s12864-018-4893-5

Vercammen-Grandjean, P. H. 1960. Les trématodes du Lac Kivu Sud (Vermes). *Annales du Musée Royal de l'Afrique Centrale*, 5:1–176

Verneau, O., du Preez, L. H., Laurent, V., Raharivololoniaina, L., Glaw, F. & Vences, M. 2009. The double odyssey of Madagascan polystome flatworms leads to new insights on the origins of their amphibian hosts. *Proceedings of the Royal Society of London B: Biological Sciences*, 276:1575–1583. https://doi.org/10.1098/rspb.2008.1530

Verneau, O., Palacios, C., Platt, T., Alday, M., Billard, E., Allienne, J.-F., ... du Preez, L. H. 2011. Invasive species threat: parasite phylogenetics reveals patterns and processes of host-switching between non-native and native captive freshwater turtles. *Parasitology*, 138:1778–1792. https://doi.org/10.1017/s0031182011000333

Vimercati, G., Kruger, N. & Secondi, J. 2021. Land cover, individual's age and spatial sorting shape landscape resistance in the invasive frog *Xenopus laevis*.

Vimercati, G., Labadesse, M., Dejean, T. & Secondi, J. 2020. Assessing the effect of landscape features on pond colonisation by an elusive amphibian invader using environmental DNA. *Freshwater Biology*, 65:502–513. https://doi.org/10.1111/fwb.13446

von Linstow, O. F. B. 1879. Helminthologische Untersuchungen. *Jahresbericht des Vereins für vaterländische Naturkunde in Würtemberg*, 35:313–342

von Nickisch-Rosenegk, M., Brown, W. M. & Boore, J. L. 2001. Complete sequence of the mitochondrial genome of the tapeworm *Hymenolepis diminuta*: gene arrangements indicate that platyhelminths are eutrochozoans. *Molecular Biology and Evolution*, 18:721–730. https://doi.org/10.1093/oxfordjournals.molbev.a003854

Wade, S. E. 1981. *The parasites of Xenopus laevis Daudin (South African Clawed Frog) with special reference to the bionomics and pathogenicity of Capillaria xenopodis sp. n. (Trichoidea: Trichuridae)*. Ithaca, NY: College of Veterinary Science, Cornell University. (Thesis – PhD).

Wade, S. E. 1982. *Capillaria xenopodis* sp. n. (Nematoda: Trichuroidea) from the epidermis of the South African Clawed Frog (*Xenopus laevis* Daudin). *Proceedings of the Helminthological Society of Washington*, 49:86–92

Waeschenbach, A., Brabec, J., Scholtz, T., Littlewood, D. T. J. & Kuchta, R. 2017. The catholic taste of broad tapeworms – multiple routes to human infection. *International Journal for Parasitology*, 47:831–843. https://doi.org/10.1016/j.ijpara.2017.06.004

Wang, S., Hong, Y. & Measey, G. J. 2019. An established population of African clawed frogs, *Xenopus laevis* (Daudin, 1802), in mainland China. *BioInvasions Records*, 8:457–464. https://doi.org/10.3391/bir.2019.8.2.29

Warburton, E. M., Kohler, S. L. & Vonhof, M. J. 2016. Patterns of parasite community dissimilarity: the significant role of land use and lack of distance-decay in a bat-helminth system. *Oikos*, 125:374–385. https://doi.org/10.1111/oik.02313

Ward, R. D., Zemlak, T. S., Innes, B. H., Last, P. R. & Hebert, P. D. 2005. DNA barcoding Australia's fish species. *Philosophical Transactions of the Royal Society of London B*, 360:1847–1857. https://doi.org/10.1098/rstb.2005.1716

Warton, D. I., Duursma, R. A., Falster, D. S. & Taskinen, S. 2012. smatr 3: an R package for estimation and inference about allometric lines. *Methods in Ecology and Evolution*, 3:257–259. https://doi.org/10.1111/j.2041-210X.2011.00153.x

Warton, D. I. & Weber, N. C. 2002. Common slope tests for errors-in-variables models. *Biometrical Journal*, 44:161–174. https://doi.org/10.1002/1521-4036(200203)44:2⟨161::AID-BIMJ161⟩3.0.CO;2-N

Weldon, C., de Villiers, A. L. & du Preez, L. H. 2007. Quantification of the trade in *Xenopus laevis* from South Africa, with implications for biodiversity conservation. *African Journal of Herpetology*, 56:77–83. https://doi.org/10.1080/21564574.2007.9635553

Wey-Fabrizius, A. R., Podsiadlowski, L., Herlyn, H. & Hankeln, T. 2013. Platyzoan mitochondrial genomes. *Molecular Phylogenetics and Evolution*, 69:365–375. https://doi.org/10.1016/j.ympev.2012.12.015

Whitfield, A. K. & Heeg, J. 1977. On the life cycles of the cestode *Ptychobothrium belones* and nematodes of the genus *Contracaecum* from Lake St Lucia, Zululand. *South African Journal of Science*, 73:121–122

Wickham, H. 2016. *ggplot2: Elegant Graphics for Data Analysis*. New York: Springer-Verlag.

Wickham, H., Averick, M., Bryan, J., Chang, W., D'Agostino McGowan, L., François, R., ... Yutani, H. 2019. Welcome to the tidyverse. *Journal of Open Source Software*, 4, art. 1686. https://doi.org/10.21105/joss.01686

Wickham, H., Francois, R., Henry, L. & Müller, K. 2017. dplyr: a grammar of data manipulation. R package version 0.7.4 https://CRAN.R-project.org/package=dplyr

Williams, J. B. 1959. Preliminary notes on the anatomy of a polystome from the bladder of *Xenopus laevis* Daud. *Journal of Helmintology*, 33:207–208. https://doi.org/10.1017/S0022149X00033459

Yamaguti, S. 1961. *The Nematodes of Vertebrates. Parts 1 & 2*, Vol. Systema Helminthum III. New York: Interscience Publishers.

Yang, Z. 1994. Maximum likelihood phylogenetic estimation from DNA sequences with variable rates over sites: approximate methods. *Journal of Molecular Evolution*, 39:306–314. https://doi.org/10.1007/BF00160154

Ye, F., King, S. D., Cone, D. K. & You, P. 2014. The mitochondrial genome of *Paragyrodactylus variegatus* (Platyhelminthes: Monogenea): differences in major non-coding region and gene order compared to *Gyrodactylus*. *Parasites & Vectors*, 7, art. 377. https://doi.org/10.1186/1756-3305-7-377

Yeh, L. S. 1960a. On a reconstruction of the genus *Camallanus* Railliet and Henry, 1915. *Journal of Helminthology*, 34:117–124. https://doi.org/10.1017/s0022149x00020435

Yeh, L. S. 1960b. On *Camallanus johni* sp. nov., collected from *Xenopus* in Tanganyika territory. *Journal of Helminthology*, 34:103–106. https://doi.org/10.1017/S0022149X00020411

Yorke, W. & Maplestone, P. A. 1926. *The Nematode Parasites of Vertebrates*. Philadelphia, Pennsylvania: P. Blakiston's Son & Co.

Zahiri, R., Christian Schmidt, B., Schintlmeister, A., Yakovlev, R. V. & Rindoš, M. 2019. Global phylogeography reveals the origin and the evolutionary history of the gypsy moth (Lepidoptera, Erebidae). *Molecular Phylogenetics and Evolution*, 137:1–13. https://doi.org/10.1016/j.ympev.2019.04.021

Zhang, D., Li, W. X., Zou, H., Wu, S. G., Li, M., Jakovlić, I., ... Wang, G. 2019a. Homoplasy or plesiomorphy? Reconstruction of the evolutionary history of mitochondrial gene order rearrangements in the subphylum Neodermata. *International Journal for Parasitology*, 49:819–829. https://doi.org/10.1016/j.ijpara.2019.05.010

Zhang, D., Li, W. X., Zou, H., Wu, S. G., Li, M., Jakovlić, I., ... Wang, G. T. 2018a. Mitochondrial genomes of two diplectanids (Platyhelminthes: Monogenea) expose paraphyly of the order Dactylogyridea and extensive tRNA gene rearrangements. *Parasites & Vectors*, 11, art. 601. https://doi.org/10.1186/s13071-018-3144-6

Zhang, D., Li, W. X., Zou, H., Wu, S. G., Li, M., Jakovlić, I., ... Wang, G. T. 2020. Mitochondrial genomes and 28S rDNA contradict the proposed obsoletion of the order

Tetraonchidea (Platyhelminthes: Monogenea). *International Journal of Biological Macromolecules*, 143:891–901. https://doi.org/10.1016/j.ijbiomac.2019.09.150

Zhang, D., Zou, H., Jakovlić, I., Wu, S. G., Li, M., Zhang, J., ... Wang, G. T. 2019b. Mitochondrial genomes of two *Thaparocleidus* species (Platyhelminthes: Monogenea) reveal the first rRNA gene rearrangement among the Neodermata. *International Journal of Molecular Sciences*, 20, art. 4214. https://doi.org/10.3390/ijms20174214

Zhang, D., Zou, H., Wu, S. G., Li, M., Jakovlić, I., Zhang, J., ... Wang, G. T. 2018b. Three new Diplozoidae mitogenomes expose unusual compositional biases within the Monogenea class: implications for phylogenetic studies. *BMC Evolutionary Biology*, 18, art. 133. https://doi.org/10.1186/s12862-018-1249-3

Zhang, D., Zou, H., Wu, S. G., Li, M., Jakovlić, I., Zhang, J., ... Li, W. X. 2017. Sequencing of the complete mitochondrial genome of a fish-parasitic flatworm *Paratetraonchoides inermis* (Platyhelminthes: Monogenea): tRNA gene arrangement reshuffling and implications for phylogeny. *Parasites & Vectors*, 10, art. 462. https://doi.org/10.1186/s13071-017-2404-1

Zhang, D., Zou, H., Wu, S. G., Li, M., Jakovlić, I., Zhang, J., ... Li, W. X. 2018c. Sequencing, characterization and phylogenomics of the complete mitochondrial genome of *Dactylogyrus lamellatus* (Monogenea: Dactylogyridae). *Journal of Helminthology*, 92:455–466. https://doi.org/10.1017/S0022149X17000578

Zhang, D. X. & Hewitt, G. M. 1997. Insect mitochondrial control region: a review of its structure, evolution and usefulness in evolutionary studies. *Biochemical Systematics and Ecology*, 25:99–120. https://doi.org/10.1016/S0305-1978(96)00042-7

Zhang, D. X., Szymura, J. M. & Hewitt, G. M. 1995. Evolution and structural conservation of the control region of insect mitochondrial DNA. *Journal of Molecular Evolution*, 40:382–391

Zhang, J., Wu, X., Li, Y., Xie, M. & Li, A. 2016. The complete mitochondrial genome of *Tetrancistrum nebulosi* (Monogenea: Ancyrocephalidae). *Mitochondrial DNA Part A*, 27:22–23. https://doi.org/10.3109/19401736.2013.867441

Zhang, J., Wu, X., Li, Y., Zhao, M., Xie, M. & Li, A. 2014. The complete mitochondrial genome of *Neobenedenia melleni* (Platyhelminthes: Monogenea): mitochondrial gene content, arrangement and composition compared with two *Benedenia* species. *Molecular Biology Reports*, 41:6583–6589. https://doi.org/10.1007/s11033-014-3542-6

Zhang, J., Wu, X., Xie, M. & Li, A. 2012. The complete mitochondrial genome of *Pseudochauhanea macrorchis* (Monogenea: Chauhaneidae) revealed a highly repetitive region and a gene rearrangement hot spot in Polyopisthocotylea. *Molecular Biology Reports*, 39:8115–8125. https://doi.org/10.1007/s11033-012-1659-z

Zhang, J., Wu, X., Xie, M., Xu, X. & Li, A. 2011. The mitochondrial genome of *Polylabris halichoeres* (Monogenea: Microcotylidae). *Mitochondrial DNA*, 22:3–5. https://doi.org/10.3109/19401736.2011.588223

Zhu, X., D'Amelio, S., Hu, M., Paggi, L. & Gasser, R. B. 2001. Electrophoretic detection of population variation within *Contracaecum ogmorhini* (Nematoda: Ascaridoidea: Anisakidae). *Electrophoresis*, 22:1930–1934. https://doi.org/10.1002/1522-2683(200106)22:10⟨1930::AID-ELPS1930⟩3.0.CO;2-Z

Zuur, A. F., Hilbe, J. M. & Ieno, E. N. 2015. *A Beginner's Guide to GLM and GLMM with R: A Frequentist and Bayesian Perspective for Ecologists*. Newburgh: Highland Statistics Limited.

Zuur, A. F. & Ieno, E. N. 2016. A protocol for conducting and presenting results of regression-type analyses. *Methods in Ecology and Evolution*, 7:636–645. https://doi.org/10.1111/2041-210X.12577

Zuur, A. F., Ieno, E. N. & Elphick, C. S. 2010. A protocol for data exploration to avoid common statistical problems. *Methods in Ecology and Evolution*, 1:3–14. https://doi.org/10.1111/j.2041-210X.2009.00001.x

Appendix A

Information on water bodies where *Xenopus laevis* were collected for parasitological surveys

Table A.1: Detailed information on collection localities from four continents where *Xenopus laevis* specimens were sampled for parasitological surveys. Included are specimens from 14 water bodies from previously published works from Chile (Castillo *et al.*, 2017), Portugal (Rodrigues, 2014) and California, USA (Kuperman *et al.*, 2004) and the 47 water bodies from western France, Portugal and southern Africa surveyed in the present study. Localities in southern Africa are named according to the nearest town and province. The surveyed water bodies in southern Africa were classified according to habitat type for the analyses in chapter 5 (Habitat). Water bodies in southern Africa, France and Portugal were further classified according to the phylogeographic lineage of the collected *X. laevis* (SA1–7), following de Busschere *et al.* (2016), for the analyses in chapter 6 (Lineage). In addition, for each surveyed water body, collection month (Date), latitude and longitude in decimal degrees (Coordinates) and number of *X. laevis* screened for parasites (Sample size) are given, along with the chapters, referred to by their number, that included the particular locality in analyses (Chapter(s)).

Locality	Habitat	Lineage	Date	Coordinates	Sample size	Chapter(s)
Southern Africa						
Adelaide, Eastern Cape	Peri-urban	SA6	November 2017	32.6879 °S; 26.2951 °E	4	4,5,6
Barrydale 1, 2 & 4, Western Cape	Natural	SA3	November 2017	33.9264 °S; 20.5917 °E	2	4,5,6
	Unvegetated artificial	SA3		33.9283 °S; 20.5915 °E	3	4,5,6
	Unvegetated artificial			33.9313 °S; 20.5873 °E	4	4,5
Bloemfontein, Free State	Peri-urban		November 2019	29.0636 °S; 26.2188 °E	6	4,5,7
Cape Town, Western Cape	Peri-urban	SA1	June 2017	33.8355 °S; 18.5528 °E	14	2,3,4,5,6,B
Colesberg, Northern Cape	Unvegetated artificial		December 2017	29.5848 °S; 24.0146 °E	7	4,5
Debshan ranch, Zimbabwe		SA5	November 2017	19.6825 °S; 29.1547 °E	1	4,6
Dullstroom, Mpumalanga Province	Natural	SA5	April 2017	25.3981 °S; 30.0380 °E	10	2,3,4,5,6,B
Durbanville, Western Cape	Vegetated artificial	SA1	July 2017	33.8392 °S; 18.6003 °E	5	2,3,4,5,6,B
George, Western Cape	Peri-urban	SA2	February 2018	33.9455 °S; 22.4637 °E	3	4,5,6
Hermanus, Western Cape	Vegetated artificial	SA1	June 2017	34.3702 °S; 19.2571 °E	7	2,3,4,5,6,B
Hopetown, Northern Cape	Vegetated artificial	SA5	December 2017	33.3528 °S; 20.4255 °E	2	4,5,6
Johannesburg, Gauteng Province	Peri-urban	SA5	February 2018	26.1251 °S; 27.9222 °E	6	4,5,6
Jonkershoek, Western Cape		SA1	February 2020	33.9584 °S; 18.9169 °E	1	6
Ladismith, Western Cape	Natural	SA3	November 2017	33.4637 °S; 21.0970 °E	6	4,5,6
Laingsburg, Western Cape	Natural	SA3	November 2017	33.3528 °S; 20.4255 °E	2	4,5,6
Louis Trichardt, Limpopo Province	Vegetated artificial	SA5	February 2019	23.0728 °S; 30.0711 °E	6	4,5,6
Matjiesfontein, Western Cape		SA3	February 2020	33.2294 °S; 20.5816 °E	3	6
Modimolle, Limpopo Province	Vegetated artificial	SA5	April 2017	24.6384 °S; 28.4369 °E	6	2,3,4,5,6,B
Polokwane, Limpopo Province	Unvegetated artificial		April 2017	23.7693 °S; 29.4047 °E	7	2,4,5

Table A.1: Detailed information on collection localities from four continents where *Xenopus laevis* specimens were sampled for parasitological surveys (*continued*).

Locality	Habitat	Lineage	Date	Coordinates	Sample size	Chapter(s)
Potchefstroom, North-West Province	Vegetated artificial	SA5	March 2017	26.7555 °S; 27.0506 °E	9	2,3,4,5,6,B
Richards Bay, KwaZulu Natal				28.7928 °S; 26.0506 °E	15	2
Riversdale, Western Cape	Natural	SA3	November 2017	33.7033 °S; 21.1762 °E	5	4,5,6
Three Sisters, Western Cape	Vegetated artificial	SA4	November 2017	31.8950 °S; 23.0957 °E	5	4,5,6
	Natural	SA4		31.8526 °S; 23.2645 °E	2	4,5,6
Tzaneen, Limpopo Province	Unvegetated artificial	SA5	May 2017	23.7988 °S; 30.1951 °E	10	2,3,4,5,6,B
Ugie, Eastern Cape	Vegetated artificial	SA6	December 2017	31.3049 °S; 28.2646 °E	6	4,5,6
Vanrhynsdorp, Western Cape	Natural	SA7	November 2017	31.7361 °S; 18.8255 °E	7	3,4,5,6
Verkykerskop, Free State	Vegetated artificial	SA5	January 2018	27.7833 °S; 29.3363 °E	7	4,5,6
Wakefield, KwaZulu Natal	Natural	SA5	February 2018	29.4797 °S; 29.8877 °E	7	4,5,6
			April 2019	29.4825 °S; 29.8889 °E	1	5,6
Wellington 1 & 2, Western Cape	Natural		November 2017	33.5560 °S; 18.8437 °E	2	4,5
	Unvegetated artificial	SA1		33.5714 °S; 18.8401 °E	6	3,4,5,6
White River 1 & 2, Mpumalanga Province	Peri-urban	SA5	April 2017	25.3391 °S; 31.0226 °E	8	2,3,4,5,6,B
				25.3320 °S; 31.0433 °E	6	2,4,5,6
Chile						
Batuco Lagoon, Batuco			1997–2014	33.2000 °S; 70.8333 °W	43	4
Carén stream, Alhue			1997–2014	34.0660 °S; 71.2517 °W	3	4
Chilcas stream, Las Chilcas			1997–2014	32.8715 °S; 70.8453 °W	8	4
Córdova stream, El Tabo			1997–2014	33.4334 °S; 71.6457 °W	9	4
Ibacache stream, Ibacache			1997–2014	33.4514 °S; 71.3332 °W	24	4
La Patagua			1997–2014	34.7165 °S; 71.3850 °W	79	4
Les Molles Dam, El Yali National Park			1997–2014	33.8010 °S; 71.6970 °W	2	4
Maipo River, Tejas Verdes			1997–2014	33.6284 °S; 71.6086 °W	3	4
Tinguiririca River, Palmilla			1997–2014	34.5970 °S; 71.3556 °W	3	4
Universidad de Chile, La Pintana			1997–2014	33.5733 °S; 70.6327 °W	5	4
France						
Sites 1–6		FR	July 2017	47.3440 °N; 0.7636 °W	8	4,6

Table A.1: Detailed information on collection localities from four continents where *Xenopus laevis* specimens were sampled for parasitological surveys (*continued*).

Locality	Habitat	Lineage	Date	Coordinates	Sample size	Chapter(s)
				46.9280 °N; 0.3332 °W	10	4
		FR		46.9401 °N; 0.3686 °W	10	4,6
				47.0261 °N; 0.3447 °W	5	4
		FR		47.0328 °N; 0.3474 °W	4	4,6
				47.0407 °N; 0.3339 °W	6	4
Ambillou-Château		FR	June 2019	47.2386 °N; 0.3445 °W	9	5,6
Bouillé-Saint-Paul		FR	June 2019	47.0273 °N; 0.3443 °W	13	5,6
Brézé		FR	June 2019	47.1726 °N; 0.0729 °W	10	5,6
Cersay 1 & 2		FR	May 2019	47.0531 °N; 0.3648 °W	11	5,6
			July 2019	47.0531 °N; 0.3648 °W	8	5,6
Chalonnes-sur-Loire		FR	June 2019	47.3440 °N; 0.7636 °W	6	5,6
Épieds			June 2019	47.1413 °N; 0.0606 °W	12	5
La Butte			May 2019	46.9185 °N; 0.2803 °W	7	5
Le Coudray-Macouard		FR	June 2019	47.1872 °N; 0.1151 °W	11	5,6
Massais		FR	June 2019	47.0106 °N; 0.3582 °W	16	5,6
Saint-Martin-de Sanzay		FR	May 2019	47.0729 °N; 0.1898 °W	8	5,6
Portugal						
Lage and Barcena streams, Oeiras			June–August 2013	38.7307 °N; 9.3187 °W	80	4
				38.6922 °N; 9.3154 °W		4
				38.7517 °N; 9.2898 °W		4
				38.7460 °N; 9.2869 °W		4
				38.7450 °N; 9.2867 °W		4
				38.7420 °N; 9.2856 °W		4
				38.7439 °N; 9.2874 °W		4
				38.7378 °N; 9.2834 °W		4
				38.7354 °N; 9.2821 °W		4
				38.7091 °N; 9.2731 °W		4
Lisbon		PT	February 2019	38.7136 °N; 9.2897 °W	1	6

Table A.1: Detailed information on collection localities from four continents where *Xenopus laevis* specimens were sampled for parasitological surveys (*continued*).

Locality	Habitat	Lineage	Date	Coordinates	Sample size	Chapter(s)
United States						
Dulzura Creek System, San Diego County, California			1999–2001	32.6250 °N; 116.7761 °W	68	4
Rancho Jamul System, San Diego County, California			1999–2001	32.6675 °N; 116.8633 °W	132	4
Santa Ana River, Riverside County, California			1999–2001	33.9667 °N, 117.6453 °W	30	4

Appendix B

Investigation of the intraspecific morphometric variation of *Protopolystoma xenopodis* (Monogenea: Polystomatidae) from divergent host lineages in its native range

B.1 Background and aim

Intra-specific morphological variation has been recorded before in the monogenean *Protopolystoma xenopodis* (Price, 1943) Bychowsky, 1957 (Monogenea: Polystomatidae), with genital spine length increasing markedly from the southernmost to the more northerly populations of this parasite (Tinsley & Jackson, 1998b). The geographical variation in other taxonomically important traits in the genus *Protopolystoma* (following Tinsley & Jackson, 1998b), such as number of lateral and medial diverticula and post-ovarian inter-caecal anastomoses and shape and size of the large hamuli and eggs, was investigated as part of this PhD project on a small sample of worms. The aim of this investigation was to see whether morphological differences exist between *P. xenopodis* from the summer and winter rainfall regions that correspond with the divergent phylogeography of both the parasite and its host *Xenopus laevis* (Daudin, 1802) (Anura: Pipidae).

B.2 Morphometrics

Permanent mounts were made of 13 polystomatids from the northerneastern lineage of the host (SA5 localities) and 10 from the southwestern lineage (SA1 localities), representing nine localities, namely Dullstroom, Modimolle, Potchefstroom, White River (two localities), Tzaneen, Hermanus and Cape Town (two localities). Polystomatids preserved in both 10% neutral buffered formalin and 70% ethanol were hydrated through a decreasing ethanol series to tap water. The specimens were stained overnight in acetocarmine. Thereafter, the specimens were dehydrated in an increasing ethanol series to absolute ethanol, with colour corrections by hydrochloric acid incorporated whilst the specimens were in the 70% ethanol. The specimens were cleared in xylene and mounted on a microscope slide under coverslip pressure in Canada balsam (Sigma-Aldrich Co., Steinheim, Germany). The mounts were dried at 60℃ for approximately 48 hours. Throughout the procedure, care was taken to ensure that the specimens were not exposed to air, as this leads to discolouration. Measurements and photomicrographs were taken on a Nikon ECLIPSE E800 compound microscope in conjunction with the software NIS-Elements Documentation *version* 3.22.09 (Nikon Instruments Inc., Tokyo, Japan).

B.3 Statistical analyses

After measurement, the 12 characters with minimal missing data points among the measured worms were compared statistically between the two groups in R *version* 3.5.1 (R Core Team, 2018). Missing data points were imputed by the random forest method in the R package *missForest* (Stekhoven, 2013). This method was preferred since it has a non-parametric approach suitable to the small sample size and because it can handle mixed variable types (Stekhoven & Bühlmann, 2012). Since certain characters can vary with parasite age, or its proxy, body size, the median body length and width and haptor length and width were compared between the two groups with the non-parametric Wilcoxon-Mann-Whitney (WMW) test before other comparisons were conducted. The WMW test was further employed to test whether there was a significant difference in the median number of post-ovarian inter-caecal anastomoses and lateral and medial diverticula (averaged for left and right) and the median length of the terminal hook and dorsal and ventral roots of the large hamuli (also averaged for left and right sides of worms) and egg length and width between the two groups of *P. xenopodis*. A principal components analysis (PCA), which is commonly employed in numerical taxonomy, also that of monogeneans (Hahn *et al.*, 2011), was employed to evaluate the correlation among polystomatids from different localities based upon the variance in the characters that were shown to be significantly different between the two groups. The PCA specifically tested whether the combination of significantly different morphological characters could

discriminate between polystomatids from hosts from the two phylogeographic lineages, despite overlap in the measurements of all these characters between the two groups, without taking into account geographical origin *a priori*. The visualisation further identified the characters that contributed most to the variation between groups. Since the Euclidean distances utilised in a PCA are very sensitive to different units of measurement, the data were column-standardised beforehand in the R package *vegan* (Oksanen *et al.*, 2019) as recommended by Thorpe (1981). The PCA itself was also performed in R, utilising the singular value decomposition method.

B.4 Significant morphological variation among South African *Protopolystoma xenopodis*

In their re-description of *P. xenopodis*, Tinsley & Jackson (1998b) noted that the species displayed significant, but continuous, geographical variation in the size of the genital spines between southern and more northerly populations of *X. laevis*. In addition, they identified certain key characteristics which could be used to discriminate between the six species of *Protopolystoma*, namely variation in the morphology of the gut, large hamulus and genital spines (Tinsley & Jackson, 1998b). Therefore, these characters were specifically selected to explore geographical variation in *P. xenopodis* in southern Africa.

It would seem as if general body size, which can influence the size of other structures in the body, was not significantly different between the polystomatids that were measured from the northerneastern lineage (SA5) and those measured from the southwestern lineage (SA1). Neither median body length (WMW test, median_{SA1} = 1854.0 μm, median_{SA5} = 1769.5 μm, p = 0.5224) and width (WMW test, median_{SA1} = 712.5 μm, median_{SA5} = 677.0 μm, p = 0.9274), nor median haptor length (WMW test, median_{SA1} = 437.5 μm, median_{SA5} = 387.1 μm, p = 0.1535) and width (WMW test, median_{SA1} = 367.0 μm, median_{SA5} = 329.0 μm, p = 0.4458) were significantly different between the two groups. Since body size was controlled for between the two groups, the significant differences in the number of post-ovarian inter-caecal anastomoses (WMW test, median_{SA1} = 2, median_{SA5} = 2, $p < 0.05$), lateral (WMW test, median_{SA1} = 27, median_{SA5} = 24 μm, $p < 0.05$) and medial diverticula (WMW test, median_{SA1} = 26 μm, median_{SA5} = 20 μm, $p < 0.05$), terminal hook length (WMW test, median_{SA1} = 46.8 μm, median_{SA5} = 37.8 μm, $p < 0.05$) and egg length (WMW test, median_{SA1} = 237.9 μm, median_{SA5} = 220.8 μm, $p < 0.05$) were the products of geographical divergence in morphology. Three of the measured characters, namely length of the dorsal (WMW test, median_{SA1} = 137.5 μm, median_{SA5} = 136.0 μm, p = 1) and ventral roots of the hamuli (WMW test, median_{SA1} = 149.0 μm, median_{SA5} = 135.9 μm, p = 1) and egg diameter (WMW test, median_{SA1} = 81.8 μm, median_{SA5} = 79.1 μm, p = 0.0880), did not differ significantly between the two groups. In sum, *P. xenopodis* from the southwestern parts of the region displayed less variation in the number of anastomoses (one or two

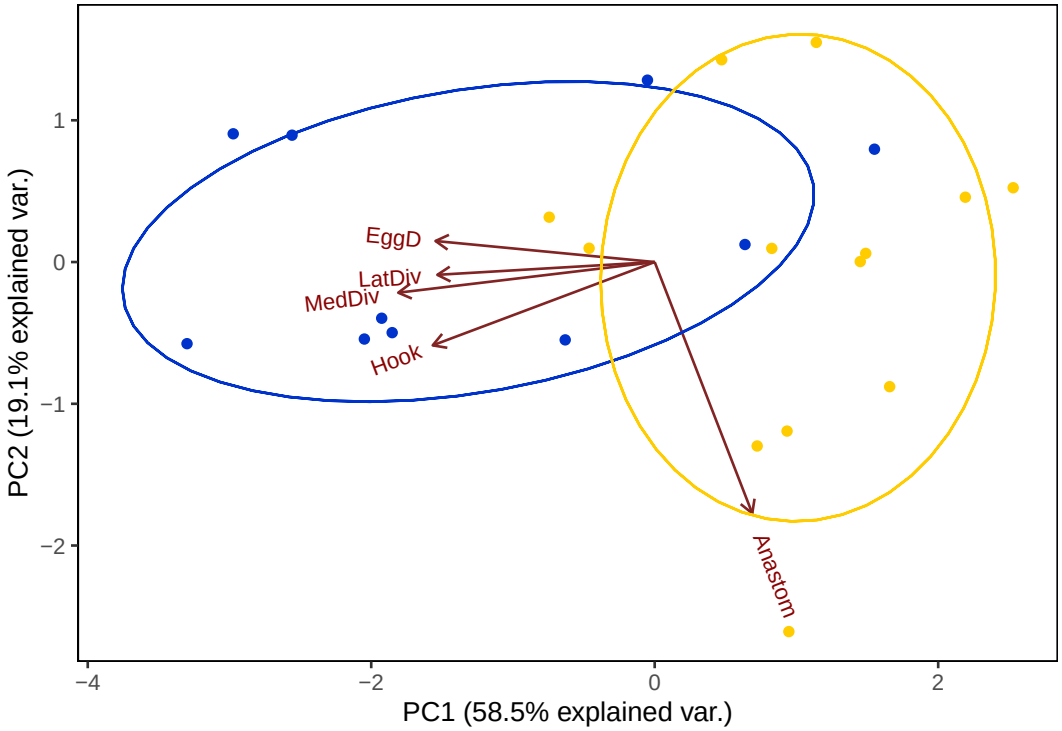

Figure B.1: Principal components analysis of the morphological traits of *Protopolystoma xenopodis* from two phylogeographic lineages of the host *Xenopus laevis*. Principal components were calculated from five morphometric variables, namely egg length (EggD), number of lateral (LatDiv) and medial (MedDiv) diverticula, post-ovarian inter-caecal anastomoses (Anastom) and length of the terminal hook of the hamuli (Hook), of polystomatids from the southwestern (SA1 in blue) and northerneastern (SA5 in yellow) phylogeographic lineages of the host. Ellipses indicate the normal contour line of one standard deviation (68%) from the mean for each group.

versus one to four), possessed more diverticula, both laterally and medially, had longer terminal hooks on the hamuli and had longer eggs than their northern counterparts.

This trend was emphasised by the results of the PCA, which was able to partially discriminate polystomatids from the two host lineages from one another based upon the five significantly diverging morphological characters (Figure B.1). The first two principal components accounted for 58.6% and 19.33% of the observed variance, together explaining 77.93% of the variance in the data.

B.5 Implications

In sum, the results indicate that there is significant morphological variation between the southern African lineages of *P. xenopodis*. Interestingly, this involves some of the characters that are important for species delineation in the genus, such as the number of anastomoses and gut and hamulus morphology (Tinsley & Jackson, 1998b), underscoring

the importance of these traits as possible role players in incipient speciation. Moreover, the traits that differed significantly between the two groups were either involved in reproduction, feeding or attachment. Since feeding and attachment are directly linked to host characteristics (in the light of the fact that the host bladder is both the attachment substrate and the food source), the observed divergence may well represent adaptation to different lineages of the host. Variation in egg dimensions, an aspect of reproduction, may further hint at a mechanism for reproductive isolation.

However, before jumping to conclusions, one must keep in mind that the examined parasites hailed from the two most geographically distanced lineages of the host, which also happen to inhabit two vastly different climatic regions. Tellingly, the influence of the environment on egg production in *P. xenopodis* is well documented (Jackson & Tinsley, 1988). With the addition of specimens from the lineages that lie between these two (geographically speaking), it is not unrealistic to imagine that morphological variation will present itself on a spectrum that correlates closely with geographical distance between the groups. In fact, the slight overlap of group means, as illustrated by the PCA, hints at a form of continuous variation rather than divergent selection. This is in accordance with the ”significant, but continuous” variation in penis armature that was observed in the previous study (Tinsley & Jackson, 1998b), albeit on a larger geographical scale.

All in all, these findings are not necessarily valuable for species delineation from a taxonomic viewpoint, as it has been for gyrodactylid monogeneans parasitising salmon and trout (Hahn *et al.*, 2011). What these findings do bring to light, however, is a possible link between host and parasite morphological and genetic variation. In turn, this link hints at a possibility of shared evolutionary history between host and parasite, making this system an ideal model to tease out the processes involved for new species to emerge from existing ones.